

University of Nottingham
UK | CHINA | MALAYSIA

PROCESS AND OPTIMIZATION OF PALM-OIL BASED WATER-IN-OIL-IN-WATER (W/O/W) MULTIPLE NANOEMULSION ENCAPSULATING TOCOTRIENOLS AND CAFFEIC ACID WITH CISPLATIN AS A SYNERGISTIC ANTICANCER TREATMENT

REVATHI RAVIADARAN, MEng (Hons).

Thesis submitted to the University of Nottingham for the Degree of Doctor of Philosophy

July 2021

ABSTRACT

Water-in-oil-in-water (W/O/W) multiple emulsion consist of oil globules containing small internal water droplets dispersed in an external continuous water phase. They possess the potential to encapsulate active compounds such as drugs, nutrients and flavonoids to protect them from degradation by external stresses such as pH, light, temperature, oxygen and gastrointestinal conditions during the transit. Despite their potential for sustained release, multiple emulsion is not widely used due to their thermodynamic instability culminating in phase separation. With rising fatality due to cancer, as well as the tumour resistance and severe side effects of the most commonly used chemotherapeutic drug, cisplatin-cis-diamminedichloroplatinum (CIS), it is essential to explore a combined therapy of using CIS with natural chemopreventive active compounds. Through this, the toxic dosage of CIS could be reduced and synergistic effects could be achieved. This study aims to formulate stable natural tocotrienol rich fraction (TRF) and caffeic acid (CA) encapsulated in palm oil-based W/O/W multiple nanoemulsion and evaluate its anticancer and toxicity effects towards cancer and normal cell lines, respectively. This was achieved through multi-faceted experimentations which commenced with the formulation of stable water-in-palm oil (W/O) nanoemulsion using ultrasonicator and microfluidizer emphasizing on the interaction between the oil and emulsifier to form rigid oil-water interface. For this, the effects of the addition of polyglycerol polyricinoleate (PGPR), medium-chain triglyceride (MCT), lecithin and sodium chloride (NaCl) towards the stability of nanoemulsion were mainly evaluated. Following this, stable W/O/W multiple nanoemulsion encapsulating TRF and CA was formulated using ultrasonicator and microfluidizer, as well as focused on the energy consumption and oxidation of palm oil in the processed emulsion. The effects of Sucragel (oil-soluble thickener) for the oil phase and Xanthan gum (water-soluble thickener) for the internal water phase, as well as tonicity such as hypotonic, isotonic and hypertonic towards the stability of multiple nanoemulsion, were evaluated. Finally, the anticancer and toxicity effects of TRF and CA encapsulated W/O/W multiple nanoemulsion with CIS towards cancer (A549 and HEP G2) and normal (HEK 293) cell lines were examined. Stable

palm oil-based W/O nanoemulsion was produced using 61.25 wt% of palm oil, 26.25 wt% of MCT, 2.5 wt% of PGPR and 10.0 wt% of water. The W/O nanoemulsion was formed under optimized ultrasonicator conditions of 40% amplitude, 180 s of irradiation time, while for microfluidizer it was 350 bar and six cycles. The obtained mean droplet diameter (MDD) and dispersity index (DI) of W/O nanoemulsion were 143.1±8.8 nm and 0.131±0.094, respectively, with no sedimentation observed for 2 weeks. PGPR's polyricinoleate non-polar fatty acids were found to bound to palm oil's non-polar fatty acids through van der Waals intermolecular forces. At the same time, it's polyglycerol polar head interacted with water molecules through hydrogen bonding and bound to glyceride units of palm oil that strengthened its interaction at the interface. The addition of NaCl further reduced MDD by 70 nm and improved the stability of nanoemulsion through electrostatic repulsions attributed to the dissociation of Na^+ and Cl^- ions. Then, W/O/W multiple nanoemulsion was formed under optimized ultrasonicator conditions of 40% amplitude, 180 s of irradiation time, while for microfluidizer it was 350 bar and eight cycles. This is the first work that successfully utilized Sucragel (oil-based thickener) in imparting enhanced stability in W/O/W multiple nanoemulsion. Through this, the thickened oil phase retained and protected the internal water droplets by forming a packed and stable network in the oil globules and rigid stability at the oil-water interface. W/O/W multiple nanoemulsion with isotonic stabilization gave the lowest change in MDD, concentration of NaCl and water content by 1.34%, 2.97% and 0.40%, respectively, due to the reduced movement of water. The optimized W/O/W multiple nanoemulsion consist of 10.0 wt% of W/O nanoemulsion, 89.0 wt% of water and 1.0 wt% of Tween 80. The W/O nanoemulsion consist of 10.0 wt% of water, 1.0 wt% of Sucragel, 2.5 wt% PGPR and 86.5 wt% of palm oil (70:30 of palm oil:palm MCT oil). It possessed 175.5±9.8 nm and 0.232±0.012 of MDD and DI, respectively. After 180 days of storage for the TRF and CA encapsulated W/O/W multiple nanoemulsion, <4% change in water content, conductivity, NaCl concentration, as well as the concentration of TRF and CA were measured. ~99% and ~98% encapsulation efficiencies of

TRF and CA, respectively, were obtained. Higher TRF and CA concentrations in the range of 100.0% - 237.5% were required to achieve inhibitory concentration (IC 50) for A549 and HEP G2 in solution as compared to nanoemulsion. TRF, CA and CIS synergistically improved apoptosis in the late apoptotic phase in A549 and HEP G2 by 23.1% and 24.9%, respectively. The generation of reactive oxygen species was enhanced using TRF:CA:CIS by 16.9% and 30.2% for A549 and HEP G2, respectively. Cell cycle analysis showed enhanced cell arrest in the G0/G1 phase for both A549 and HEP G2. TRF, CA and CIS led to cell death in A549 and HEP G2. For HEK 293, ~33% cell viability was found when only CIS was used, while ~95% cell viability was observed when TRF, CA and CIS were used. These outcomes distinctly show that stable TRF and CA encapsulated W/O/W multiple nanoemulsion was successfully formulated, which synergistically treated cancer cell lines, as well as increased the viability of normal cell line due to reduced toxicity. These are especially true for the cancer and normal cell lines evaluated in this study. Overall, this work contributed to the advancement of knowledge and application of palm oil-based W/O/W multiple nanoemulsion encapsulating natural active compounds to be used synergistically with chemotherapeutic drug for more effective and less toxic cancer treatment.

LIST OF JOURNAL PUBLICATIONS

- R. Raviadaran, M. H. Ng, D. Chandran, K. K. Ooi, S. Manickam, Stable W/O/W multiple nanoemulsion encapsulating natural tocotrienols and caffeic acid with cisplatin synergistically treated cancer cell lines (A549 and HEP G2) and reduced toxicity on normal cell line (HEK 293). Materials Science & Engineering: C. 121 (2021) 111808. https://doi.org/10.1016/j.msec.2020.111808.
- R. Raviadaran, M. H. Ng, S. Manickam, D. Chandran, Ultrasound-assisted production of palm oil-based isotonic W/O/W multiple emulsion with enhanced stability using oil-based Sucragel. Ultrasonics Sonochemistry. 64 (2020) 104995. https://doi.org/10.1016/j.ultsonch.2020.104995.
- R. Raviadaran, M. H. Ng, S. Manickam, D. Chandran, Ultrasound-assisted water-in-palm oil nano-emulsion: Influence of polyglycerol polyricinoleate and NaCl on its stability. Ultrasonics Sonochemistry. 52 (2019) 353-363. https://doi.org/10.1016/j.ultsonch.2018.12.012.

LIST OF BOOK CHAPTER

- R. Raviadaran, M.H. Ng, K. Muthoosamy, S. Manickam (2018). Simple and Multiple Emulsions Emphasizing on Industrial Applications and Stability. In C.O. Mohan, E. Carvajal-Millan, C.N. Ravishankar, & A. K. Haghi (Eds.), Food Process Engineering and Quality Assurance (pp. 179-230). New York: Apple Academic Press. https://doi.org/10.1201/9781315232966.

LIST OF CONFERENCES

- R. Raviadaran. Effects of ultrasonication and microfluidization on nano-emulsion degradation. UNMC LINK'18 PG Conference. University of Nottingham, Malaysia, 26 July 2018.
- R. Raviadaran, M.H. Ng and S. Manickam. Multiple emulsion (W/O/W) as a drug carrier for hydrophilic and hydrophobic compounds. The Royal Society of Chemistry Twitter Poster Conference. 06-07 March 2018.
- R. Raviadaran, M.H. Ng, S. Manickam and K. Muthoosamy. Investigation on the effects of different types of emulsifiers towards the stability of palm oil-based W/O nanoemulsion for encapsulating Tocotrienol. MPOB International Palm Oil Congress (PIPOC 2017): Chemistry, Processing Technology & Bio-energy. Kuala Lumpur, Malaysia, 14-16 Nov 2017, pp. 32.
- R. Raviadaran, S. Manickam and M.H. Ng, Multiple emulsion (W/O/W): A single drug carrier for hydrophilic and hydrophobic compound in: UNMC Postgraduate Research Showcase. University of Nottingham, Malaysia, 27 Sept 2017.
- R. Raviadaran, M.H. Ng, S. Manickam and K. Muthoosamy, Comparative studies between ultrasound cavitation and microfluidizer in generating palm oil-based oil-in-water (O/W) tocotrienol nanoemulsion. MPOB National Seminar on Palm Oil Milling, Refining, Environment and Quality (POMREQ 2016). Kuala Lumpur, Malaysia, 29-30 Nov 2016, pp. 82.

DEDICATION

For my father,

Ravindaran Ragavan Pillay

ACKNOWLEDGEMENTS

I would like to acknowledge the supervision provided by Prof. Sivakumar Manickam, Dr. Ng Mei Han and Dr. Davannendran Chandran from the University of Nottingham (Malaysia Campus), Malaysian Palm Oil Board and Sunway University, respectively. I have improved myself as a whole, from the knowledge and experience gained from them.

I would also like to express my gratitude to the Malaysian Palm Oil Board for funding this project. I am thankful for the facilities provided at the Malaysian Palm Oil Board, the University of Nottingham (Malaysia Campus), Sunway University and Universiti Putra Malaysia, for completing this project.

I would like to convey my gratitude for the support and encouragement provided by my mother, Indirawathy Balakrishnan Nair and sister, Hema Raviadaran, in completing my post-graduate study. Thank you for being there at all the crucial times in my life.

I would like to thank someone special who has always been a well-wisher in my life for his consistent guidance, encouragement, support and most of all, as an inspiration himself.

I would also like to take this opportunity to acknowledge the support provided by Filzah, Khairani and Fareez, as well as all those throughout my research.

I thank my Master, Prem Rawat and The Almighty for blessing me to complete this task successfully.

TABLE OF CONTENTS

ABSTRACT i

LIST OF JOURNAL PUBLICATIONS iv

LIST OF BOOK CHAPTER iv

LIST OF CONFERENCES v

DEDICATION vi

ACKNOWLEDGEMENTS vii

TABLE OF CONTENTS viii

LIST OF ABBREVIATIONS xiii

LIST OF FIGURES xv

LIST OF TABLES xviii

CHAPTER 1-INTRODUCTION 1

CHAPTER 2-LITERATURE REVIEW 19

2.1 Stability mechanism of W/O/W multiple emulsion 19

2.1.1 Production of W/O/W multiple emulsion 21

2.1.2 Composition of W/O/W multiple emulsion 23

2.1.2.1 Oil and water 23

2.1.2.2 Emulsifiers 24

2.1.2.3 Thickeners 27

2.1.2.4 Additives 29

2.2 Evaluation of existing studies which produced W/O/W multiple emulsion for oral application 31

2.3 Potential of TRF and CA in W/O/W multiple emulsion for cancer therapy 38

2.4 Summary 42

CHAPTER 3- FORMULATION FOR THE GENERATION OF STABLE PALM OIL-BASED W/O NANOEMULSION USING ULTRASONICATOR AND MICROFLUIDIZER 44

3.1 Background 44

3.2 Materials and methods 45

3.2.1 Materials 45

3.2.2 Selection of hydrophobic emulsifier for forming stable palm oil-based W/O emulsion 46

3.2.2.1 Determination of critical micelle concentration (CMC) 46

3.2.3 Comparison between ultrasonicator and microfluidizer for the formation of W/O nanoemulsion 47

3.2.3.1 Preparation of W/O emulsion 47
3.2.3.2 Ultrasonication for the generation of W/O nanoemulsion 47
3.2.3.3 Microfluidization for the generation of W/O nanoemulsion 48
3.2.3.4 Peroxide value 48
3.2.3.5 Analysis of fatty acid composition 49
3.2.3.6 FTIR analysis 49
3.2.4 Effect of phase volume ratio towards the formation of W/O nanoemulsion 50
3.2.5 Effect of palm MCT oil, lecithin and NaCl towards the formation and stability of W/O nanoemulsion 50
3.2.5.1 Effect of the blending of palm oil and palm MCT oil towards the formation of W/O nanoemulsion 50
3.2.5.2 Effect of blending of lecithin with PGPR on the formation of W/O nanoemulsion 51
3.2.5.3 Effect of addition of NaCl on the formation of W/O nanoemulsion 51
3.2.6 Droplet size and dispersity index 51
3.2.7 Validation tests for the type of nanoemulsion formed (O/W or W/O) 52
3.2.8 Interfacial tension 53
3.2.9 Measurement of sedimentation index 53
3.2.10 Measurement of viscosity 53
3.2.11 Analysis using scanning transmission electron microscopy (STEM) 54
3.3 Results and discussion 54
3.3.1 Selection of hydrophobic emulsifier for the formation of stable W/O emulsion using palm oil 54
3.3.1.1 Determination of CMC of PGPR in palm oil 58
3.3.2 Comparison between ultrasonicator and microfluidizer processing for the formation of W/O nanoemulsion 60
3.3.2.1 Effect of ultrasonicator parameters (amplitude and total irradiation time) on the formation of W/O nanoemulsion 60
3.3.2.2 Effect of microfluidizer parameters (operating pressure and number of cycles) on the formation of W/O nanoemulsion 61
3.3.2.3 Energy consumption 64
3.3.2.4 Oxidation of nanoemulsion 65
3.3.3 Effect of phase volume ratio (oil to water) on the formation of W/O nanoemulsion 68
3.3.4 Effect of palm MCT oil, soybean lecithin and NaCl on the formation and stability of W/O nanoemulsion 69
3.3.4.1 Effect of blending of palm oil and palm MCT oil on the formation of W/O nanoemulsion 69
3.3.4.2 Effect of blending of lecithin with PGPR on the formation of W/O nanoemulsion 72
3.3.4.3 Effect of addition of NaCl on the formed W/O nanoemulsion 75
3.3.5 Morphological analysis of formed W/O nanoemulsion using STEM 78

3.4 Summary 79

CHAPTER 4- FORMULATION FOR THE GENERATION OF STABLE PALM OIL-BASED W/O/W MULTIPLE NANOEMULSION USING ULTRASONICATOR AND MICROFLUIDIZER 80

4.1 Background 80

4.2 Materials and methods 81

4.2.1 Materials 81

4.2.2 Comparison between ultrasonicator and microfluidizer for the formation of W/O/W multiple nanoemulsion 81

4.2.2.1 Preparation of W/O/W multiple nanoemulsion 81

4.2.2.2 Ultrasonication for the generation of W/O/W multiple nanoemulsion 82

4.2.2.3 Microfluidization for the generation of W/O/W multiple nanoemulsion 82

4.2.3 Effect of phase volume ratio (water to W/O), the concentration of hydrophilic emulsifier, thickeners and tonicities on the generation of W/O/W multiple nanoemulsion 83

4.2.4 Analyses 84

4.2.5 Imaging 84

4.3 Results and discussion 85

4.3.1 Comparison between ultrasonicator and microfluidizer processing for the formation of W/O/W multiple nanoemulsion 85

4.3.1.1 Effect of ultrasonicator parameters (amplitude and total irradiation time) on the formation of W/O/W multiple nanoemulsion 85

4.3.1.2 Effect of microfluidizer parameters (operating pressure and number of cycles) on the formation of W/O/W multiple nanoemulsion 88

4.3.1.3 Energy consumption 91

4.3.1.4 Oxidation of W/O/W multiple nanoemulsion 92

4.3.2 Effect of phase volume ratio (water to W/O) on the formation of W/O/W multiple nanoemulsion at 40% amplitude 95

4.3.3 Effect of concentration of hydrophilic emulsifier (Tween 80) on the stability of W/O/W multiple nanoemulsion 96

4.3.4 Effect of thickener on W/O/W multiple nanoemulsion 98

4.3.4.1 Comparison on the stability of W/O/W multiple nanoemulsion stabilized by oil-based thickener (Sucragel), water-based thickener (Xanthan gum) and without thickener 98

4.3.4.2 Effect of concentration of oil-soluble thickener (Sucragel) on the formation of W/O/W multiple nanoemulsion 101

4.3.5 Effect of hypotonicity, isotonicity and hypertonicity on the stability of W/O/W multiple nanoemulsion 104

4.3.6 Morphological analysis of W/O/W multiple nanoemulsion using STEM 108

4.4 Summary 110

CHAPTER 5- EVALUATION OF ANTICANCER EFFECTS OF ENCAPSULATED TRF AND CA IN W/O/W MULTIPLE NANOEMULSION WITH CIS TOWARDS A549 AND HEP G2 CANCER CELL LINES 111
5.1 Background 111
5.2 Materials and methods 112
5.2.1 Materials 112
5.2.2 Preparation of W/O/W multiple nanoemulsion 113
5.2.3 Evaluation of the stability 113
5.2.3.1 Processing stability 113
5.2.3.2 Storage stability 113
5.2.3.3 Stability of TRF/CA 114
5.2.3.4 Stability of the refrigeration cycle 114
5.2.3.5 Comparison of TRF and CA stability in emulsion and solution form 114
5.2.4 Encapsulation efficiency and loading capacity 115
5.2.5 Antioxidant and phenolic activity 116
5.2.5.1 Antioxidant activity 116
5.2.5.2 Total phenolic activity 116
5.2.6 Cell culture 116
5.2.7 Cell viability assay 117
5.2.8 Analysis of cell apoptosis using flow cytometry 117
5.2.9 Intracellular ROS measurements 118
5.2.10 Analysis of cell cycle using flow cytometry 119
5.2.11 Toxicity study 119
5.2.12 Analyses 119
5.3 Results and discussion 121
5.3.1 Evaluation of the stability 121
5.3.1.1 Processing stability 121
5.3.1.2 Storage stability 122
5.3.1.3 Stability of TRF/CA 126
5.3.1.4 Stability of the refrigeration cycle 128
5.3.1.5 Comparison of TRF and CA stability in emulsion and solution form 129
5.3.2 Encapsulation efficiency and loading capacity 131
5.3.3 Antioxidant and phenolic activity 132

5.3.4 Evaluation of cell viability 133
5.3.5 Flow cytometry analysis of cell apoptosis for A549 and HEP G2 cell lines 143
5.3.6 Intracellular ROS generation for A549 and HEP G2 cell lines 146
5.3.7 Flow cytometry analysis of cell cycle for A549 and HEP G2 cell lines 148
5.3.8 Toxicity study 150
5.4 Summary 152
CHAPTER 6-CONCLUSIONS AND RECOMMENDATIONS FOR FURTHER WORK 153
6.1 Conclusions 153
6.2 Recommendations for further work 158
REFERENCES 160

LIST OF ABBREVIATIONS

CA	caffeic acid
CI	combination index
CIS	cisplatin-cis-diamminedichloroplatinum
CMC	critical micelle concentration
DI	dispersity index
DMEM	Dulbecco's Modified Eagle Medium
DMSO	dimethyl sulphoxide
DNA	deoxyribonucleic acid
FBS	fetal bovine serum
FDA	Food and Drug Administration
GRAS	generally recognized as safe
h	hour/hours
H	height
HLB	hydrophilic lipophilic balance
HPLC	high performance liquid chromatography
IC 50	inhibitory concentration
M	Molar (mol/dm^3)
MCT	medium chain triglyceride
MDD	mean droplet diameter
min	minute

MTT	3-(4,5-dimethylthiazol-2-yl)-2,5-diphenyltetrazolium bromide
PBS	phosphate-buffered saline
PGPR	polyglycerol polyricinoleate
PI	propidium iodide
PS	phosphatidylserine
ROS	reactive oxygen species
rpm	revolution per minute
RPMI	Roswell Park Memorial Institute
SI	sedimentation index
TRF	tocotrienol rich fraction
W/O	water-in-oil
W/O/W	water-in-oil-in-water
WPI	whey protein isolate
wt	weight

LIST OF FIGURES

Fig. 1.1 Multiple emulsion droplets 1

Fig. 1.2 Fundamental framework of the research 13

Fig. 1.3 Thesis structure 17

Fig. 2.1 Destabilization in W/O/W multiple emulsion 20

Fig. 3.1 Overview of experimentations in Chapter 3 44

Fig. 3.2 Sedimentation index with time for palm oil-based W/O nanoemulsion using PGPR and Span 80 55

Fig. 3.3 Sedimentation index with time for W/O nanoemulsion using different types of oils 57

Fig. 3.4 Effect of concentration of PGPR on the interfacial tension at the interface of palm oil-water 59

Fig. 3.5 Effect of irradiation time at different amplitude on the generated mean droplet diameter 60

Fig. 3.6 Effect of number of cycles at different operating pressure on the resultant mean droplet diameter of formed W/O nanoemulsion 62

Fig. 3.7 Comparison of FTIR spectra in the formation of palm oil-based W/O nanoemulsion using ultrasonicator and microfluidizer 67

Fig. 3.8 Effect of irradiation time at 40% amplitude for different phase volume ratio on the mean droplet diameter of formed W/O nanoemulsion 68

Fig. 3.9 Mean droplet diameter at different palm oil to palm MCT oil blend ratio 70

Fig. 3.10 Comparison of the mean droplet diameter of formed W/O nanoemulsion with and without lecithin blend at an amplitude of 40% 74

Fig. 3.11 Morphology of W/O nanoemulsion. 78

Fig. 4.1 Overview of experimentations in Chapter 4 80

Fig. 4.2 Effect of irradiation time towards droplet size at different amplitudes 86

Fig. 4.3 Images of W/O/W multiple nanoemulsion with increased amplitude and irradiation time.....87

Fig. 4.4 Illustration of W/O/W multiple nanoemulsion with the movement of water between the internal and external water phases 87

Fig. 4.5 Effect of number of cycles towards droplet size of W/O/W multiple nanoemulsion 89

Fig. 4.6 Images of W/O/W multiple nanoemulsion with increasing operating pressure and number of cycles 90

Fig. 4.7 FTIR spectra of generated W/O/W multiple nanoemulsion using ultrasonicator and microfluidizer.....94

Fig. 4.8 Effect of 40% amplitude and irradiation time towards droplet size 96

Fig. 4.9 Movement of water in (a) hypotonic, (b) isotonic and (c) hypertonic conditions 104

Fig. 4.10 Calibration curve for the conductivity values of NaCl solution 107

Fig. 4.11 STEM image of W/O/W multiple nanoemulsion 109

Fig. 5.1 Overview of experimentations in Chapter 5.1.....111

Fig. 5.2 STEM images of W/O/W multiple nanoemulsion encapsulating TRF and CA at (a) 0 day, (b) 30 days, (c) 60 days, (d) 90 days, (e) 120 days, (f) 150 days, (g) 180 days and (g) after refrigeration cycles 125

Fig. 5.3 Zeta potential of W/O/W multiple nanoemulsion encapsulating TRF and CA for 180 days 126

Fig. 5.4 HPLC calibration for TRF.....127

Fig. 5.5 HPLC calibration for CA.....128

Fig. 5.6 UV-Vis calibration for gallic acid.....133

Fig. 5.7 Cell viability of (a) A549 and (b) HEP G2 with the treatment of TRF, CA and CIS 134

Fig. 5.8 Cell viability of A549 for treatment using (a) TRF and (b) CA in emulsion and solution form 136

Fig. 5.9 Cell viability of HEP G2 for treatment using (a) TRF and (b) CA in emulsion and solution form.....137

Fig. 5.10 Isobologram of (a) TRF:CA, (b) TRF:CIS and (c) CA:CIS for A549.....139

Fig. 5.11 Isobologram of (a) TRF:CA, (b) TRF:CIS and (c) CA:CIS for HEP G2.....140

Fig. 5.12 Analysis of cell viability at 3, 6, 12, 24 and 48 h for TRF-treated, CA-treated, CIS- treated, TRF:CA treated and TRF:CA:CIS treated for (a) A549 and (b) HEP G2..... 142

Fig. 5.13 Cell distribution at live, early apoptosis, late apoptosis and necrosis phase for (a) A549 Annexin analysis and (b) HEP G2 Annexin analysis 145

Fig. 5.14 Intracellular generation of ROS for untreated, control, TRF-treated, CA-treated, CIS-treated, TRF/CA-treated and TRF:CA:CIS treated A549 and HEP G2 ..... .147

Fig. 5.15 Cell distribution at G0/G1, S and G2/M phase for (a) A549 cell cycle analysis and (b) HEP G2 cell cycle analysis..... 149

Fig. 5.16 Cell viability analysis of HEK 293 for untreated, control, TRF-treated, CA-treated, CIS-treated, TRF:CA treated and TRF:CA:CIS treated A549 and HEP G2 dosages. 151

LIST OF TABLES

Table 1.1 Bibliographic studies on the applications of multiple emulsion 3

Table 2.1 Bibliographic studies of W/O/W multiple emulsion formulated using ultrasonicator and microfluidizer .. 33

Table 3.1 Distribution guide recommended by Malvern for Dynamic Light Scattering (DLS) 52

Table 3.2 Validation tests for the type of emulsion formed using different hydrophobic emulsifiers 55

Table 3.3 Validation tests for the type of emulsion formed using different types of oils with PGPR 57

Table 3.4 Optimized parameters for the formation of palm oil-based W/O nanoemulsion using ultrasonicator 61

Table 3.5 Optimized parameters for the formation of palm oil-based W/O nanoemulsion using microfluidizer 63

Table 3.6 Comparison of peroxide values for the formation of palm oil-based W/O nanoemulsion 65

Table 3.7 Comparison of fatty acid composition for the formation of palm oil-based W/O nanoemulsion 66

Table 3.8 Properties of W/O nanoemulsion formed at different phase volume ratio 69

Table 3.9 Viscosity of W/O nanoemulsion formed at different palm oil to palm MCT oil blend ratio 70

Table 3.10 Properties of W/O nanoemulsion formed at different palm oil to palm MCT oil blend ratio 71

Table 3.11 Properties of W/O nanoemulsion stabilized with a blend of lecithin and PGPR 73

Table 3.12 Comparison of mean droplet diameter for the formed W/O nanoemulsion with different stabilizers 76

Table 3.13 Comparison of mean droplet diameter for the formed W/O nanoemulsion with different concentration of NaCl 78

Table 4.1 Optimized parameters for the formation of palm oil-based W/O/W multiple nanoemulsion using ultrasonicator 88

Table 4.2 Optimized parameters for the formation of palm oil-based W/O/W multiple nanoemulsion using microfluidizer 91

Table 4.3 Comparison of peroxide values for the formation of W/O/W multiple nanoemulsion 92

Table 4.4 Comparison of fatty acid composition for the formation of W/O/W multiple nanoemulsion 93

Table 4.5 Comparison of concentration of hydrophilic emulsifier (Tween 80) for the formation of W/O/W multiple nanoemulsion 97

Table 4.6 Comparison of different thickeners for the formation of W/O nanoemulsion and W/O/W multiple nanoemulsion 98

Table 4.7 Viscosity of W/O nanoemulsion and W/O/W multiple nanoemulsion with different thickeners 99

Table 4.8 Comparison of water content in W/O/W multiple nanoemulsion with different thickeners..... 100

Table 4.9 Comparison of the stability of W/O/W multiple nanoemulsion at different concentrations of Sucragel .. 102

Table 4.10 Viscosity of W/O/W multiple nanoemulsion at different concentrations of Sucragel 103

Table 4.11 Conductivity values of W/O/W multiple nanoemulsion at different tonicities..... 105

Table 4.12 Effect of NaCl concentration towards W/O/W multiple nanoemulsion 106

Table 4.13 Effect of different tonicities towards droplet size of W/O/W multiple nanoemulsion 107

Table 4.14 Optimized parameters for the formation of palm oil-based W/O/W multiple nanoemulsion with Sucragel using ultrasonicator..... 108

Table 5.1 Optimized processing parameters of W/O/W multiple nanoemulsion using ultrasonicator and microfluidizer 113

Table 5.2 Concentrations of treatments used for A549 and HEP G2 118

Table 5.3 Comparison of TRF/CA retainment in W/O/W multiple nanoemulsion processed using ultrasonicator and microfluidizer 121

Table 5.4 Storage stability of W/O/W multiple nanoemulsion for 180 days 123

Table 5.5 Stability of W/O/W multiple nanoemulsion with the refrigeration cycle 129

Table 5.6 Comparison of TRF/CA concentration in the W/O/W multiple nanoemulsion and solution form 130

Table 5.7 Encapsulation efficiency and loading capacity of W/O/W multiple nanoemulsion encapsulating TRF and CA 131

Table 5.8 Comparison of antioxidant and phenolic activity of TRF and CA in W/O/W multiple nanoemulsion and solution form 132

Table 5.9 IC 50 values for TRF, CA and CIS for A549 and HEP G2 135

Table 5.10 Comparison of IC 50 values of TRF and CA in W/O/W multiple nanoemulsion and solution form 138

Table 5.11 Combination index for A549 and HEP G2 141

CHAPTER 1: INTRODUCTION

Multiple emulsion, also known as double emulsion or emulsion of the emulsion has emerged as a popular tool due to its capability to enhance drug delivery, especially for pharmaceutical applications [1, 2]. There are two types of multiple emulsion such as oil-in-water-in-oil (O/W/O), as well as water-in-oil-in-water (W/O/W) [3, 4]. W/O/W multiple emulsion is typically more commonly researched due to its advantage for transport and bioavailability in the human body [5]. In a W/O/W multiple emulsion system, the oil globules contain smaller internal water droplets which are dispersed in an external continuous water phase, as shown in Fig. 1. It can be simply explained as an organic phase (hydrophobic) which separates the internal and external aqueous phases [3, 6].

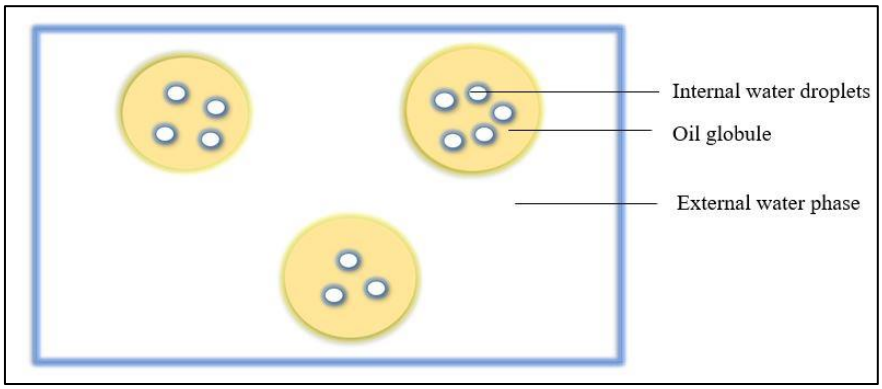


Fig. 1.1 Multiple emulsion droplets.

W/O/W multiple emulsion is typically produced in two stages, commenced with the formation of W/O emulsion, followed with the formation of multiple W/O/W emulsion. Ultrasonication and microfluidization are the two commonly employed methods to produce multiple nanoemulsion. Nanoemulsion refers to the formulation of nano-sized droplets in the emulsion. Ultrasonic cavitation results in the collapse of vapor cavities which leads to the radiation of powerful shock waves throughout the medium, breaking the dispersed phase into smaller droplets [7, 8]. While, microfluidizer uses high pressure to direct the flow stream

through microchannels towards the impingement area, which creates a very high shearing action into forming smaller droplets [8, 9].

Besides pharmaceutical applications, multiple emulsion is also beneficial for use in food and nutraceutical applications due to their ability to encapsulate natural active compounds [10-12]. Encapsulation enables protection for the active compounds from degradation by reducing their exposure to the external environment [13]. The encapsulate is also protected from external stresses such as pH, light, temperature, oxygen and gastrointestinal conditions during the transit. Lamba et al. [14] reported that the encapsulation of active compounds in multiple emulsion prevents the loss of functionality in the food matrix and during the gastrointestinal transit.

Table 1.1 demonstrates the utilization of multiple emulsion for food, nutraceuticals and pharmaceuticals applications. For food applications, multiple emulsion serves to reduce fat content. While, for the nutraceutical and pharmaceutical applications, multiple emulsion acts a drug delivery tool which provides sustained delivery, protects encapsulated active compounds, reduces side effect and improves therapeutic efficiency.

Table 1.1 Bibliographic studies on the applications of multiple emulsion.

Application	Summary	Ref
Food		
Food	Reduced fat cheese obtained by substituting milk-fat by multiple emulsion. Normal cheese had higher fat content of 15.3% than emulsified cheese.	[15]
	Reduced fat in frankfurter by replacing pork backfat with multiple emulsion. Significant fat reduction by >60% achieved for healthier frankfurters.	[16]
Meat	Meat systems formulated with hydroxytyrosol multiple emulsion displayed oxidative stability for successful development of healthier meat products. Multiple emulsion resulted in reduced lipid, increased protein content and modified fatty acid composition.	[17]
	Multiple emulsion had promising impacts on modifying the fatty acid composition and developing both oxidatively stable beef emulsion system.	[18]
	Pork backfat was replaced by multiple emulsion to improve the fat content. Healthy meat products with water and fat binding properties, texture and colour were obtained.	[19]
Lactobacillus acidophilus	Protection of Lactobacillus acidophilus (bacteria) from gastric juice for utilizing the advantages of the probiotics. The relative viability of the bacteria included in the multiple emulsion was 49% at 2 h in the model gastric juice. In contrast, the viability of the bacteria directly dispersed in the juice declined to 1.3% at 0.67 h.	[20]
Lactobacillus plantarum	Oaxaca cheese processing conditions are harsh, and the probiotic cells, Lactobacillus plantarum could be protected in multiple emulsion.	[21]
Lactobacillus rhamnosus	The viability of Lactobacillus rhamnosus in the multiple emulsion was higher when exposed to low pH and bile salt conditions. Multiple emulsion protected Lactobacillus rhamnosus against simulated gastrointestinal tract conditions.	[22]

Table 1.1 Bibliographic studies on the applications of multiple emulsion. (Continued).

Application	Summary	Ref
Pharmaceuticals		
Urease	Multiple emulsion was used for enzyme immobilization.	[23]
Chlorpheniramine maleate	Multiple emulsion provided gradual and consistent drug release.	[24]
Indomethacin	Multiple emulsion showed sustained drug release in both *in vitro* and *in vivo* studies.	[25]
Nattokinase	Multiple emulsion provided sustained drug release. Blood clotting time in mouse was prolonged and the carrageenan-induced tail thrombosis was improved.	[26]
Chloroquine	Multiple emulsion enabled taste masking.	[27]
Diclofenac sodium	Improved drug delivery and achieved targetted delivery as multiple emulsion retarded the reticuloendothelial system uptake mainly to liver and brain. Targetted delivery to non-reticuloendothelial system tissues such as lungs and inflammatory tissue.	[28]
Vaccine adjuvant of surface antigen hemagglutinin.	Multiple emulsion formulation was more effective in eliciting an immune response against influenza virus in rats than the conventional vaccine due to their adjuvant properties. A single administration of multiple emulsion proved to stimulate more effective immune response in rats than the conventional vaccine.	[29, 30]
Boron	The delivery of boron multiple emulsion in tumour, normal liver tissue and blood was superior than conventional emulsion for hepatocellular carcinoma treatment.	[31]
5-fluorouracil	Multiple emulsion showed better radioactivity in the regional lymph nodes after intratesticular injection as compared to the conventional emulsion with the utilization of smaller dose.	[32]

Table 1.1 Bibliographic studies on the applications of multiple emulsion. (Continued).

Application	Summary	Ref
Pharmaceuticals		
Epirubicin	Clinical studies showed enhanced bioavailability and improved survival rate using multiple emulsion formulation. Targetted delivery to hepatoma carcinoma cancer cells with reduced side effects.	[33, 34]
Aqueous oxygen	Multiple emulsion as red blood cell substitute. Haemoglobin in multiple emulsion had an oxygen content of 14 ml/100 ml emulsion.	[35]
Insulin	Multiple emulsion protected against enzymatic degradation caused by pepsin, trypsin and a-chymotrypsin.	[36]
	Insulin encapsulated in multiple emulsion promoted resident time of emulsion at the intestinal mucosal membrane.	[37]
	Multiple emulsion for oral administration of insulin showed hypoglycaemic activity for an extended period after administration to rats.	[38]
Tacrolimus	Targetted delivery by multiple emulsion increased delivery to the liver and spleen. Decreased delivery to the brain and kidney.	[39]
Aspirin	Multiple emulsion provided sustained delivery and had pronounced anti-inflammatory and analgesic effects in rats.	[40]
Doxorubicin hydrochloride	Multiple emulsion provided sustained delivery and higher concentration in tissue distribution in Sprague Dawley rats. Reduced side effects due to the reduced drug distribution in kidney and heart cells.	[41]
Etoposide	Multiple emulsion provided sustained release.	[42]
6-mercaptopurine	Multiple emulsion with sustained-release in blood, with reduced dosage.	[43]

Table 1.1 Bibliographic studies on the applications of multiple emulsion. (Continued).

Application	Summary	Ref
Pharmaceuticals		
Methotrexate and Cytarabine (cytosine arabinoside)	Multiple emulsion with sustained-release and enhanced therapeutic activity against the mouse lymphoma and rat Walker tumour with reduced dosage. Multiple emulsion in a single dose demonstrated chemotherapeutic effect similar to that of five daily doses of cytosine arabinoside and methotrexate in aqueous solution for the treatment of acute lymphocytic and granulocytic leukaemia.	[44]
Pentazocine	Multiple emulsion showed good tolerance to various pH range of the gastrointestinal tract during *in vitro* studies. *In vivo* studies carried out in mice showed sustained drug levels in multiple tissues after oral administration.	[45]
Vancomycin	Multiple emulsion administered intravenously to rats showed sustained drug concentration in plasma as compared to the Vancomycin solution.	[46]
Nutraceuticals		
Betalain	Multiple emulsion showed sustained release and protection of compound during in vitro digestion.	[47]
Anthocyanins	Multiple emulsion provided sustained release and improved stability under gastrointestinal conditions.	[48]
Vitamin A	The stability of vitamin A multiple emulsion was high, with a concentration of 56.9% at 50 °C after 4 weeks.	[49]
Vitamin B12	Encapsulation of vitamin B12 in multiple emulsion retained the vitamin loss by >90% during *in vitro* gastric digestion.	[50]
Apigenin	The *in vivo* pharmacokinetics revealed that apigenin-loaded multiple emulsion had a high oral bioavailability through the digestive tract and potential as a targeted delivery system.	[51]
Rifampicin	The plasma level implied that the multiple emulsion provided sustained drug release.	[52]

In addition to the potential of multiple emulsion as demonstrated in Table 1.1, multiple emulsion can also encapsulate both hydrophobic and hydrophilic active compounds in a single drug delivery tool which could be beneficial for cancer therapy. This feature is however yet to be exploited. With the rise in cancer cases and limited success rate in the current treatments, it is necessary to explore the potential of natural active compounds encapsulated in multiple emulsion for cancer therapy.

Cancer was determined as the second leading cause of fatality in 2018 globally, with a total estimate of 9.6 million deaths. Approximately 70% of the deaths due to cancer occurred in low-income and middle-income countries. The total annual economic cost of cancer was estimated at US$ 1.16 trillion in 2010 [53]. Considering the growing burden of increasing cancer patients, deaths and cost, it is imperative to deduce an effective and affordable treatment, patient compliant, using natural compounds and with reduced side effects.

Lung cancer is among the most common cancers worldwide, contributing up to 12.3% of the total number of newly diagnosed cancer cases in 2018 [54]. Lung cancer is the leading cause of cancer death among both men and women [55]. There are two main types of lung cancer such as non-small cell lung cancers (NSCLC) and small cell lung cancer (SCLC) [56]. The types of cancer are named based on the kinds of cells found in the cancer and how the cells look under a microscope [57]. The subtypes of NSCLC are adenocarcinoma, squamous cell carcinoma, and large cell carcinoma. About 85% of lung cancers are NSCLC. At the time of diagnosis, approximately 30 to 40% of NSCLC patients had developed metastatic disease [58-60]. Metastasis occurs when the lung cancer cells travelled through the blood or lymph system and formed new tumours in other parts of the body. Liver metastasis is found to be with the worst prognostic factor [61].

Currently, the standard treatment for lung cancer and liver metastases is surgery, followed by chemotherapy or a combination of chemotherapy and radiation therapy to prevent cancer from recurring. These treatments are given based on the stage of cancer after being diagnosed. Targeted therapy and immunotherapy are also provided. Notably, chemotherapy is the primary treatment for cancer.

Cisplatin-cis-diamminedichloroplatinum (CIS) is the most commonly used chemotherapeutic agent [62]. CIS is the first drug with platinum compound used for cancer treatment which obtained approval from the United States Food and Drug Administration (FDA) in 1978 [63]. CIS is also the critical chemotherapy drug used for NSCLC and liver metastases [62, 64]. However, chemotherapy for NSCLC is unsatisfactory as the current prognosis remains poor, with only 10 to 15% survival for 5 years. The clinical efficacy of CIS is limited due to tumour resistance and severe side effects [63, 65]. The side effects of CIS include nephrotoxicity, ototoxicity, neurotoxicity, hepatotoxicity, increased risk of infection, nausea and vomiting [66, 67].

To address this limitation, a combined therapy which uses a commercially potent chemotherapeutic compound such as CIS coupled with natural chemopreventive compounds is observed as a feasible approach. This is chiefly due to the potential of improving the therapeutic values synergistically, while lowering the side effects by reducing the dosage of chemotherapy drug. Natural chemopreventive compounds that are readily available, affordable, as well as with the benefit of inhibiting or reversing tumour growth are required. In line with this, there are various natural phytochemicals with chemopreventive properties that may modulate signalling pathways involved in cell proliferation and apoptosis in transformed cells, enhance the host immune system and sensitize malignant cells to cytotoxic agents [68]. Tocotrienol and caffeic acid (CA) are among the natural active compounds which have these required properties.

Tocotrienol is a vitamin E with three double bonds at positions 3', 7', and 11' in the alkyl side chain. Tocotrienol rich fraction (TRF) has a composition of α-tocopherol, α-tocomonoenol, α-tocotrienol, β-tocotrienol, γ-tocotrienol and δ-tocotrienol [69-71]. It is reported to possess antioxidant [72, 73], anti-inflammatory [74, 75], anti-proliferative [76, 77] and anti-cancer [78, 79] properties. While, CA (3,4-dihydroxycinnamic acid) is a phenolic compound which possesses an aromatic ring bearing two hydroxyl groups. CA is reported to have anti-oxidant [80, 81], anti-cancer [82], anti-tumour [83] and anti-proliferative [84, 85] properties. Both compounds have the potential to be used for cancer treatment. The combination of phytonutrients could synergistically enhance the therapeutic effect as compared to a single phytonutrient [86]. The enhanced therapeutic effect of combined phytonutrients could also reduce the required concentration of chemotherapy drug resulting in lower toxicity level.

Despite the beneficial properties of TRF and CA, the combined effects of these two compounds for NSCLC with liver metastases are typically yet to be reported till present. Hence, to investigate the combined effects for these two compounds, a suitable drug delivery carrier is firstly required. Essentially, TRF is hydrophobic, while CA is hydrophilic. W/O/W multiple emulsion is observed as the best candidate for encapsulating both hydrophobic and hydrophilic compounds in a single carrier for drug delivery [10]. This is significant as both the internal water and oil compartments are available for encapsulating hydrophilic and hydrophobic compounds, respectively. Successful formulation of these two compounds could produce synergistic effect.

Nevertheless, before encapsulating the active compounds, stable W/O/W multiple emulsion needs to be formulated. Thermodynamic instability which could culminate in phase separation [87-90] is among the major challenge faced for producing stable W/O/W multiple emulsion. This is among the reason why multiple emulsion is yet to reach the commercialization stage. For W/O/W

multiple emulsion, the loss of internal water droplets from the oil globules could occur through coalescence in the droplets and due to the difference in the osmotic pressure [91]. Among the possibilities of coalescence in the droplets are between the internal water droplets and oil globules.

The majority of the existing studies focused on enhancing the stability of multiple emulsion by balancing the osmotic pressure difference through thickeners [92, 93] and additives [94, 95]. However, thickeners and additives are secondary approaches to stabilize W/O/W multiple emulsion since they aim to control the movement between the internal and external water droplets. Instead, priority should be given to firstly formulate stable W/O emulsion before forming W/O/W multiple emulsion. The formulation of a stable W/O emulsion is dependent on the interaction between the oil and emulsifier to build a rigid oil-water interface. This could be achieved through deep anchoring of the emulsifier in the oil.

Upon successful formulation of stable W/O emulsion by ensuring rigid oil-water interface, next, diffusion or osmotic transfer which could result in loss of internal water droplets or rupture of oil globules need to be prevented to produce stable W/O/W multiple emulsion [91]. Usage of thickeners and tonicity stabilization is observed essential to prevent diffusion or osmotic transfer.

Majority of the existing studies investigated the usage of thickeners in the internal water phase of W/O/W multiple emulsion emphasized on the sustained release of the active compound. Thickeners that were commonly used for the internal water phase were proteins such as sodium caseinate [96, 97], whey protein [92, 98], gelatin [99, 100] and polysaccharides such as starch [101, 102] and xanthan gum [103, 104]. Notably, limited studies investigated the usage of thickeners for evaluating the stability of W/O/W multiple emulsion. Furthermore, the utilization of thickeners in the oil phase and its effect on the stability of W/O/W multiple emulsion is yet to be reported until

now. Furthermore, not readily available oil-soluble thickeners and limited choices for oral-based formulations present another challenge.

Sucragel AOF is a 100% natural oil-soluble thickener biocomposed of Prunus Amygdalus Dulcis (sweet almond) oil, glycerine, sucrose laurate and Citrus Aurantium Dulcis (orange) fruit water. The stabilizing effect of Sucragel as an oil phase thickener in palm oil-based W/O/W multiple emulsion is yet to be reported. Schmidt et al. [105] investigated the stabilizing effect of water-based thickener in the water globule of O/W/O multiple emulsion. The authors reported that there was increased stability against coalescence of internal oil droplets due to the reduced movement of droplets. Hence, it is essential to evaluate the effect of thickener in the oil globule for the stability in W/O/W multiple emulsion.

With respect to tonicity stabilization, majority of the existing studies altered the additive concentrations in the internal and external water phases of W/O/W multiple emulsion to evaluate the release rate and transport mechanism. Balcaen et al. [106] formed W/O/W multiple emulsion encapsulating 0.2 M glucose in both internal and external water phase, aimed to evaluate the release of glucose in hypotonic, hypertonic and isotonic solutions. The authors reported that hypotonic and isotonic solutions released the encapsulated glucose unlike hypertonic solution. Zhu et al. [107] formed W/O/W multiple emulsion with 2.0 M magnesium chloride in the internal water phase aimed to evaluate the slow release of magnesium to ensure its applicability for good quality tofu. The authors reported that both hypotonic and isotonic released the encapsulated compounds unlike hypertonic condition influenced by the utilized emulsifiers.

Kawashima et al. [108] formed W/O/W multiple emulsion encapsulating glucose/NaCl using Span 80 and Tween 20 as the hydrophobic and hydrophilic emulsifiers, respectively. The authors investigated the transfer of additives between the internal and external water phases of

W/O/W multiple emulsion by simulating isotonic, hypertonic and hypotonic conditions. Kawashima et al. [108] concluded that high concentration of additives in the internal water phase can improve the encapsulation efficiency of single drug in the internal water phase of W/O/W multiple emulsion. The studies by Balcaen et al. [106] and Zhu et al. [107] focused on transport mechanism for the slow release of encapsulated compounds while, the study by Kawashima et al. [108] focused on improving the encapsulation efficiency of a single drug. At present, limited studies have reported on the effect of tonicity on the stability of W/O/W multiple emulsion. Hence, there is a need to evaluate the effect of tonicity on the stable formulation of W/O/W multiple emulsion.

The present study aims to formulate and generate W/O/W multiple nanoemulsion encapsulating natural TRF and CA, followed by the evaluation of its anticancer and toxicity effects towards cancer and normal cell lines, respectively as displayed in Fig. 1.2.

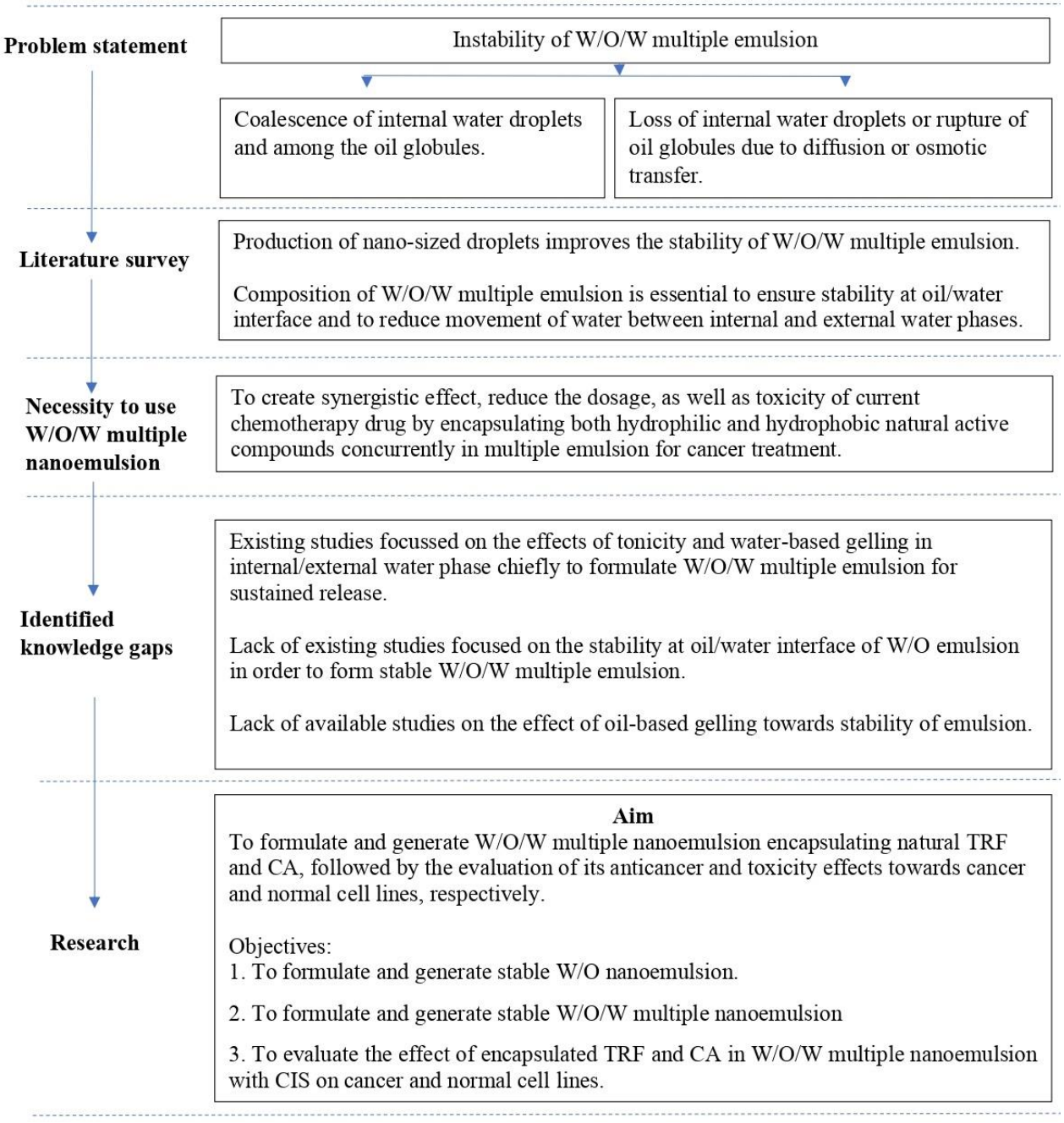


Fig. 1.2 Fundamental framework of the research.

The specific objectives of this investigation are:

- Formulation and generation of stable W/O nanoemulsion using ultrasonicator and microfluidizer emphasizing on the interaction between the oil and emulsifier to form rigid oil-water interface.
- Formulation and generation of stable W/O/W multiple nanoemulsion emphasizing on the energy consumption and oxidation of palm oil in the emulsion processed using ultrasonicator and microfluidizer, as well as the effect of thickener and tonicity towards the stability of multiple nanoemulsion.
- Evaluation of the anticancer and toxicity effect of the encapsulated TRF and CA in W/O/W multiple nanoemulsion with CIS, towards cancer (A549 and HEP G2) and normal (HEK 293) cell lines, respectively.

To achieve the objectives in a considerable depth within the given 36 months of PhD, the scope was defined and executed according to the schedule. Palm-based oil was used as the feedstock of interest considering the availability of palm oil in Malaysia. Palm oil was chosen since it is cheap, popular and the second most traded oil in the world after soy. Also, palm oil's health benefits, especially anti-cancer properties, have been reported by Sambanthamurthi et al. [109] and Olafisoye et al. [110]. Generation of nanoemulsion using ultrasonicator and microfluidizer were chosen based on the capability of these high energy-intensive equipments in producing nanoemulsion. Ultrasonicator and microfluidizer are high energy processing methods that are easy to control, reproducible and result in small droplet size. Established international standard methods were utilized for the analyses based on the requirement and suitability of the testing facilities.

The experimentation commenced with the determination of a suitable hydrophobic emulsifier for formulating stable W/O emulsion using palm oil followed with the comparison of W/O nanoemulsion generation using ultrasonicator and microfluidizer. Then, the effects of phase volume ratio of oil to water, medium-chain triglyceride (MCT) oil, soybean lecithin and sodium chloride (NaCl) addition towards the stability of W/O nanoemulsion were evaluated.

This was then followed with the evaluation of the generated palm oil-based W/O/W multiple nanoemulsion using ultrasonicator and microfluidizer focusing on the energy consumption and oxidation of palm oil in the emulsion. Subsequently, the effects of thickeners such as Sucragel (oil-soluble thickener) for the oil phase and Xanthan gum (water-soluble thickener) for internal water phase, as well as the tonicity effects such as hypotonic, isotonic and hypertonic towards the stability of W/O/W multiple nanoemulsion were evaluated.

Finally, the effectiveness of TRF and CA encapsulated stable W/O/W multiple nanoemulsion with CIS towards treating human lung and liver cancer cells, as well as toxicity effect on human kidney cells were evaluated. The cell viability, quantification of apoptosis phases, ROS generation and cell cycle arrest which led to the cell death in A549 and HEP G2 cancer cell lines were investigated.

The primary significance of this study is the successful formulation of stable W/O/W multiple nanoemulsion encapsulating TRF and CA, as well as its effectiveness towards treating cancer cell lines. Through the performed experimentations, W/O/W multiple nanoemulsion is proven to be a suitable drug delivery tool to encapsulate TRF and CA for the intended treatment. This outcome recommends that the encapsulated TRF and CA in W/O/W multiple nanoemulsion with CIS could progress to the next stage of animal study, followed by the clinical trial and then commercialization.

The specific original contributions to knowledge from this study are:

- Successful generation of stable palm oil-based W/O nanoemulsion using palm oil, palm MCT oil, polyglycerol polyricinoleate (PGPR) and water. Through this work, the suitability of PGPR as an emulsifier to form strong interaction at the oil-water interface was elucidated. The addition of NaCl reduced the mean droplet diameter (MDD) and improved stability through electrostatic repulsions attributed to the dissociation of Na^+ and Cl^- ions.
- Successful generation of stable isotonic palm oil-based W/O/W multiple nanoemulsion with Sucragel. This is the first work that successfully utilized Sucragel (oil-based thickener) in imparting enhanced stability for W/O/W multiple nanoemulsion.
- Encapsulated TRF and CA in W/O/W multiple nanoemulsion with CIS synergistically led to death in cancer cell (A549 and HEP G2) lines.
- The combined therapy of TRF and CA in W/O/W multiple nanoemulsion with CIS had lower toxicity effect on normal kidney cell by having cell viability of ~95% as compared to ~33% of cell viability when treated with CIS only.

Aligned with the aim and scope of this study, the structure of this thesis is displayed in Fig. 1.3.

Chapter 1 Presents the background of the performed work and highlights the novelty/contribution of this study

↓

Chapter 2 Presents the conducted literature survey in three phases:

1. First phase: The influence of production and composition towards the stability of W/O/W multiple emulsion.
2. Second phase: The existing studies that produced W/O/W multiple emulsion using ultrasonicator and microfluidizer for oral application.
3. Third phase: The potential of TRF and CA as encapsulates in W/O/W multiple nanoemulsion for cancer therapy.

↓

Chapter 3 Presents the formulation of palm oil-based W/O nanoemulsion in four stages of work:

1. First stage: Suitable emulsifier was determined.
2. Second stage: A comparison was made between the generation of W/O nanoemulsion using ultrasonicator and microfluidizer.
3. Third stage: The effects of the phase volume ratio of oil to water (90:10 and 80:20) on the stability of nanoemulsion were evaluated.
4. Fourth stage: The impacts with MCT oil, soybean lecithin and NaCl towards the formulation and stability of W/O nanoemulsion were investigated.

↓

Chapter 4 Presents the formulation of palm oil-based W/O/W multiple nanoemulsion in two stages:

1. First stage: The production of palm oil-based W/O/W multiple nanoemulsion using ultrasonicator and microfluidizer was investigated.
2. Second stage: Evaluation on the effect of thickeners and tonicity towards the stability of W/O/W multiple emulsion.

↓

Chapter 5 Presents the experimentations carried out in two stages:

1. First stage: The encapsulation of TRF and CA in W/O/W multiple nanoemulsion was investigated by evaluating the stability, encapsulation efficiency and loading capacity.
2. Second stage: The effects of TRF and CA encapsulated in W/O/W multiple nanoemulsion with CIS towards cancer and normal cell lines were investigated.



Chapter 6 Presents the conclusions drawn from this study followed with the recommendations for further work

Fig. 1.3 Thesis structure.

CHAPTER 2: LITERATURE REVIEW

The literature review emphasizes three parts. Firstly, the influences of production and composition towards the stability of W/O/W multiple emulsion were evaluated. Secondly, the existing studies that produced W/O/W multiple emulsion for the oral application using ultrasonicator and microfluidizer were assessed. Thirdly, the potential of natural compounds such as TRF and CA as encapsulates in W/O/W multiple nanoemulsion for cancer therapy was examined. The direction of this study was then derived based on the identified knowledge gaps from the performed literature survey.

2.1 Stability mechanism of W/O/W multiple emulsion

W/O/W multiple emulsion is composed of internal water droplets which are dispersed in oil globules. These oil globules are dispersed in an external water phase [111]. Multiple emulsion can be considered as multiple nanoemulsion when its size ranges between 20 nm and 500 nm [112]. The long-term stability of nanoemulsion is associated with its nanosized droplets that enable the nanoemulsion to remain dispersed with no apparent flocculation or coalescence.

However, nanoemulsion is thermodynamically unstable as with the given sufficient time, phase separation occurs [87, 88]. Thermodynamic instability could lead to breakdown through various physicochemical mechanisms such as flocculation, coalescence, Ostwald ripening and creaming [89, 112]. Flocculation is a process where two or more droplets come together to form aggregation in the emulsion, although at the same time, these droplets can retain their integrity [113]. Flocculation occurs when the kinetic energy released during droplet collision brings the droplets over the repulsive force barrier into a region where attractive forces cause the droplets to attach [114]. Coalescence is a process where two or more droplets merge to form a single large droplet [113]. Coalescence can only occur when the droplets are close to

each other and the interfacial membranes are disrupted. Ostwald ripening is a process whereby large droplets grow at the expense of smaller ones [115]. This phenomenon occurs since the Laplace pressure inside the smaller droplets is higher than the pressure inside larger droplets, which drives the smaller droplets to merge with larger droplets [116]. Gupta et al. [112] indicated that Ostwald ripening is the dominant destabilization mechanism in the emulsion. Creaming refers to phase separation into oil phase, unseparated emulsion and water phase. Jiao and Burgess [117] stated that flocculation may or may not cause creaming, and thus, it is not considered as a mark of instability for emulsions. Coalescence and Ostwald ripening represent potential steps towards creaming.

Since 2015, there has been limited progress on W/O/W multiple emulsion for oral pharmaceutical applications. One primary reason that prevents the advancement of W/O/W multiple emulsion is its stability, mainly described by the unwanted loss of the internal water droplets or rupture of oil globules [118]. Firstly, this could occur due to coalescence in the internal water droplets and between the oil globules. Secondly, diffusion or osmotic transfer could also result in the loss of internal water droplets or rupture of the oil globules [91]. These phenomena are described in Fig. 2.1.

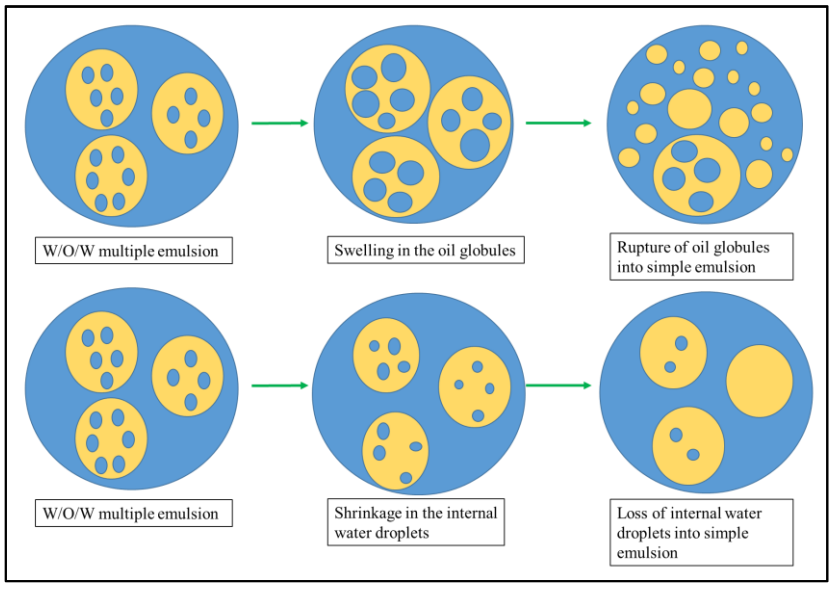


Fig. 2.1 Destabilization in W/O/W multiple emulsion.

To evaluate stability, the majority of the existing studies have utilized methods such as measuring the change in droplet size [37, 119, 120] and the encapsulation efficiency [121-123] in the W/O/W multiple emulsion. In sections 2.1.1 and 2.1.2, the effects of production and composition of W/O/W multiple emulsion towards the stability are elaborated, respectively.

2.1.1 Production of W/O/W multiple emulsion

The production of W/O/W multiple emulsion involves two stages. W/O emulsion is firstly formed followed by W/O/W multiple emulsion. To ensure stability, the formation of the smallest possible droplet size of W/O/W multiple emulsion is required. For this, the method for producing multiple emulsion is critical. Small droplet size ensures stability against gravitational separation as it ensures domination of Brownian motion against gravitational forces [87]. Thus, it could provide greater stability to droplet aggregation as compared to the conventional emulsion [124]. This phenomenon could be described using Stokes' law from Eq. 2.1 where, the velocity of a droplet moving upward is influenced by gravity (g), droplet radius (R), the density difference between the continuous and dispersed phases ($\Delta\rho$), and the viscosity of the continuous phase (μ). An increase in the droplet radius directly increases the velocity of the droplet movement. In the case of the higher density of dispersed phase than the continuous phase, the droplet moves upwards and vice versa.

$$V_{stokes} = \frac{2}{9}\frac{(\Delta\rho)}{\mu} gR^2 \qquad \text{Eq. 2.1} \qquad [115]$$

Concerning the formation of nanoemulsion, it is a non-spontaneous process, and a large amount of emulsifier or energy is required to break a droplet. Notably, for nanoemulsion used for pharmaceutical/nutraceutical application, only a permitted amount of emulsifier could be utilized due to human oral consumption. Hence, high energy emulsification devices such as

microfluidizer and ultrasonicator are commonly employed due to its capability to produce stable nanoemulsion with a reduced amount of emulsifier.

The microfluidic technology was patented in 1985 [125] and among the firstly reported work using this technology was published in 1987 [126]. It consists of an air-driven intensifier pump and a fixed-geometry interaction chamber. The intensifier pump provides constant high pressure to force the coarse emulsion through the interaction chamber [127]. The pumped coarse emulsion is then divided into two streams that enter two well-defined microchannels where the emulsion is accelerated to a high velocity as they pass through the chamber. Here, the two jets of emulsion collide with each other [8]. The streams are forced through the microchannels toward an impingement area, creating a tremendous shearing action for the production of nanoemulsion [128-130]. The interaction chamber efficiently converts the high pressure into the combination of high shear and impact forces, as well as hydrodynamic cavitation [131].

Concerning ultrasonicator, ultrasound is an acoustic wave with a frequency beyond the threshold human can hear >16 kHz [132]. Ultrasound immersion horn consists of a power generator, a piezoelectric crystal sealed converter and a probe. The piezoelectric quartz crystal in response to alternating current can expand and contract forming mechanical vibration and cavitation, when the sonicator probe comes into contact with the medium (emulsion) [129]. Cavitation is the formation of vapor bubbles when the local pressure is reduced to that of the vapour in the medium at ambient temperature because of local velocity changes [133]. As these bubbles grow rapidly and collapse, pressurized shock waves are sent to the medium [134]. This leads to the droplet break-up within the vicinity of the collapsing bubble. The accumulative effect of these miniature implosion results in the droplet break-up, leading to the production of nanoemulsion.

Microfluidization is influenced by the operating pressure and number of cycles, while ultrasonication is influenced by the sonication amplitude and irradiation time. Microfluidization is unfavourable under higher pressure and longer emulsification time (number of cycles), while ultrasonication is unfavourable at higher amplitude and longer irradiation time. Both microfluidization and ultrasonication form nanoemulsion through disruptive forces. The final droplets size from these two methods is usually dictated by two opposite phenomena which are the droplet disruption and droplet coalescence [124, 135]. "Over-processing" is a phenomenon which occurs due to the higher coalescence rate of droplets than disruption rate of droplets, culminating in the increase in droplets size [128, 136]. Over-processing is related to the slow absorption rate of the emulsifier, the short residence time in the emulsification zone, high-rate of coalescence and also applying intense energy for forming emulsion [136-138]. As such, optimization of the process parameters along with the selection of emulsifier and oil is crucial. Through this, over-processing can be prevented and stable nanoemulsion could be produced with optimized process conditions and adequate concentration of emulsifier [136].

2.1.2 Composition of W/O/W multiple emulsion

The composition of emulsion formulation is fundamental to ensure its stability. The emulsion is formed using oil, water, emulsifiers, thickeners and additives.

2.1.2.1 Oil and water

Oil and water phases are essential components in the formulation due to their ability to solubilize lipophilic and hydrophilic active compounds, respectively. Usually, the employed oil phase for oral-based emulsion formulation is of vegetable origin (soybean, sesame, olive, peanut, safflower, palm, sunflower, corn, castor, canola and rapeseed oil), mineral oil (liquid paraffin oil) and speciality oil (Moringa oleifera oil, orange oil and grape oil). Mineral oil is

slowly metabolized as compared to the vegetable oil [139]. MCT can also be used since it is easily digested than long-chain triglyceride of vegetable oil [140]. Also, the gastrointestinal tract absorption depends upon the chain length of the fatty acid [141].

The viscosity of the oil phase is vital for stabilization since it controls the transfer rates of solutes across the oil membrane [142]. Omotosho et al. [143] reported that oil phase with high water solubility could result in the tendency of water movement from the internal phase to the external phase in a multiple emulsion causing the shrinkage of droplets or vice versa. The chemical structure of the oil such as the chain length of fatty acids and the number of unsaturated bonds is essential for the stability of the emulsion [144]. In short, the properties of oil phase such as its viscosity, water-solubility, density, polarity, refractive index and interfacial tension can affect the formation and stability in emulsion [145].

Phase volume ratio is the ratio between the dispersed and continuous phase in an emulsion. In a W/O/W multiple emulsion, the primary W/O emulsion is the dispersed phase, and the external water phase is the continuous phase. This ratio can also influence the stability of emulsion. Lovelyn and Attama [146] highlighted that high phase volume ratios might result in coalescence during emulsification. Cameron [147] found that the droplet size of the emulsion increases significantly with an increase in the volume ratio.

2.1.2.2 Emulsifiers

Emulsifier is a surface-active agent that promotes the formation and stabilization of an emulsion. Emulsifiers are used in the formulation of emulsion to bind to the oil-water interface to prevent coalescence, which can culminate in phase separation [124]. Emulsifiers work by improving the stability of the emulsion by overcoming the tension at the oil-water interface. With regards to this, nanoemulsion has a large surface area with abundant free interfacial

energy. This free interfacial energy is associated with the interfacial tension, which can be mathematically represented in Eq. 2.2, where G is the interfacial free energy, γ is the interfacial tension, V is the volume and R is the radius. The equation shows that lowering the interfacial tension leads to a reduction of the free interfacial energy hence, providing stability for the emulsion.

$$\Delta G = \gamma \frac{3V}{R} \qquad \text{Eq. 2.2} \qquad [148]$$

Also, the Gibbs-Marangoni effect states that, during stretching at the oil-water interface, there would be an increase in surface tension [149, 150]. The surface tension gradient would cause the emulsifier to flow towards the stretched region to provide a 'healing' force and resists against further thinning. In brief, emulsifiers adsorb at the oil-water interface forming a film to prevent the coalescence of droplets by reducing the interfacial tension. Long term stability is dependent on the strength of this film [151]. Jiao and Burgess [151] also stated that for the film to be an effective barrier, it should remain intact at all the points between two droplets. It should also have surface elasticity to reform rapidly once broken.

Besides, emulsifiers could also prevent flocculation by providing repulsive forces to overcome the van der Waals attraction between the droplets when they are in close proximity with each other. Emulsifiers could create this repulsive force by electrostatic and steric stabilization. Electrostatic stabilization is the formation of electrical double layers where repulsive Coulomb forces act between the negatively charged colloidal droplets [152]. While, steric stabilization is achieved by the emulsifiers adsorbing at the interface and forming a layer of coating to separate the droplets.

Concerning the selection of emulsifiers for food-based/pharmaceutical/nutraceutical emulsion for human oral consumption, the use of emulsifiers at a permissible quantity that is 'generally recognized as safe' (GRAS) by FDA is required. The type of emulsifiers that could

be used are such as non-ionic (monomeric/polymeric), zwitterionic and ionic (cationic/anionic). The non-ionic emulsifiers are usually preferred for use in oral formulations [153]. Florence and Whitehill [4] stated that non-ionic emulsifiers are preferred for pharmaceutical use not only because of their lower toxicity but also due to their less likely interactions with ionic compounds. Matsumoto et al. [154] reported that non-ionic emulsifiers produced stable emulsion.

Due to the complex nature of multiple emulsion, the utilization of emulsifier must be carefully considered to ensure long-term stability. Multiple emulsion requires at least two emulsifiers to be present in the system using the hydrophilic-lipophilic balance (HLB) values. HLB numbers range from ~1-30 where an emulsifier with a low HLB is considered oil soluble (hydrophobic) whereas HLB of 15 and beyond is considered water soluble (hydrophilic) [155]. Schmidts et al. [156], suggested that hydrophobic emulsifier with a low HLB value of 3-8 can be used to stabilize the W/O emulsion. Whereas, a hydrophilic emulsifier with a high HLB value of 9-12 can be used to stabilize the W/O/W multiple emulsion.

Existing studies have utilized several types of non-ionic emulsifiers to formulate W/O/W multiple emulsion. In a study by Kim et al. [157], the authors encapsulated cytarabine in paraffin oil-based W/O/W multiple emulsion using emulsifiers of the Tween and Span types. The authors reported that the combination of Tween 20/80 and Span 20/80 as a hydrophilic and hydrophobic emulsion system, respectively, produced stable multiple emulsion exhibiting a controlled release. Wang et al. [158] encapsulated resveratrol in Miglyol 812 based-W/O/W multiple emulsion using PGPR as the hydrophobic emulsifier and Tween 80 as the hydrophilic emulsifier. Ye et al. [159] in a study successfully encapsulated tea polyphenol in the W/O/W multiple emulsion using grape oil with Tween 80 as the hydrophilic emulsifier and Span 80 as the hydrophobic emulsifier. Mishra et al. [160] successfully encapsulated pentazocine in W/O/W multiple emulsion prepared with liquid paraffin containing Span 80 as the hydrophobic

emulsifier and Tween 40 as the hydrophilic emulsifier. Nakhare et al. [161] encapsulated rifampicin in a liquid paraffin-based W/O/W multiple emulsion using Span 80 as the hydrophobic emulsifier and Tween 80 as the hydrophilic emulsifier. Owusu et al. [162] successfully prepared W/O/W multiple emulsion using kerosene oil by utilizing Span 80 and Tween 20 as the hydrophobic and hydrophilic emulsifiers, respectively. Based on this, the commonly used emulsifiers for formulating multiple emulsion are Spans, Tweens, PGPR and lecithin.

In relevance to the emulsifiers used for W/O/W multiple emulsion, insufficient concentration of hydrophilic and hydrophobic emulsifier may result in destabilization due to coalescence in the internal water droplets and oil globules, respectively. While, higher concentration of hydrophobic and hydrophilic emulsifiers can contribute to micelles formation promoting water movement through micellar transport [163, 164].

2.1.2.3 Thickeners

Thickeners are required for the formulation of multiple emulsion to increase the viscosity of the internal and external water phases for inhibiting the movement between the phases and also to prevent loss of internal water droplets [165]. Lutz et al. [166] indicated that the utilization of thickeners provided better packing and elasticity at the interface. This ‘stiffens’ the interface resulting in a decreased interfacial mobility. Benichou et al. [167] suggested that thickeners play a crucial role to stabilize the emulsion system through steric and electrostatic stabilization. Macromolecules such as proteins and polysaccharides can act as natural thickeners at the interface by forming an interfacial layer comprised of loops and tails that can be well anchored into the oil and water phases [168, 169]. The addition of these proteins and polysaccharide to

the internal or external water phases have also shown to improve the stability of multiple emulsion [170-172].

Zhu et al. [107] reported that protein molecules could adsorb at the interface together with the non-ionic emulsifier and this interfacial interaction cause the formation of a thick and strong interfacial film. This could impart elasticity and resistance which could inhibit the loss of the internal water droplets by reducing the coalescence rate of emulsion droplets, resulting in improved stability. While, polysaccharides act as emulsion stabilizers by forming an extended network in the continuous phase which becomes highly viscous [173] and can even form a gel [172, 174]. Proteins and polysaccharides can adsorb at a globule surface, thereby decreasing the interfacial tension and enhancing the interfacial elasticity. Examples of such protein-based thickeners are caseins [96], whey proteins [98] and gelatin [100]. While, for polysaccharide, xanthan gum [103], alginates [93], gum Arabic [175] and hydroxypropyl methylcellulose [25] could be used.

Existing studies have successfully utilized proteins and polysaccharides for improving the stability of W/O/W multiple emulsion. Iqbal et al. [98] demonstrated that the stability of W/O/W multiple emulsion improved when whey protein isolate (WPI) at 20 wt% was included in the internal water phase. Perez-Moral et al. [93] prepared W/O/W multiple emulsion using 1 wt% of alginate solutions in the internal water phase and xanthan gum in the external water phase. The authors reported that the thickening of the internal water droplets with alginate reduced the size of the water droplets due to the reduced recoalescence rates. Opperman et al. [176] utilized gelatin in the internal water phase and WPI in the external water phase. The authors summarized that the thickened phases hindered the deformation of the oil globules. W/O emulsions stabilized by WPI in the internal water phase had larger MDD than those without WPI. This suggests that it may be more challenging to break up the W/O phase when WPI was present. Also, W/O/W multiple emulsions containing thickened water droplets

were observed to be more stable than those containing non-thickened water droplets [92]. Balcaen et al. [177] reported that upon thickening of the internal water phase, it was possible to produce multiple emulsions with small droplet and a narrow size distribution while maintaining a higher enclosed water volume fraction as compared to samples with non-thickened internal water.

2.1.2.4 Additives

The presence of hydrophobic and hydrophilic emulsifiers in the W/O/W multiple emulsion can lead to the movement of water between the internal and external water phases [178]. This is because the oil layer in the W/O/W multiple emulsion can act as a water-permeable membrane, especially when both these emulsifiers are present in excess [179]. To address this, additives are utilized to enhance the stability at the oil-water interface of the W/O emulsion and also to reduce the movement of the internal and external water phases by balancing the osmotic pressure.

Additives strengthen the W/O interface by increasing the adsorption density and lowering the interfacial tension [180]. NaCl, glucose and glycerol are among the commonly utilized additives. Sunflower oil-based W/O emulsion was formulated with PGPR containing calcium chloride as an additive in the internal water phase, as reported by Márquez et al. [181]. The authors indicated that the increasing concentration of PGPR and/or calcium chloride content gave more stable emulsion. Scherze et al. [182] prepared W/O emulsion with phosphatidylcholine depleted lecithin and PGPR as emulsifying agents. The addition of NaCl as an additive was essential to achieve stable emulsion prepared with PGPR. However, the presence of NaCl favoured the coalescence of water droplets and phase separation in emulsion containing lecithin. Hino et al. [183] in a study prepared W/O/W multiple emulsion

encapsulating tryptophan or theophylline. The authors reported that addition of NaCl in the internal water phase played a vital role in the suppression of the separation and encapsulation of the drug.

Besides strengthening the W/O interface, additives are also used to balance the osmotic pressure by simulating the conditions of isotonic, hypotonic and hypertonic. The growth and shrinkage of internal water droplets can be hindered when the osmotic pressure is controlled [91, 171, 184]. Imbalance in the osmotic pressure could cause the internal water droplets to swell, thinning the oil layer and eventually results in the rupture of oil layer when the water transports from the external to internal water phase [4, 185, 186]. An imbalance could also lead to inversion from W/O/W multiple emulsion to simple O/W emulsion when the water transports from the internal to the external water phase. Kawashima et al. [108] reported that the W/O/W multiple emulsion with a hypertonic internal water phase delayed the separation and enhanced its stability. Zhu et al. [107] reported that under hypotonic conditions, the osmotic pressure gradients promoted the swelling process, implying increased movement of water molecules from the external to the internal water phase followed by rupturing. Whereas, Momeny et al. [187] successfully formulated stable W/O/W multiple emulsion in a hypotonic medium for the encapsulation of β-Sitosterol.

In contrast, existing study has also reported that despite the presence of additive, movement of water from the internal phase still occurred due to the presence of hydrophobic emulsifier in the oil phase [11]. Benichou et al. [178] reported that despite the osmotic pressure of the two phases was equilibrated, the coalescence of internal water droplets still takes place. The authors also reported that the water droplets can still be transported out, controlled by the viscosity of the oil phase and the nature of the oil membrane. Aston et al. [188] reported that even with close-packed molecular areas of emulsifier and additive in the internal water phase, transport of water between the internal and external phase was still observed.

2.2 Evaluation of existing studies on the production of W/O/W multiple emulsion for oral application

From the performed literature survey, the majority of the reported work produced W/O/W multiple emulsion used high shear homogenizers [189-191]. Until now, only a few studies as summarized in Table 2.1 employed ultrasonicator and microfluidizer for producing oral-based W/O/W multiple emulsion. It could be noted that ultrasonicator is more commonly employed as compared to microfluidizer. It is observed that majorly, nano-sized droplet was formed when both primary W/O and W/O/W multiple emulsion were produced using ultrasonicator or microfluidizer [1, 120, 122, 192]. In contrast, micron-sized droplet was formed when either W/O emulsion or W/O/W multiple emulsion was produced using ultrasonicator or microfluidizer [123, 177].

Nevertheless, in a few studies, micron range droplet sizes were formed despite ultrasonication was utilized for both primary W/O emulsion and secondary W/O/W multiple emulsion production [95, 193, 194]. Direct comparison on the effect of processing parameters towards the formed droplet size for these studies was not possible due to the differences in the utilized amplitudes, irradiation time, compositions and sonotrodes. Also, the objective of these studies was not to optimize the processing parameters for formulating W/O/W multiple emulsion. Hence, a thorough investigation of the effect of homogenization parameters on droplet size was not carried out in these studies. Therefore, the reason for the droplet size in the micron range despite utilizing ultrasonication for both W/O and W/O/W productions could not be deduced.

Contrastingly, Bamba et al. [119] obtained nano range droplet size despite utilizing microfluidizer only for the production of W/O/W multiple emulsion. Notably, the optimization of process parameters for the production of W/O/W multiple emulsion was among the objectives of this study. The authors, however, only evaluated the use of microfluidizer between

50 MPa and 200 MPa for the W/O/W multiple emulsion formulations. No thorough investigation was performed for the utilization of microfluidizer for both W/O and W/O/W multiple emulsion production. Hence, the judgement could not be made for the droplet sizes obtained in the nano range due to the lack of information on the W/O emulsion droplet formation and size. Besides, the droplet sizes in the existing studies as shown in Table 2.1 are expressed in terms of Z-average, surface-weighted and volume-weighted. The variation in expressing the droplet sizes also presents a challenge in making direct comparison of the best-optimized process parameters for the production of W/O/W multiple emulsion.

Concerning the emulsifiers used for oral-based formulations, either Span 80 or PGPR has been commonly used as hydrophobic emulsifier, while Tween 80 as hydrophilic emulsifier. For thickeners, existing studies have shown improvement in the stability by either thickening the internal water phase [1, 120, 194], external water phase [119, 123, 193] or both [106, 122, 192] as shown in Table 2.1. Notably, thickening was only investigated for the water phases.

For tonicity, few studies have altered the osmotic pressure to improve the stability in W/O/W multiple emulsion, as illustrated in Table 2.1. These studies recommended either hypotonic [1, 120], hypertonic [194] or isotonic [95, 177, 193] for stable W/O/W multiple emulsion formulations. Hence, no judgement can be made on which tonicity delivers stable W/O/W multiple emulsion.

Table 2.1 Bibliographic studies of W/O/W multiple emulsion formulated using ultrasonicator and microfluidizer.

Ref	Methodology	Hydrophobic emulsifier & oil	Phase volume ratio	Hydrophilic emulsifier	Thickeners	Tonicity	Droplet size	Encapsulation efficiency
[194]	W/O: Homogenized 8 min at 6000 rpm using Ultra-Turrax T25 homogenizer (IKA Labortechnik) and sonicated 4 min using probe sonicator (VCX 130, Sonics and Materials Inc.) at frequency 20 kHz and amplitude 40% (3 s on, 3 s off). W/O/W: Homogenized 4 min at 2000 rpm and sonicated 2 min at frequency 20 kHz and amplitude 30% (3 s on, 3 s off).	5% PGPR & olive oil.	25:75	1% Tween 80.	3% of gelatin in internal water.	Hypertonic: 2% NaCl in external water.	Volume weighted droplet diameter ($d_{4,3}$) ~4 µm.	91 ± 3% of curcumin and 93 ± 2% of catechin.
[119]	W/O: Homogenized 10 min at 10000 rpm using Polytron PT 2500E homogenizer (Kinematica AG, Luzern, Switzerland). W/O/W: Homogenized 15 min at 6000 rpm and microfluidized at 50 MPa and 1 cycle using (Microfluidics M-110P Microfluidizer, ATS Scientific Inc., Burlington, ON, Canada).	4% PGPR & corn oil.	30:70		2.5 wt% of WPI in external water.		Surface-weighted droplet diameter / sauter diameter, ($d_{3,2}$) ~400 nm.	>80% of blueberry polyphenols and anthocyanins.

Table 2.1 Bibliographic studies of W/O/W multiple emulsion formulated using ultrasonicator and microfluidizer. (Continued).

Ref	Methodology	Hydrophobic emulsifier & oil	Phase volume ratio	Hydrophilic emulsifier	Thickeners	Tonicity	Droplet size	Encapsulation efficiency
[193]	W/O: Homogenized 8 min at 6000 rpm using high-speed homogenizer (Ultra-Turrax, Janke & Kundel, Staufen, Germany) and sonicated 180 s using P400S Hielscher sonicator (Hielscher Ultrasound Technology, Teltow, Germany) at frequency 24 kHz and amplitude 40%. W/O/W: Homogenized 4 min at 6000 rpm and sonicated 90 s at frequency 24 kHz and amplitude 30%.	5% PGPR & corn oil.	30:70	1.5 wt% lecithin.	Sodium carboxymethylcellulose in external water.	Isotonic: 0.1 M NaCl in both internal and external water.	MDD, ~3-8 µm	>90% of anthocyanins. .
[122]	W/O: Homogenized 2 min at 6000 rpm using high shear mixer (Greerco Corp., Hudson, NH, USA) and microfluidized at 12000 psi using (Model M-110Y with F20Y & H30Z Chambers, Microfluidics Corporation, Newton, MA, USA). W/O/W: Microfluidized at 3000 psi.	8% PGPR & Orange terpene oil.	10:90		4% gelatin in internal water and 16% gum Arabic in external water.		MDD, 0.75 µm.	>85% of Yellow#6.

Table 2.1 Bibliographic studies of W/O/W multiple emulsion formulated using ultrasonicator and microfluidizer. (Continued).

Ref	Methodology	Hydrophobic emulsifier & oil	Phase volume ratio	Hydrophilic emulsifier	Thickeners	Tonicity	Droplet size	Encapsulation efficiency
[95]	W/O: Homogenized 8 min at 6000 rpm using Ultra-Turrax T25 and somicated at 400 W with UPS400S Hielscher sonicator (Hielscher Ultrasound Technology, Teltow, Germany) using 22 mm sonotrode at frequency 24 kHz. W/O/W: Homogenized 4 min at 3000 rpm using Ultra-Turrax T25 and sonicated 90 s at 50 µm.	5% PGPR & corn oil.	25:75	2% Tween 80.		Isotonic: 0.1 M NaCl in both internal and external water.	MDD, ~4 µm.	89.31 ± 1.07% of phenolic-rich extract from mango peel.
[177]	W/O: Homogenized at 5400 rpm using Ultra-Turrax (type S50N-G45F, IKA®-Werke, Germany). W/O/W: Homogenized 1 min at 6500 rpm microfluidized at 140 bar for 4 cycles using (M110S, Microfluidics) .	5% PGPR & sunflower oil.	50:50		5wt% WPI in internal water and 2 wt% sodium caseinate in external water.	Isotonic: 0.1 M KCl in internal and external water.	Volume weighted droplet diameter, ($D_{4,3}$) ~5 µm.	

Table 2.1 Bibliographic studies of W/O/W multiple emulsion formulated using ultrasonicator and microfluidizer. (Continued).

Ref	Methodology	Hydrophobic emulsifier & oil	Phase volume ratio	Hydrophilic emulsifier	Thickeners	Tonicity	Droplet size	Encapsulation efficiency
[123]	W/O: Homogenized 10 min at 16000 rpm using high-speed homogenizer (IKA T25 Digital UltraTurrax, Selangor, Malaysia) and sonicated 10 min using ultrasonicator (Sonic Ruptor 400, OMNI International the Homogenizer Company, Georgia, USA) at frequency 120 kHz (50% pulse). W/O/W: Homogenized 60 min at 300 rpm using magnetic stirrer (Heidolph MR 3001 K, Heidolph Instruments GmbH & Co, Schwabach, Germany).	3% PGPR & sunflower oil.	40:60	0.05% sodium alginate.	15% sodium caseinate in external water.		MDD, 5.8 µm.	94.1% of NaCl.
[192]	W/O: Homogenized 15 min at 24000 rpm using rotor-stator homogenizer (24,000 rpm for 15 min, Heidolph DIAX900, Germany) and sonicated 10 min with probe sonicator (UP400S, Hielscher, Germany) using 3mm microtip ultrasonic horn at frequency 20 kHz and amplitude 70% (3 s on; 3 s off).	8.74% Span 80 & soybean oil.	80:20		8% Whey-protein & 1.97% pectin in external water.		MDD, ~250 nm	91% of oleuropein.

Table 2.1 Bibliographic studies of W/O/W multiple emulsion formulated using ultrasonicator and microfluidizer. (Continued).

Ref	Methodology	Hydrophobic emulsifier & oil	Phase volume ratio	Hydrophilic emulsifier	Thickeners	Tonicity	Droplet size	Encapsulation efficiency
Cont.	W/O/W: Sonicated 10 min at frequency 20 kHz and amplitude 70% (3 s on; 3 s off).							
[1, 120]	W/O: Homogenized 5 min using vortex mixer and sonicated 90 s using Ultrasound Processor VCX 750 (Sonics & Materials, Inc., Newtown, USA) at amplitude 40%. W/O/W: Ultrasonicated 60 s at amplitude 20%.	1.25% Span 80 & castor oil and lauroglycol 90 (1:1).	25:75	0.5% Cremophor EL	1% gelatin in internal water.	Isotonic: 1% glucose in both internal & external water. Hypotonic: 1% glucose in internal water & 0.5% glucose in external water.	MDD, ~400 nm.	~98% of aspirin.

2 stages with pre-emulsification were performed in all the studies.

2.3 Potential of TRF and CA in W/O/W multiple emulsion for cancer therapy

Anti-oxidant, anti-proliferative, anti-tumour and anti-inflammatory properties of natural active compounds such as TRF and CA exhibits potential for cancer treatment. These natural active compounds also have the potential to lower the toxicity and reduce the side effects of existing therapeutics when utilized for cancer treatment.

At present, several existing studies have demonstrated the potential of TRF and CA for use in cancer treatment. Rajasinghe et al. [195] postulated that TRF inhibited cell proliferation and induced apoptosis via the downregulation of the Notch-1/NF-κB pathways in NSCLC cells. In another study, Husain et al. [196] reported that δ-tocotrienol inhibited metastasis of human pancreatic tumour through inhibition of extracellular matrix tumour, migration, invasion, angiogenesis, cancer stem cell signalling and induction of apoptosis. Ji et al. [197] reported that δ-tocotrienol augmented CIS-induced suppression of NSCLC via the inhibition of the Notch-1 pathway. Pierpaoli et al. [198] reported that the anticancer effects of δ and γ tocotrienols are mainly related to the direct induction of oxidative stress, senescent-like growth arrest and apoptosis of mammary gland tumour cells in HER-2/neu transgenic mice.

Concerning CA, Min et al. [199] reported that the synergistic anticancer activity of CA with paclitaxel enhanced the apoptosis of NSCLC *in vivo* and *in vitro*. In a study by Lin et al. [200], the authors justified that CA with paclitaxel-induced anti-proliferation and apoptosis in lung cancer cells through the NF-κB pathway. Sirota et al. [201] reported that the CIS cytotoxicity was enhanced with co-treatment using CIS and CA on ovarian cancer cells. Koraneekit et al. [202] reported that the synergistic effects of CIS with CA induced apoptosis in human cervical cancer cells via the mitochondrial pathway. Prasad et al. [84] identified that CA enhanced the lipid peroxidation markers and increased reactive oxygen species (ROS) levels in the human fibrosarcoma cell line. CA has also significantly inhibited superoxide production in A549 cells [203].

With regards to the beneficial properties inherited by TRF, only two existing studies have been found to explore the potential of TRF encapsulation in nanoemulsion for cancer therapy to date. Alayoubi et al. [204] prepared O/W nanoemulsion for the concurrent delivery of TRF and simvastatin as a combination of cancer therapy. The authors reported that the nanoemulsion demonstrated anti-proliferative activity against human mammary tumour cells (MCF-7 and MDA-MB-231). Also, the IC 50 for TRF nanoemulsion and simvastatin when used individually for treating the cells was higher as compared to the IC 50 when TRF nanoemulsion was combined with Simvastatin on both MCF-7 and MDA-MB-231. This shows that when combined therapy with more than one active compound is utilized, the nanoemulsion possessed a synergistic effect and achieved IC 50 at a lower concentration. Steuber et al. [205] formulated O/W nanoemulsion encapsulating TRF and curcumin for combined cancer therapy. This nanoemulsion induced apoptosis in the breast (MCF-7) and ovarian (OVCAR-8) cancer cells. The authors concluded that the combined therapy produced superior cytotoxicity profiles with lower concentration of IC 50. Thus, this shows the synergistic effect of both curcumin and TRF achieved better therapeutic effect with a lower dosage. Concerning CA, no existing study has typically reported on the encapsulated CA in nanoemulsion formulation for cancer therapy till now.

Taking into consideration the limited knowledge in terms of encapsulated TRF and CA in nanoemulsion for cancer therapy, the required investigation and analysis to evaluate its efficacy for cancer treatment were identified. Firstly, it is necessary to evaluate the cell viability upon incubation with the encapsulated W/O/W multiple emulsion. Cell viability is the measurement of the number of cancer cells that are alive upon incubation [206]. This analysis will provide information on the required dosage for the inhibitory concentration of the cancer cells at 50%, commonly denoted as IC 50. Commonly, the non-radioactive colorimetric assay using tetrazolium salt, 3-(4,5-dimethylthiazol-2-yl)-2,5-diphenyltetrazolium bromide (MTT) is

utilized. MTT assay is the best-known method for determining mitochondrial dehydrogenase activities in the living cells [207]. Cancer cells that are alive and metabolically active would convert the water-soluble MTT to a water-insoluble purple MTT-formazan crystal catalyzed by mitochondrial succinate dehydrogenase [208]. The amount of formazan dye produced is directly proportional to the number of metabolically active cells.

Next, the analysis of apoptotic stages for the cancer cell due to the formulation is necessary. This is because it is essential to evaluate whether the cells are undergoing apoptosis (programmed cell death) or necrosis (traumatic cell death) upon incubation with the formulation [209]. If the formulation or the dosage used is toxic, cells will die dramatically instead of undergoing the sequence of apoptosis leading to cell death. This phenomenon is known as necrosis and should be avoided. Apoptosis plays a regulatory function during development and tissue homeostasis controlled by an intracellular death program [209, 210]. One early event in the signalling cascade includes alterations in the organization of phospholipids in the plasma membrane of most cells where the phosphatidylserine (PS) translocate from the cytoplasmic to the extracellular surface of the membrane [211]. PS exposure is recognized by phagocytes *in vivo*, which engulf and thereby remove apoptotic cells. This coordinated process prevents inflammatory reactions.

In contrast, necrosis results from acute cellular injury caused by external factors such as toxins [212]. It is characterized by the loss of cell membrane integrity and an uncontrolled release of cytoplasmic components which initiate inflammatory reactions in the surrounding tissue. PS translocation precedes the loss of membrane integrity, which accompanies the later stages of cell death resulting from necrotic process. *In vitro* externalized PS can be detected by Annexin V. In the presence of Ca^{2+}, Annexin V binds to the negatively charged phospholipids such as PS with high affinity for labelling apoptotic cells [213]. Annexin V can be conjugated to fluorochromes while retaining its high affinity for PS and thus serves as a sensitive probe for

flow cytometric analysis of cells undergoing apoptosis [214]. While, propidium iodide (PI) intercalates into deoxyribonucleic acid (DNA) and is membrane impermeable. Therefore, it is usually excluded from viable cells and can be used to identify necrotic cells [215]. Thus, staining with Annexin V is typically used in conjunction with a vital dye such as PI for the identification of apoptotic and necrotic cells.

The next critical analysis would be the cell cycle analysis that determines the stage cancer cell growth is arrested. This analysis can be used as a base to evaluate the function of gene therapy on cancer cells using the formulation as a further study. The first step in preparing the cancer cells for cell cycle analysis is the permeabilization of the plasma membranes [216]. This is usually done by fixating them in ethanol. PI is used to label DNA in cells undergoing various phases of cell growth [217]. As the dye directly intercalates with the base pairs on a DNA strand, its fluorescence intensity is directly proportional to the DNA content of the cell. This can reliably distinguish cells arrested in different growth phases (G0/G1, S & G2/M) [218, 219].

Considering that TRF and CA are antioxidants, the quantification of ROS in the cancer cells need to be evaluated. When ROS production is increased or decreased, this will lead to the loss of ROS homeostasis in cancer cells. This imbalance could lead to oxidative stress-induced cell death in cancer cells [220]. When cancer cells are incubated with active compounds encapsulated in W/O/W multiple emulsion, the presence of ROS could be detected by staining using 5-(and-6)-carboxy-2,7-dichlorodihydrofluorescein diacetate. This is a membrane-permeable dye that can diffuse into the cells where it becomes hydrolyzed by intracellular esterase and reacts with the ROS to generate the fluorescent 2,7-dichlorofluorescein [221]. Thus, the amount of ROS produced by the cells can be estimated by this fluorescence intensity.

Lastly, the toxicity effect on normal kidney cells to evaluate the side effects using W/O/W multiple emulsion encapsulated with TRF and CA could be verified by the cell viability

assay. This analysis would quantify the number of living cells upon incubation with the formulation. Hence, the cytotoxicity of the formulation on the normal kidney cells could be evaluated.

Collectively, the information derived from these assays can indicate whether a cell population that has been exposed to the formulation is: (1) healthy or dying, (2) actively dividing or in stasis, and (3) committed to an apoptotic pathway or underwent necrosis.

2.4 Summary

Based on the performed literature survey, the utilization of both ultrasonicator and microfluidizer to formulate W/O/W multiple emulsion with the emphasis on the production and optimization should be thoroughly investigated. Optimization of processing parameters should also be carried out to avoid 'over-processing' phenomena. The usage of palm oil for the formulation of W/O/W multiple emulsion should be investigated considering that no study has reported on the usage of palm oil for oral-based multiple emulsion, as well as since Malaysia being the second-largest producer of palm oil in the world. The usage of both Span 80 and PGPR as a hydrophobic emulsifier, as well as Tween 80 as the hydrophilic emulsifier, should be investigated. The concentration of emulsifier should be optimized to formulate stable W/O/W multiple emulsion since higher quantity can result in the movement of water between the internal and external water phases. The effect of thickener for oil phase towards the stability of W/O/W multiple emulsion should be investigated considering no study has been reported in this area. The tonicity effect towards the stable formulation of W/O/W multiple emulsion also needs to be evaluated since judgement could not be made based on the existing studies.

Then, the possibility of encapsulating TRF and CA in oil and internal water phases of W/O/W multiple nanoemulsion, respectively, as well as their efficacy towards lung and liver

cancer cell lines should be investigated. This is due to the potential possessed by both these active compounds and lack of investigation for the encapsulation of both these compounds simultaneously for cancer therapy. Considering that CIS is the standard chemotherapeutic agent that is used for treating cancer, here, the formulated W/O/W multiple emulsion encapsulating TRF and CA would be simultaneously used with CIS to evaluate its efficacy on the lung and liver cancer cells. As TRF and CA are natural compounds, it is hypothesized that the W/O/W nanoemulsion encapsulating these active compounds should not have toxicity effect on normal cells as a side effect during treatment on the cancer cells. As such, the formulated W/O/W multiple emulsion would also be analysed to substantiate its non-toxic effect on normal kidney cells.

CHAPTER 3: FORMULATION FOR THE GENERATION OF STABLE PALM OIL-BASED W/O NANOEMULSION USING ULTRASONICATOR AND MICROFLUIDIZER

This chapter presents the details of experimentation carried out to formulate stable palm oil-based W/O nanoemulsion as outlined in Fig. 3.1. The formulation of stable nanoemulsion is dependent on the interaction between the oil and hydrophobic emulsifier to form rigid oil-water interface. This could be achieved through deep anchoring of the emulsifier in the oil.

First stage To determine a suitable hydrophobic emulsifier for formulating stable W/O emulsion using palm oil.

↓

Second stage To compare the generation of W/O nanoemulsion using ultrasonicator and microfluidizer.

↓

Third stage To evaluate the effects of phase volume ratio of oil to water (90:10 and 80:20) on the stability of nanoemulsion.

↓

Fourth stage To evaluate the effects of MCT oil, soybean lecithin and NaCl towards the formulation and stability of W/O nanoemulsion.

Fig. 3.1 Overview of experimentation in Chapter 3.

3.1 Background

As discussed in the literature review (Chapter 2), the majority of studies have focused on enhancing the stability of multiple emulsion by balancing the osmotic pressure difference through thickeners and additives. However, thickeners and additives are secondary approaches in stabilizing multiple emulsion since they are only aimed to control the movement between the internal and external water droplets. Instead, importance should be given to form a rigid oil-

water interface in W/O nanoemulsion before generating multiple nanoemulsion. On this context, four-stage experimentation was carried out aimed to formulate and investigate the factors that affect the stability of palm oil-based W/O nanoemulsion. The first stage was to determine a suitable hydrophobic emulsifier for formulating stable W/O emulsion using palm oil.

The second stage was to compare the generation of W/O nanoemulsion using ultrasonicator and microfluidizer. The third stage evaluated the effects of phase volume ratio of oil to water (90:10 and 80:20) on the stability of nanoemulsion.

In the fourth stage, the effects with MCT oil, soybean lecithin and NaCl towards the formulation and stability of W/O nanoemulsion were evaluated. MCT was used because it has been reported to have health benefits, especially for digestibility and absorbability in human body [222]. Soybean lecithin was used as it is a natural emulsifier obtained from the cell membranes of soybeans [223] to fulfill the growing demand for a natural-based formulation of food/pharmaceutical products [224]. NaCl was investigated here as it has been reported to improve the stability of nanoemulsion in existing studies [95, 193, 194].

3.2 Materials and methods

3.2.1 Materials

Refined palm olein (palm oil) purchased from Sime Darby Food (Malaysia), palm MCT oil purchased from KLK Oleo (Malaysia), sunflower oil purchased from Yee Lee Edible Oils (Malaysia), liquid paraffin from Sigma Aldrich (Malaysia), Span 80 from Sigma Aldrich (Malaysia), PGPR from Palsgaard (Denmark) and liquid soy lecithin purchased from Guangzhou Hisoya Biological Science and Technology (China) were used in producing the nanoemulsion. Water obtained from Milli-Q® Plus apparatus (USA) was used in the

formulations of nanoemulsion. 300-mesh formvar-coated copper grid purchased from Agar Scientific Ltd. (United Kingdom) was used for scanning transmission electron microscope (STEM) analysis.

3.2.2 Selection of hydrophobic emulsifier for forming stable palm oil-based W/O emulsion

Firstly, two GRAS certified hydrophobic emulsifiers by FDA such as Span 80 and PGPR were used to form W/O emulsion, independently. The organic phase constituted 5.0 wt% of hydrophobic emulsifier dissolved in palm oil (85.0 wt%), which was stirred for 2 min using a magnetic stirrer at 500 rpm. Subsequently, deionized water (10.0 wt%) was added to the organic phase and stirred for 15 min using a magnetic stirrer at 700 rpm. This study was carried out to evaluate the stability of W/O emulsion due to the interaction of different hydrophilic heads in the emulsifiers with palm oil.

Secondly, the stability of W/O emulsion due to the interaction of hydrophobic tail in PGPR and various oils such as palm oil, liquid paraffin, palm MCT oil and sunflower oil was evaluated. The stability was observed for 28 days by evaluating the sedimentation index (SI). The composition of the organic phase consists of 5.0 wt% of PGPR dissolved in 85.0 wt% of oil was stirred for 2 min using a magnetic stirrer at 500 rpm. Subsequently, deionized water (10.0 wt%) was added to the organic phase and stirred for 15 min using a magnetic stirrer at 700 rpm to form W/O emulsion.

3.2.2.1 Determination of critical micelle concentration (CMC)

CMC was evaluated by plotting the concentration of emulsifier in oil against interfacial tension at the oil-water interface. PGPR concentrations of 0.5, 1.0, 2.0, 3.0, 5.0 and 7.0 wt% in palm

oil were prepared, independently. The interfacial tension between water and these oils at different PGPR concentrations was measured as described in section 3.2.8. CMC is the point at which the emulsifier is saturated at the surface where the lowest interfacial tension can be expected. Beyond this point, the interfacial tension is expected to level off despite an increase in the concentration of emulsifier.

3.2.3 Comparison between ultrasonicator and microfluidizer for the formation of W/O nanoemulsion

3.2.3.1 Preparation of W/O emulsion

W/O emulsion was prepared using palm oil as the continuous phase and deionized water as the dispersed phase. Firstly, PGPR was added to the oil phase and stirred for 2 min using a magnetic stirrer at 500 rpm. Subsequently, coarse W/O emulsion was prepared by adding the aqueous phase to the oil phase and mixed using a Ultra-Turrax T18 Basic high-speed homogenizer (Germany) at 700 rpm for 20 min. The composition of W/O emulsion for the organic phase consisted of 3.0 wt% of PGPR and 87.0 wt% of palm oil, while the aqueous phase constituted of 10.0 wt% of deionized water. The coarse emulsion resulted in an MDD of 982.4±10.1 nm and dispersity index (DI) at 1.

3.2.3.2 Ultrasonication for the generation of W/O nanoemulsion

The coarse W/O emulsion was then subjected to a 20 kHz VCX 750W Ultrasonic Processor (USA) with ¼ ” stepped microtip. Ultrasound was dissipated in a pulse mode (3 s on and 10 s off). This ultrasonic immersion horn system primarily consisted of a power generator, a piezoelectric lead zirconate titanate crystal sealed converter and a microtip probe. For each

generation, a sample size of 50 ml was used. For the generation of W/O nanoemulsion sonication at different amplitudes, i.e. 20, 30, 40 and 50% were employed. Samples were then collected after a total irradiation time of 10, 30, 45, 60, 90, 120, 150, 180, 220 and 240 s at each amplitude. The influences of amplitude and irradiation time towards the MDD of the formed W/O nanoemulsion were investigated.

3.2.3.3 Microfluidization for the generation of W/O nanoemulsion

The coarse W/O emulsion was microfluidized using M-110Y Microfluidics (USA) at the operating pressures of 150, 250, 350 and 450 bar. A sample size of 200 ml was utilized for each generation. Samples were then collected after 2, 3, 4, 5, 6, 7, 8, 9, 10 and 12 cycles for each of the studied operating pressure. The influences of operating pressure and the number of cycle on the MDD of the generated W/O nanoemulsion were also investigated. Throughout the preparation coarse W/O emulsion and generation of W/O nanoemulsion using ultrasonicator and microfluidizer, the temperature was maintained below 32 °C.

3.2.3.4 Peroxide value

Peroxide value for the W/O nanoemulsion was determined according to Peroxide value - AOCS method (AATM 516-01) [225]. 5 g of W/O nanoemulsion sample was taken in a 250 ml conical flask followed by the addition of 30 ml of acetic acid-chloroform solution. Then, 0.5 ml of saturated potassium iodide (KI) solution was added and swirled vigorously for 1 min. 30 ml of deionized water was then added and the flask was shaken vigorously to liberate the iodine from the chloroform layer. Then, 1 ml of starch solution was added to the mixture. The resulting mixture was titrated by using 0.1 N sodium thiosulfate ($Na_2S_2O_3$) solution until the

disappearance of purple colour. The peroxide value was calculated by using the following Eq. 3.1.

$$Peroxide\ value\ (meq) = \frac{titration \times Nthiosulfate \times 1000}{weight\ of\ sample} \qquad \text{Eq. 3.1}$$

3.2.3.5 Analysis of the composition of fatty acids

Perkin Elmer's Autosystem XL (USA) gas chromatography was used to determine the composition of fatty acids. The gas chromatography column has a length of 60 m, the internal diameter of 0.25 mm with a coating of 0.25 µm. The column was held for 1 min and then ramped to 40 °C at 20 °C/min and finally held at 240 °C for 13 min. The transfer line of gas chromatography was kept at 240 °C. Helium was used as the carrier gas at a flow rate of 1.5 ml/min. Other gases used were hydrogen and purified air.

3.2.3.6 FTIR analysis

FTIR spectra were obtained using Perkin Elmer's Frontier FTIR (USA) spectrometer. The spectrometer covered the wavenumber range from 400 and 4000 cm^{-1} at a resolution of 4 cm^{-1} and interval 1 cm^{-1}. Each FTIR spectrum was produced from an accumulative of 16 scans. The functional groups of concern were aldehydes (C=O stretch at 1750-1625 cm^{-1}, C-H stretch off C=O at 2850-2800 cm^{-1}, and C-H stretch off C=O at 2750-2700 cm^{-1}), ketones (C=O stretch at 1750-1625 cm^{-1}) and carboxylic acid (C=O stretch at 1730-1650 cm^{-1} and hydrogen-bonded O-H stretch at 3400-2400 cm^{-1}) [226].

3.2.4 Effect of phase volume ratio towards the formation of W/O nanoemulsion

The effect of phase volume ratio of 80:20 of oil:water on the formation of W/O nanoemulsion was evaluated in comparison to 90:10 of oil:water. The organic phase of W/O nanoemulsion had a composition of 3.0 wt% of PGPR and 77.0 wt% of palm oil, while the aqueous phase constituted 20.0 wt% of deionized water. The steps followed for the formation of W/O nanoemulsion have been described in section 3.2.3.1. An amplitude of 40% at different irradiation time of 10, 30, 45, 60, 90, 120, 150, 180, 220 and 240 s was employed. The selection of applying an amplitude of 40% was based on the optimization study, as discussed in section 3.2.3.2.

3.2.5 Effect of palm MCT oil, lecithin and NaCl towards the formation and stability of W/O nanoemulsion

3.2.5.1 Effect of blending of palm oil and palm MCT oil towards the formation of W/O nanoemulsion

The effect of blending palm oil with palm MCT oil for the formation of W/O nanoemulsion was evaluated. The procedure followed for the formation of W/O emulsion was described in section 3.2.3.1. The experiments were conducted at amplitude of 40% and at different irradiation time of 10, 30, 45, 60, 90, 120, 150, 180, 220 and 240 s. The composition of W/O nanoemulsion for the organic phase consisted of 3.0 wt% of PGPR, 87.0 wt% of oil (varied by blending palm oil and palm MCT oil at the following ratios of 100:0, 70:30, 50:50 and 0:100), while the aqueous phase constituted of 10.0 wt% of deionized water.

3.2.5.2 Effect of blending of lecithin with PGPR on the formation of W/O nanoemulsion

The effect of blending lecithin with PGPR on the formation of W/O nanoemulsion was examined. The procedure for the formation of W/O emulsion was described in section 3.2.3.1. The experiments were conducted at amplitude of 40% for a total irradiation time of 180 s. The composition of W/O nanoemulsion for the organic phase consisted of 3.0 wt% of emulsifiers (varied by blending lecithin and PGPR in the oil phase at the following ratios: 3:0, 2:1, 1:2 and 0.5:2.5), 87.0 wt% of palm oil and palm MCT oil at the ratio of 70:30, while the aqueous phase constituted of 10.0 wt% of deionized water.

3.2.5.3 Effect of addition of NaCl on the formation of W/O nanoemulsion

The effect of the addition of NaCl on the formation of W/O nanoemulsion was studied. The procedure for the formation of W/O emulsion was described in section 3.2.3.1. The experiments were conducted at amplitude of 40% for an irradiation time of 180 s. The composition of W/O nanoemulsion for the organic phase consisted of 3.0 wt% of emulsifiers, 87.0 wt% of palm oil and palm MCT oil at the ratio of 70:30, while the aqueous phase constituted of 10.0 wt% of deionized water added with NaCl (2.0 M).

3.2.6 Droplet size and dispersity index

The droplet size and DI of W/O nanoemulsion were determined using Malvern Zetasizer Nano ZS (United Kingdom). Each run (test) was produced from an accumulative of 12 scans. The average duration for each run was ~15 s. Triplicate measurements were performed using He–Ne laser at a wavelength of 633 nm and a scattering angle of 173° at 25 ℃. Intensity weighted average hydrodynamic diameter was computed from intensity autocorrelation data with

cumulant method using DTS (nano) software (Version 5.0). The Z-average diameter is reported as the MDD of the generated W/O nanoemulsion. DI is a dimensionless measure of the width of size distribution calculated from the cumulant analysis and ranging from 0 to 1. Table 3.1 shows the guideline given by Malvern to evaluate the obtained DI [227].

Table 3.1 Distribution guide recommended by Malvern for Dynamic Light Scattering (DLS) [227].

Monodisperse		**Polydisperse**	
Uniform	**Narrow**	**Moderate**	**Broad**
0.0	0.0-0.1	0.1-0.4	>0.4

3.2.7 Validation tests for the type of nanoemulsion formed (O/W or W/O)

Two validation methods, i.e., conductivity analysis and dilution test were performed to evaluate the type of nanoemulsion formed (O/W or W/O) [228]. For the conductivity analysis, Eutech Instruments CyberScan PCD650 (Singapore) conductivity meter was used to measure the conductivity of the formed nanoemulsion. The conductivity probe was lowered into a 50 ml beaker containing nanoemulsion. W/O type emulsion was determined to be formed if the conductivity value is 0 µS/m. This is because the electric current do not pass through the medium when oil is the continuous phase.

For the dilution test, a few drops of prepared nanoemulsion were added into two different containers having 20 ml of oil and deionized water. If the emulsion dissolves into oil, then, a W/O type emulsion was formed. This is because the continuous oil phase enables the dispersion of emulsion into the oil.

3.2.8 Interfacial tension

Interfacial tension was measured using Kruss K6 tensiometer (United Kingdom) equipped with a platinum ring in accordance to the standard test method for interfacial tension of oil against water by the ring method (ASTM D971 – 12) [229]. Firstly, the ring was washed with water, followed by acetone and left to dry. Then, the ring was heated to red-orange colour using a gas burner. Distilled water was added to a beaker and calibrated to the surface tension of 72-73 mN/m. The oil was then carefully layered on the surface of the water. It was left for 1 min to reach equilibrium before taking any measurements. It was ensured that the ring was immersed into the water by 5 mm, whereas the oil was ensured not to cover the crossbar of the ring. The ring was kept in the middle to prevent its contact with the wall of the beaker.

3.2.9 Measurement of sedimentation index

The separation of the oil phase could be expressed as SI by relating between the upper oil phase (H) and the initial height of emulsion (H_0) using the Eq. 3.2. This measurement was used to evaluate the stability of W/O nanoemulsion.

$$SI = \frac{H}{H_0} \times 100\% \qquad \text{Eq. 3.2}$$

3.2.10 Measurement of viscosity

Brookfield DV-E (USA) digital viscometer was used to measure the apparent viscosity of the nanoemulsion. The viscosity measurements were performed using spindle S86 with 15 ml of the sample placed in the extension. The speed of the spindle was adjusted to 1 rpm and the obtained viscosity is reported in centipoise (cP).

3.2.11 Analysis using STEM

FEI Quanta 400F FESEM (USA) field emission scanning electron microscope was used to investigate the morphology of the formed W/O nanoemulsions. For this, the sample was at first diluted with oil (1:5). This ratio was chosen as the images obtained at this ratio were clear. Then, a drop of nanoemulsion was added to 300-mesh formvar-coated copper grid from Agar Scientific Ltd. (United Kingdom) using a micropipette. Excess solution was drawn-off with a Whatman filter paper. Samples were then made electrically conductive, employing negative staining using 2.0 wt% of phosphotungstic acid. The samples were then dried at room temperature for 30 s before analysis using STEM at a higher vacuum of 2660 Pa and an acceleration voltage of 20 kV. The morphology and size of emulsion droplets were confirmed by using an xTMicroscope Control imaging software.

The experiments were repeated two times. For each experiment, two samples were collected. For each sample, the analyses were repeated two times. For the graphs in the results section, error bars based on standard errors are shown to provide an estimated precision of the measured parameters. While, for the tables, error bars based on standard deviations are shown to show the dispersion of the measured parameters.

3.3 Results and discussion

3.3.1 Selection of hydrophobic emulsifier for the formation of stable W/O emulsion using palm oil

The outcome shown in Table 3.2 confirms that the formed emulsion is W/O type from both the dilution (soluble in oil) and conductivity test (0 µS/m). From Fig. 3.2, W/O emulsion had lower SI formulated using PGPR than Span 80. After 28 days, SI using PGPR was at 12.14%, while for Span 80 it was at 100.00% (completely separated). For Span 80, there was a continuous

increase in SI and water phase-separated within 28 days. While, for W/O emulsion formed with PGPR, SI stabilized over time. Similar outcome had also been reported by other studies where vegetable oil-based W/O emulsion showed better stability by using PGPR than Span 80. Merhnia et al. [230] reported better stability by using PGPR as compared to Span 80, where olive oil was used to form Crocin W/O emulsion. In another study, Aditya et al. [194] reported that PGPR formed more stable W/O emulsion to encapsulate Catechin using sunflower oil as compared to Span 80.

Table 3.2 Validation tests for the type of emulsion formed using different hydrophobic emulsifiers.

W/O emulsion	Conductivity (µS/m)	Dilution
Palm oil:PGPR	0	Soluble in oil
Palm oil:Span 80	0	Soluble in oil

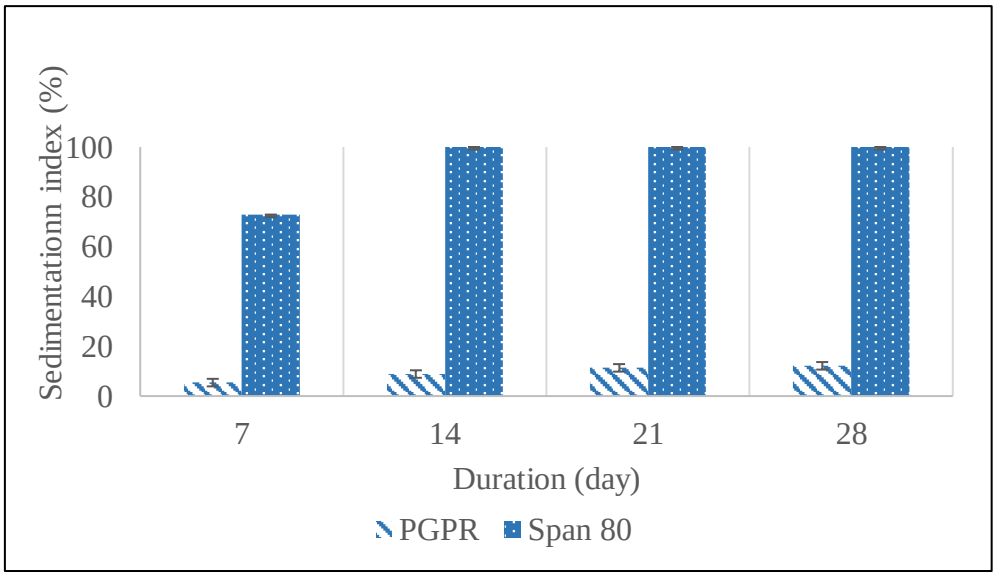


Fig. 3.2 Sedimentation index with time for palm oil-based W/O emulsion using PGPR and Span 80.

Both sorbitol and polyglycerol, which are the hydrophilic moieties in Span 80 and PGPR, respectively, can form hydrogen bonds with water molecules in the W/O emulsion. Besides, PGPR has a polyglycerol head which interacts with the glyceride units of palm oil and strengthens the interaction at the oil-water interface supplementary to the hydrogen bonds formed with water molecules. This is supported by Ushikubo and Cunha [144], where the authors reported the formation of a structured interface in the vegetable oil-based W/O emulsion due to PGPR. Different from PGPR, Span 80 possesses a hexagonal cyclic ring instead of a linear glycerol head. Thus, there is no interaction with the glyceride units of palm oil to form a strong network structure. Also, PGPR has multiple fatty acid chains as compared to Span 80 in establishing a network with the fatty acid chains of oil. As a result, 100.0% phase separation was observed over time in Span 80 stabilized W/O emulsion. Hence, palm oil-based W/O emulsion formed using PGPR is more stable as compared to Span 80.

A further study was carried out to evaluate the interaction of hydrophobic tails between oils and PGPR at the oil-water interface towards the formation of a stable W/O emulsion. For this, mineral oil which is a mixture of hydrocarbon chains, sunflower oil with different fatty acid chains (more unsaturation) and a palm-based MCT oil which has shorter and saturated fatty acid chains were used to formulate W/O emulsion with PGPR. All the emulsions formed with PGPR using palm MCT oil, liquid paraffin and sunflower oil were of W/O type as confirmed by the conductivity test (0 µS/m) and dilution test (soluble in oil) as shown in Table 3.3. PGPR showed excellent stability in all the vegetable oils (sunflower oil, palm oil and palm MCT oil) used. Whereas, W/O emulsion formed with mineral oil and PGPR was poorly stable with the highest SI at 63.30% ± 0.08 at the end of 28 days, as shown in Fig. 3.3.

Table 3.3 Validation tests for the type of emulsion formed using different types of oils with PGPR.

W/O emulsion	Conductivity (µS/m)	Dilution
Sunflower oil:PGPR	0	Soluble in oil
Palm MCT oil:PGPR	0	Soluble in oil
Liquid paraffin:PGPR	0	Soluble in oil

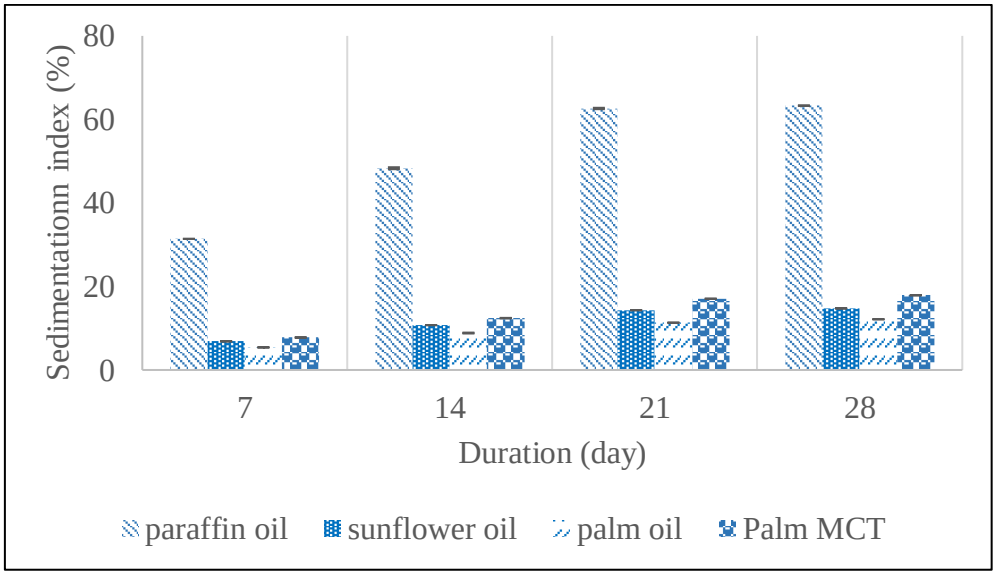


Fig. 3.3 Sedimentation index with time for W/O emulsion using different types of oils.

PGPR could form more stable W/O emulsion with vegetable oils than with liquid paraffin oil due to the binding between the fatty acid (ricinoleic acid) in PGPR and the fatty acid in the vegetable oils. The non-polar fatty acid chains interact together through van der Waal's forces. This is in agreement with the observations of Benichou et al. [231] where they have demonstrated that the fatty acid chains of PGPR have strong anchoring ability into the chains of fatty acid of oil ensuring good elasticity at the interface. On the other hand, the W/O emulsion formed using liquid paraffin and PGPR had poor stability due to the weak anchoring between the fatty acid of PGPR and the linear hydrocarbon chain of liquid paraffin. The hydrocarbon chain of liquid paraffin is a saturated linear chain while the fatty acid chains of

palm oil are branched with unsaturation. Therefore, it is anticipated that the saturated linear chains in liquid paraffin do not promote strong anchoring into the fatty acid chains of PGPR. This is supported by Ushikubo and Cunha [144] where the authors reported that oil with linear saturated carbon chain did not form stable W/O emulsion with PGPR.

Amongst the evaluated vegetable oils, palm oil had the lowest SI at the end of 28 days at 12.14±0.04 followed by sunflower oil at 14.75±0.05 and finally palm MCT oil at 17.88±0.01. This outcome could be related to the viscosities of these oils in which palm oil (~77.2 cP) has the highest viscosity, followed by sunflower oil (~48.8 cP) and finally palm MCT oil (~27 cP). The higher viscosity of palm oil as compared to other oils could have reduced the rate of sedimentation by resisting the motion of water droplets within the continuous oil phase and resulted in lower SI. Likewise, the lowest SI in palm oil could also be related to the highest density of palm oil (~925 kg/m^3) than sunflower oil (~919 kg/m^3) and palm MCT oil (~910 kg/m^3). This is because higher density of oil (closer to density of water 1000 kg/m^3) could retard separation due to the effect of gravitational force [115]. Based on the effects of interaction between emulsifier and oil, viscosity and density of oil, as well as SI, palm oil is determined to be suitable in forming a stable emulsion with PGPR.

3.3.1.1 Determination of CMC of PGPR in palm oil

As shown in Fig. 3.4, the interfacial tension between palm oil and water decreased with increasing concentration of PGPR, and eventually plateau could be noted. The lowest interfacial tension was obtained (1.5 mN/m) at 3.0 wt% of PGPR, and at this concentration, the oil-water interface was saturated with PGPR (CMC).

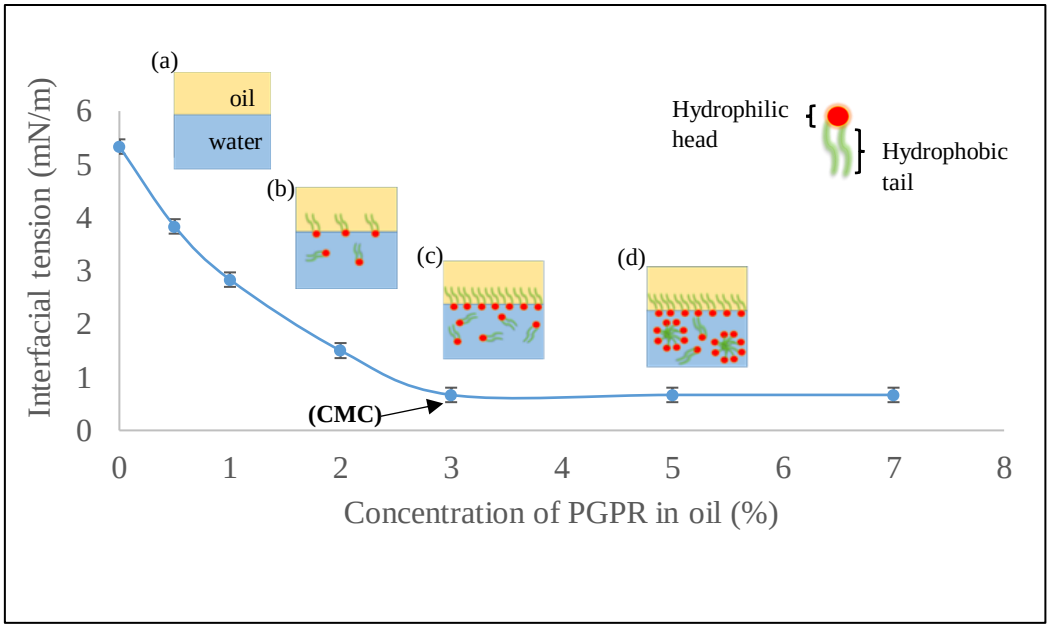


Fig. 3.4 Effect of concentration of PGPR on the interfacial tension at the interface of palm oil-water.

A similar trend was reported by Gulseran et al. [232] where the authors investigated the influence of PGPR concentration by measuring the interfacial tension between soybean oil and water using drop tensiometer. The authors reported that with an increase in PGPR concentration, the interfacial tension decreased and eventually plateaued at about 1.8 mN/m.

Fig. 3.4 (a) shows the oil-water interface in the absence of an emulsifier (0%). Whereas, Fig. 3.4 (b) shows that as the concentration of emulsifier increases, the emulsifier aligns themselves at the interface. Interfacial tension is lowered with increase in the concentration of PGPR. Fig. 3.4 (c) shows that at CMC (3.0%), there is a saturation of emulsifier at the interface. At this CMC, the lowest possible interfacial tension is obtained. Increasing the concentration beyond CMC resulted in excess emulsifier in the bulk oil and forms micelles, as shown in Fig. 3.4 (d). Thus, a further reduction in the interfacial tension is not observed beyond CMC. Following this, a saturated emulsifier content at the oil-water interface is obtained at 3.0 wt% of PGPR.

3.3.2 Comparison between ultrasonicator and microfluidizer processing for the formation of W/O nanoemulsion

3.3.2.1 Effect of ultrasonicator parameters (amplitude and total irradiation time) on the formation of W/O nanoemulsion

From Fig. 3.5, at all evaluated amplitudes, it could be observed that MDD decreased with increased irradiation time. At a higher amplitude and irradiation time, more bubbles could be generated, and their subsequent miniature implosion intensified the degree of cavitation activity [9]. Thus, higher cavitation intensity increased droplet break up which led to the decrease in MDD, in agreement to existing studies [120, 233].

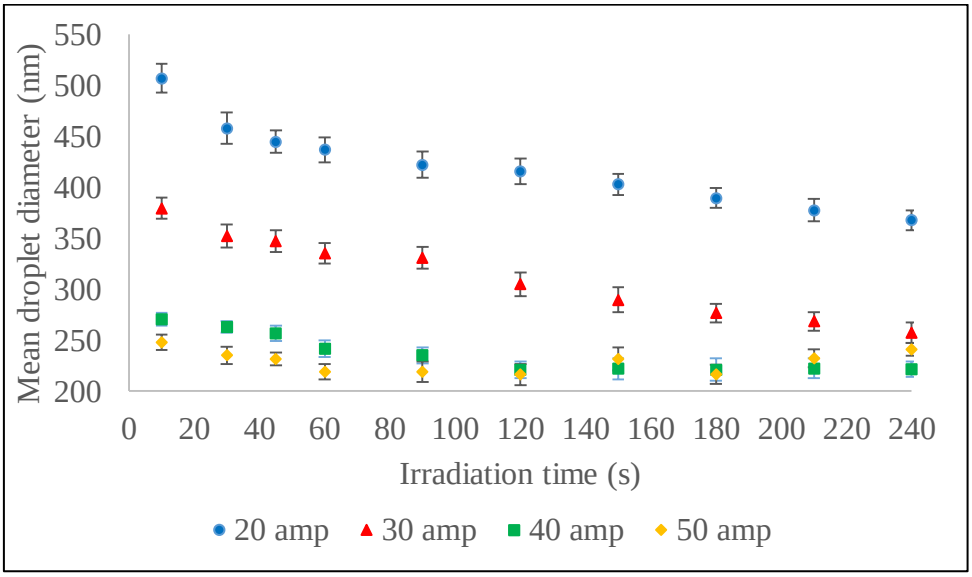


Fig. 3.5 Effect of irradiation time at different amplitude on the generated mean droplet diameter.

Besides, a plateau in MDD could be noted at 40% amplitude and irradiation time of 120 s (Fig. 3.5). The plateau showed that equilibrium was attained at 120 s as no further decrease in MDD was observed at similar concentration of emulsifier. However, the DI at the irradiation time of 180 s (0.115±0.044) was smaller as compared to the irradiation time of 120 s (0.246± 0.054) and 150 s (0.198±0.048). As the irradiation time increased, the emulsion was retained

longer in the system. This assisted to smoothen the droplet break up, thus, lowered the dispersity of formed nano-droplets. Hence, 40% amplitude and 180 s of irradiation time formed droplets with smallest MDD and DI at 221.4±1.1 nm and 0.115±0.044, respectively. The obtained smallest MDD and DI agrees well with the findings reported by Higgins and Skauen [133] in which an optimum energy for attaining the maximum effect of acoustic emulsification has been demonstrated. Table 3.4 shows the optimized parameters for the formation of palm oil-based W/O nanoemulsion using PGPR.

Table 3.4 Optimized parameters for the formation of palm oil-based W/O nanoemulsion using ultrasonicator.

Parameters	Optimized values
Amplitude (%)	40
Irradiation time (s)	180
PGPR concentration (%)	3
Mean droplet diameter (nm)	221.4±1.1
Dispersity index	0.115±0.044

3.3.2.2 Effect of microfluidizer parameters (operating pressure and number of cycles) on the formation of W/O nanoemulsion

As shown in Fig. 3.6, for all the evaluated operating pressure, the MDD decreased with increased number of cycles. This is in agreement to the existing studies [9, 70]. Higher operating pressure increases the flowrate and velocity of two streams entering the interaction chamber in the microfluidizer. The higher velocity results in higher shear rate forming smaller MDD when the streams impinge against each other. This can be explained using Eq. 3.3, where ΔP is the Laplace pressure, γ is the oil-water interfacial tension, and R is the radius of curvature. It could

be noted that as the droplets get smaller, Laplace pressure in the droplets becomes higher, requiring high energy source for droplet breakup. Hence, an increase in the supplied energy is required to overcome the Laplace pressure to form smaller droplets.

$$\Delta P = 2\gamma/R \qquad \text{Eq. 3.3} \qquad [234]$$

However, at 350 bar, a plateau was observed after 6 cycles. Here, maximum droplet break-up occurred to obtain the smallest MDD and DI. This indicates that an operating pressure of 350 bar is optimum to obtain the lowest MDD. The optimized parameters for the formation of W/O nanoemulsion using microfluidizer are shown in Table 3.5. The smallest droplet size was obtained at 209.8±0.5 nm with DI at 0.012±0.032 at an operating pressure of 350 bar with 6 cycles.

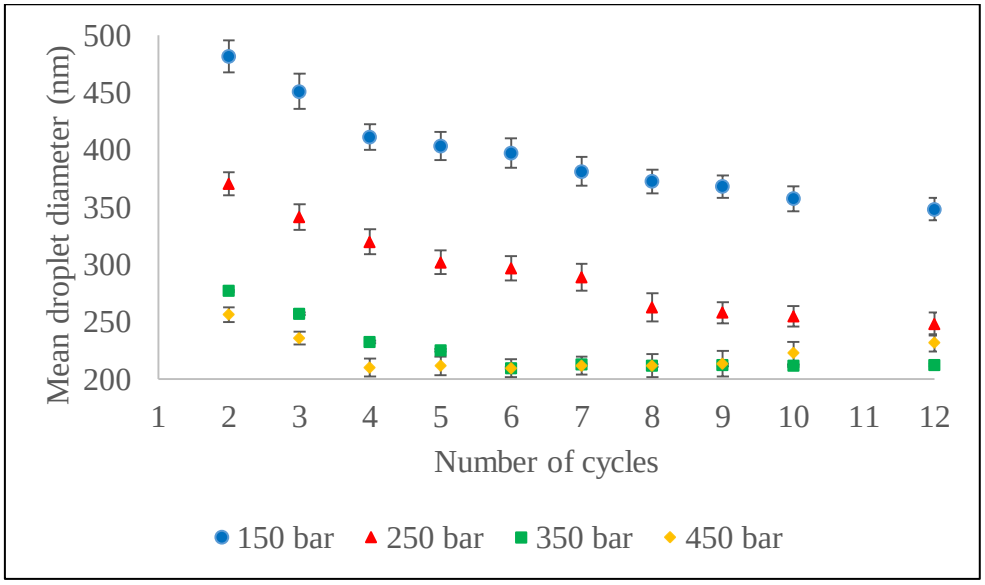


Fig. 3.6 Effect of the number of cycles at different operating pressure on the resultant mean droplet diameter of formed W/O nanoemulsion.

Table 3.5 Optimized parameters for the formation of palm oil-based W/O nanoemulsion using a microfluidizer.

Parameters	Optimized values
Operating pressure (bar)	350
Number of cycles	6
PGPR concentration (%)	3
Mean droplet diameter (nm)	209.8±0.5
Dispersity index	0.012±0.032

Additionally, for both ultrasonicator (50% amplitude) and microfluidizer (450 bar), MDD did not decrease further in comparison to the optimized MDD at 40% amplitude (~220 nm) and 350 bar (~210 nm), respectively. The droplet size of emulsion is the result of an equilibrium of droplet break-up and its recoalescence [8]. The energy induced by ultrasonicator and microfluidizer led to droplet disruption, followed by the stabilization of fresh interface by the emulsifier to prevent the recoalescence of newly formed droplets [9]. Hence, beyond the optimized parameters at the same emulsifier concentration, the droplet breakup and recoalescence did not result in further reduction of MDD.

Furthermore, at 50% amplitude and 240 s of irradiation time, an increase in MDD by 8.95% as compared to the optimum droplet size (~220 nm) was noted. Also, at 450 bar and 12 cycles, an increase in MDD was observed by 10.49% as compared to the optimum droplet size (~210 nm). This shows that supplying more energy beyond optimum level did not lower the MDD, but, led to an increase in MDD. This phenomenon shows the occurence of 'over-processing'. Over-processing leads to recoalescence of droplets at higher pressure/amplitude and at longer emulsification time. This can result in an increase in MDD especially due to

insufficient concentration of emulsifier in the system. However, from this system, over-processing and an increase in MDD occurred despite the presence of sufficient emulsifier concentration at CMC. This is probably because of the continuous supply of energy which caused the system to become unstable. It is suggested that this could have energised the droplets and caused constant collision among the droplets. This might have depleted the emulsifier layering at the oil-water interface leading to the increase in the MDD due to the recoalescence.

3.3.2.3 Energy consumption

Based on optimisation, a final droplet size of 221.4±1.1 nm and 209.8±0.5 nm were obtained using ultrasonicator and microfluidizer, respectively. Energy consumption was calculated using Eq. 3.4 for ultrasonication and Eq. 3.5 for microfluidization, where m is the mass, Cp is the specific heat capacity, ΔT is the difference between initial and final temperature, P is the operating pressure, Q is the volumetric flowrate and t is the residence time. Based on the performed calculation, ultrasonicator required 4.65 kJ of energy, while the microfluidizer required 42.08 kJ to obtain a nanoemulsion with MDD of ~215 nm. For taking into account the required volume for processing, energy density was calculated using Eq. 3.6. 50 ml and 200 ml of volume was required for processing W/O nanoemulsion using ultrasonicator and microfluidizer, respectively. 2.3 times higher energy density was required by microfludizer than ultrasonicator for producing W/O nanoemulsion. The differences in the energy consumed by microfluidizer and ultrasonicator could be associated to the different working principles of the equipment. Microfluidizer utilizes pump to create high pressure for shearing action in the interaction camber to form nano-droplets. While, ultrasound employs cavitation and implosion of the formed bubbles to break the droplets into nano-size. This agrees to the observations of Tang et al. [9] where they reported the requirement of higher energy for microfluidizer as compared to ultrasonicator by 18 times. The formation O/W nanoemulsion by Tang et al. [9]

as compared to the formation W/O nanoemulsion in this study could have influenced the differences in the energy requirements between these studies.

Energy consumption for ultrasound (kJ) = m (kg) x Cp (kJ/kg°C) x ΔT (°C) Eq. 3.4

Energy consumption for microfluidizer (kJ) = P (kPa) x Q (m^3/s) x t (s) Eq. 3.5

Energy density, kJ/m^3= $\frac{\text{Energy comsumption (kJ)}}{\text{Sample volume } (m^3)}$ Eq. 3.6

3.3.2.4 Oxidation of nanoemulsion

Three analyses were performed to evaluate the oxidation of nanoemulsion. Firstly, the peroxide value was calculated to assess whether the high energy generated by ultrasonicator or microfluidizer oxidized the fatty acid of oil. As shown in Table 3.6, the peroxide value remained constant before and after nanoemulsion formulation at ~15 meq/kg using both ultrasonicator and microfluidizer. This indicates that primary oxidation products were not formed in both the emulsion processed using ultrasonication and microfluidization.

Table 3.6 Comparison of peroxide values for the formation of palm oil-based W/O nanoemulsion.

W/O emulsion	**Peroxide value (meq/kg)**	
	After sample preparation	**After 1 week**
Coarse	15.2	15.3
Ultrasonicator processed	15.4	15.6
Microfluidizer processed	15.2	15.4

As shown in Table 3.7, the fatty acid compositions of C10:0, C12:0, C14:0, C16:0, C16:1, C18:0, C18:1, C18:2 and C18:3 after processing under ultrasonicator and microfluidizer

did not change significantly as compared to the coarse emulsion (before processing). For all the fatty acid compositions, the maximum difference was <3.33% as compared between before processing and after processing (both ultrasonicator and microfluidizer). This observed change could be due to the measurement errors from the instrument.

Table 3.7 Comparison of fatty acid composition for the formation of palm oil-based W/O nanoemulsion.

Fatty acid	Before processing		Ultrasonicator processed		Microfluidizer processed	
	Mean	SD	Mean	SD	Mean	SD
C10:0	0.02	0	0.02	0	0.02	0
C12:0	0.30	0	0.29	0	0.29	0
C14:0	0.99	0.01	0.97	0.01	0.98	0.01
C16:0	37.64	0.34	37.65	0.31	37.63	0.26
C16:1	0.71	0.02	0.69	0.03	0.72	0.03
C18:0	4.00	0.10	4.01	0.10	3.98	0.09
C18:1	44.16	0.14	44.15	0.11	44.17	0.11
C18:2	11.43	0.21	11.48	0.22	11.46	0.23
C18:3	0.74	0.03	0.73	0.03	0.74	0.03
C20:0	0.03	0	0.03	0	0.03	0

Thirdly, FTIR analysis was carried out to determine any structural change before and after the processing of W/O emulsion. As shown in Fig. 3.7, the FTIR spectra remained unchanged between before and after processing (both ultrasonicator and microfluidizer). The absence of key functional groups such as aldehydes (C=O stretch at 1750-1625 cm^{-1}, C-H stretch off C=O at 2850-2800 cm^{-1}, and C-H stretch off C=O at 2750-2700 cm^{-1}), ketones (C=O stretch at 1750-1625 cm^{-1}) and carboxylic acid (C=O stretch at 1730-1650 cm^{-1} and hydrogen-bonded O-H stretch at 3400-2400 cm^{-1}) show that no secondary oxidation products were formed

due to processing under ultrasonicator as well as microfluidizer. This shows that the processed W/O nanoemulsion did not oxidize under processing of ultrasonicator and microfluidizer. For ultrasonicator processed nanoemulsion, cooling was provided for the emulsion during processing by immersion in a water bath. While, microfluidizer processed nanoemulsion utilizes shearing principle for droplet break-up which was also supplemented with a cooling jacket and water bath to ensure cooling in the emulsion. The utilized cooling system for both ultrasonicator and microfluidizer could have prevented oxidation of the emulsion which can be promoted at high temperature. Similar findings of the absence of oxidation products processed using ultrasonicator were also reported in existing studies [235, 236]. Comparisons were not made possible with emulsion processed using microfluidizer since limited studies reported on this.

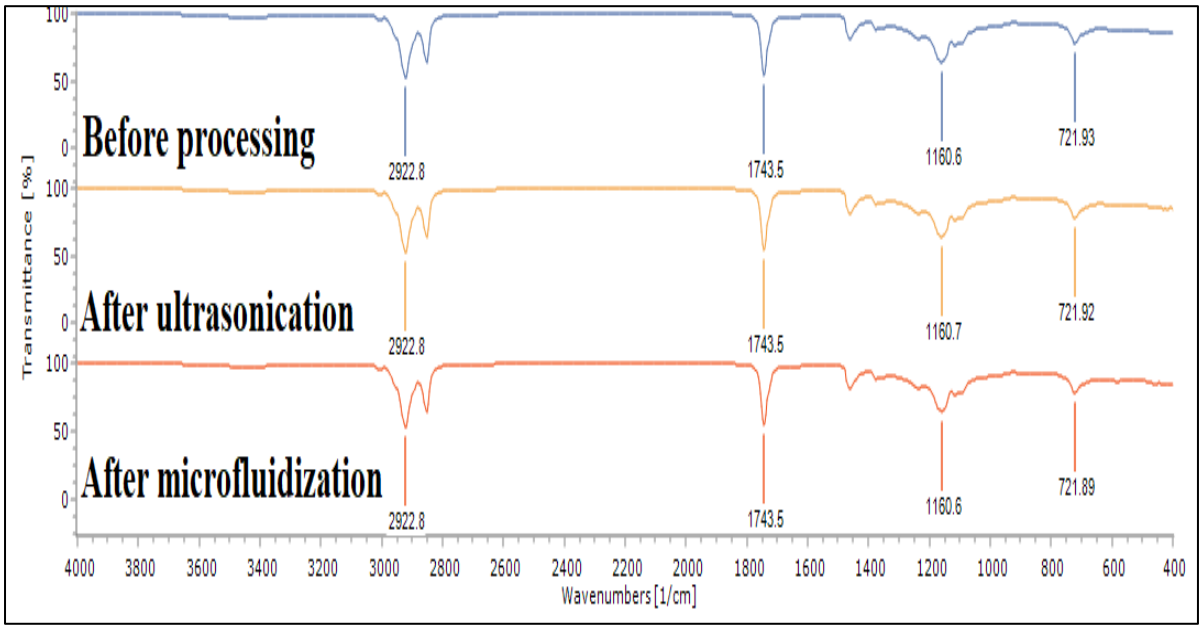


Fig. 3.7 Comparison of FTIR spectra in the formation of palm oil-based W/O nanoemulsion using ultrasonicator and microfluidizer.

3.3.3 Effect of phase volume ratio (oil to water) on the formation of W/O nanoemulsion

From Fig. 3.8, it could be noted that 180 s of total irradiation time was required to obtain smallest MDD (~220 nm) for the formed W/O nanoemulsion at 80:20 phase volume ratio. While, for 90:10 phase volume ratio, only 120 s of total irradiation time was required. As the dispersed phase volume decreased, lower irradiation time was required for the droplet break-up and for the stabilisation of new interface to achieve equilibrium at the same amplitude [237].

The MDD at 120 s was larger by 8.33% at the phase volume ratio of 80:20 as compared to 90:10 (Table 3.8). Furthermore, after a week, the MDD increased by 9.84% and 3.48% for phase volume ratio of 80:20 and 90:10, respectively. In a study by Mollakhalili Meybodi et al. [238], the authors reported smaller MDD for higher oil to water ratio. At a fixed emulsifier concentration and a higher dispersed phase volume ratio, there is a possibility of incomplete coverage of emulsifier onto the oil-water interface which could increase the MDD due to coalescence [237].

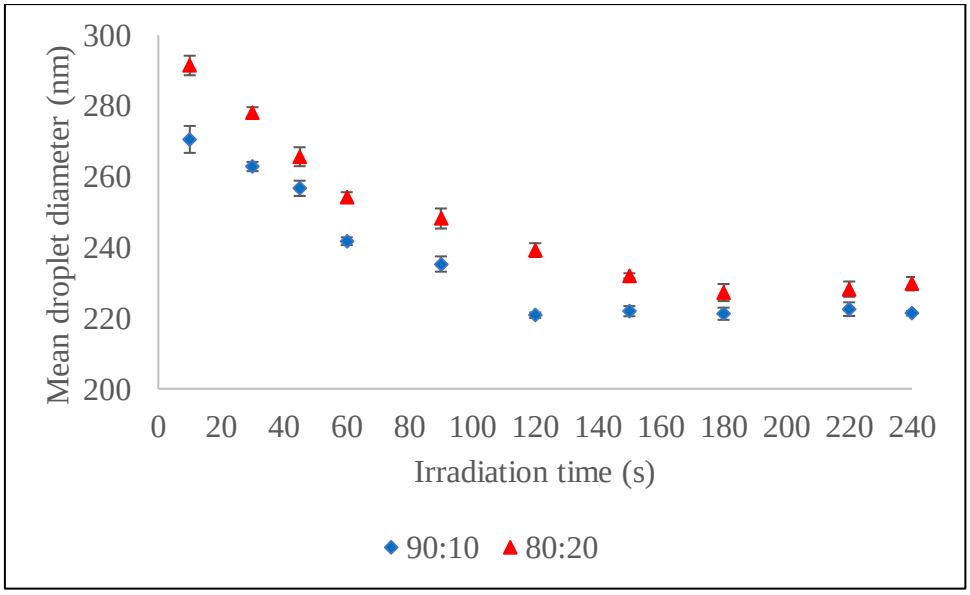


Fig. 3.8 Effect of irradiation time at 40% amplitude for different phase volume ratio on the mean droplet diameter of formed W/O nanoemulsion.

Table 3.8 Properties of W/O nanoemulsion formed at different phase volume ratio.

The phase volume ratio of oil:water	Sedimentation index (%)	Mean droplet diameter (nm)		Dispersity index	
	1 week	Initial	1 week	Initial	1 week
90:10	0	221.4±1.1	229.1±1.0	0.115±0.011	0.121±0.002
80:20	2.83±0.02	229.7±0.3	252.3±0.9	0.358±0.044	0.517±0.031

Distinctly, the obtained DI was high at ~0.4 (polydispersed) for 80:20 phase volume ratio, while the DI was around 0.1 (monodispersed) for 90:10 of phase volume ratio. After 1 week, 2.83% of SI was observed for phase volume ratio of 80:20 while, no sedimentation was observed for 90:10, as shown in Table 3.8. The higher DI and SI for phase volume ratio 80:20 could also be related to the incomplete coating of emulsifier at the oil-water interface of the droplets as compared to the 90:10. These could have prevailed coalescence. As the DI was initially higher for phase volume ratio of 80:20 (0.358±0.044) than at 90:10 (0.115±0.011), it is suggested that the smaller droplets could have merged into larger droplets due to Ostwald ripening [152]. Thus, W/O nanoemulsion with a phase volume ratio at 90:10 had better stability as compared to 80:20.

3.3.4 Effect of palm MCT oil, soybean lecithin and NaCl on the formation and stability of W/O nanoemulsion

3.3.4.1 Effect of blending of palm oil and palm MCT oil on the formation of W/O nanoemulsion

Notably, when higher amount of palm MCT oil was used, the viscosity of W/O nanoemulsion decreased, as shown in Table 3.9. From Fig. 3.9, as the irradiation time increased, MDD decreased and a plateau was observed for all the cases (0 wt%, 30.0 wt%, 50.0 wt% and 100.0 wt% blend of MCT oil). However, when 100.0 wt% and 70.0 wt% of palm oil were utilized in

the oil phase, independently, the plateau was observed at 120 s. Whereas, W/O nanoemulsion formed with 50.0 wt% and 0 wt% of palm oil in the oil phase, independently, a plateau was observed at 60 s. Thus, higher amount of palm MCT oil in the emulsion shortened the irradiation time required for obtaining the smallest MDD. Additionally, as shown in Table 3.10, when higher amount of palm MCT oil was used, the MDD of W/O nanoemulsion obtained decreased. The MDD was smallest at 187.1±0.7 nm when 100.0 wt% of MCT oil was utilized.

Table 3.9 Viscosity of W/O nanoemulsion formed at different palm oil to palm MCT oil blend ratio.

Palm oil:Palm MCT oil blend ratio	**Viscosity (cP)**
100:0	171.6 ± 5.3
70:30	127.3 ± 7.7
50:50	109.6 ± 5.7
0:100	67.6 ± 8.1

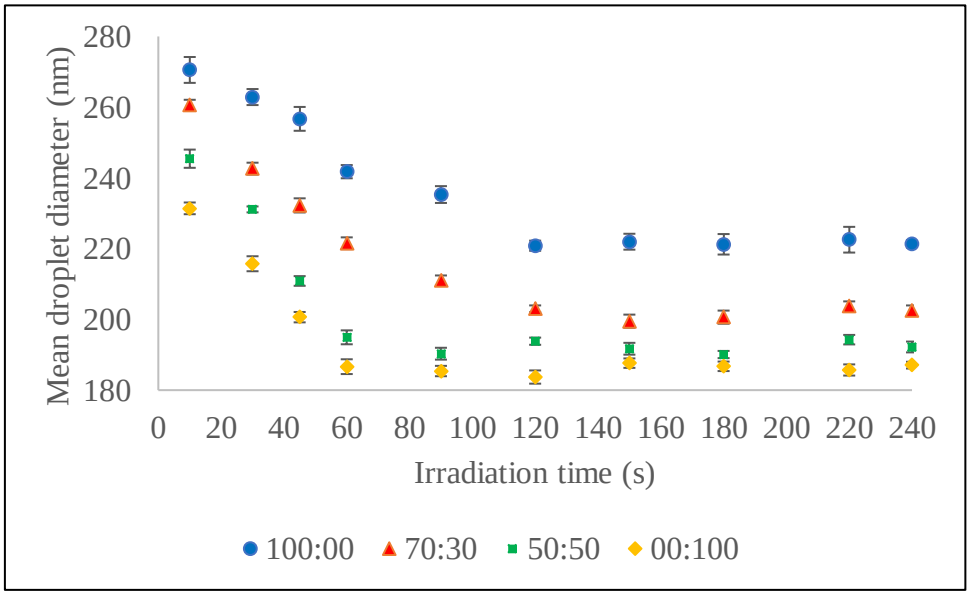


Fig. 3.9 Mean droplet diameter at different palm oil to palm MCT oil blend ratio.

Table 3.10 Properties of W/O nanoemulsion formed at different palm oil to palm MCT oil blend ratio.

Palm oil: Palm MCT oil blend ratio	Sedimentation index (%)	Mean droplet diameter (nm)		Dispersity index	
	1 week	Initial	1 week	Initial	1 week
100:0	0	221.4±1.1	229.1±1.3	0.115±0.011	0.121±0.002
70:30	0.85± 0.005	207.9±1.3	208.7±0.5	0.125±0.003	0.140±0.007
50:50	1.51± 0.008	197.2±1.1	201.5±0.4	0.151±0.005	0.166±0.004
0:100	3.82±0.008	187.1±0.7	191.5±0.4	0.112±0.007	0.116±0.004

The shorter irradiation time required to produce the smallest MDD with the utilization of higher amount of palm MCT oil could be related to the viscosity of the formed W/O nanoemulsion. In ultrasound cavitation, there is formation, growth and implosive collapse of bubbles [7]. Cavitation leads to highly localized turbulence driven by the intense shock waves generated from the implosion sites. These implosions which are highly influenced by the viscosity of the emulsion, induce powerful shock waves forming high velocity liquid jets which are suggested to promote droplet break-up and mixing of the emulsion [134]. High viscosity of emulsion is suggested to suppress implosion and also reduce the radiation of powerful shockwaves [239, 240]. This is inline with the study reported by Tang et al. [9]. The authors indicated that smaller MDD could be produced by using less viscous medium due to better propagation of acoustic waves generated by the transducer. This observation has also been reported in other existing study [241].

After 1 week of storage, sedimentation was not observed in W/O nanoemulsion with 100.0 wt% of palm oil whereas 100.0 wt% of palm MCT oil produced highest SI. This could also be related to the viscosity of the emulsion, where at lower viscosity the mobility of droplets

increased. This could have prevailed flocculation of droplets and led to the increase in SI. Tadros et al. [152] suggested that Brownian motion could have increased the mobility of droplets within the continuous oil phase.

However, as shown in Table 3.10, the MDD and DI of W/O nanoemulsion showed a maximum change of <3.48% and <5.22%, respectively, after a week for all the cases (0 wt%, 30 wt%, 50 wt% and 100 wt% blend of MCT oil). It could be assumed here that coalescence did not occur predominantly, as the emulsifier (PGPR) in the system could coat the droplets thoroughly at the interface. Additionally, it is proposed that the blending of palm oil and palm MCT oil resulted in a strong interaction between the fatty acid chains (hydrophobic moieties) of the mixture of oils with PGPR at the oil-water interface, preventing coalescence. This is also supported by Wooster et al. [89], where the authors showed that the blending of oil which consists of long-chain triglyceride by at least 50% for the formation of nanoemulsion, enabled the prevention of Ostwald ripening. Therefore, to incorporate palm MCT oil in the oil phase of W/O nanoemulsion formulation, the blending of palm oil to palm MCT oil at 70:30 is found to be appropriate to form a stable formulation.

3.3.4.2 Effect of blending of lecithin with PGPR on the formation of W/O nanoemulsion

In this study, it was observed that by using 3.0 wt% of emulsifier consisting of only lecithin led to the formation of a condensed gel-like structure. With a dilution test, the type of nanoemulsion formed was confirmed to be O/W nanoemulsion as it did not dissolve in the oil phase. This trend was also observed by Atluntas et al. [191], when only lecithin was used to form W/O nanoemulsion without blending with PGPR.

Through the dilution test (nanoemulsion dissolved in oil), the blending ratios of lecithin to PGPR at 1:2 and 2:1 were found to enable the formation of W/O nanoemulsion. The viscosity

of formed W/O nanoemulsion was lower with lesser concentration of lecithin (Table 3.11). Additionally, when W/O nanoemulsion was stabilized by lecithin to PGPR blend ratio of 2:1, the MDD was more than 1 µm with DI at 1. While, at the blend ratio of 1:2, the MDD was <500 nm but with a high DI of ~0.7 (polydispersed). This could be linked to the viscosity of the formed W/O nanoemulsion. The viscosity of lecithin is 120,000 cP at 25 ℃. The high viscosity of emulsion resulted in increased flow resistance and absorbing effect of the emulsion medium, hindering the turbulence effect of shock waves generated at the implosion sites. Also, it could be possible that the cavitation-induced disruptive forces at 40% amplitude was not able to break-up the droplets in the viscous medium [237].

Table 3.11 Properties of W/O nanoemulsion stabilized with a blend of lecithin and PGPR.

Lecithin: PGPR blend ratio	**Validation (Dilution test)**	**Viscosity (cP)**	**Mean droplet diameter (nm)**	**Dispersity index**
2:1	W/O	412.7±16.5	>1000	1
1:2	W/O	317.3±15.2	449.3± 11.4	0.683±0.024
0.5:2.5	W/O	191.3± 8.2	208.9±5.8	0.197±0.012
0:3	W/O	127.3±7.7	207.9±1.3	0.125±0.003

From Table 3.11, it could also be noted that when the lecithin to PGPR blend ratio of 0.5:2.5 was used, a stable W/O nanoemulsion with MDD 208.9±5.8 nm with and DI of 0.197 ±0.012 (monodispersed) was achieved. Fig. 3.10 shows the formation of W/O nanoemulsion from 70.0 wt% of palm oil and 30.0 wt% of palm MCT oil with and without lecithin blend in PGPR. Both the formulation with and without lecithin resulted in MDD of ~210 nm as shown in Fig. 3.10. However, for the formulation without lecithin, the equilibrium MDD (no further drop) was attained at 120 s. While, for the formulation with lecithin, the equilibrium MDD was attained at 180 s. So, the formulation with lecithin required longer duration by 60 s to attain

equilibrium MDD as compared to the formation without lecithin. The increase in the irradiation time is linked with the viscosity of W/O nanoemulsion. As illustrated earlier, an increase in the viscosity in the nanoemulsion could inhibit the propagation of acoustic waves generated by the transducer leading to a decrease in the droplet break-up rate [237]. Additionally, in a study by Ushikubo and Cunha [144], the authors summarized that lecithin molecules migrate slowly toward the oil-water interface probably due to the presence of charged groups in the hydrophilic moiety. This slow migration could also influence the increase in irradiation time for the formation of W/O nanoemulsion with lecithin.

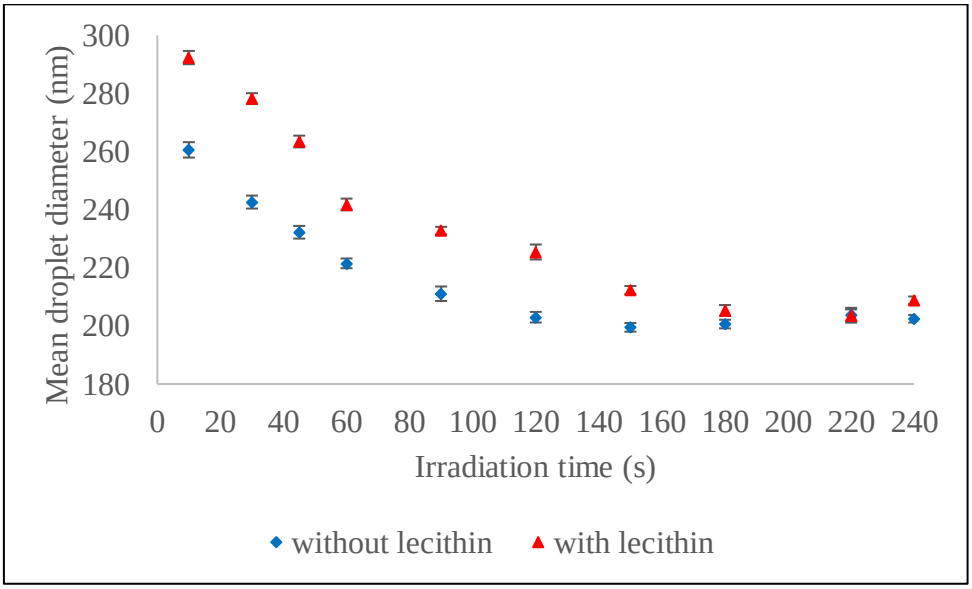


Fig. 3.10 Comparison of the mean droplet diameter of the formed W/O nanoemulsion with and without lecithin blend at amplitude of 40%.

3.3.4.3 Effect of addition of NaCl on the formed W/O nanoemulsion

From Table 3.12, lower initial MDD by 50 nm was obtained from W/O nanoemulsion stabilized using PGPR-lecithin blend with NaCl as compared to without NaCl. However, much lower initial MDD by 20 nm was obtained from W/O nanoemulsion stabilized using PGPR with NaCl as compared to PGPR-lecithin blend with NaCl. Therefore, adding NaCl provided a positive impact by contributing to a decrease in its MDD. The W/O nanoemulsion formed only by PGPR with NaCl addition caused a higher drop in MDD due to the viscosities of the formed emulsion. The addition of lecithin (with NaCl) increased the viscosity, and thus the propagation of acoustic waves could have been hindered, leading to a lesser decrease in MDD as compared to without lecithin (with NaCl).

Additionally, emulsification process includes two steps: the break-up of droplets and stabilization of the freshly generated interface by the emulsifier to prevent recoalescence of the newly formed droplets. Jafari et al. [135] concluded that a reduction in recoalescence was more important than improving the disruption of droplets. In other words, MDD is influenced not because of a stronger droplet break-up, but rather with a better stabilization of the disrupted droplets. With regards to this, when NaCl was added into the water phase, being an ionic compound, it dissociated into Na^+ and Cl^- in water. Thus, these ions improved the stability at the oil-water interface.

Table 3.12 Comparison of mean droplet diameter for the formed W/O nanoemulsion with different stabilizers.

Stabilizers for W/O nanoemulsion		**Sedimentation index (%)**	**Mean droplet diameter (nm)**		**Dispersity index**	
		2 weeks	**Initial**	**2 weeks**	**Initial**	**2 weeks**
PGPR and lecithin at 2.5:0.5	Without NaCl	0	205.3±0.4	229.1±4.0	0.133±0.024	0.190±0.042
PGPR and lecithin at 2.5:0.5	With NaCl (2.0 M)	0	166.3±5.0	186.5±4.2	0.154±0.031	0.177±0.045
Only PGPR at 2.5%	With NaCl (2.0 M)	0	143.1±8.8	151.2±6.5	0.131±0.094	0.156±0.025

The stability at the oil-water interface could be through electrostatic or steric repulsions [152]. In the absence of NaCl, only steric repulsion exists. The emulsifiers, lecithin and PGPR in the W/O nanoemulsion coat the droplets thereby providing a barrier for the interaction of droplets. However, in the presence of NaCl, an additional electrostatic repulsion also exists. The ions in the water caused repulsion in the droplets and led to improved stability due to the reduced recoalescence which resulted in a decrease in MDD. Márquez et al. [181] concluded that the stabilizing effect of calcium salt was attributed to the decrease in the size of water droplets, a decrease in the attractive force between water droplets, as well as due to an increase in the adsorption density of the emulsifier. This is in agreement with the studies of Scherze et

al. [182] where they demonstrated the necessity of NaCl to obtain a stable emulsion prepared with PGPR that could resist coalescence.

With the addition of NaCl, both the W/O nanoemulsions stabilized by the blends of PGPR and lecithin, as well as only PGPR, showed a reduction in MDD. To ensure long-term stability of the emulsion, it is firstly governed by the emulsifier interaction at the oil-water interface, followed by the smallest droplet size and finally the viscosity. Smaller droplets of 20 nm and better stability at the oil-water interphase were obtained by W/O nanoemulsion formulated using PGPR with NaCl as compared to PGPR with lecithin and NaCl stabilized W/O nanoemulsion. Therefore, PGPR with NaCl would be used.

A further study was carried out to evaluate the MDD of W/O nanoemulsion formed with different concentrations of NaCl at 0.1, 0.5, 1.0 and 2.0 M. As shown in Table 3.13, a maximum change of <7.84% or <10.4 nm in MDD was observed as a result of varying the concentration of NaCl between 0.1 and 2.0 M. Beyond the required concentration of NaCl, the ions are suggested to be saturated throughout the bulk water phase and not just at the interface which do not further reduce the MDD. This observed outcome corroborates with the study reported by Wolf et al. [242] in which the authors highlighted that NaCl concentration did not have significant impact on the MDD. In choosing the suitable NaCl concentration based on the results obtained, 0.1 M and 2.0 M of NaCl concentration is observed to produce MDD beyond 140 nm. While, 0.5 M and 1.0 M of NaCl concentration produced MDD below 135 nm. Notably, despite the 1.0 M of NaCl concentration produced 1.66% higher MDD than 0.5 M, 1.0 M resulted in 8.55% lower DI than 0.5 M. Since lower DI reflects more uniform MDD, 1.0 M was chosen as the suitable NaCl concentration and would be used for subsequent work.

Table 3.13 Comparison of mean droplet diameter for the formed W/O nanoemulsion with different concentration of NaCl.

NaCl concentration (mol/dm^3)	0.1	0.5	1	2
Mean droplet diameter (nm)	141.3±6.1	132.7±7.9	134.9±5.3	143.1±8.8
Dispersity index	0.155±0.051	0.152±0.0420	0.139±0.072	0.131±0.094

3.3.5 Morphological analysis of formed W/O nanoemulsion using STEM

Fig. 3.11 shows the STEM image of W/O nanoemulsions produced from optimized parameters of 40% amplitude, 180 s irradiation time, 2.5 wt% PGPR, 90:10 phase volume ratio and 1.0 M NaCl. The morphology of the STEM image revealed that the produced nanoemulsions comprised of spherical droplets. The water droplets at ~150 nm corroborates with the obtained MDD and DI from the Zetasizer at 134.9±5.3 nm and 0.139±0.072, respectively. The increase in MDD here could be attributed to the sample preparation technique of staining. Thompson et al. [243] prepared liposomes from milk fat globule membrane and analysed the morphology using electron microscopy. The authors indicated that the sample preparation technique influenced the obtained image for liposome.

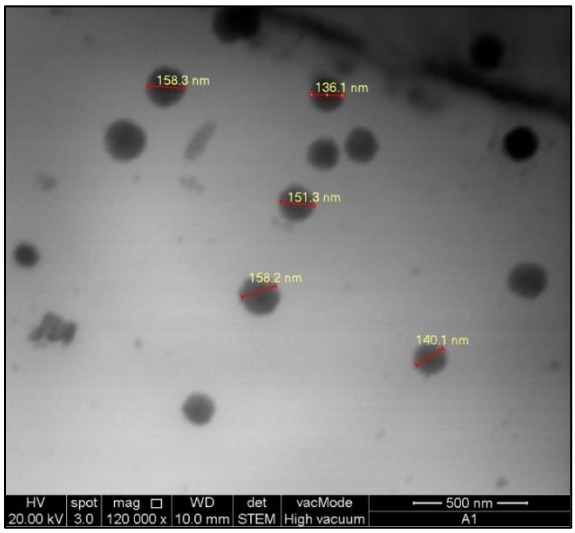


Fig. 3.11 Morphology of W/O nanoemulsion.

3.4 Summary

Despite both ultrasonicator and microfluidizer were able to form stable W/O nanoemulsion, which consists of palm oil, MCT oil, PGPR and water, the former required lower energy than the latter. Lipid peroxidation was not detected in the samples processed under both methods. Addition of MCT oil reduced the viscosity of the nanoemulsion and hence prevailed sedimentation. Although the addition of lecithin reduced the required PGPR to produce stable W/O nanoemulsion, it, however, did not decrease the MDD. While, the addition of NaCl decreased the MDD and further enhanced the W/O nanoemulsion stability through electrostatic and steric repulsions. In the next chapter, the formulation of stable palm oil-based W/O/W multiple nanoemulsion would be investigated.

CHAPTER 4: FORMULATION FOR THE GENERATION OF STABLE PALM OIL-BASED W/O/W MULTIPLE NANOEMULSION USING ULTRASONICATOR AND MICROFLUIDIZER

This chapter presents the details of investigations carried out to formulate stable palm oil-based W/O/W multiple nanoemulsion as outlined in Fig. 4.1.

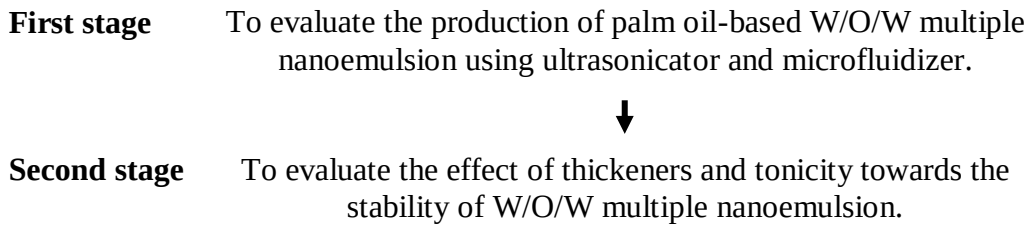


Fig. 4.1 Overview of experimentations in Chapter 4.

4.1 Background

The experimentation in this chapter to formulate stable W/O/W multiple nanoemulsion was performed after the successful formulation of stable palm oil-based W/O nanoemulsion as described in Chapter 3. In the first stage, the production of palm oil-based W/O/W multiple nanoemulsion using ultrasonicator and microfluidizer was evaluated. The energy consumption and oxidation of palm oil in the emulsion subjected to both the processing methods were discussed. The effects of varying the concentration of hydrophilic emulsifier and the phase volume ratio on the formation of W/O/W multiple nanoemulsion were also discussed.

In the second stage, the effects of thickeners and tonicity towards the stability of formulated W/O/W multiple nanoemulsion were evaluated. The effects of oil-soluble thickener (Sucragel) and water-soluble thickener (Xanthan gum) were studied for oil and internal water phases, respectively, on the stability of W/O/W multiple nanoemulsion. This is the first work

which evaluated the stabilizing effect of Sucragel for palm oil-based W/O/W multiple emulsion. For tonicity, three conditions such as hypotonic, isotonic and hypertonic were simulated by modifying the concentration of NaCl in the internal and external water phases to assess their effects on the stability of W/O/W multiple nanoemulsion.

4.2 Materials and methods

4.2.1 Materials

Palm oil, palm MCT oil and PGPR were sourced from Sime Darby (Malaysia), KLK Oleo (Malaysia) and Palsgaard (Denmark), respectively. The following chemicals were also use to produce the multiple nanoemulsion: Tween 80 from Sigma Aldrich (Malaysia), Sucragel AOF Bio from Alfa Chemicals (United Kingdom) and Xanthan gum from Sigma Aldrich (Malaysia). Deionized water produced from the Milli-Q® Plus (USA) was utilized for the generation of nanoemulsions. For STEM analysis, formvar-coated copper grid with 300 mesh procured from Agar Scientific Ltd. (United Kingdom) was used.

4.2.2 Comparison between ultrasonicator and microfluidizer for the formation of W/O/W multiple nanoemulsion

4.2.2.1 Preparation of W/O/W multiple nanoemulsion

W/O coarse and nanoemulsion were prepared using palm oil (palm oil:palm MCT oil at 70:30 ratio) as the continuous phase and deionized water as the dispersed phase using the optimized parameters presented in Chapter 3. The composition of W/O emulsion for the organic phase consisted of 2.5 wt% of PGPR and 87.5 wt% of palm oil, while the aqueous phase constituted of 10.0 wt% of deionized water with 1.0 M NaCl. The obtained coarse emulsion was then

subjected to optimized ultrasonication parameters of 180 s at 40% amplitude. This led to the formation of W/O nanoemulsion (~150 nm). The W/O nanoemulsion of 10.0 wt% was added with 89.0 wt% of deionized water and 1.0 wt% of Tween 80 to make up the W/O/W coarse multiple emulsion.

4.2.2.2 Ultrasonication for the generation of W/O/W multiple nanoemulsion

W/O/W multiple nanoemulsion was formed using VCX 750W Ultrasonic Horn Processor (USA) with 1⁄4'' (6 mm) stepped microtip in a pulse mode (60 s on and 60 s off) at 20 kHz. Amplitudes of 20, 30, 40 and 50% were utilized to produce the W/O/W multiple nanoemulsion. Irradiation time of 10, 30, 45, 60, 90, 120, 150, 180, 220 and 240 s was utilized for sonication at each amplitude. The composition of W/O/W multiple nanoemulsion constituted of 10.0 wt% of W/O nanoemulsion, 89.0 wt% of deionized water, and 1.0 wt% of Tween 80. Each generation consisted of 50 ml of sample size.

4.2.2.3 Microfluidization for the generation of W/O/W multiple nanoemulsion

M-110Y Microfluidics (USA) with the cooling jacket was also used to form W/O/W multiple nanoemulsion. Operating pressure at 150, 250, 350 and 450 bar was utilized. At each operating pressure, the effect of the number of cycles at 2, 3, 4, 5, 6, 7, 8, 9, 10 and 12 cycles on W/O/W multiple nanoemulsion formation were evaluated. The composition of W/O/W multiple nanoemulsion constituted of 10.0 wt% of W/O nanoemulsion, 89.0 wt% of deionized water, and 1.0 wt% of Tween 80. The sample size for each generation was 200 ml. The temperature was maintained below 32 °C during the preparation of coarse and generated W/O/W multiple nanoemulsion using ultrasonicator and microfluidizer.

4.2.3 Effect of phase volume ratio (water to W/O), the concentration of hydrophilic emulsifier, thickeners and tonicities on the generation of W/O/W multiple nanoemulsion

80:20 and 90:10 of phase volume ratios consisting of deionized water:W/O nanoemulsion on the generation of W/O/W nanoemulsion were evaluated. For this, 40% amplitude with an irradiation time of 10, 30, 45, 60, 90, 120, 150, 180, 220 and 240 s was employed. For the effects of concentration of hydrophilic emulsifier on the formation W/O/W multiple nanoemulsion, 0.5, 1.0 and 2.0 wt% of Tween 80 were compared. 40% amplitude and 180 s of irradiation time were employed. For the effects of thickener on the stability of W/O/W multiple nanoemulsion, oil-based thickener (Sucragel), water-based thickener (Xanthan gum) and without the addition of thickener were compared. To thicken the oil phase, firstly, during the formation of W/O nanoemulsion, 1.0 wt% of Sucragel was included in the oil phase. Whereas, for the thickening of the water phase, Xanthan gum at 1.0 wt% was added to the internal water phase during the formation of W/O nanoemulsion. This was followed with the evaluation of the stability of W/O/W multiple nanoemulsion with varying concentration of oil-based Sucragel at 0.5, 1.0 and 2.0 wt%.

Next, the effects of tonicities on the stability of W/O/W multiple nanoemulsion were also evaluated. The W/O nanoemulsion contains 1.0 M NaCl in the internal water phase (Chapter 3). To evaluate the effects of tonicities, 0.5 M, 1.0 M, and 2.0 M of NaCl in the external water phase of W/O/W multiple nanoemulsion were used to simulate hypotonicity, isotonicity, and hypertonicity, respectively. For the effects of thickeners and tonicity towards the stability of W/O/W multiple nanoemulsion, 40% amplitude and 180 s of irradiation time were employed.

4.2.4 Analyses

Among the performed analyses for the generated W/O/W multiple nanoemulsion were peroxide value, FTIR, fatty acid compositions, droplet size, DI, viscosity, conductivity and water content. Peroxide value and FTIR analyses were conducted to determine the formation of primary and secondary oxidation products. Fatty acid composition analysis was performed to ascertain the changes in fatty acid composition after being processed under ultrasonicator and microfluidizer. The droplet size and DI were performed to compare the sizes of the formed droplets using ultrasonicator and microfluidizer. Viscosity, conductivity and water content analyses were performed to evaluate the stability of the generated W/O/W multiple nanoemulsion. Detailed explanations for peroxide value, FTIR, fatty acid composition, droplet size, DI, viscosity and conductivity analyses, as well as the utilized equipment, have been presented in Chapter 3 section 3.2.

For water content, the separated oil phase (supernatant) from 50 ml of the emulsion, after centrifuged at 15000 rpm for 15 min was used for the analysis. Metrohm 831 KF Coulometer (Switzerland) was used to analyse the internal water content. 2.0 g of the collected sample was utilized according to ISO 12937 [244] for the analysis of water content.

4.2.5 Imaging

The images and morphology of the generated W/O/W multiple nanoemulsion were analysed using light microscope and field emission scanning electron microscope, respectively. Nikon light microscope (Japan) was used to obtain the images of W/O/W multiple nanoemulsion. The images were captured using Nikon DS-Fi1 Camera Head and analysed using Nikon NIS-Elements D 3.0 software. No dilution was used. A drop of W/O/W multiple nanoemulsion was placed on the top of the glass slide, and the coverslip was lowered before analysis. For

morphology, the W/O/W multiple nanoemulsion sample was diluted with deionized water (1:100). This ratio was chosen as the images obtained at this ratio were clear. Detailed explanations for morphology analysis and the equipment used have been presented in Chapter 3 section 3.2.11.

Each experiment was performed twice. Two samples were collected from each experiment. Each analysis was performed twice for each sample. For the graphs in the results section, error bars based on standard errors are shown. While, for tables, error bars based on standard deviations are shown.

4.3 Results and discussion

4.3.1 Comparison between ultrasonicator and microfluidizer processing for the formation of W/O/W multiple nanoemulsion

4.3.1.1 Effect of ultrasonicator parameters (amplitude and total irradiation time) on the formation of W/O/W multiple nanoemulsion

As shown in Fig. 4.2, the MDD of W/O/W multiple nanoemulsion decreased with an increase in amplitude and irradiation time. For 20% and 30% of amplitude, a plateau for MDD was yet to form until 240 s of irradiation time. For 40% amplitude, a plateau for MDD was observed at 150 s of irradiation time. However, the DI obtained at the irradiation time of 180 s (0.248±0.011) was smaller than the irradiation time at 150 s (0.362±0.034). As such, more uniform droplets were obtained at 180 s compared to 150 s. Thus, for 40% amplitude, 180 s is the optimum irradiation time for achieving maximum droplet break-up with the usage of 1.0 wt% of Tween 80. As the sonication intensity increased, the cavitation activity was amplified enhancing the droplet breakup [7]. The obtained droplets with smaller MDD with increasing

sonication intensity in W/O/W multiple nanoemulsion is inline with other reported studies [9, 120].

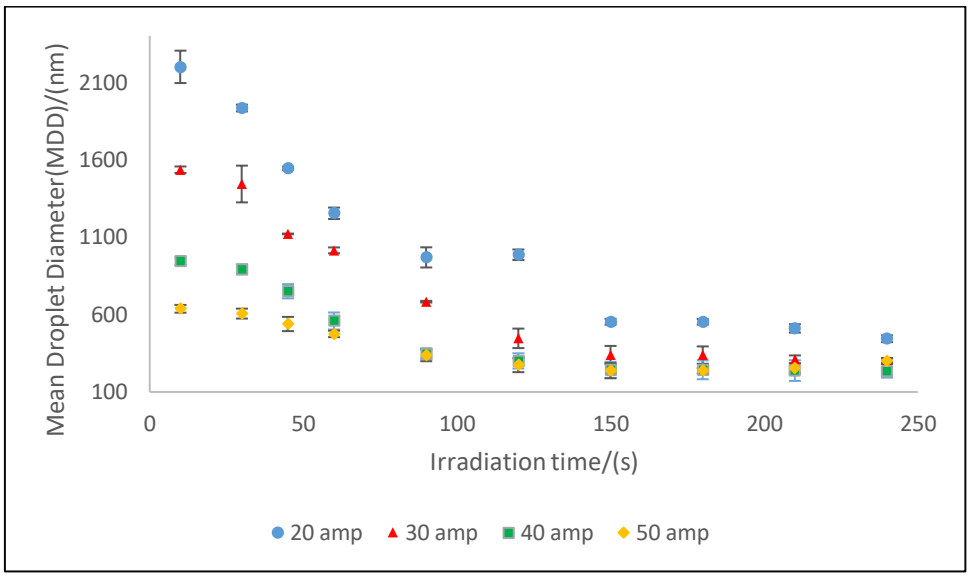


Fig. 4.2 Effect of irradiation time towards droplet size at different amplitudes.

Fig. 4.3 shows the microscopic images obtained for the W/O/W multiple nanoemulsion droplets. These images demonstrated the reduction in MDD of W/O/W multiple nanoemulsion with increased amplitude and irradiation time. The droplets of W/O/W multiple nanoemulsion became more monodispersed with increased irradiation time. However, a further increase in amplitude to 50%, despite produced droplet with MDD of ~240 nm and DI of 0.252±0.012 at a shorter irradiation time of 150 s, 26.04% of higher MDD was obtained at 240 s as compared to 40% amplitude at similar irradiation time. As the cavitation intensity increased, the power generated renders instability especially at the interface of the internal water droplets. It is suggested that the instability leads to the coalescence and droplet enlargement in the internal water droplets during the recoalescence and stabilization at the interface during processing [7]. This could cause rupture in the oil globules and hence the loss of internal water droplets, as illustrated in Fig. 4.4. This was also confirmed with the increased DI by 89.52% at 240 s for

50% amplitude as compared to the optimum condition of 180 s at 40% amplitude. Thus, in this work, 40% amplitude was observed as the optimal parameter as compared to the 50% amplitude for the formation of W/O/W multiple nanoemulsion.

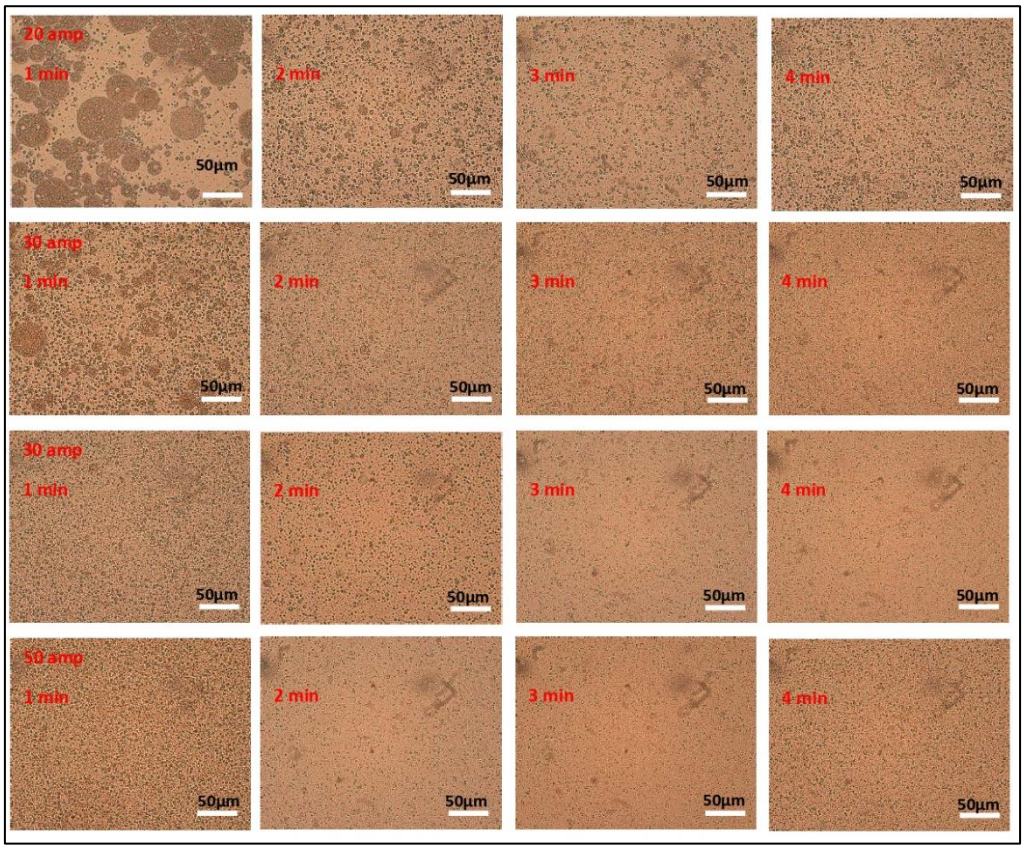


Fig. 4.3 Images of W/O/W multiple nanoemulsion with increased amplitude and irradiation time.

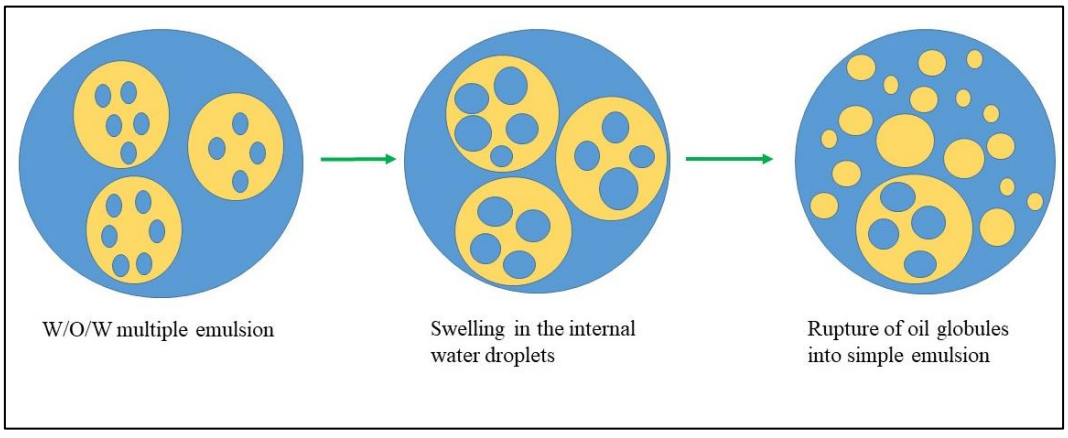


Fig. 4.4 Illustration of W/O/W multiple nanoemulsion with the movement of water between the internal and external water phases.

From Table 4.1, W/O/W multiple nanoemulsion with 243.3±10.7 nm and 0.248±0.011 of droplet size and DI, respectively, were obtained by utilizing 1.0 wt% of Tween 80 and optimized ultrasonicator at 40% and 180 s of amplitude and total irradiation time, respectively.

Table 4.1 Optimized parameters for the formation of palm oil-based W/O/W multiple nanoemulsion using ultrasonicator.

Parameters	Optimized values
Amplitude (%)	40
Irradiation time (s)	180
Tween 80 concentration (%)	1
Mean droplet diameter (nm)	243.3±10.7
Dispersity index (DI)	0.248±0.011

4.3.1.2 Effect of microfluidizer parameters (operating pressure and number of cycles) on the formation of W/O/W multiple nanoemulsion

The MDD of W/O/W multiple nanoemulsion droplets decreased with increased operating pressure and number of cycles, as demonstrated in Fig. 4.5. The higher pressure enhanced the shearing rate of droplets, resulting in the reduction of droplet sizes [7]. Similar findings were also reported in existing study [9].

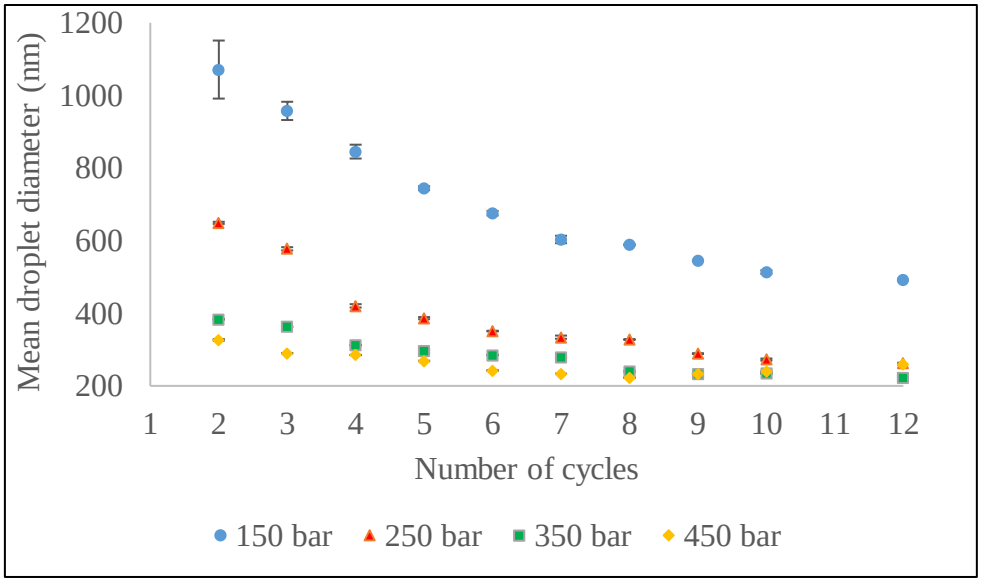


Fig. 4.5 Effect of the number of cycles towards droplet size of W/O/W multiple nanoemulsion.

For 150 bar and 250 bar, the MDD was yet to plateau up to 12 cycles. For 350 bar of operating pressure, a plateau was observed after 8 cycles. This was observed as the optimum condition to obtain MDD of 233.2±7.3 nm and DI of 0.205±0.008 at 1.0 wt% of hydrophilic emulsifier (Tween 80). Fig. 4.6 shows the microscopic images of W/O/W multiple emulsion droplets. The images exhibited reduced droplet size with increased number of cycles and operating pressure. Droplets of multiple nanoemulsion were seen to become more monodispersed as the number of cycles increased.

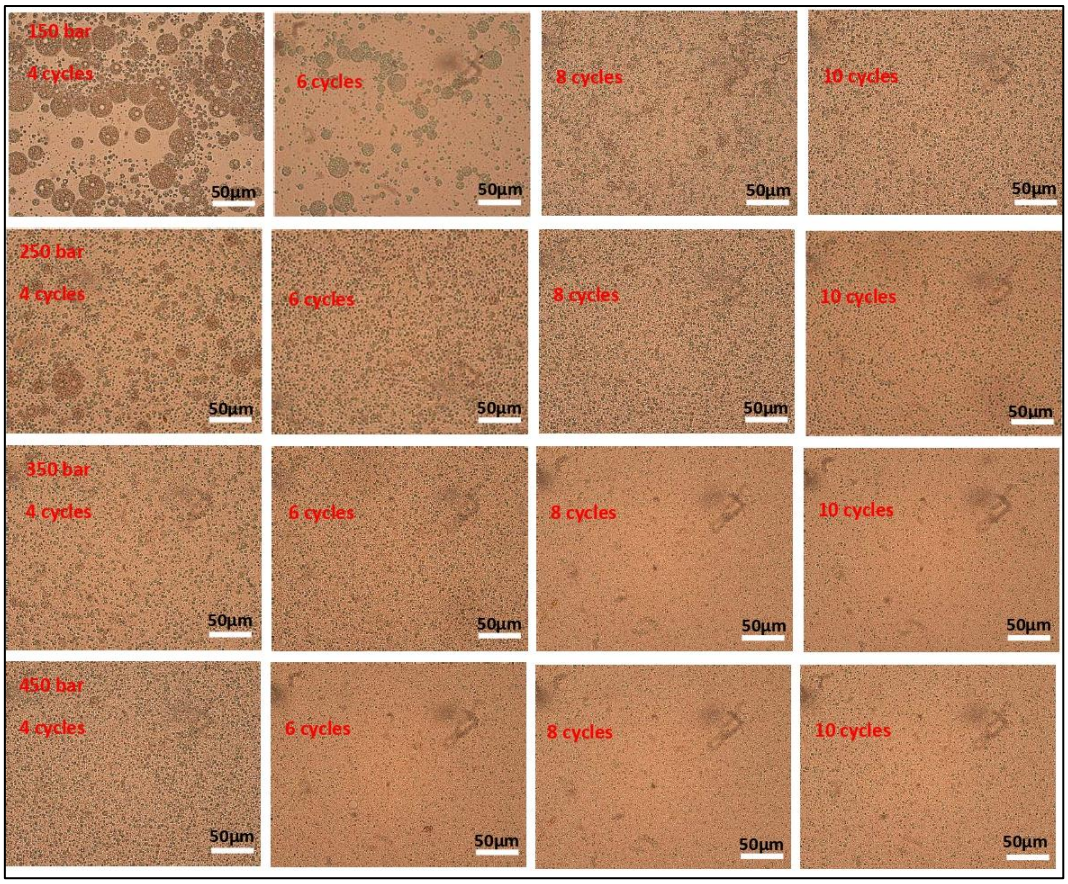


Fig. 4.6 Images of W/O/W multiple nanoemulsion with increasing operating pressure and number of cycles.

Increased operating pressure to 450 bar produced droplets with MDD ~240 nm much faster at 6 cycles. The higher operating pressure could have led to a reduction in the number of cycles required. However, microfluidization at 450 bar after 12 cycles led to increase of 16.40% and 46.80% for MDD and DI, respectively, as compared to 350 bar after 12 cycles. Increased operating pressure and number of cycles rendered instability, especially at the interface of the internal water-oil as shown in Fig. 4.4 (explained in section 4.3.1.1 for ultrasonication). This phenomenon commonly known as 'over-processing' describes the increase in MDD and DI. Thus, in this work, 350 bar was observed as the optimal parameter as compared to the 450 bar for the formation of W/O/W multiple nanoemulsion. As shown in Table 4.2, 233.2 ±7.3 nm of

MDD and 0.205±0.008 of DI was generated using microfluidizer at 350 bar of operating pressure with 8 cycles.

Table 4.2 Optimized parameters for the formation of palm oil-based W/O/W multiple nanoemulsion using a microfluidizer.

Parameters	Optimized values
Operating pressure (bar)	350
Number of cycles	8
Tween 80 concentration (%)	1
Mean droplet diameter (nm)	233.2±7.3
Dispersity index	0.205±0.008

4.3.1.3 Energy consumption

At optimum conditions, ultrasonicator and microfluidizer generated W/O/W multiple nanoemulsion with a final droplet size of 243.3±10.7 nm and 233.2.5±7.3 nm, respectively. Energy consumption was calculated using Eq. 3.4 for ultrasonication and Eq. 3.5 for microfluidization while, energy density was calculated using Eq. 3.6. The ultrasonicator and microfluidizer utilized 4.62 kJ and 53.71 kJ of energy consumption, respectively, to produce W/O/W multiple nanoemulsion with the droplet size of ~235 nm. Higher energy consumption by ~12 times was required by microfluidizer as compared to ultrasonicator to generate a comparable droplet size of ~235 nm. For processing W/O/W multiple nanoemulsion, 50 ml and 200 ml of volume was required for ultrasonicator and microfluidizer, respectively. This resulted in 2.9 times lesser energy density required by ultrasonicator than microfluidizer for processing W/O/W multiple nanoemulsion. A similar outcome was reported by Tang et al. [9], where ultrasonicator required lesser energy by 18 times than microfluidizer to produce O/W

nanoemulsion encapsulating aspirin. Tang et al. [9] utilized Lauroglycol 90 oil, Cremophor EL emulsifier and produced O/W type nanoemulsion. While, palm oil, PGPR emulsifier and W/O/W type multiple nanoemulsion was produced in this study. These differences such as different oils, emulsifiers and type of emulsion produced could be associated to the difference in the energy required between the study by Tang et al. [9] and this study.

4.3.1.4 Oxidation of W/O/W multiple nanoemulsion

Three analyses were performed to determine the oxidation of W/O/W multiple nanoemulsion processed using microfluidizer and ultrasonicator. Firstly, the peroxide value of formed W/O/W multiple nanoemulsion using ultrasonication and microfluidization remained unchanged in comparison to the coarse W/O/W emulsion at ~15 meq/kg, as shown in Table 4.3. This indicated that the primary oxidation products were absent when W/O/W multiple nanoemulsion was processed using ultrasonicator and microfluidizer.

Table 4.3 Comparison of peroxide values for the formation of W/O/W multiple nanoemulsion.

W/O /W emulsion	**Peroxide value (meq/kg)**	
	After sample preparation	**After 1 week**
Coarse	15.4	15.3
Ultrasonicator-processed	15.8	15.5
Microfluidizer-processed	15.2	15.5

Secondly, among the unsaturated fatty acid composition such as palmitoleic acid (C16:1), oleic acid (C18:1), linoleic acid (C18:2) and linolenic acid (C18:3), ~2.70% of maximum difference was observed between before and after processing under both the

equipment, independently as shown in Table 4.4. This change observed could have resulted from instrument measurement errors. This result indicated that the fatty acid composition of palm oil were not altered due to processing under ultrasonicator and microfluidizer.

Table 4.4 Comparison of fatty acid composition for the formation of W/O/W multiple nanoemulsion.

Fatty acid	Coarse emulsion		Ultrasonicator-processed		Microfluidizer-processed	
	Mean	SD	Mean	SD	Mean	SD
C10:0	0.02	0	0.02	0	0.02	0
C12:0	0.29	0	0.29	0	0.30	0
C14:0	0.97	0.01	0.98	0.01	0.98	0.01
C16:0	37.64	0.34	37.63	0.32	37.64	0.27
C16:1	0.74	0.02	0.73	0.04	0.73	0.04
C18:0	3.99	0.10	4.00	0.10	3.98	0.09
C18:1	44.17	0.14	44.17	0.11	44.15	0.11
C18:2	11.43	0.21	11.45	0.23	11.46	0.23
C18:3	0.74	0.03	0.72	0.03	0.73	0.03
C20:0	0.03	0	0.03	0	0.03	0

Thirdly, FTIR analysis was performed to ascertain any changes in terms of functional groups before and after the processing under ultrasonicator and microfluidizer, independently. From the performed three analyses to determine the oxidation of processed W/O/W multiple nanoemulsion, FTIR analysis was the most important. This is because shall oxidation had taken place, it will eventually lead to the formation of secondary oxidation products which could be detected from the FTIR spectra. As shown in Fig. 4.7, the functional groups before and after processing under both equipment, independently, remained unchanged. Importantly, key functional groups for secondary oxidation products such as carboxylic acid (hydrogen-bonded O-H stretch at 3400-2400 cm^{-1} and C=O stretch at 1730-1650 cm^{-1}), ketones (C=O stretch at

1750-1625 cm^{-1}) and aldehydes (C-H stretch off C=O at 2750-2700 cm^{-1}, C=O stretch at 1750-1625 cm^{-1} and C-H stretch off C=O at 2850-2800 cm^{-1}) were not detected. This shows that the processed W/O/W multiple nanoemulsion did not oxidize under ultrasonicator and microfluidizer. As explained in sub-section 3.3.2.4, the not oxidized multiple nanoemulsion could be related to the utilized cooling system during processing by ultrasonicator and microfluidizer, independently. The cooling system controlled the rise in temperature during processing and hence prevented oxidation from taking place. Similar findings of the absence of oxidation products were also reported in existing studies [235, 236]. However, comparison was not made possible for emulsion processed using microfluidizer since limited studies reported on the oxidation aspect.

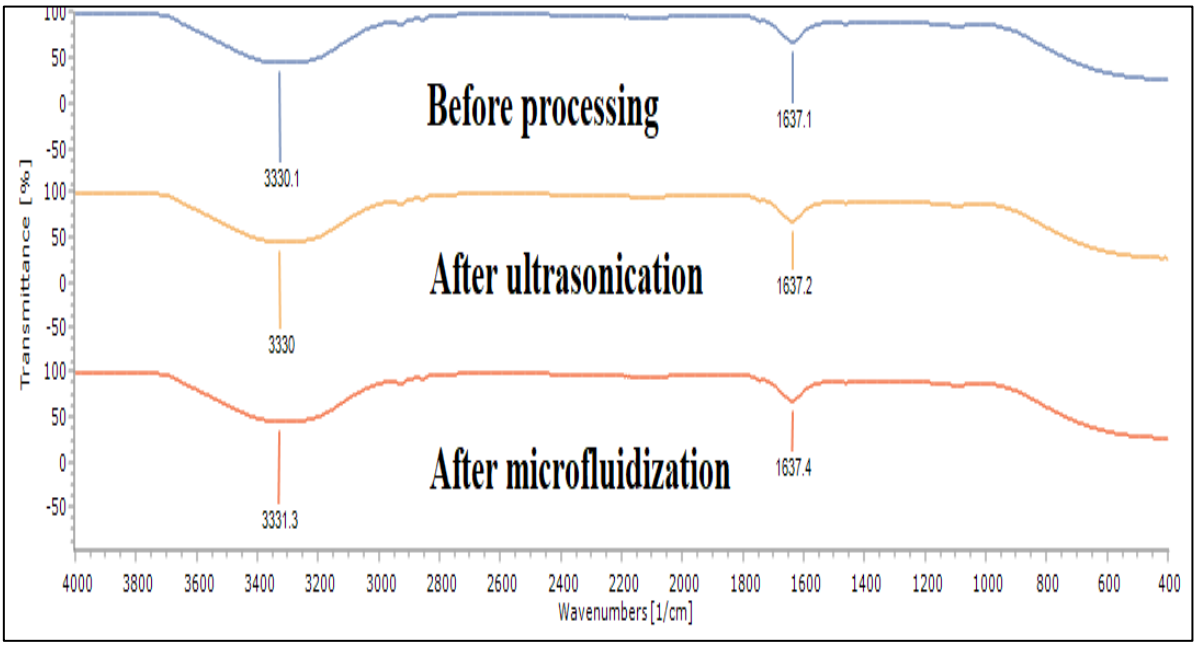


Fig. 4.7 FTIR spectra of generated W/O/W multiple nanoemulsion using ultrasonicator and microfluidizer.

4.3.2 Effect of phase volume ratio (water to W/O nanoemulsion) on the formation of W/O/W multiple nanoemulsion at 40% amplitude

Fig. 4.8 shows the comparison between the phase volume ratio of water:W/O nanoemulsion, at 90:10 and 80:20. Reductions in MDD with increase in the irradiation time for both the phase volume ratios have been noted. For 90:10 phase volume ratio, a plateau for the MDD was observed at 150 s, while, for 80:20 phase volume ratio, a plateau was not observed up to 240 s. This reflected that when higher phase volume ratio was utilized, equilibrium was not attained up to 240 s. 117.02% larger MDD was observed at 150 s for 80:20 phase volume ratio as compared to 90:10. 88.95% larger DI was observed for 80:20 (0.684±0.048) than 90:10 (0.362±0.034) phase volume ratio. From Section 4.3.1.1, the optimized parameters at 40% amplitude and 180 s of irradiation time were required for the formation of W/O/W multiple namoemulsion. However, for phase volume ratio of 80:20, these optimized parameters could not obtain droplets with smallest MDD and DI due to the presence of a higher volume of W/O nanoemulsion as compared to the phase volume ratio of 90:10. When higher volume of W/O nanoemulsion was used at similar concentration of emulsifier (Tween 80), there was insufficient concentration of emulsifier in the system to enable the formation of W/O/W multiple nanoemulsion with the smallest MDD and DI. Onuki et al. [95] reported that the increase in the W/O nanoemulsion from 14.3% to 33.3% in the W/O/W multiple nanoemulsion resulted in larger droplet size by 11.39%. The authors suggested that this was due to the agglomeration of internal droplets. This agglomeration could be related to insufficient concentration of emulsifier present in the system for further break-up of droplets or longer emulsification time that was required for the formation of droplets with lower MDD and DI at higher phase volume ratio. Similar findings were also observed in existing studies [171, 245].

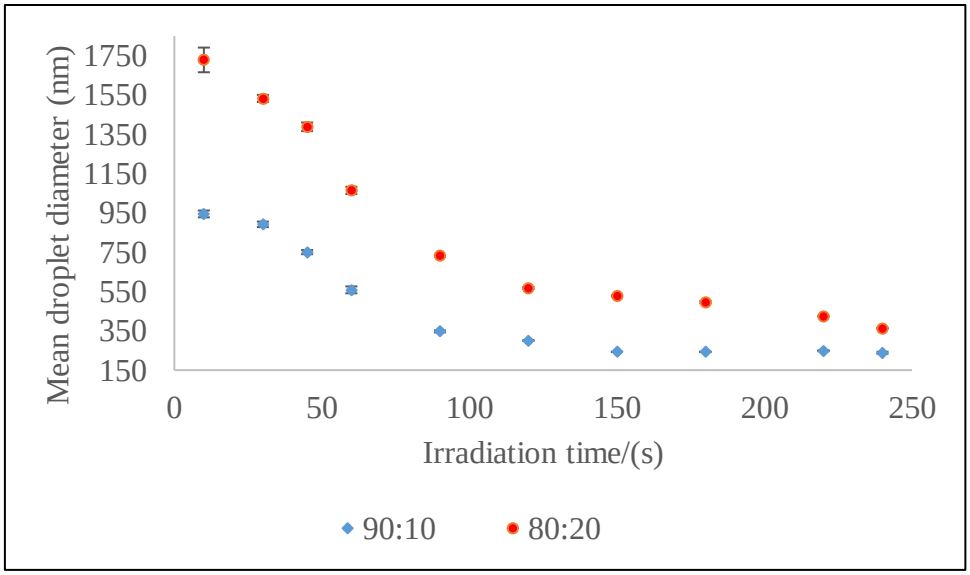


Fig. 4.8 Effect of 40% amplitude and irradiation time towards droplet size.

4.3.3 Effect of concentration of hydrophilic emulsifier (Tween 80) on the stability of W/O/W multiple nanoemulsion

The initial and after 1 week of MDD and DI were larger for W/O/W multiple nanoemulsion stabilized with 0.5 wt% of Tween 80 as compared to 1.0 wt% of Tween 80, as shown in Table 4.5. At an optimal amplitude of 40% and an irradiation time of 180 s, 0.5 wt% of Tween 80 was insufficient in obtaining a smaller droplet size as compared to 1.0 wt% of Tween 80. Therefore, it is suggested that coalescence prevailed at the water-oil interface leading to an increase in MDD and DI by 14.83% and 15.76% after 1 week, respectively.

Table 4.5 Comparison of concentration of hydrophilic emulsifier (Tween 80) for the formation of W/O/W multiple nanoemulsion.

Concentration of Tween 80 (wt%)	W/O/W multiple nanoemulsion	Initial	1 week
0.5	Mean droplet diameter (nm)	355.06±7.8	407.7±12.9
	Dispersity index	0.368±0.037	0.426±0.029
1.0	Mean droplet diameter (nm)	212.6±2.6	234.9±2.1
	Dispersity index	0.231±0.032	0.276±0.041
3.0	Mean droplet diameter (nm)	166.5±3.5	244.5±3.4
	Dispersity index	0.235±0.016	0.356±0.004
5.0	Mean droplet diameter (nm)	163.7±2.5	328.9±2.3
	Dispersity index	0.188±0.009	0.417±0.015

Furthermore, after 1 week, at 1.0 wt%, 3.0 wt% and 5.0 wt% of Tween 80, there were changes in MDD by 10.49%, 46.84%, 100.92%, and DI by 19.48%, 51.49%, and 121.81%, respectively. As the concentration of Tween 80 increased, the MDD and DI increased, which agreed with existing studies [117, 246]. The utilization of high concentration of hydrophilic emulsifier may lead to the migration of internal hydrophobic emulsifier and the external hydrophilic emulsifier. This movement can cause instability at the oil-water interfaces, promoting the movement of water in between the external and internal water phases. This led to the increase in the MDD and DI. Jiao and Burgess et al. [117] also highlighted that the micelles might carry the hydrophobic emulsifier into the external continuous water phase, hence, rupturing the oil globules and causing the loss of internal water droplets. 1.0 wt% of Tween 80 was the optimum concentration of hydrophilic emulsifier that can be used to formulate W/O/W multiple nanoemulsion.

4.3.4 Effect of thickener on W/O/W multiple nanoemulsion

4.3.4.1 Comparison on the stability of W/O/W multiple nanoemulsion stabilized by oil-based thickener (Sucragel), water-based thickener (Xanthan gum) and without thickener

From Table 4.6, oil-based thickener produced the smallest initial MDD by 46.62% and 35.86% as compared to without thickener and water-based thickener, respectively, for W/O nanoemulsion. After 1 week, there were changes in MDD by 5.43%, 6.64% and 9.15% respectively, for oil, water and non-thickened W/O nanoemulsion. Both the water and oil-thickened W/O nanoemulsion had smaller change in MDD after 1 week as compared to the non-thickened W/O nanoemulsion. The thickened W/O nanoemulsion was more stable since the thickeners improved the physicochemical interaction at the oil-water interface by forming complex stable networks [247, 248]. However, it is to be noted that initial DI was smaller for the non-thickened W/O nanoemulsion (0.102±0.062) than both the oil (0.137±0.025) and water-thickened (0.323±0.014) W/O nanoemulsion. This was because the lower viscosity of the non-thickened W/O nanoemulsion as shown in Table 4.7 enabled better dispersion of the cavitation-induced forces which resulted in emulsion with more uniform droplets.

Table 4.6 Comparison of different thickeners for the formation of W/O nanoemulsion and W/O/W multiple nanoemulsion.

Type of thickener		**W/O nanoemulsion**		**W/O/W multiple nanoemulsion**	
		Initial	**1 week**	**Initial**	**1 week**
Without thickener	Mean droplet diameter (nm)	143.1±8.8	156.2±6.5	242.9±1.4	281.9±3.6
	Dispersity index	0.102±0.062	0.283±0.051	0.247±0.025	0.318±0.055
Oil thickener	Mean droplet diameter (nm)	97.6±3.23	102.9±1.4	175.4±4.3	197.9±1.4
	Dispersity index	0.137±0.025	0.219±0.020	0.225±0.005	0.263±0.023
Internal water thickener	Mean droplet diameter (nm)	132.6±1.1	141.4±1.9	182.7±1.7	228.9±2.0
	Dispersity index	0.323±0.014	0.467±0.037	0.324±0.037	0.467±0.014

The larger initial MDD by 35.86% produced using water thickener than oil thickener could be associated with the higher viscosity of the water-thickened W/O nanoemulsion as compared to the oil-thickened W/O nanoemulsion. The high propagation of acoustic waves in a less viscous medium provided stronger cavitation-induced forces [9]. Furthermore, the water thickener is also suggested unable to improve the stability at the oil-water interface as compared to the oil thickener due to the absence of multiple OH^- groups and fatty acid chains.

Notably, oil-based thickened W/O nanoemulsion had the smallest MDD and DI after 1 week. This outcome is suggested to be attributed to the presence of Sucragel in the oil phase which composed of glycerine, sucrose laurate, Prunus Amygdalus Dulcis (Sweet Almond) oil and Citrus Aurantium Dulcis fruit water that enhanced hydrogen bonding and fatty acid-binding with PGPR stabilized at the palm oil-water interface. The sucragel solubilized well within palm oil which improved the binding strength.

Table 4.7 Viscosity of W/O nanoemulsion and W/O/W multiple nanoemulsion with different thickeners.

Type of thickener	**Viscosity (cP)**	
	W/O nanoemulsion	**W/O/W nanoemulsion**
Without thickener	127.2±6.2	102.1±7.8
Oil thickener	145.3±5.4	128.0±4.5
Internal water thickener	162.3±9.6	144.2±12.3

Importantly, despite the lower viscosity, the initial MDD of the non-thickened W/O/W multiple nanoemulsion was larger by 32.95% and 38.48% as compared to the water and oil thickened W/O/W multiple nanoemulsion, respectively. This was because of the higher strength at the inner water-oil interface for both the thickened in comparison to the non-thickened

W/O/W multiple nanoemulsion. The thickened entities imparted better strength that could withstand high-power processing during the recoalescence and stabilization resulting in smaller MDD than the non-thickened.

Water content analysis was performed to evaluate the loss of internal water molecules, as shown in Table 4.8. The increase in internal water content was 25.57%, 7.56%, and 13.13% for non-thickened, oil-thickened, and water-thickened W/O/W multiple nanoemulsion, respectively, after 1 week. The increase in internal water content was the smallest for the oil thickened W/O/W multiple nanoemulsion. The thickened oil is suggested to be able to retain and protect the internal water droplets within the oil phase by forming a stable and robust network within the oil globules and hence, better stability at the oil-water interface. Sucragel's solubility in palm oil increased the viscosity of the oil phase and enhanced the stability at the oil-water interface by co-interacting with PGPR. This resulted in the formation of the smallest MDD and DI for the oil thickened. Comparison with other studies was not possible since existing studies majorly utilized water-based thickeners focussing on sustained release [1, 93, 99, 100].

Table 4.8 Comparison of water content in W/O/W multiple nanoemulsion with different thickeners.

W/O/W nanoemulsion	**Water content (%)**	
	Initial	**After 1 week**
No thickener	0.8252±0.0023	1.0362±0.0029
Oil thickener	0.8268±0.0031	0.8893±0.0046
Internal water thickener	0.8139±0.0008	0.9208±0.0071

However, increased MDD and water content by 12.83% and 7.56%, respectively, was observed for oil-thickened W/O/W multiple nanoemulsion after 1 week as compared to the initial. Therefore, the required concentration of oil thickener and tonicity stabilization need to be determined for improving the stability of W/O/W multiple nanoemulsion. These would be elaborated in section 4.3.4.2 and 4.3.5.

4.3.4.2 Effect of concentration of oil-soluble thickener (Sucragel) on the formation of W/O/W multiple nanoemulsion

From Table 4.9, the initial MDD and DI of W/O/W multiple nanoemulsion formulated with 0.5 wt% of Sucragel were larger by 3.31% and 4.00%, respectively, when compared to the formulation with 1.0 wt% of Sucragel. While, the formulation of W/O/W multiple nanoemulsion with 2.0 wt% of Sucragel produced larger initial MDD and DI by 21.09% and 60.89%, respectively, as compared to the formulation with 1.0 wt% of Sucragel. After 1 week, the MDD increased by 17.49%, 12.83% and 14.03% for the W/O/W multiple nanoemulsion formulated with 0.5 wt%, 1.0 wt% and 2.0 wt% of Sucragel, respectively. While, the water content increased by 14.25%, 7.56% and 2.51% for the W/O/W multiple nanoemulsion formulated with 0.5 wt%, 1.0 wt% and 2.0 wt% of Sucragel, respectively, after 1 week.

Table 4.9 Comparison of the stability of W/O/W multiple nanoemulsion at different concentrations of Sucragel.

Concentration of Sucragel (wt%)	**W/O/W multiple Nanoemulsion**	**Initial**	**After 1 week**
0.5	Mean droplet diameter (nm)	181.2±4.3	212.9±8.7
	Dispersity index	0.234±0.072	0.322±0.025
	Water content (%)	0.8142±0.0021	0.9302±0.0018
1.0	Mean droplet diameter (nm)	175.4±4.3	197.9±1.4
	Dispersity index	0.225±0.005	0.263±0.023
	Water content (%)	0.8268±0.0031	0.8893±0.0046
2.0	Mean droplet diameter (nm)	212.4±4.8	242.2±2.3
	Dispersity index	0.362±0.008	0.488±0.005
	Water content (1%)	0.8314±0.0012	0.8523±0.0028

1.0 wt% of Sucragel in W/O/W multiple nanoemulsion was observed to have better resistance to changes in water content and MDD as compared to 0.5 wt% of Sucragel. As given in Table 4.10, the 6.86% increase in viscosity of the W/O/W multiple nanoemulsion with the addition of 0.5 wt% of Sucragel was not able to retain the internal water droplets within the oil globule. Thus, the increase in viscosity when 0.5 wt% of Sucragel was utilized was unable to form oil phase with a rigid and packed network. As such, retainment of internal water droplets was poor.

Table 4.10 Viscosity of W/O/W multiple nanoemulsion at different concentrations of Sucragel.

Concentration of Sucragel (wt%)	Viscosity of W/O/W multiple nanoemulsion (cP)
0	102.1±7.8
0.5	109.1±12.3
1.0	128.0±4.5
2.0	187.2±7.8

While, W/O/W multiple nanoemulsion formulated with 2.0 wt% of Sucragel had higher viscosity than 1.0 wt% of Sucragel. The higher viscosity could have reduced the propagation of acoustic waves resulting in larger initial MDD and DI as compared to the formulation with 1.0 wt% of Sucragel. The higher DI could have promoted flocculation and coalescence in W/O/W multiple nanoemulsion, increasing the MDD and DI after 1 week. However, notably, the high viscosity of W/O/W multiple nanoemulsion formulated using 2.0 wt% of Sucragel had the lowest change in water content as compared to with 0.5 wt% and 1.0 wt% of Sucragel. The increase in viscosity of W/O/W multiple nanoemulsion with 1.0 and 2.0 wt% of Sucragel is suggested to form rigid oil phase with a packed network. Furthermore, the internal water droplet could have been retained due to the strengthened interaction at the rigid oil water interphase. Comparison with existing study was not made possible as no study has reported on the usage of oil thickener for the stable formation of W/O/W multiple nanoemulsion.

1.0 wt% of Sucragel was the optimum concentration for the formation of W/O/W multiple nanoemulsion since the increase in viscosity improved the water retention and produced optimal MDD and DI. In section 4.3.5, the influence of tonicity to control the water movement would be discussed.

4.3.5 Effect of hypotonicity, isotonicity and hypertonicity on the stability of W/O/W multiple nanoemulsion

Three conditions in the W/O/W multiple nanoemulsion, i.e., hypotonic, isotonic, and hypertonic, were simulated. Hypotonic is a condition in which the concentration of NaCl in the external water phase (0.5 M) is lower than the internal water phase (1.0 M). Isotonic is a condition where both the external and internal water phases have similar concentrations of NaCl (1.0 M). Lastly, hypertonic is a condition where the external water phase (2.0 M) has a higher concentration of NaCl than the internal water phase (1.0 M).

From Fig. 4.9, hypotonic promoted the movement of water from the external water phase to the internal water phase. While, hypertonic promotes water movement from the internal water phase to the external water phase. This was followed by the isotonic condition that has a balanced water potential with none/minimal water movement.

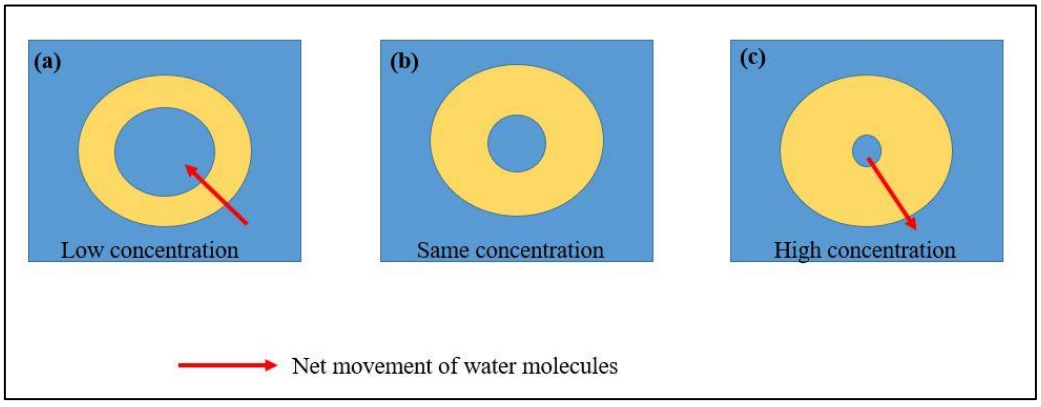


Fig. 4.9 Movement of water in (a) hypotonic, (b) isotonic and (c) hypertonic conditions.

W/O/W multiple nanoemulsion simulating the hypotonic condition showed an increasing trend in the conductivity values when analysed for 10 days, as shown in Table 4.11. The initial concentration of NaCl was 0.522 M, and there was an increase to 0.782 M after 10 days, as provided in Table 4.12. The concentration of NaCl was obtained based on Fig. 4.10 which showed the calibration of conductivity values for a concentration of NaCl solution

between 0 and 2.5 M. The best-fit line obtained was used to calculate the concentration of NaCl in the external water phase using the conductivity values obtained for W/O/W multiple nanoemulsion. There was also an increase of 4.10% of water content in the internal water phase. Also, as shown in Table 4.13, after 10 days, there was an increase in MDD by 4.34% for the hypotonic condition. Based on osmosis, since the water potential is higher in the external phase than the internal phase, the water moves from the external to internal phase during the hypotonic condition. Thus, this explains the increase in conductivity, concentration of NaCl, water content and MDD in W/O/W multiple nanoemulsion.

Table 4.11 Conductivity values of W/O/W multiple nanoemulsion at different tonicities.

Osmotic condition	**Conductivity values (µ/s)**					
	Day					
	Initial	**2**	**4**	**6**	**8**	**10**
Hypotonic	15.44±2.10	16.35±1.84	17.78±1.20	19.95±2.11	20.31±1.15	22.75±1.14
Isotonic	26.35±1.08	26.78±1.13	26.88±1.31	26.74±1.25	26.42±1.31	27.10±1.42
Hypertonic	53.81±1.61	50.22±2.17	47.76±1.14	44.23±1.30	42.85±1.21	41.90±1.22

For the isotonic condition, a stable trend was observed with a difference of 0.75µ/s between the highest and lowest conductivity values obtained in 10 days, as given in Table 4.11. As shown in Table 4.12, the concentration of NaCl initially and after 10 days were 0.910 M and 0.937 M, respectively, as calculated using the best fit line. There was also increase of 0.40% in the internal water content after 10 days. Table 4.13 shows both the MDD and DI had an increase of 1.34% and 3.11%, respectively, after 10 days. Due to the similar concentration in NaCl at 1.0 M in the internal and external phase, the water potential was identical. Thus, this reduced the movement of water in and out of both the internal and external water phases. This

resulted in lowest change in the conductivity, concentration of NaCl, water content and MDD as compared to hypertonic and hypotonic conditions.

Table 4.12 Effect of NaCl concentration towards W/O/W multiple nanoemulsion.

Osmotic condition	**Initial**		**After 10 days**	
	Concentration of NaCl (mol/dm^3)	**Water content (%)**	**Concentration of NaCl (mol/dm^3)**	**Water content (%)**
Hypotonic	0.522	0.8368±0.0044	0.782	0.8711±0.0054
Isotonic	0.910	0.8235±0.0058	0.937	0.8268±0.0031
Hypertonic	1.888	0.8282±0.0038	1.464	0.7703±0.0087

Whereas, the hypertonic condition showed a decreasing trend in the conductivity values. This reflected in the initial concentration of NaCl at 1.888 M, decreasing to 1.464 M after 10 days calculated using the best fit line as shown in Table 4.12. A decrease in the internal water content by 6.99% was also observed. Based on Table 4.13, there was a decrease of 5.58% in the MDD of W/O/W multiple nanoemulsion simulating the hypertonic condition. Due to osmosis, the water potential is higher in the internal water phase in comparison to the external water phase. Hence, water moved from the internal to external phase resulted in decreased conductivity, concentration of NaCl, water content and MDD in the W/O/W multiple nanoemulsion.

Table 4.13 Effect of different tonicities towards droplet size of W/O/W multiple nanoemulsion.

Osmotic condition	W/O/W multiple Nanoemulsion	Initial	After 10 days
Hypotonic	Mean droplet diameter (nm)	175.3±4.8	182.9±7.2
	Dispersity index	0.214±0.013	0.308±0.077
Isotonic	Mean droplet diameter (nm)	172.2±5.4	174.5± 9.8
	Dispersity index	0.225±0.008	0.232± 0.012
Hypertonic	Mean droplet diameter (nm)	182.6±3.8	172.4±6.7
	Dispersity index	0.281±0.014	0.235±0.022

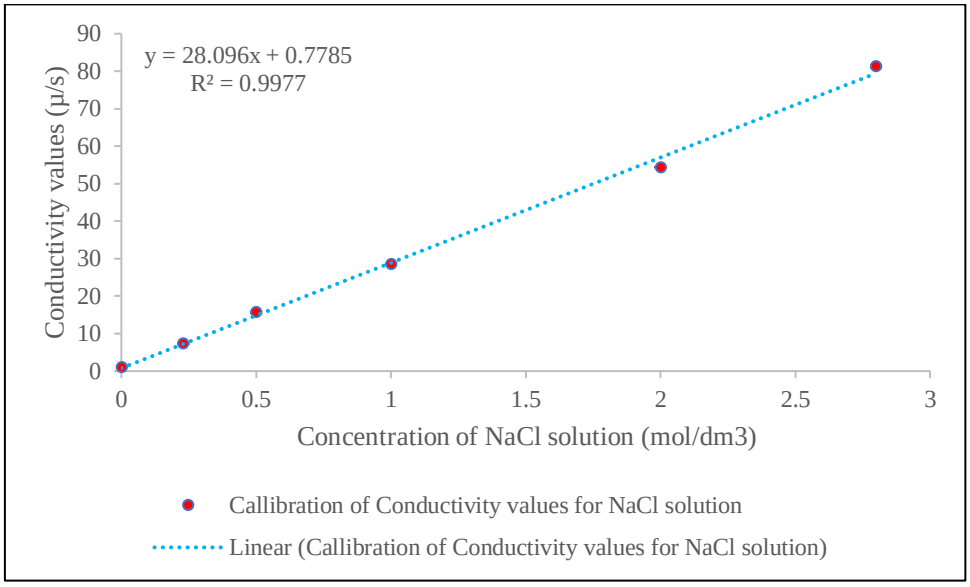


Fig. 4.10 Calibration curve for the conductivity values of the NaCl solution.

Thus, for the oil thickened W/O/W multiple nanoemulsion, the isotonic condition provided the best stability. Table 4.14 shows the final optimized parameters with 1.0 wt% of Sucragel and isotonicity used to generate stable W/O/W multiple nanoemulsion. Corroborating with this work, Zhang et al. [249] formed W/O/W multiple emulsion that was isotonic-stabilized with NaCl. The authors reported that they achieved stability for at least 2 months.

Notably, the obtained conductivity values for the W/O/W multiple nanoemulsion also proved that the formed emulsion was of W/O/W type.

Table 4.14 Optimized parameters for the formation of palm oil-based W/O/W multiple nanoemulsion with Sucragel using ultrasonicator.

Parameters	Optimized values
Amplitude (%)	40
Irradiation time (s)	180
Tween 80 concentration (wt%)	1.0
Sucragel concentration (wt%)	1.0
Tonicity	Isotonic (1.0 M)
Mean droplet diameter (nm)	175.5±9.8
Dispersity index (DI)	0.232±0.012

4.3.6 Morphological analysis of W/O/W multiple nanoemulsion using STEM

Fig. 4.11 shows the STEM image of W/O/W multiple nanoemulsion produced from optimized parameters of 40% amplitude, 180 s irradiation time, 90:10 phase volume ratio, 0.25 wt% PGPR, 1.0 wt% Tween 80, 1.0 wt% of Sucragel and isotonic condition (1.0 M). The morphology of the STEM image revealed that an internal water droplet is shown entrapped within the oil droplet. The internal water droplet showed an average diameter of ~120 nm, while the oil globule showed an average diameter of ~190 nm. ~25.0% reduction in internal water droplet diameter is observed when compared between W/O nanoemulsion (Fig 3.11) as compared to W/O/W multiple nanoemulsion (Fig 4.11). The observed reduction is suggested due to the reprocessing effect of W/O nanoemulsion during processing W/O/W multiple nanoemulsion. Comparison of this was not made possible with existing study since no study

has typically reported on this till present. The entrapped water droplet indicated the successful formulation that complied with the MDD and DI obtained at 175.5±9.8 nm and 0.232±0.012, respectively, for the optimized W/O/W multiple nanoemulsion. The increased MDD could be related to the sample preparation procedure involving staining using phosphotungstic acid solution. In a study by Thompson et al. [243], the authors indicated that the sample preparation techniques can influence the image obtained using electron microscope.

Fig. 4.11 successfully showed the differences in the morphology of W/O/W multiple nanoemulsion as compared to W/O nanoemulsion (Fig. 3.11). In specific, there was presence oil globule for W/O nanoemulsion (Fig. 3.11) while, there was an internal water droplet within the oil globule for W/O/W multiple nanoemulsions (Fig. 4.11). The obtained morphology of W/O/W multiple emulsion through STEM corroborated with the study by Tang et al. [1]. The authors in the study reported entrapped internal water droplet within the oil globule (oil globule ~540 nm and internal water droplet ~320 nm in size). The authors also indicated that this type of multiple emulsion formation as the single-core W/O/W multiple nanoemulsion. As such, the formed W/O/W multiple nanoemulsion in this study could also be indicated as single-core W/O/W multiple nanoemulsion.

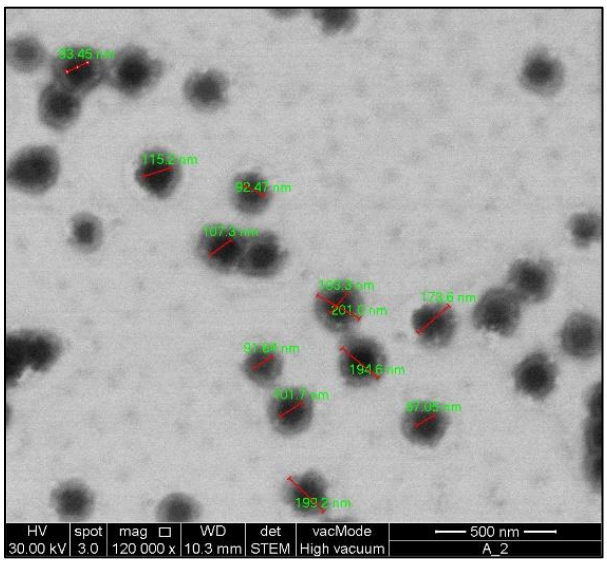


Fig. 4.11 STEM image of W/O/W multiple nanoemulsion.

4.4 Summary

Based on the carried out investigations, both ultrasonicator and microfluidizer were able to formulate stable palm oil-based W/O/W multiple nanoemulsion. Ultrasonicator was however found more energy-efficient than microfluidizer. No oxidation product was detected from the processed W/O/W multiple nanoemulsion under both the methods. More stable W/O/W multiple nanoemulsion was formulated from the phase volume ratio of 90:10 as compared to 80:20. Increased Tween 80 concentration adversely affected the stability of W/O/W multiple nanoemulsion as it promoted migration of emulsifiers between the internal and external water-oil interfaces. Utilization of Sucragel and isotonic condition further enhanced the stability of W/O/W multiple nanoemulsion by forming rigid oil-water interface and reduced movement of water between the water phases, respectively. In the next chapter, encapsulation of TRF and CA in W/O/W multiple nanoemulsion would be investigated. This would then be followed with the evaluation of its efficacy to be used with CIS for cancer treatment.

CHAPTER 5: EVALUATION OF ANTICANCER EFFECTS OF ENCAPSULATED TRF AND CA IN W/O/W MULTIPLE NANOEMULSION WITH CIS TOWARDS A549 AND HEP G2 CANCER CELL LINES

This chapter presents the details of investigation carried out to evaluate the efficacy of encapsulated TRF and CA in W/O/W multiple nanoemulsion with CIS towards cancer cell lines as outlined in Fig. 5.1.

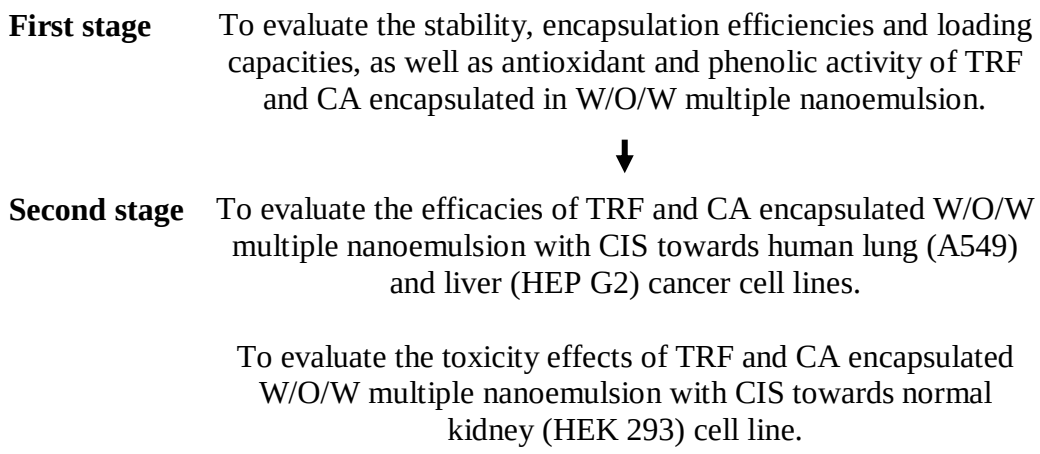


Fig. 5.1 Overview of experimentations in Chapter 5.

5.1 Background

The experimentation in this chapter was after the successful formulation of stable palm oil-based W/O/W multiple nanoemulsion reported in Chapter 4. Aligned with the knowledge gap presented concerning the combination effect of TRF and CA on lung and liver cancer cell lines as detailed in Chapter 2, the first stage evaluated the stability, encapsulation efficiency and loading capacity, as well as antioxidant and phenolic activity of TRF and CA encapsulated W/O/W multiple nanoemulsion.

In the second stage, there are two sub-stages. In the first sub-stage, the efficacies of TRF and CA encapsulated W/O/W multiple nanoemulsion with CIS towards human lung (A549), and liver (HEP G2) cancer cell lines were investigated. In the second sub-stage, the toxicity effects of encapsulated TRF and CA in W/O/W multiple nanoemulsion with CIS towards normal kidney cell line were evaluated.

5.2 Materials and methods

5.2.1 Materials

PGPR, palm MCT oil and palm oil were procured from Palsgaard (Denmark), KLK Oleo (Malaysia) and Sime Darby Food (Malaysia), respectively. TRF-70 was purchased from Carotino (Malaysia), while CA and CIS were purchased from Sigma Aldrich (Malaysia). The following chemicals were also used in this investigation to produce W/O/W multiple nanoemulsion: Tween 80 from Sigma Aldrich (Malaysia) and Sucragel AOF Bio from Alfa Chemicals (United Kingdom). Deionized water from Milli-Q® Plus apparatus (USA) was used for nanoemulsion formulations. Copper grid (300-mesh & formvar-coated) from Agar Scientific Ltd. (United Kingdom) was utilized for the analysis of STEM.

Human lung epithelial adenocarcinoma cell line (A549), human liver hepatocellular carcinoma cell line (HEP G2) and human embryonic kidney epithelial cells (HEK 293) were purchased from ATCC-The Global Bioresource Centre (USA). Roswell Park Memorial Institute (RPMI) media, Dulbecco's Modified Eagle Medium (DMEM), phosphate-buffered saline (PBS) and streptomycin/penicillin solution purchased from Nacalai Tesque (Japan) were used to culture cells. Foetal bovine serum (FBS) was purchased from Tico (Europe).

5.2.2 Preparation of W/O/W multiple nanoemulsion

Firstly, W/O nanoemulsion with an MDD of ~150 nm was generated as presented in Chapter 3. TRF (0.0008 M) and CA (0.0008 M) were added into the oil and water phases, respectively, prior to processing W/O nanoemulsion. Secondly, W/O/W multiple nanoemulsion with an MDD of ~180 nm was produced, as presented in Chapter 4.

5.2.3 Evaluation of the stability

5.2.3.1 Processing stability

W/O/W multiple nanoemulsion was formed using the optimized parameters for ultrasonicator and microfluidizer. The optimized parameters for the processing of both W/O nanoemulsion and W/O/W multiple nanoemulsion, as presented in Chapter 3 and Chapter 4, respectively, are shown in Table 5.1. The concentrations of TRF and CA in the W/O/W multiple nanoemulsion after being subjected to these processes with the optimized conditions were evaluated using high performance liquid chromatagraphy (HPLC), as explained in section 5.2.12.

Table 5.1 Optimized processing parameters of W/O/W multiple nanoemulsion using ultrasonicator and microfluidizer.

	W/O nanoemulsion	**W/O/W multiple nanoemulsion**
Process 1: Ultrasonication	40 amplitude, 180 s	40 amplitude, 180 s
Process 2: Microfluidization	350 bar, 6 cycles	350 bar, 8 cycles

5.2.3.2 Storage stability

50.0 ml of W/O/W multiple nanoemulsion in a glass container wrapped with an aluminium foil was stored at room temperature (~25 °C) in the dark. The droplet size, DI, water content,

conductivity value, NaCl concentration and zeta potential were measured at predetermined intervals of 0, 30, 60, 90, 120, 150 and 180 days.

5.2.3.3 Stability of TRF/CA

The concentrations of the encapsulated TRF and CA within W/O/W multiple nanoemulsion were evaluated at predetermined intervals of 30, 60, 90, 120, 150 and 180 days. Methanol was added to the W/O/W multiple nanoemulsion at a ratio of 1:1 and thoroughly mixed. The W/O/W multiple nanoemulsion encapsulating TRF and CA were centrifuged at 15000 rpm for 15 min [194]. The supernatant was obtained and diluted with methanol, while TRF and CA were quantified using HPLC, as explained in section 5.2.12.

5.2.3.4 Stability of the refrigeration cycle

50 ml of W/O/W multiple nanoemulsion in a glass container wrapped with an aluminium foil was exposed to six cycles at 4 °C (refrigeration temperature) and 25 °C (room temperature) for 12 h each. At the end of each cycle, the MDD, DI, as well as TRF and CA concentrations were evaluated.

5.2.3.5 Comparison of TRF and CA stability in emulsion and solution form

TRF and CA were prepared individually in the form of W/O/W multiple nanoemulsion and ethanol solution at a concentration of 0.008 M. The samples were kept in a glass bottle, covered with aluminium foil and kept in the dark (without exposure to light) at room temperature (~25 °C) for 28 days. The concentrations of TRF and CA in both the forms were then analysed at predetermined intervals of 7, 14, 21 and 28 days using HPLC analysis, as explained in section 5.2.12.

5.2.4 Encapsulation efficiency and loading capacity

The encapsulation efficiencies and loading capacities of TRF and CA in W/O/W multiple nanoemulsion were measured using HPLC, as described in section 5.2.12. 5.0 ml of the W/O/W multiple nanoemulsion containing CA and TRF was centrifuged at 15000 rpm for 15 min. 1 ml syringe was used to collect the unencapsulated CA and TRF from the external water phase, which accumulated at the bottom of the centrifugation tube. The collected external water phase was filtered using a 0.22 µm syringe to remove oil droplets. The filtrate was used to detect the unencapsulated CA and TRF. The encapsulation efficiencies for CA and TRF was obtained using Eq. 5.1 and Eq. 5.2, respectively [250].

$$Encapsulation\ efficiency_{CA}\ (\%) = \frac{W_{1CA} - W_{2CA}}{W_{1CA}} \times 100 \qquad \text{Eq. 5.1}$$

$$Encapsulation\ efficiency_{TRF}(\%) = \frac{W_{oil\,TRF} - W_{2TRF}}{W_{oil\,TRF}} \times 100 \qquad \text{Eq. 5.2}$$

The loading capacities for CA and TRF was obtained using Eq. 5.3 and Eq. 5.4, respectively.

$$Loading\ capacity_{CA}(\%) = \frac{W_{1CA} - W_{2CA}}{W_1} \times 100 \qquad \text{Eq. 5.3}$$

$$Loading\ capacity_{TRF}(\%) = \frac{W_{oil\,TRF} - W_{2TRF}}{W_{oil}} \times 100 \qquad \text{Eq. 5.4}$$

W_{1CA} is the amount of CA added to the internal water phase, W_{2CA} is the amount of CA that has seeped into the external water phase, $W_{oil\ TRF}$ is the amount of TRF added to the oil phase and W_{2TRF} is the amount of TRF that has seeped to the external water phase. W_1 and W_{oil} are the total amount of water added as the internal water phase and the total amount of oil added as the oil phase, respectively.

5.2.5 Antioxidant and phenolic activity

5.2.5.1 Antioxidant activity

The antioxidant activity was evaluated using 0.2 mM 2,2-diphenyl-1-picrylhydrazyl (DPPH) in ethanol. The solution was added to the W/O/W multiple nanoemulsion encapsulating TRF only and CA only at a ratio of 1:3, independently. This mixture was kept in the dark at room temperature (~25 °C) for 30 min. The analysis was conducted using the Shimadzu UV 1800 UV-Vis Spectrophotometer (Japan) at a wavelength of 517 nm [251, 252]. The purple DPPH solution would be reduced to the yellow coloured, diphenylpicryl hydrazine, due to the presence of antioxidant [253]. The DPPH scavenging effect was calculated using Eq. 5.5.

DPPH scavenging effect (%) = $[(A_{control} - A_{sample})/A_{control}] \times 100$ Eq. 5.5

5.2.5.2 Total phenolic activity

W/O/W multiple nanoemulsion encapsulating TRF and CA was mixed with 0.2 ml of Folin-Ciocalteu reagent, 2.0 ml of H_2O, 1.0 ml of 15% Na_2CO_3 and kept in the dark for 2 h at room temperature (~25 °C). A standard curve was plotted where alcoholic dilutions of gallic acid (2.5-20.0 µM) were analysed by using a UV-Vis Spectrophotometer at a wavelength of 765 nm [254]. Gallic acid was used as a standard and the total phenolics were expressed as gallic acid equivalents (GAE). Phenolics react with the Folin-Ciocalteu reagent to form a blue chromophore constituting of phosphotungstic-phosphomolybdic complex [255].

5.2.6 Cell culture

A549 and HEP G2 were cultured in RPMI media supplemented with 10.0% FBS and 1.0% penicillin/streptomycin, while HEK 293 was cultured in DMEM supplemented with 10.0% FBS

and 1% penicillin/streptomycin. All cell lines were maintained at 37 °C in a humidified 5% CO_2 atmosphere using Memmert CO_2 Incubator (Germany).

5.2.7 Cell viability assay

A549 and HEP G2 cells were seeded in 96-well plates and incubated for 24 h, independently. The medium was aspirated and replaced with medium containing the W/O/W multiple nanoemulsion encapsulating TRF only and CA only formed at a concentration of 400.0 µM. Serial dilution in the RPMI medium was carried out and added to the wells of the 96-well plates to obtain a final concentration ranging between 0.05 µM and 400.0 µM for both A549 and HEP G2 cell lines. This was also repeated for a 400.0 µM solution of CA, TRF and CIS in ethanol. The unencapsulated W/O/W multiple nanoemulsion was also evaluated as a control. After 24 h of incubation at 37 °C, 20 µl solution of MTT in PBS (2 mg/ml) was added to each well, and the plates were then incubated at 37 °C for 2 h. The medium was then aspirated, and dimethyl sulphoxide (DMSO) at 100 µl was added to dissolve the precipitate. The absorbance of each well was measured at the wavelength of 570 nm using a Tecan Infinite 200 (Switzerland) microplate reader [256].

5.2.8 Analysis of cell apoptosis using flow cytometry

A549 and HEP G2 cells were seeded in 6-well plates and incubated for 24 h, independently. These cells were subjected to treatments 1 to 5, as shown in Table 5.2, independently. The unencapsulated W/O/W multiple nanoemulsion acted as a control. The cells were harvested, then washed with ice-cold PBS and resuspended with 500 µl ice-cold 1× binding buffer. Next, cells were stained with 10 µL of Annexin V–FITC (recombinant annexin V conjugated to fluorescein isothiocyanate) and 8 µL of PI. Cells in flowcytometer tubes were kept in dark (wrapped in aluminium foil) for 30 min at room temperature (~25 °C) before analysis. The

measurement of apoptosis was performed using a FACSCalibur™ BD Biosciences Flow Cytometer (USA) equipped with CellQuestPro software™ [256]. Bi-colour analysis (band pass filter for FITC is 530 nm and PI is 600 nm) was used for analysis.

Table 5.2 Concentrations of treatments used for A549 and HEP G2.

Treatment	Active compound	Concentration (µM)	
		A549	**HEP G2**
1	TRF (IC 50)	1.00	0.80
2	CA (IC 50)	1.50	1.60
3	CIS (IC 50)	0.45	0.25
4	TRF: CA (IC 75 of TRF: IC 75 of CA)	0.18:0.14	0.10:0.14
5	TRF:CA:CIS (IC 80 of TRF : IC 80 of CA: IC 90 of CIS)	0.13:0.10:0.02	0.07:0.10:0.08

5.2.9 Intracellular ROS measurements

A549 and HEP G2 cells were seeded in 6-well plates and incubated for 24 h, independently. These cells were subjected to treatments 1 to 5, as shown in Table 5.2, independently. The unencapsulated W/O/W multiple nanoemulsion acted as a control. The cells were harvested, washed with PBS and incubated with 1 ml of 10.0 µM of 5-(and-6)-Carboxy-2′,7′-dichlorodihydrofluorescein diacetate in PBS. Cells were seeded in 96-well black plate and incubated in dark (wrapped in aluminium foil) in CO_2 incubator for 1 h before analysis. Excitation wavelength and an emission wavelength of 485 nm and 535 nm, respectively, were used to measure the fluorescence via microplate reader [257].

5.2.10 Analysis of cell cycle using flow cytometry

A549 and HEP G2 cells were seeded in 6-well plates and incubated for 24 h, independently. These cells were subjected to treatments 1 to 5, as shown in Table 5.2, independently. The unencapsulated W/O/W multiple nanoemulsion acted as a control. The cells were harvested and washed with ice-cold PBS. Then, 70% of ethanol was added for cell fixing and stored at -20 °C for 24 h. Next, the cells were washed with ice-cold PBS again to remove the ethanol and rehydrate the cells. This was followed by the addition 50 µl of RNase A (1 mg/ml) and 50 µl PI (1 mg/ml) to stain the cells. Cells in flow cytometer were kept for 30 min at room temperature (~25 °C) in the dark (wrapped in aluminium foil) before analysis. Cell cycle analysis was carried out via flow cytometer equipped with CellQuestPro software™ [258]. The PI fluorescence was measured at 488 nm.

5.2.11 Toxicity study

HEK 293 cell line was cultured for 24 h in 96-well plates. Then, the medium was aspirated and the treatments 1 to 5, as shown in Table 5.2 were added to the wells and incubated for 24 h at 37 °C. 20 µl solution of MTT in PBS (2 mg/ml) was added to each well and incubated for 2 h at 37 °C in dark (wrapped in aluminium foil). The medium was then aspirated, and DMSO at 100 µl was added to dissolve the precipitate. The absorbance of each well was measured at the wavelength of 570 nm using a microplate reader [256].

5.2.12 Analyses

Among the performed analyses for the generated W/O/W multiple nanoemulsion were droplet size, DI, zeta potential, conductivity and water content. The droplet size, DI, conductivity, water content and zeta potential were performed to evaluate the stability of W/O/W multiple

nanoemulsion. The zeta potential of the nanoemulsion was measured using Malvern Zetasizer Nano ZS (United Kingdom). The zeta potential indicates the charge on the droplet surface. It is determined by measuring the electrophoretic mobility in mV which is computed from the measured Doppler shifted frequency, under a given applied electric field. The morphology of the generated W/O/W multiple nanoemulsion was also analysed using field emission scanning electron microscope. Detailed explanations for these analyses and the utilized equipment can be obtained from Chapter 3 and Chapter 4.

The concentrations of TRF and CA in the W/O/W multiple nanoemulsion were determined by RP-HPLC method, as described by Aditya et al. [250]. 20 µl sample was injected into Agilent ZORBAX Extend-C18 (USA), 4.6 mm x 150 mm x 5 µm analytical column. The flow rate of the mobile phase was 1.0 ml/min. TRF and CA concentrations were detected separately at 295 nm and 330 nm, respectively. Samples were injected into Agilent HPLC equipped with online degasser, Agilent Infinity 1260 Quaternary LC Pump (USA) and a VWD UV detector. The Agilent ChemStation software was used for instrument control, data acquisition and data analysis.

For cell lines related investigations, the experiments and analyses were repeated three times. For the rest, two repetitions were performed for each experiment, two sample were collected from each experiment and two repetitions of analysis were performed for each sample. The differences in repetitions performed were because of the different minimum requirements of engineering and biology related investigations. Error bars based on standard deviation and standard errors are shown for tables and figures, respectively, in the results section.

5.3 Results and discussion

5.3.1 Evaluation of the stability

5.3.1.1 Processing stability

From Table 5.3, the concentrations of TRF and CA were 0.007432 M and 0.007298 M, respectively, for W/O/W multiple nanoemulsion processed using Process 1 (ultrasonication). While, for W/O/W multiple nanoemulsion processed using Process 2 (microfluidization), the concentrations of TRF and CA were 0.007490 M and 0.007214 M, respectively. For ultrasonication, a decrease of 7.64% and 9.62% in concentrations for TRF and CA, respectively, were observed after processing. Whereas, for microfluidization, a decrease of 6.81% and 10.90% in concentrations were observed after processing for TRF and CA, respectively. The decrease in active compounds concentrations for both ultrasonication and microfluidization were in between 6.0% and 11.0%. This outcome contradicts to the study reported by Salvia-Trujillo et al. [259] in which the authors compared the antimicrobial activities of lemongrass encapsulated nanoemulsion processed using ultrasonication and microfluidization. The authors reported that microfluidizer processed nanoemulsion had higher antimicrobial activities than the ultrasonicator processed nanoemulsion. This could be associated with the differences in the outlet temperature reported between the two processes, where ultrasonication had a maximum temperature gain up to 47 °C, whereas microfluidization was maintained below 20 °C.

Table 5.3 Comparison of TRF/CA retainment in W/O/W multiple nanoemulsion processed using ultrasonicator and microfluidizer.

	Concentration of TRF (M)	**Concentration of CA (M)**
Process 1: Ultrasonication	0.007432	0.007298
Process 2: Microfluidization	0.007490	0.007214

Contrastingly, the outlet temperatures for both ultrasonicator and microfluidizer processed W/O/W multiple nanoemulsion in this study were maintained between 30 °C and 32 °C. In addition, the W/O/W multiple nanoemulsion processed in this study had a double layer to protect the encapsulates as compared to the simple emulsion reported by Salvia-Trujillo et al. [259]. Notably, in this study, the concentrations of active compounds were measured, while in the study by Salvia-Trujillo et al. [259], antioxidant activity was measured. This too, might have influenced the differently obtained outcomes. Furthermore, 0.008 M of TRF and CA concentrations were encapsulated, independently, in the W/O/W multiple nanoemulsion. It is suggested that the loss of TRF and CA could also be linked to the loss of encapsulates during extraction using methanol. Since similar retainments of TRF and CA were found in W/O/W multiple nanoemulsion generated from both ultrasonicator and microfluidizer, ultrasonicator processing would be used for the subsequent work. Ultrasonicator was mainly chosen due to its lower energy requirement to produce similar MDD size as compared to microfluidizer as explained in Chapter 3 section 3.3.2.3 and Chapter 4 section 4.3.1.3.

5.3.1.2 Storage stability

As shown in Table 5.4, the changes in MDD, DI, water content, conductivity and NaCl concentration were monitored for 180 days. Zero was used as the initial value for all the monitored parameters. 45.13%, 19.83%, 0.49%, 3.71%, and 3.83% changes for MDD, DI, water content, conductivity and NaCl concentration, respectively, were observed when measured after 180 days. Although MDD showed an increase of up to 254.7±15.6 nm after 180 days, it was still within the nano range of between 20 nm and 500 nm [112, 260, 261]. This corroborates with the existing study that demonstrated the droplet size in nano-range when stored for 90 days [1].

Table 5.4 Storage stability of W/O/W multiple nanoemulsion for 180 days.

Days	**0**	**30**	**60**	**90**	**120**	**150**	**180**
Mean droplet diameter (nm)	175.5 ±9.8	186.4±8.1	192.3±7.2	210.1±11.1	225.4±14.5	231.2±8.8	254.7±15.6
Dispersity index	0.232 ±0.012	0.238±0.015	0.240±0.024	0.243±0.019	0.251±0.022	0.256±0.016	0.278±0.014
Water content (%)	0.8235±0.0021	0.8256±0.0021	0.8270±0.0015	0.8265±0.0025	0.8268±0.0009	0.8272±0.0011	0.8275±0.0032
Conductivity value (µ/s)	26.43±2.21	26.57±3.40	26.82±6.42	27.13±4.82	27.40±2.23	27.53±6.41	27.41±4.81
Concentration of NaCl (mol/dm^3)	0.913	0.918	0.927	0.938	0.945	0.952	0.948
Concentration of TRF (mol/dm^3)	0.007432	0.007415	0.007406	0.07354	0.007351	0.007248	0.007231
Concentration of CA (mol/dm^3)	0.007298	0.007227	0.007202	0.007183	0.007169	0.007140	0.007122

The increase in MDD and DI is interrelated, while the increase in conductivity value is associated with the increase in NaCl concentration due to the movement between the water phases. The increase in water content and NaCl could be associated with the movement of water from the external to the internal water phase. This shows that despite stabilization measures had been performed, such as the utilization of oil based-thickener, emulsifiers with good anchoring and binding properties, as well as tonicity adjustments, the movement of water in and out of the internal and external water phases cannot be prevented [178, 262]. It can, however, be minimalized. In line with it, the changes observed after 180 days were less than ~4% for the water content, the concentration of NaCl and conductivity values.

Fig. 5.2 show the STEM images of the W/O/W multiple emulsion from 0 to 180 days. An increase in the oil globule size with time was observed. Notably, the single-core W/O/W multiple nanoemulsion was observed during the study for 180 days.

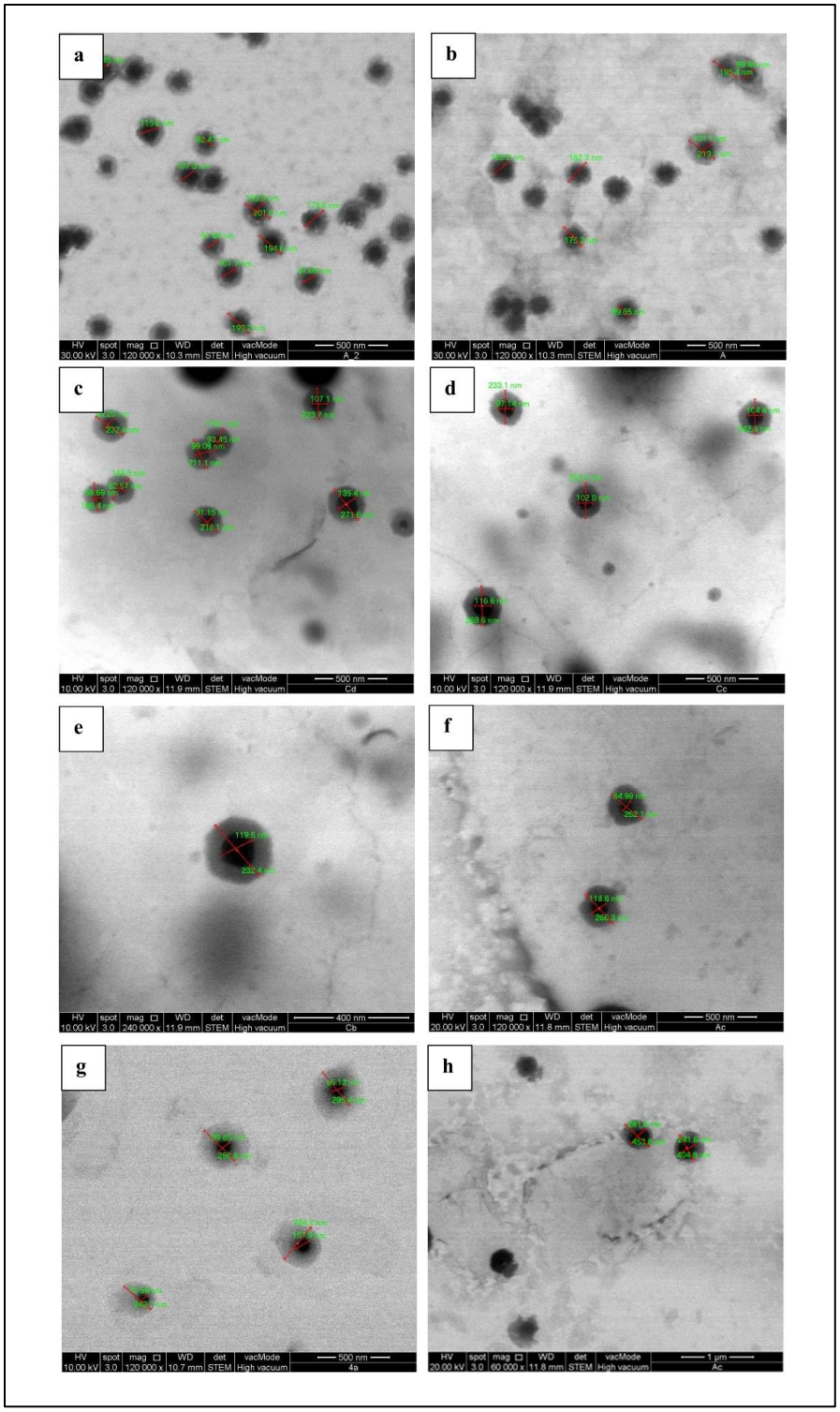


Fig. 5.2 STEM images of W/O/W multiple nanoemulsion encapsulating TRF and CA at (a) 0 day, (b) 30 days, (c) 60 days, (d) 90 days, (e) 120 days, (f) 150 days, (g) 180 days and (h) after refrigeration cycles.

Fig. 5.3 shows the zeta potential measurements of the W/O/W multiple nanoemulsion for 180 days. Zeta potential close to -30.0 mV (-27.8±1.2 to -29.9±1.8 mV) was measured for 180 days. In general, the zeta potential of about ±30.0 mV and higher, indicates stable droplets that can avoid aggregation, sedimentation or phase separation [263]. The formation of Na^+ and Cl^- charges due to the presence of NaCl in the external water phase is suggested to have influenced the obtained zeta potential values.

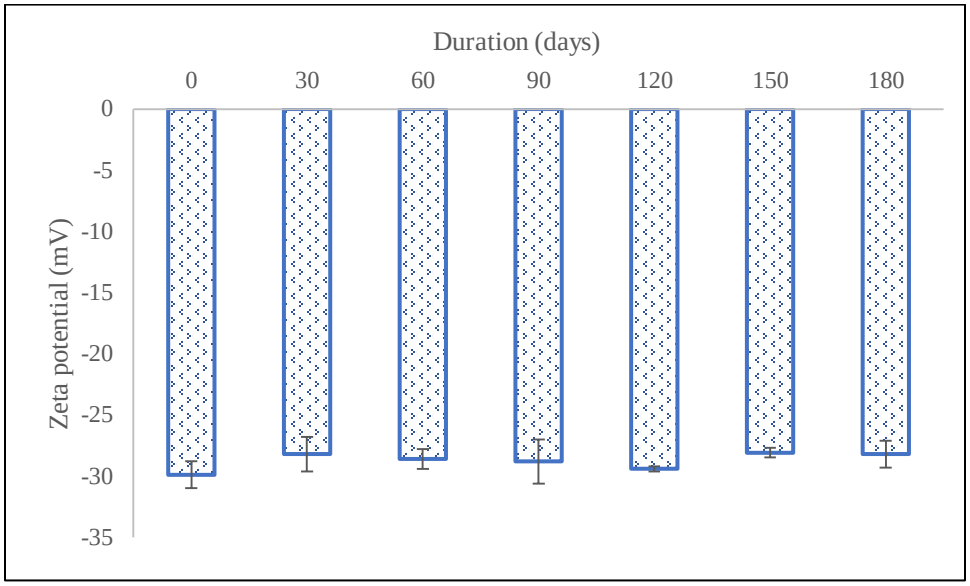


Fig. 5.3 Zeta potential of W/O/W multiple nanoemulsion encapsulating TRF and CA for 180 days.

5.3.1.3 Stability of TRF/CA

Based on Table 5.4, the concentrations of TRF and CA in the W/O/W multiple nanoemulsion decreased by 2.70% and 2.41%, respectively, when analysed after 180 days. Despite being encapsulated in the emulsion and stored without direct sunlight, decrease in the concentrations of TRF and CA were still observed. The concentrations of TRF and CA were evaluated through the HPLC calibration graphs, as shown in Fig. 5.4 and Fig. 5.5, respectively. Notably, the reduction

in the concentration value was less than 4% for both the compounds. This could also be inclusive of the extraction losses. Antioxidants are sacrificial compounds preventing oxidation from occurring. Since oxidation is a natural phenomenon, the present antioxidants could have reacted with the surrounding, preventing oxidation from taking place. This occurrence is suggested to have reduced the concentration of TRF and CA in the nanoemulsion stored for 180 days. This finding corroborates with the study by Aditya et al. [194] in which the authors reported reduced curcumin and catechin concentration in the W/O/W multiple emulsion with time by ~8% and ~30%, respectively, analysed after 15 days of storage at 23 °C.

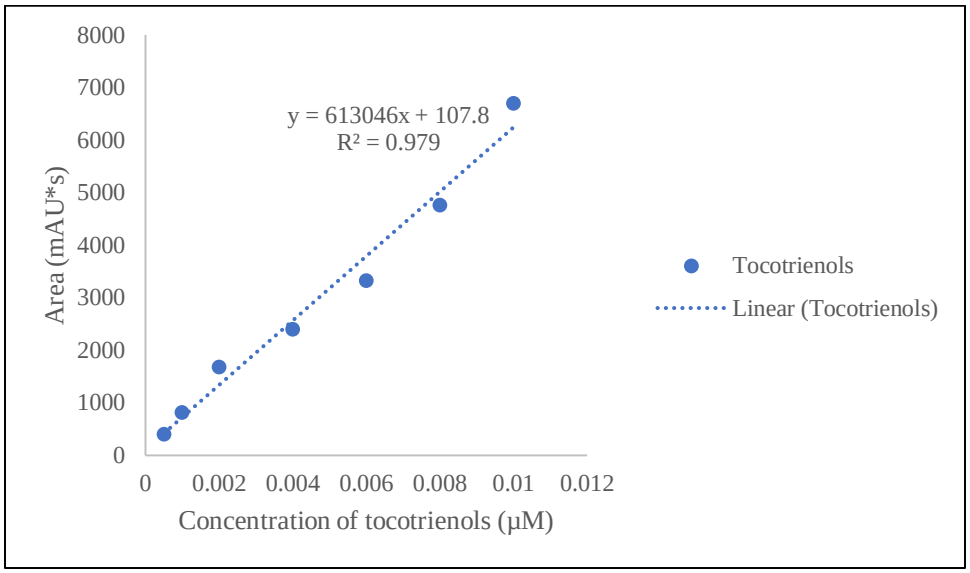


Fig. 5.4 HPLC calibration for TRF.

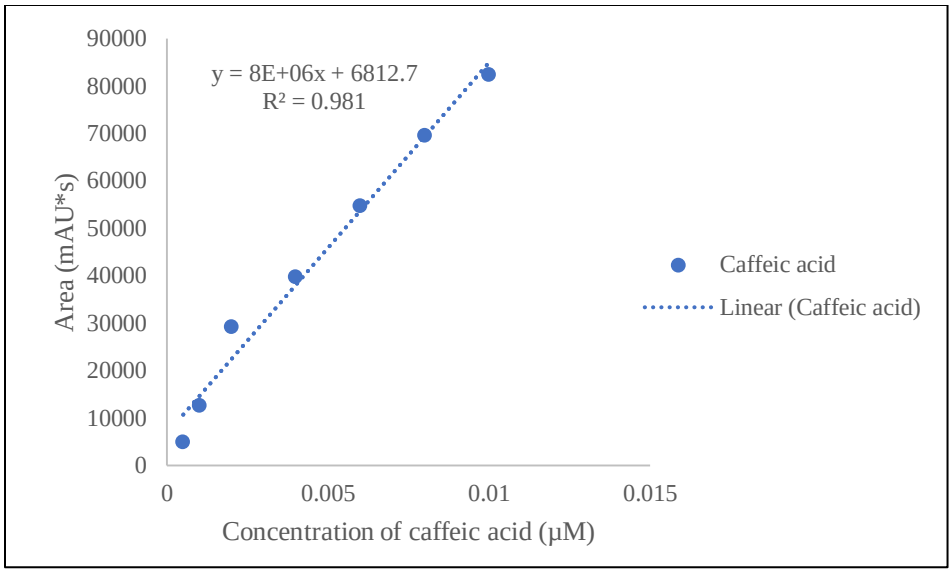


Fig. 5.5 HPLC calibration for CA.

5.3.1.4 Stability of the refrigeration cycle

Table 5.5 shows the MDD, DI and concentration of TRF and CA after 6 refrigeration cycles. 6 refrigeration cycles were chosen to represent 6 days of the typical expected lifespan of the W/O/W multiple nanoemulsion encapsulated with the natural active compounds after first use. MDD and DI increased by 107.52% and 47.84%, respectively. This observation is suggested due to the weakened binding and anchoring properties of emulsifiers/thickeners at the oil-water interface caused by the refrigeration cycles. When the nanoemulsion was subjected to a cycle of temperatures (room temperature and refrigeration), the weakened binding at the interface could have promoted the movement of water between the internal and external water phases, that could have resulted in the increase in MDD and DI. Notably, the MDD of the W/O/W multiple nanoemulsion after 6 refrigeration cycles of 364.2±11.2 nm was still within the nano range. Fig. 5.2 (h) shows the STEM image of W/O/W multiple nanoemulsion after the refrigeration cycles with an increase in MDD as compared to Fig. 5.2 (a). The droplet size of the oil gobule in the STEM image is ~425 nm. Here, the droplet size is higher when compared to the MDD obtained

from zetasizer which could be attributed to the staining technique as mentioned earlier (Chapter 4 section 4.3.6).

0.13% of TRF and 1.18% of CA were lost from the oil and internal water phases, respectively, in the W/O/W multiple nanoemulsion. However, these losses were lower when compared to the losses of TRF and CA in their respective phases when analysed after 180 days at room temperature (~25 °C) (Section 5.3.1.3). When nanoemulsion was refrigerated, the natural phenomenon of oxidation could have been suppressed due to low refrigeration temperature. This could have improved the retainment of refrigerated active compounds in W/O/W multiple nanoemulsion than stored at room temperature. This finding corroborates with the study by Aditya et al. [194] which reported higher retainment of active compounds in W/O/W multiple emulsion stored for 15 days at 4 °C than at 23 °C.

Table 5.5 Stability of W/O/W multiple nanoemulsion with the refrigeration cycles.

	Refrigeration cycles	
	Initial	**Final**
Mean droplet diameter (nm)	175.5±9.8	364.2±11.2
Dispersity index	0.232±0.012	0.343±0.048
Concentration of TRF (mol/dm^3)	0.007432	0.007422
Concentration of CA (mol/dm^3)	0.007298	0.007212

5.3.1.5 Comparison of TRF and CA stability in emulsion and solution form

After 28 days, TRF and CA concentrations decreased by 0.23% and 0.97%, respectively, in W/O/W multiple nanoemulsion. Whereas, the TRF and CA concentrations decreased by 17.42% and 11.81%, respectively, in the solution form, as shown in Table 5.6. This outcome of higher

stability of active compounds in the emulsion as compared to in solution form could be attributed to the encapsulation of TRF and CA in the oil and water phases, respectively. Contrastingly, in the solution form, there are no oil and water phases for encapsulation that could act as a protective layer. Additionally, in the emulsion, the presence of emulsifier at the oil-water interphase, as well as the solubility of TRF and CA in the oil and water phases, respectively, could have enhanced its retainment in comparison to the solution. This outcome was also observed by Aditya et al. [194], where the authors compared the stability of curcumin and catechin in the form of W/O/W multiple emulsion and solution. The authors reported a retainment of curcumin and catechin by 83% and 55%, respectively, in emulsion form. Whereas, in the solution form, retainment of 60% and 42% was reported for curcumin and catechin, respectively.

Table 5.6 Comparison of TRF/CA concentration in the W/O/W multiple nanoemulsion and solution form.

		Days	
		Initial (0)	**Final (28)**
Concentration of TRF (mol/dm^3)	**W/O/W multiple nanoemulsion**	0.007432	0.007415
	Solution	0.007521	0.006211
Concentration of CA (mol/dm^3)	**W/O/W multiple nanoemulsion**	0.007298	0.007227
	Solution	0.007613	0.006714

5.3.2 Encapsulation efficiency and loading capacity

As shown in Table 5.7, high encapsulation efficiencies of ~99% and ~98% for TRF and CA, respectively, in W/O/W multiple nanoemulsion were obtained. Concerning loading capacities, ~215% and ~90% of TRF and CA, respectively, were obtained for a concentration of 5.0 M. The high encapsulation efficiency and loading capacity achieved in this study could be related to the utilized PGPR as emulsifier, which has strong binding and anchoring properties that assisted in retaining the active compounds within the W/O/W multiple nanoemulsion. The firm anchoring properties between PGPR and palm oil have been presented and explained in Chapter 3 section 3.3.1. Besides the influence of emulsifier towards encapsulation efficiency and loading capacity, the solubility of TRF and CA in oil and water, respectively, could have also contributed to it.

Table 5.7 Encapsulation efficiency and loading capacity of W/O/W multiple nanoemulsion encapsulating TRF and CA.

Active compounds	**TRF**	**CA**
Encapsulation efficiency (%)	~99	~98
Loading capacity (%)	215.31	89.78

Comparatively, Chen et al. [264] reported 65.5% and 97.2% of encapsulation efficiencies for epigallocatechin-3-gallate and quercetin, respectively, in W/O/W multiple emulsion. The authors also reported low loading capacities of 0.262% and 0.097% for epigallocatechin-3-gallate and quercetin, respectively. These were attributed to the poor solubility of the compounds in the water and oil phases.

5.3.3 Antioxidant and phenolic activity

As shown in Table 5.8, for the antioxidant activities of TRF at 1.0 µM and 10.0 µM, 0.15% and 0.47% of differences were observed, respectively, between W/O/W multiple nanoemulsion and solution. Whereas, for the phenolic activities of CA at 1.0 µM and 10.0 µM, 0.1 GAE of differences were observed for both concentrations were observed between W/O/W multiple nanoemulsion and solution. Due to the minimal differences, similar antioxidant activities were observed for TRF in solution and emulsion forms. Likewise, similar phenolic activities were observed for CA in solution and emulsion forms which were determined using UV-Vis calibration graph, as shown in Fig. 5.6. Similar activities were due to the presence of similar concentrations of TRF and CA in emulsion or solution form. Thus, these outcomes indicate that the encapsulation of compounds in emulsion or solution form neither induce deterioration nor improvement of antioxidant and phenolic activities. The antioxidant and phenolic activities of TRF and CA, respectively, are dependent on the concentration of active compounds present. It was not influenced by the encapsulation in the nanoemulsion or its free availability in the form of solution.

Table 5.8 Comparison of antioxidant and phenolic activity of TRF and CA in W/O/W multiple nanoemulsion and solution form.

Concentration (µM)	**TRF antioxidant activity using DPPH reagent (%)**		**CA phenolic activity using Folin-Ciocalteu reagent (GAE)**	
	W/O/W multiple nanoemulsion	**Solution**	**W/O/W multiple nanoemulsion**	**Solution**
1	9.19	9.34	1.10	1.20
10	34.36	33.89	2.50	2.40

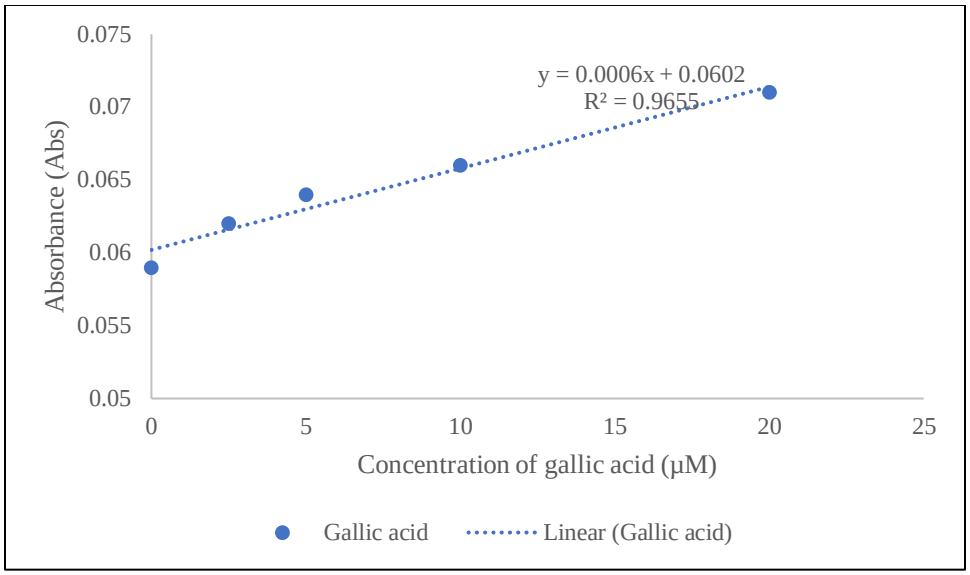


Fig. 5.6 UV-Vis calibration for gallic acid.

5.3.4 Evaluation of cell viability

From Fig. 5.7 (a) and (b), increased concentrations of TRF, CA and CIS reduced the viability of A549 and HEP G2 cancer cell lines. From Table 5.9, for A549 cells, IC 50 values for treatments were 1.00 µM, 1.50 µM and 0.45 µM using TRF, CA, and CIS, respectively, while for HEP G2, the IC 50 values for treatments were 0.80 µM, 1.60 µM and 0.25 µM using TRF, CA and CIS, respectively. The IC 50 values indicate the half-maximal inhibitory concentration as a measure of the potency of treatment in inhibiting cell proliferation.

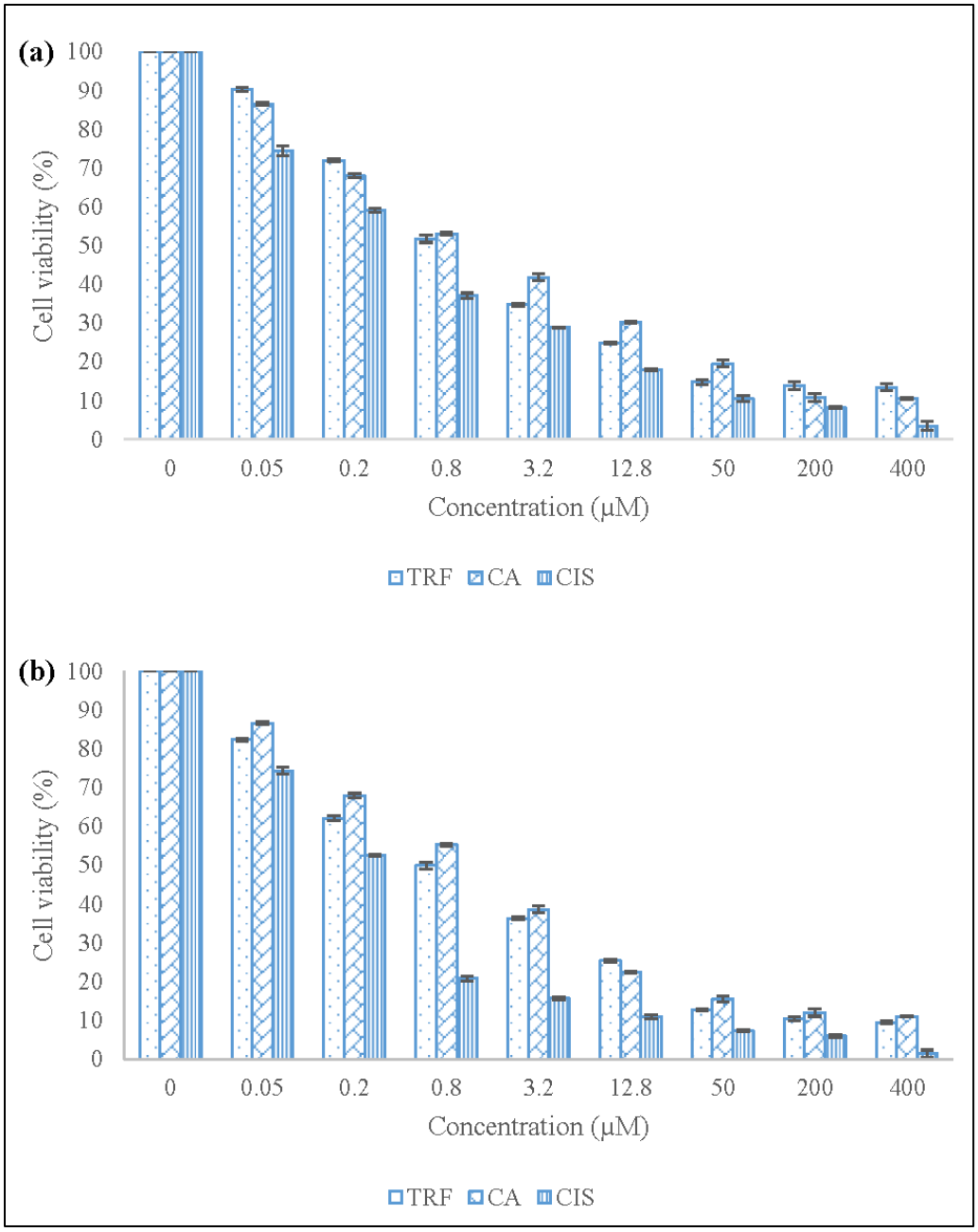


Fig. 5.7 Cell viability of (a) A549 and (b) HEP G2 with the treatment of TRF, CA and CIS.

Table 5.9 IC 50 values for TRF, CA and CIS for A549 and HEP G2.

Active compounds	Concentration (µM)	
	A549	**HEP G2**
TRF	1.00	0.80
CA	1.50	1.60
CIS	0.45	0.25

From Fig. 5.8 (a) and (b), both emulsion and solution inhibited A549 cells with increased concentrations of TRF and CA, respectively. From Fig. 5.9 (a) and (b), both solution and emulsion also inhibited the HEP G2 cells with increasing concentrations of TRF and CA, respectively. Larger number of cells were not viable as the concentrations of TRF and CA increased. However, 180.0% and 100.0% higher TRF and CA concentrations, respectively, were required in solution as compared to emulsion form to achieve IC 50 for A549 as shown in Table 5.10. Similarly, 150.0% and 237.5% higher TRF and CA concentrations, respectively, were required in solution as compared to emulsion form to achieve IC 50 for HEP G2. This shows that nano-sized emulsion required lower concentration of active compounds than in solution form to achieve IC 50. This could be attributed to the nanosized structures that allow active compounds to penetrate tissues, facilitating a smooth uptake of the active compounds by the cells [265, 266].

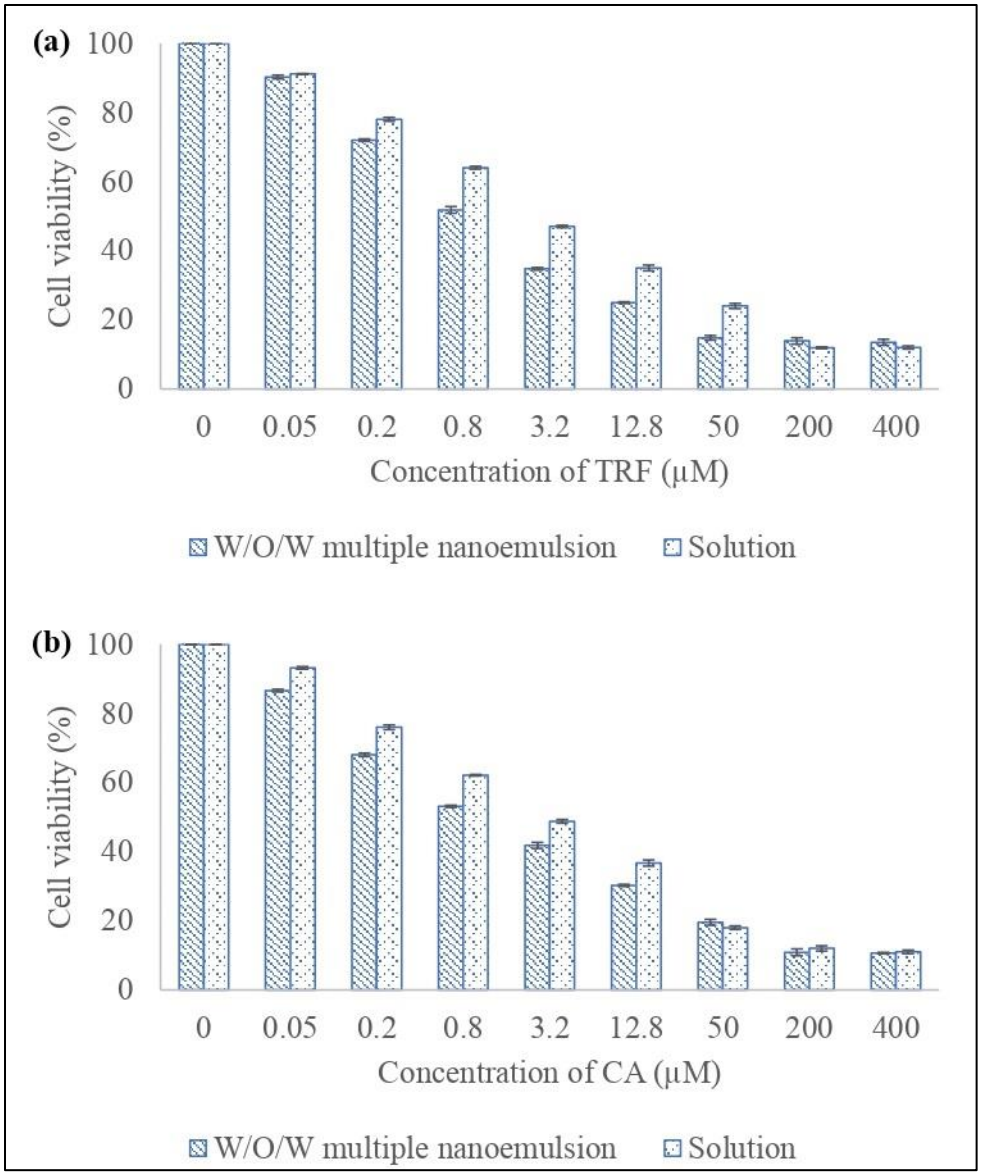


Fig. 5.8 Cell viability of A549 for treatment using (a) TRF and (b) CA in emulsion and solution form.

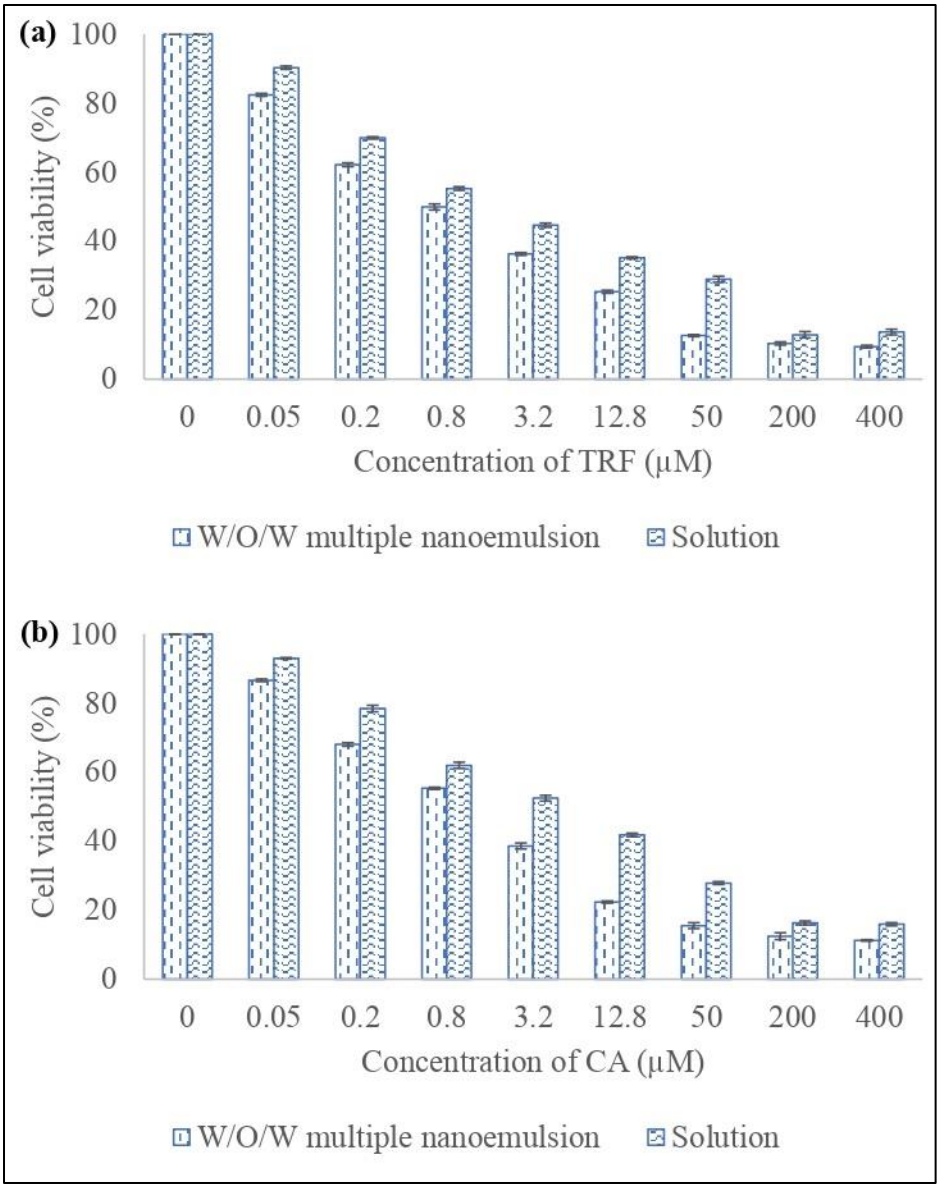


Fig. 5.9 Cell viability of HEP G2 for treatment using (a) TRF and (b) CA in emulsion and solution form.

Table 5.10 Comparison of IC 50 values of TRF and CA in W/O/W multiple nanoemulsion and solution form.

Active compounds	A549		HEP G2	
	W/O/W multiple nanoemulsion	Solution	W/O/W multiple nanoemulsion	Solution
TRF	1.00	2.80	0.80	2.00
CA	1.50	3.00	1.60	5.40

Isobologram and combination index (CI) analyses were performed to evaluate the drug interaction for cancer chemotherapy. The isobologram analysis evaluates two active compounds at a given concentration (IC 50). The line connecting these two points is the line of additivity. Synergy, additivity or antagonism is indicated when a given concentration of two active compounds is located below the line, on the line or above the line, respectively. Concerning CI, it was calculated using Eq. 5.6. CI of less than 1, equal to 1 or more than 1 indicates synergy, additivity or antagonism, respectively.

$$\text{CI} = \frac{\text{Concentration of TRF (µM)}}{IC\ 50\ TRF\ (\mu M)} + \frac{\text{Concentration of CA (µM)}}{IC\ 50\ CA\ (\mu M)} \qquad \text{Eq. 5.6}$$

From Fig. 5.10 and Fig. 5.11 which exhibited isobologram for both A549 and HEP G2, respectively, the combination of TRF:CA, TRF:CIS and CA:CIS were all below the line. This indicated synergism.

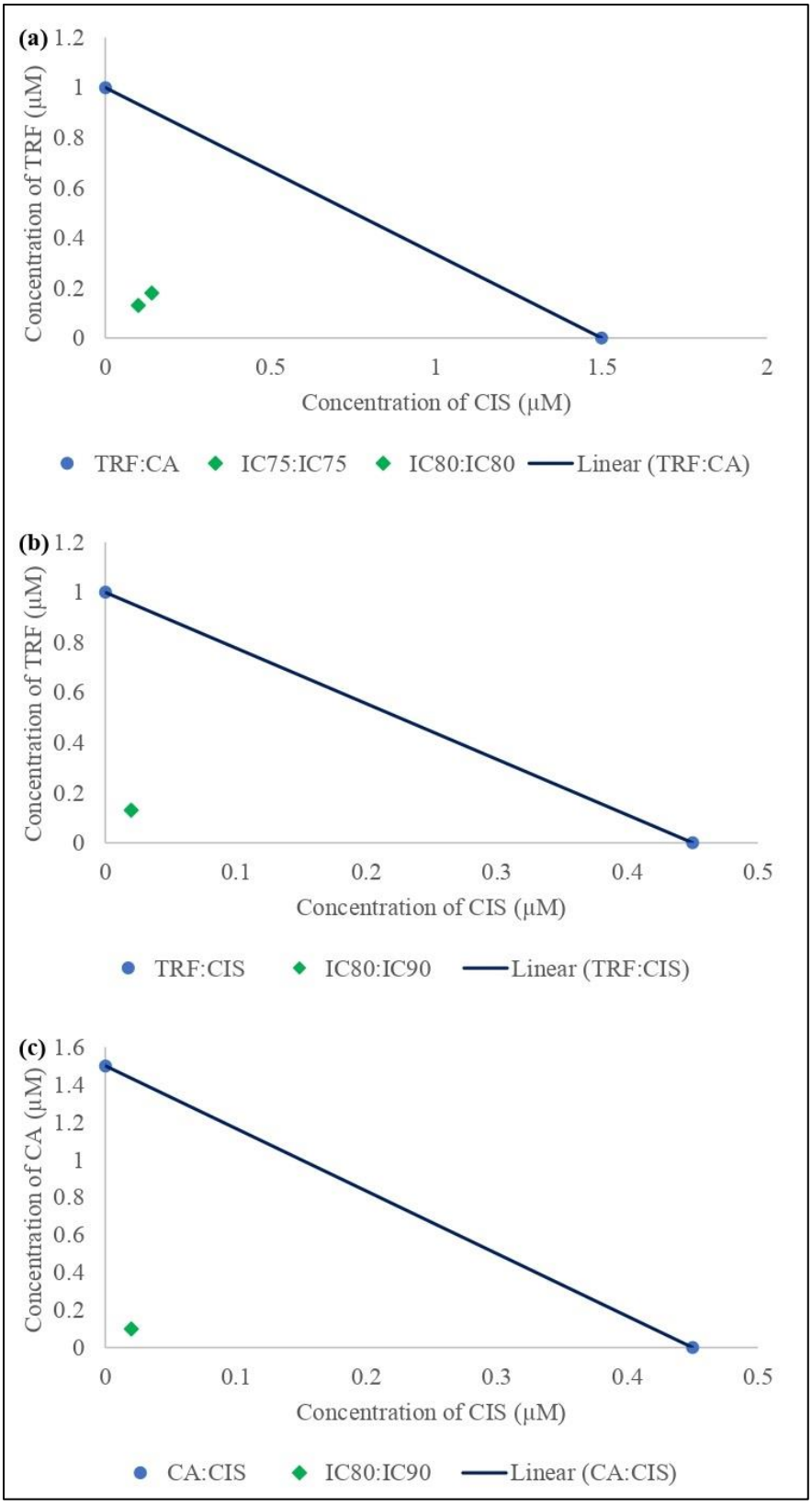


Fig. 5.10 Isobologram of (a) TRF:CA, (b) TRF:CIS and (c) CA:CIS for A549.

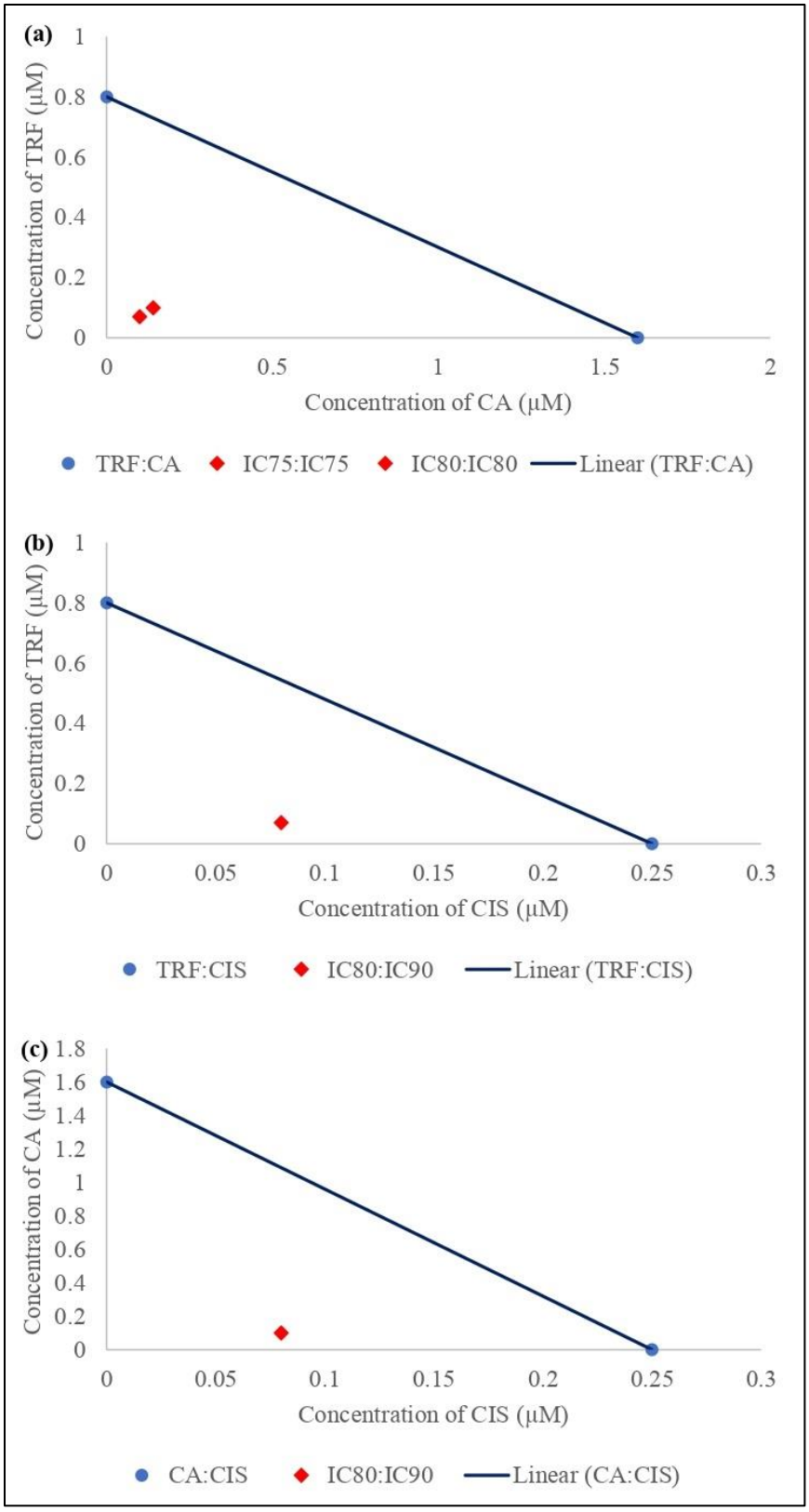


Fig. 5.11 Isobologram of (a) TRF:CA, (b) TRF:CIS and (c) CA:CIS for HEP G2.

As shown in Table 5.11, the CI values for the combination of TRF:CA, TRF:CIS and CA:CIS used at the given concentration were all less than 1. This analysis too indicated synergism for both A549 and HEP G2 cells.

Table 5.11 Combination index for A549 and HEP G2.

Active compounds	**Combination index**	
	A549	**HEP G2**
CA:TRF (IC75:IC75)	0.2733	0.2125
CA:TRF (IC80:IC80)	0.1967	0.1500
CIS:TRF (IC90:IC80)	0.1744	0.4075
CIS:CA (IC90:IC80)	0.1111	0.3825

Considering the synergism of the treatments described in Table 5.2 have been verified using isobologram and CI, the effects of these treatments towards cell viability of A549 and HEP G2 at 3, 6, 12, 24 and 48 h were then performed, independently. The investigations were carried out to evaluate the effects of the treatments on cell inhibition pattern.

From Fig. 5.12 (a) and (b), the treatments inhibited cell proliferation for both A549 and HEP G2, respectively. As the incubation duration with the treatments approached 24 h, ~IC 50 was achieved in both A549 and HEP G2, independently. Notably, even beyond 24 h, the cells were observed to be inhibited at IC 50, indicating that there were no rebound effect of cell growth. This shows that cell proliferation was not suppressed and regrown after a specific duration. Thus, the treatments utilizing TRF and CA with CIS led to cell death. In the following subsections, the quantification of apoptosis phases, the effect of generation of ROS and cell cycle arrest which led

to the cell death in A549 and HEP G2 cancer cell lines using the treatments described in Table 5.2 will be discussed.

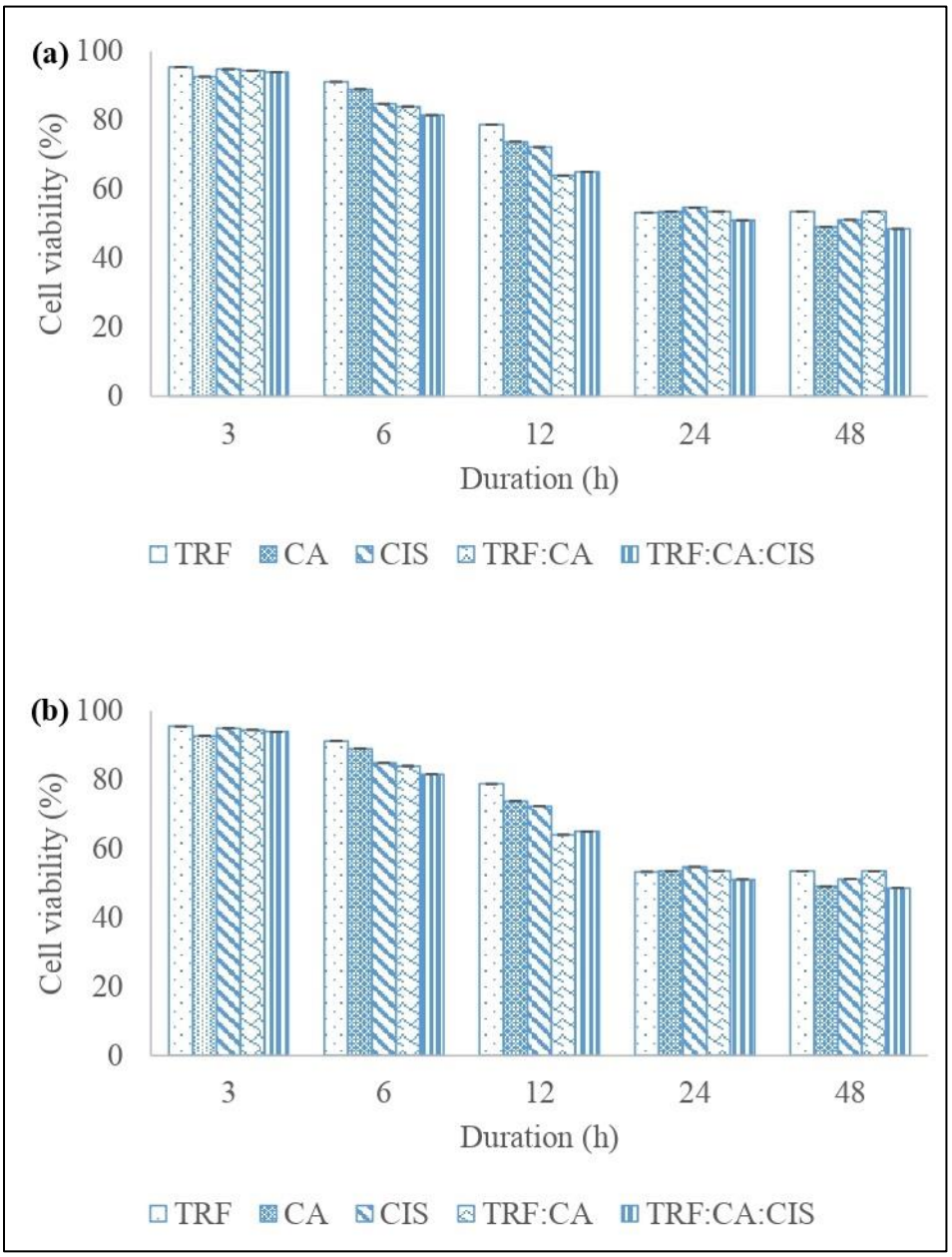


Fig. 5.12 Analysis of cell viability at 3, 6, 12, 24 and 48 h for TRF-treated, CA-treated, CIS-treated, TRF:CA treated and TRF:CA:CIS treated for (a) A549 and (b) HEP G2.

5.3.5 Flow cytometry analysis of cell apoptosis for A549 and HEP G2 cell lines

From Fig. 5.13 (a) and (b), 97.92% and 97.58% of untreated A549 and HEP G2 cell lines, respectively, are present in the live cell phase. Similar cell distributions as the untreated cells in both A549 and HEP G2 cell lines were also observed for the control (unencapsulated W/O/W multiple nanoemulsion) at ~98%. This shows that the formulated unencapsulated W/O/W multiple nanoemulsion did not induce any response in the cells and is suitable for use as a drug carrier.

For A549, TRF:CA had a cell distribution of 16.44%, while, TRF, CA and CIS only had 14.76%, 14.37% and 15.43%, respectively, in the late apoptosis phase. For HEP G2, TRF: CA had a cell distribution of 22.55%, while, TRF, CA and CIS only had 16.93%, 17.70% and 18.44%, respectively, in the late apoptosis phase. Meanwhile, TRF:CA:CIS showed the highest cell distribution for both A549 and HEP G2 cells of 23.13% and 24.89%, respectively, in late apoptosis phase. This showed that the combined use of TRF:CA and TRF:CA:CIS enhanced the apoptotic response for both A549 and HEP G2 cell lines in the late apoptotic phase.

Notably, the cell distribution for the A549 cell line was higher in the necrosis phase at 1.77% for CIS only as compared to 1.54% for TRF:CA:CIS. Likewise, the cell distribution for HEP G2 cell line was higher in the necrosis phase at 2.46% for CIS only as compared to 1.91% for TRF:CA:CIS. As indicated earlier (Table 5.2), when CIS only was used, the IC 50 concentrations were 0.55 µM and 0.35 µM for A549 and HEP G2, respectively. However, when used simultaneously with TRF and CA, the concentrations of CIS for IC 50 were 0.02 µM and 0.03 µM for A549 and HEP G2, respectively. This showed that when CIS was used at lower concentrations, the accumulated cells in the necrosis phase were lower. These findings could be associated with the mechanism of apoptosis.

Apoptosis is the process of programmed cell death. Excessive apoptosis causes atrophy, while insufficiency leads to uncontrolled cell proliferation, such as cancer. The early stages of apoptosis involve cell shrinkage and pyknosis (nuclear condensation) [209]. The late stage of apoptosis is characterized by karyorrhexis (nucleus fragmentation), where pyknotic nuclei membrane ruptures and nucleus undergoes fragmentation [209]. Necrosis is an alternative to apoptotic cell death, which is a toxic process. Necrosis involves karyolysis (nuclear fading) and cell swelling. In this, chromatin dissolves due to the action of enzymes such as deoxyribonucleases and ribonucleases.

CIS only treatment had a higher distribution of cells in the necrosis phase than TRF:CA:CIS, which is considered to be more toxic. This shows that the utilization of natural compounds reduces toxicity. This is in line with the study by Rahman et al. [267] in which the authors reported that γ-tocotrienol induced cell death in human glioma cells by apoptotic rather than a necrotic pathway. Moreover, the combined TRF:CA and TRF:CA:CIS exhibited an improved cell distribution in the late apoptotic phase due to the synergistic effect. A similar finding was also reported by Yusof et al. [268] in which the authors highlighted that there was improvement in apoptosis due to synergistic effects of γ-tocotrienol and 6-gingerol on colorectal cancer cells when used simultaneously.

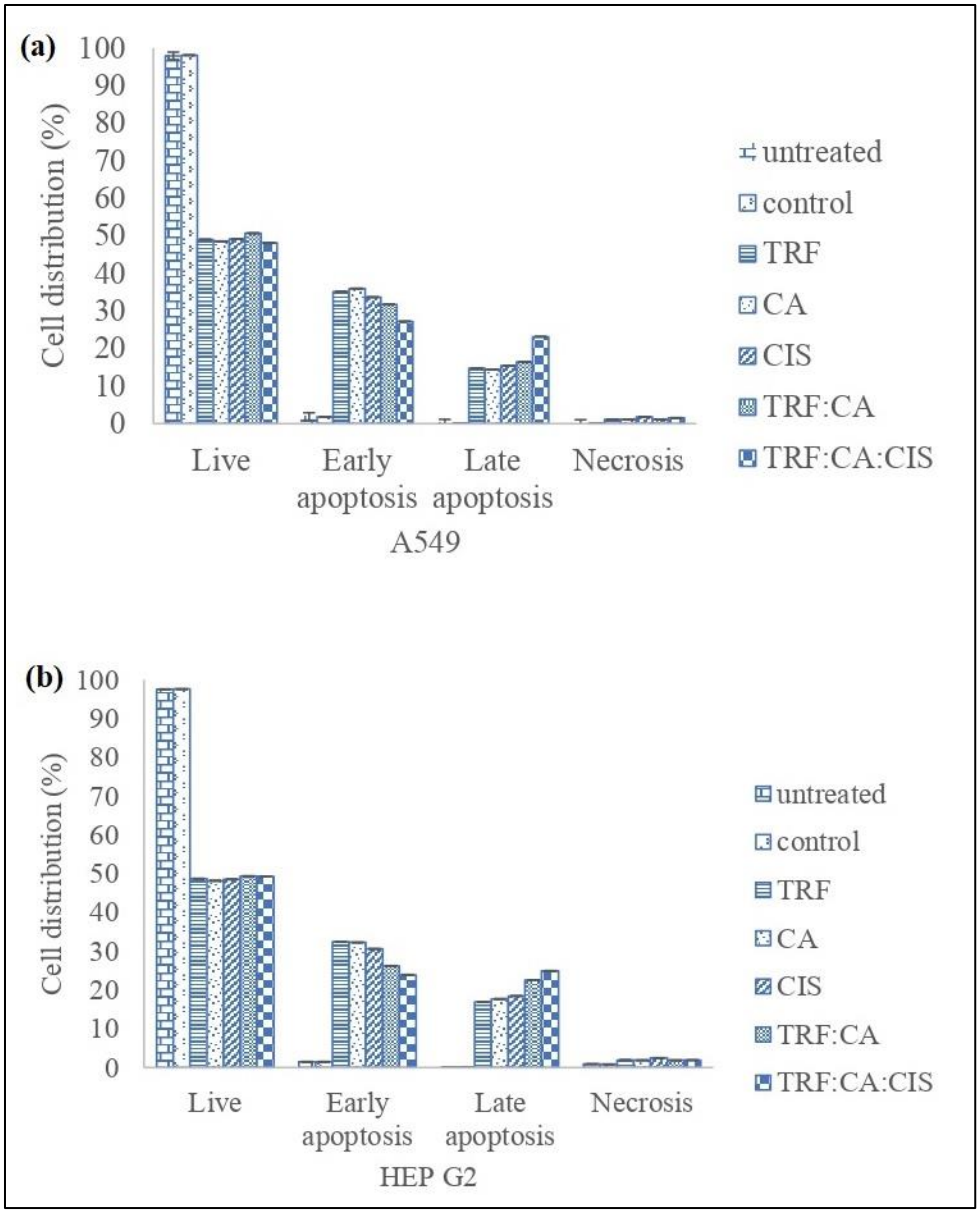


Fig. 5.13 Cell distribution at live, early apoptosis, late apoptosis and necrosis phase for (a) A549 Annexin analysis and (b) HEP G2 Annexin analysis.

5.3.6 Intracellular ROS generation for A549 and HEP G2 cell lines

The values were normalized to 100% for the untreated cells. From Fig. 5.14, both the untreated and control resulted in almost similar ROS generation of ~100% for A549 and HEP G2 cell lines. This indicated that there was no effect demonstrated by the unencapsulated W/O/W multiple nanoemulsion (control) on the cancer cell lines. Hence, suggested as a suitable carrier for drugs.

There was an increase in ROS generation for all the treatments in both A549 and HEP G2 cell lines. For A549, TRF:CA had an increase in ROS generation by 14.1%, while, TRF, CA and CIS only had an increase by 10.72%, 9.95% and 13.06%, respectively. For HEP G2, TRF:CA had an increase in ROS generation by 22.69%, while, TRF, CA and CIS only had an increase by 9.76%, 6.13% and 20.43%, respectively. Similarly, existing studies have also reported increased intracellular ROS generation induced apoptosis in cancer cell lines with the use of TRF [269, 270], CA [271, 272] and CIS [273, 274] as treatments.

Meanwhile, TRF:CA:CIS had the highest ROS generation by 16.92% and 30.22% for A549 and HEP G2 cell lines, respectively. The combined TRF:CA and TRF:CA:CIS showed a higher increase in the generation of ROS as compared to TRF, CA and CIS only treatments. The increased ROS generation due to the given treatments could be associated with the alteration of mitochondria, which affected the permeability of the membrane and damaged the respiratory chain [275]. The disruption in the mitochondrial membrane could release cytochrome c from the mitochondria leading to apoptosis [276]. In line with this, Boveris and Cadenas [277], Antunes and Cadenas [278] and Chung et al. [279] reported that an increased intracellular ROS could induce cancer cell cycle arrest, senescence and apoptosis. Besides, Noh et al. [280] and Yi et al. [281] reported increased ROS generation due to synergistic effects. Noh et al. [280] also highlighted that the synergistic effect from combined drugs could have disturbed the redox balance to kill cancer

cells more effectively. These results indicated that the combined use of TRF:CA and TRF:CA:CIS synergistically exhibited higher ROS generation that effectively led to cell death for both A549 and HEP G2 cell lines.

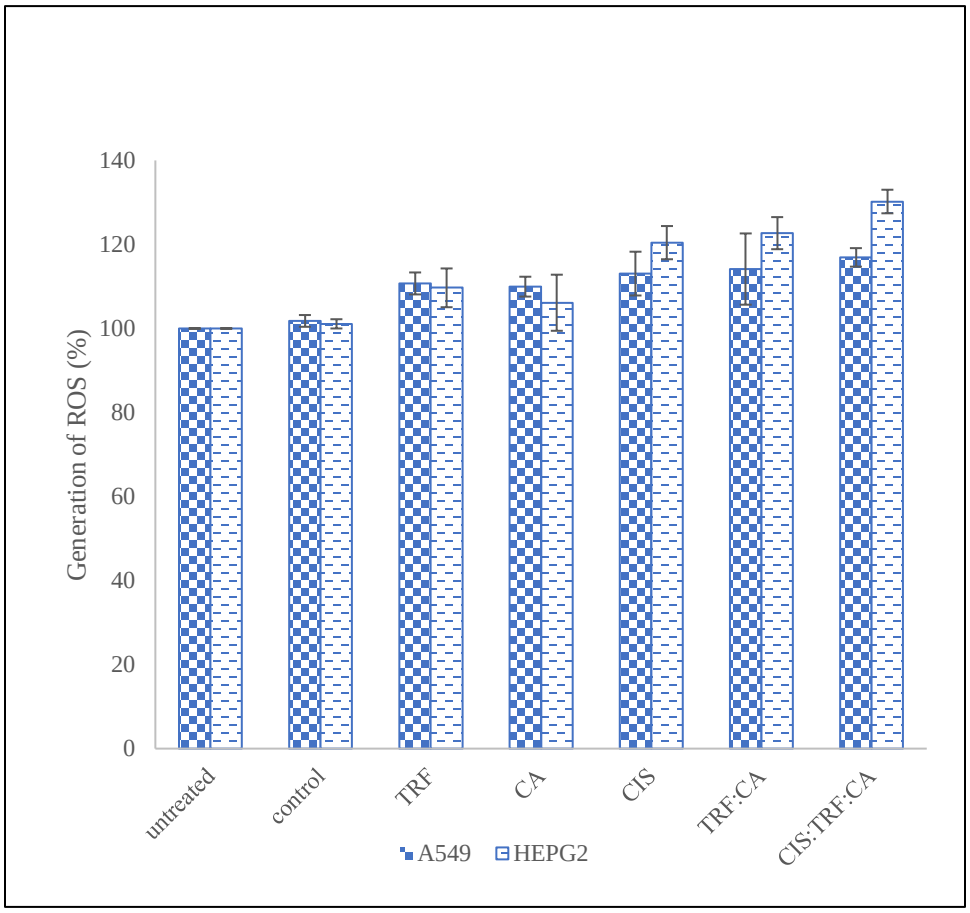


Fig. 5.14 Intracellular production of ROS for untreated, control, TRF-treated, CA-treated, CIS-treated, TRF/CA-treated and TRF:CA:CIS treated A549 and HEP G2.

5.3.7 Flow cytometry analysis of cell cycle for A549 and HEP G2 cell lines

As shown in Fig. 5.15 (a) and (b), both the untreated cell lines of A549 and HEP G2 have 61.98% and 70.15% of cells, respectively, in the G0/G1 phase. The control (unencapsulated W/O/W multiple nanoemulsion) showed similar cell distribution as the untreated cell lines. This showed that there was no influence of the unencapsulated W/O/W multiple nanoemulsion on the cancer cells. Hence, demonstrated its suitability for use as a drug carrier.

In A549 cell lines, TRF:CA increased cell accumulation in G0/G1 phase by 15.79%, while, TRF, CA and CIS only increased by 11.23%, 10.31% and 12.58%, respectively. For HEP G2 cell line, TRF:CA increased cell accumulation in G0/G1 phase by 8.0%, while, TRF, CA and CIS only increased by 2.15%, 1.75% and 5.45%, respectively. Meanwhile, TRF:CA:CIS showed highest increase in cell accumulation in G0/G1 phase for both A549 and HEP G2 cell lines by 18.88% and 10.72%, respectively. The combined use of TRF:CA and TRF:CA:CIS enhanced the apoptotic response in the G0/G1 phase for both A549 and HEP G2 cell lines. These results also indicated that the cell cycle was arrested at the G0/G1 phase when CA, TRF and CIS when treatments were given individually or simultaneously.

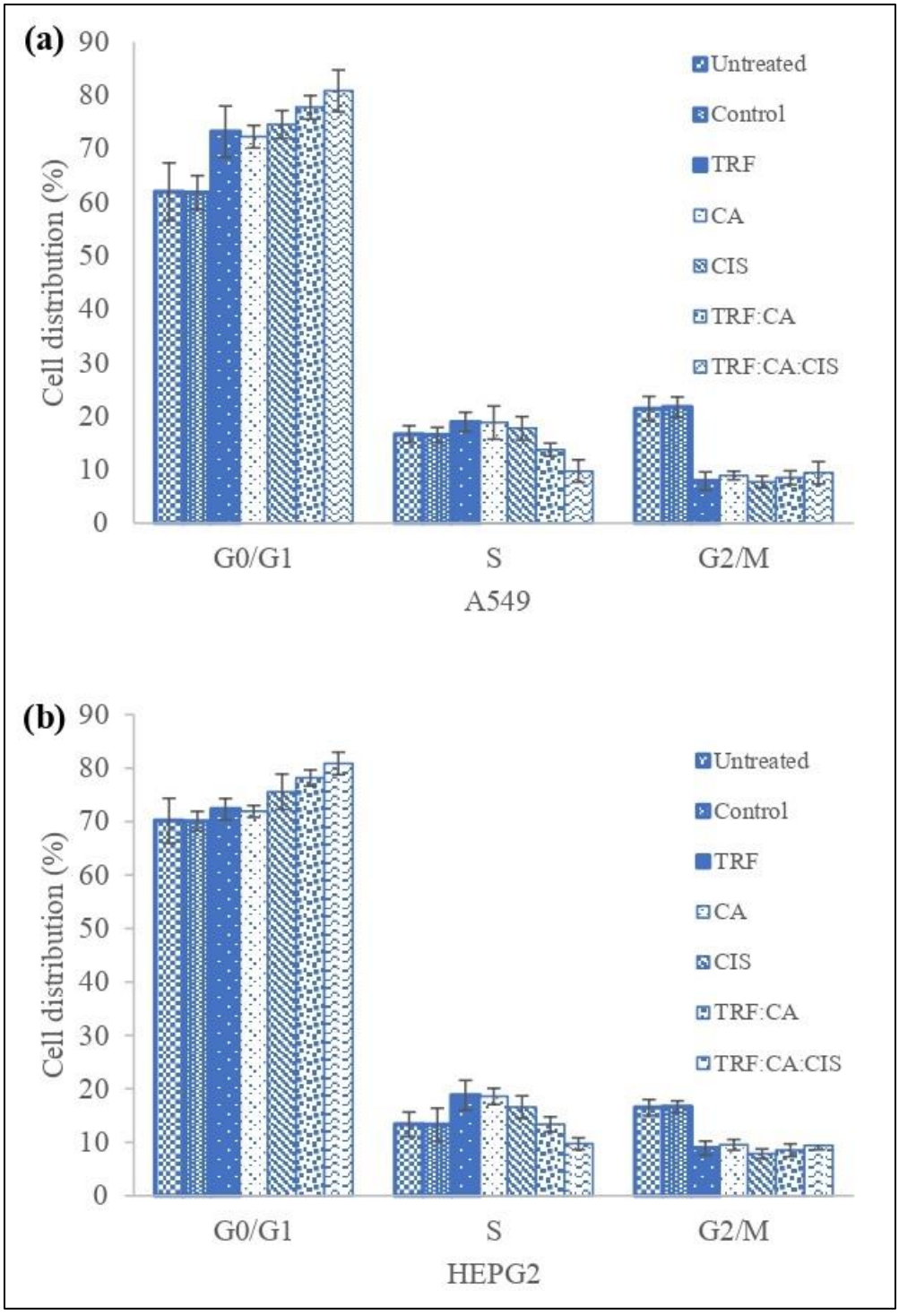


Fig. 5.15 Cell distribution at G0/G1, S and G2/M phase for (a) A549 cell cycle analysis and (b) HEP G2 cell cycle analysis.

Yang et al. [282] and Wang et al. [283] reported cell cycle arrest in the G0/G1 phase after treatment with CIS. The use of TRF has also been reported to arrest the cell cycle in the G0/G1 phase [78, 284]. Tyszka-Czochara et al. [83] and Aru et al. [285] reported cell cycle arrest in the G0/G1 phase with the use of CA.

In general, during the G0/G1 phase, the cell grows larger, copies organelles and makes the molecular building blocks it requires. In the S phase, the cell synthesizes DNA in its nucleus. It also duplicates a microtubule-organizing structure called the centrosome to separate DNA during the M phase. While, during the G2/M phase, the cell grows more, makes proteins and organelles and begins to reorganize its contents in preparation for mitosis. An increase in the G0/G1 population indicates an increase in apoptotic cells; hence, treating A549 and HEP G2 cells with TRF:CA:CIS could amplify the apoptotic cascade. Also, the higher increase in cell distribution when treated with CA:TRF and CA:TRF:CIS proves improvement due to the effect of synergism.

5.**3.8 Toxicity study**

The toxicity of the treatments, as described in Table 5.2, was evaluated on HEK293 normal kidney cell line. From Fig. 5.16, the treatments of TRF, CA and TRF:CA using the dosages used for both A549 and HEP G2 cell lines, had a viability of ~95% on HEK293 cell line. While, the treatments of CIS using the dosages used for A549 and HEP G2 cell lines had the viability of ~33% and ~43%, respectively, on the HEK293 cell line.

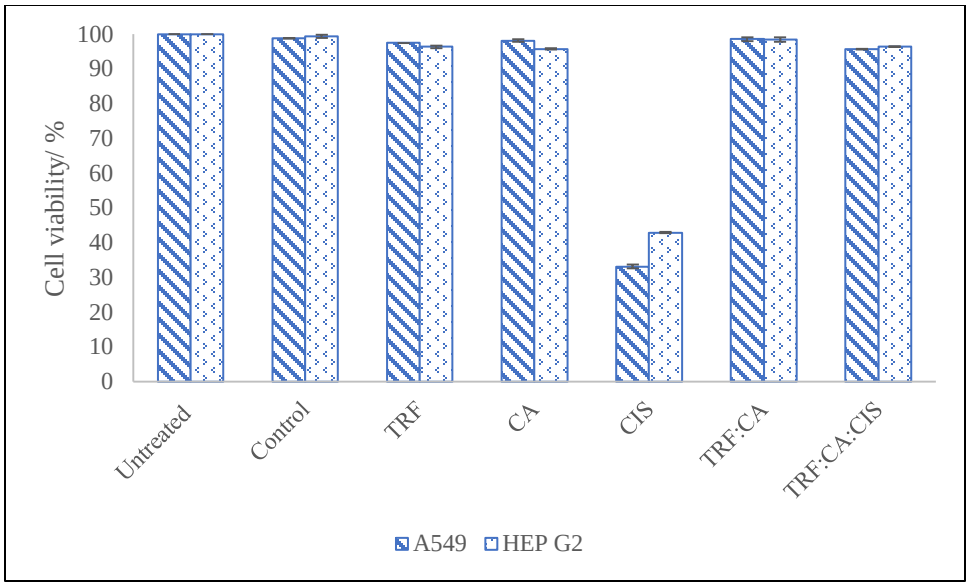


Fig. 5.16 Cell viability analysis of HEK 293 for untreated, control, TRF-treated, CA-treated, CIS-treated, TRF:CA treated and TRF:CA:CIS treated A549 and HEP G2 dosages.

The outcome of CIS on HEK293 cell line viability corroborates with the nephrotoxicity effect (side effect) of CIS during cancer treatment [286-288]. This is chiefly due to the uptake and activation of platinum within the proximal tubule cell in the kidney leading to toxicity [289]. Contrastingly, when TRF:CA:CIS was used, cell viability was ~95% for HEK 293 cell line. This is due to the lower concentration of CIS required when used simultaneously with TRF and CA. Several other studies have reported that the use of natural chemopreventive compounds could lower toxicity during cancer treatments [290, 291].

5.4 Summary

Similar concentrations of TRF and CA were retained in W/O/W multiple nanoemulsion processed using both ultrasonication and microfluidization. The stability of the formulated W/O/W multiple nanoemulsion from ultrasonicator was analysed based on the change of MDD, DI, water content, conductivity value, NaCl concentration, zeta potential, as well as TRF and CA concentrations after 180 days. The losses of the compounds were lesser with refrigeration than room temperature. Higher losses of compounds were observed in solution as compared to in emulsion form. High encapsulation efficiencies and high loading capacities were observed for both compounds in the W/O/W multiple nanoemulsion. The encapsulation of compounds (TRF and CA) in the W/O/W multiple nanoemulsion did not alter its potential. Higher concentrations of the compounds were required to obtain IC 50 in the form of solution as compared to the emulsion. The synergistic effect of the compounds and CIS determined from isobologram and CI led to the death of cancer cell lines, improved apoptosis in the late apoptotic phase, enhanced generation of ROS leading to apoptosis and intensified cell arrest in G0/G1 phase. The combined use of natural active compounds in W/O/W multiple nanoemulsion with CIS also resulted in high viability of normal kidney cell line.

CHAPTER 6-CONCLUSIONS AND RECOMMENDATIONS FOR FURTHER WORK

The present study encapsulated TRF and CA in stable palm oil-based W/O/W multiple nanoemulsion and evaluated its efficacy towards A549 and HEP G2 cancer cell lines. The key findings from this work are firstly presented, followed by recommendations for further research work.

6.1 Conclusions

An evaluation of the existing studies on multiple emulsion revealed that the majority of the studies focused on balancing the osmotic pressure difference through thickeners and additives to enhance its stability. However, these are secondary approaches considering it is aimed to control the movement between the internal and external water droplets to produce stable W/O/W nanoemulsion. Instead, emphasis on formulating stable W/O nanoemulsion with the rigid structure before forming W/O/W nanoemulsion should instead be given priority. For this reason, multi-faceted experimentations were carried out by firstly formulating stable W/O nanoemulsion emphasizing on creating a rigid structure, followed with the generation of W/O/W multiple nanoemulsion. This was then followed with the encapsulation of active compounds and subsequent evaluation of its efficacy for treating cancer cell lines. The outcomes are divided into three distinct parts, as described:

Part 1 Formulation of palm oil-based W/O nanoemulsion

- Stable palm oil-based W/O nanoemulsion was formulated using 61.25 wt%, 26.25 wt%, 2.5 wt% and 10.0 wt% of palm oil, MCT, PGPR and water, respectively. The MDD and DI of the formulated W/O nanoemulsion were 143.1±8.8 nm and 0.131±0.094, respectively. The polyricinoleate non-polar fatty acids of PGPR bound to non-polar fatty acids of palm oil through van der Waals intermolecular forces, while the polyglycerol polar head of PGPR formed hydrogen bonds with water molecules, as well as bound with glyceride units of palm oil.
- The optimized processing conditions for the formation of W/O nanoemulsion using ultrasonicator were: an amplitude of 40% and irradiation time of 180 s, while by using microfluidizer were: an operating pressure of 350 bar with 6 cycles. Lipid peroxidation did not occur for the W/O nanoemulsion processed using ultrasonicator, as well as microfluidizer. Ultrasonicator was more energy-efficient than microfluidizer as it consumed 9 times lesser energy for producing W/O nanoemulsion with an MDD of ~215 nm.
- 30.0 wt% of MCT oil with 70.0 wt% of palm oil was chosen as the optimized blend as a further addition of MCT oil lowered the viscosity of the emulsion, thereby prevailing sedimentation. The viscosity of nanoemulsion is critical as higher viscosity reduces the tendency of sedimentation, which adversely affects the formation of smaller droplet size. The CMC was obtained at 3.0 wt% of PGPR. Although the addition of lecithin further reduced the required concentration of PGPR by 0.5 wt%, which improved the stability of nanoemulsion due to increased viscosity, it, however, did not reduce the size of MDD. Instead, the addition of NaCl critically reduced the droplet size by 70.0 nm. It improved

the stability of nanoemulsion through electrostatic and steric repulsions attributed to the dissociation of NaCl into its Na^+ and Cl^- ions.

- Palm oil and MCT with PGPR and NaCl are deemed to produce stable W/O nanoemulsion.

Part 2 Formulation of palm oil-based W/O/W multiple nanoemulsion

- Stable palm oil-based W/O/W multiple nanoemulsion was successfully formed with optimized ultrasonicator conditions of 40% amplitude, 180 s of irradiation time, while for microfluidizer, it was 350 bar and 8 cycles. Ultrasonicator was more energy saving by 12 times as compared to microfluidizer to produce W/O/W multiple nanoemulsion with about similar droplet size (~235nm).
- Palm oil in W/O/W multiple nanoemulsion processed by both ultrasonicator and microfluidizer did not oxidize as there was no change in the peroxide values, fatty acid composition and FTIR indicating the absence of primary and secondary oxidation products. 90:10 of phase volume ratio was more stable with smaller MDD and DI as compared to 80:20. A higher concentration of hydrophilic emulsifier (Tween 80) led to instability in W/O/W multiple nanoemulsion with larger MDD and DI due to the enhanced migration of emulsifiers between the internal and external water-oil interfaces.
- This is the first study that successfully utilized Sucragel in imparting enhanced stability in W/O/W multiple nanoemulsion as the thickened oil retained and protected the internal water droplets within the oil phase by forming a packed and stable network within the oil globules and rigid stability at the oil-water interface. Its solubility in palm oil, increased viscosity of the oil phase and the enhanced stability by co-interaction with PGPR at the internal water-oil interface, were the keys to the formation of the smallest MDD and DI.

- Isotonic stabilized W/O/W multiple nanoemulsion gave the lowest change in MDD, the concentration of NaCl and water content by 1.34%, 2.97%, and 0.40%, respectively, due to the reduced movement of water between the internal and external water phases.
- The final optimized formation of isotonic stabilized W/O/W multiple nanoemulsion with 1.0 wt% of Sucragel had MDD and DI of 175.5±9.8 nm and 0.232±0.012, respectively.

Part 3 Efficacy of encapsulated active compounds in palm oil-based W/O/W multiple nanoemulsion towards A549 and HEP G2 cancer cell lines

- Similar concentrations of TRF and CA in the range of 0.0072 µM to 0.0074 µM were retained in W/O/W multiple nanoemulsion processed using both ultrasonicator and microfluidizer. <4.0% change in MDD, DI, water content, conductivity value, NaCl concentration, zeta potential, as well as the concentration of TRF and CA in W/O/W multiple nanoemulsion were measured after 180 days. Despite the MDD and DI increased by 107.52% and 47.84%, respectively, after 6 refrigeration cycles, the concentrations of TRF and CA were not changed.
- Higher losses of TRF and CA by 17.42% and 11.81%, respectively, were found in solution as compared to emulsion form at 0.23% and 0.97% for TRF and CA, respectively, after 28 days. The higher stability of the active compounds in the emulsion as compared to solution is due to the protection within the oil and water phases.
- High encapsulation efficiencies (~99.0% for TRF and ~98.0% for CA) and loading capacities (~215.0% for TRF and ~90.0% for CA) in W/O/W multiple nanoemulsion are related to the strong binding and anchoring properties of the PGPR emulsifier used.

- Based on the similar antioxidant (TRF) and phenolic (CA) activities of ~34.0% and ~2.5 GAE, respectively, in solution and emulsion form, the encapsulation of compounds in the emulsion is deemed not to induce deterioration nor improvement for its potential.
- For A549 cell line, 1.00 µM, 1.50 µM and 0.45 µM concentrations of TRF, CA, and CIS, respectively, were required to achieve IC 50. While, for HEP G2, 0.80 µM, 1.60 µM and 0.25 µM concentrations of TRF, CA, and CIS, respectively, were required to achieve IC 50. 180.0% and 100.0% of higher TRF and CA concentrations, respectively, were needed to achieve IC 50 in the form of solution as compared to emulsion for A549. Likewise, for HEP G2, there was an increase of 150.0% and 237.5% for TRF and CA concentrations, respectively, to achieve IC 50 in the form of solution as compared to the emulsion. The nanosized emulsion is deemed to require lower concentration of compounds to achieve IC 50 since it facilitates easy uptake of active compounds by the cells.
- By using isobologram and CI, the synergistic effects of TRF:CA, TRF:CIS and CA:CIS were determined. The combined use of TRF, CA and CIS as treatment led to cell death of A549 and HEP G2 cancer cell lines. The synergistic effect coupled with the combined use of TRF, CA and CIS improved apoptosis in the late apoptotic phase, as well as enhanced the generation of ROS, leading to apoptosis for both A549 and HEP G2 cell lines. Enhanced cell arrest in the G0/G1 phase was also determined from cell cycle analysis.
- Concerning toxicity, the use of CIS only resulted in ~33% of HEK 293 normal kidney cell line viability. Contrastingly, ~95% of HEK 293 cell viability was obtained with the combined use of TRF, CA and CIS.
- The use of TRF and CA is deemed to reduce the required CIS dose for treatment, and this resulted in reduced toxicity and side effects associated with CIS.

Stable TRF and CA encapsulated W/O/W multiple nanoemulsion was successfully formulated and its effectiveness to be used with CIS as combined therapy for treating cancer cell lines was disseminated. The original knowledge derived from this study can ultimately be commercialized as an end product for the benefit of cancer patients worldwide. This work is expected to attract more research works on W/O/W multiple nanoemulsion encapsulating natural active compounds to increase the effectiveness of existing therapy using drugs, as well as to reduce the side effects associated to it.

6.2 Recommendations for further work

In the process of progressing the research from laboratory work to commercialization as an end product for the usage of cancer patients, future investigations/work are as suggested. Firstly, the production of TRF and CA encapsulated W/O/W multiple nanoemulsion with CIS in soft gel can be investigated. Secondly, animal study can be investigated before progressing to clinical trials on cancer patients. This is the common practice of furthering the research from the *in vitro* stage to the *in vivo* stage. Lastly, upon successful completion of clinical trials, the work can be progressed towards commercialization. This would be beneficial for all lung cancer patients worldwide.

Besides, the bioavailability of W/O/W multiple nanoemulsion encapsulated with TRF and CA in human body can be investigated. This is important to know the degradation and availabilility of the active compounds after it passes through the digestive system. Among the method is by doing a rat study. Upon inducing cancer to rat, the developed emulsion can be provided for consumption. Then, by collecting the blood, urine and faeces from the rat, the bioavailability can be determined. Besides rat study, *in vitro* digestion and release can also be performed by simulating

the digestive conditions in the stomach and intestine. Effectiveness of other hydrophobic and hydrophilic natural active compounds such as curcumin and oil palm phenolics to work with CIS can also be investigated. Likewise, the effectiveness of TRF and CA with other chemotherapy drugs such as carboplatin and oxaliplatin can also be examined. Furthermore, the effectiveness of the developed compounds can also be tested on other cancer and normal cell lines. The advanced drug delivery tool from this study can be used to do these works.

REFERENCES

[1] S.Y. Tang, S. Manickam, B. Nashiru, Impact of osmotic pressure and gelling in the generation of highly stable single core water-in-oil-in-water (W/O/W) nano multiple emulsions of aspirin assisted by two-stage ultrasonic cavitational emulsification, Colloids Surf. B Biointerfaces, 102 (2013) 653-658. https://doi.org/10.1016/j.colsurfb.2012.08.036.

[2] G. Muschiolik, Multiple emulsions for food use, Curr. Opin. in Colloid Interface Sci. 12 (2007) 213-220. https://doi.org/10.1016/j.cocis.2007.07.006.

[3 D. Sahu, K. Sanjay, A. Piyush, Recent advancement, technology & applications of multiple emulsions, Innovare J. H. Sci. 1 (2013) 19-23. https://innovareacademics.in/journals/index.php/ijhs/article/view/219.

[4] A. Florence, D. Whitehill, The formulation and stability of multiple emulsions, Int. J. Pharm. 11 (1982) 277-308. https://doi.org/10.1016/0378-5173(82)90080-1.

[5] Q. Huang, H. Yu, Q. Ru, Bioavailability and delivery of nutraceuticals using nanotechnology, J. Food Sci. 75 (2010) R50-R57. https://doi.org/10.1111/j.1750-3841.2009.01457.x.

[6] N. Garti, Progress in stabilization and transport phenomena of double emulsions in food applications, LWT, 30 (1997) 222-235. https://doi.org/10.1006/fstl.1996.0176.

[7] S. Manickam, S.Y. Tang, K.W. Tan, Cavitation technology–a greener processing technique for the generation of pharmaceutical nanoemulsions, Ultrason. Sonochem. 21 (2014) 2069-2083. https://doi.org/10.1016/j.ultsonch.2014.03.025.

[8] S.M. Jafari, Y. He, B. Bhandari, Nano-emulsion production by sonication and microfluidization-a comparison, Int. J. Food Prop. 9 (2006) 475. https://doi.org/10.1080/10942910600596464.

[9] S.Y. Tang, P. Shridharan, S. Manickam, Impact of process parameters in the generation of novel aspirin nanoemulsions–comparative studies between ultrasound cavitation and microfluidizer, Ultrason. Sonochem. 20 (2013) 485-497. https://doi.org/10.1016/j.ultsonch.2012.04.005.

[10] R. Raviadaran, M.H. Ng, K. Muthoosamy, S. Manickam, Simple and multiple emulsions emphasizing on industrial applications and stability assessment, in: C.O. Mohan, E. Carvajal-Millan, C.N. Ravishankar, A. K. Haghi (Eds.), Food Process Engineering and Quality Assurance, Apple Academic Press Inc., New York, 2018, pp. 179-230. https://doi.org/10.1201/9781315232966.

[11] N. Garti, A. Benichou, Double emulsions for controlled-release applications: progress and trends, Encyclopedic handbook of emulsion technology. New York: Marcel Dekker. (2001) pp. 377-407.

[12] G. Muschiolik, E. Dickinson, Double emulsions relevant to food systems: preparation, stability, and applications, Compr. Rev. Food Sci. F. 16 (2017) 532-555. https://doi.org/10.1111/1541-4337.12261.

[13] K.G.H. Desai, H. Jin Park, Recent developments in microencapsulation of food ingredients, Dry. Technol. 23 (2005) 1361-1394. https://doi.org/10.1081/DRT-200063478.

[14] H. Lamba, K. Sathish, L. Sabikhi, Double emulsions: Emerging delivery system for plant bioactives, Food Bioproc. Tech. 8 (2015) 709-728. https://doi.org/10.1007/s11947-014-1468-6.

[15] C. Lobato-Calleros, E. Rodriguez, O. Sandoval-Castilla, E. Vernon-Carter, J. Alvarez-Ramirez, Reduced-fat white fresh cheese-like products obtained from W 1/O/W 2 multiple emulsions: Viscoelastic and high-resolution image analyses, Food Res. Int. 39 (2006) 678-685. https://doi.org/10.1016/j.foodres.2006.01.006.

[16] M. Freire, R. Bou, S. Cofrades, M.T. Solas, F. Jiménez-Colmenero, Double emulsions to improve frankfurter lipid content: impact of perilla oil and pork backfat, J. Sci. Food Agric. 96 (2016) 900-908. https://doi.org/10.1002/jsfa.7163.

[17] S. Cofrades, J. Santos-López, M. Freire, J. Benedí, F. Sánchez-Muniz, F. Jiménez-Colmenero, Oxidative stability of meat systems made with $W_1/O/W_2$ emulsions prepared with hydroxytyrosol and chia oil as lipid phase, LWT, 59 (2014) 941-947. https://doi.org/10.1016/j.lwt.2014.06.051.

[18] M. Serdaroğlu, B. Öztürk, M. Urgu, Emulsion characteristics, chemical and textural properties of meat systems produced with double emulsions as beef fat replacers, Meat Sci. 117 (2016) 187-195. https://doi.org/10.1016/j.meatsci.2016.03.012.

[19] S. Cofrades, I. Antoniou, M.T. Solas, A.M. Herrero, F. Jiménez-Colmenero, Preparation and impact of multiple (water-in-oil-in-water) emulsions in meat systems, Food Chem. 141 (2013) 338-346. https://doi.org/10.1016/j.foodchem.2013.02.097.

[20] M. Shima, Y. Morita, M. Yamashita, S. Adachi, Protection of Lactobacillus acidophilus from the low pH of a model gastric juice by incorporation in a W/O/W emulsion, Food Hydrocoll. 20 (2006) 1164-1169. https://doi.org/10.1016/j.foodhyd.2006.01.001.

[21] M. Rodríguez-Huezo, A. Estrada-Fernández, B. García-Almendárez, F. Ludena-Urquizo, R. Campos-Montiel, D. Pimentel-González, Viability of Lactobacillus plantarum entrapped in double emulsion during Oaxaca cheese manufacture, melting and simulated intestinal conditions, LWT, 59 (2014) 768-773. https://doi.org/10.1016/j.lwt.2014.07.004.

[22] D. Pimentel-González, R. Campos-Montiel, C. Lobato-Calleros, R. Pedroza-Islas, E. Vernon-Carter, Encapsulation of Lactobacillus rhamnosus in double emulsions formulated with sweet whey as emulsifier and survival in simulated gastrointestinal conditions, Food Res. Int. 42 (2009) 292-297. https://doi.org/10.1016/j.foodres.2008.12.002.

[23] S.W. May, N.N. Li, Encapsulation of enzymes in liquid membrane emulsions, in: E.K. Pye, L.B. Wingard (Eds.), Enzyme Engineering, Springer, Boston, 1974, pp. 77-82. https://doi.org/10.1007/978-1-4615-8897-9_11.

[24] L. Ghosh, N. Ghosh, R. Thakur, M. Pal, B. Gupta, Design and evaluation of controlled-release W/O/W multiple-emulsion oral liquid delivery system of chlorpheniramine maleate, Drug Dev. Ind. Pharm. 23 (1997) 1131-1134. https://doi.org/10.3109/03639049709150504.

[25] S. Roy, B.K. Gupta, In vitro-in vivo correlation of indomethacin release from prolonged release w/o/w multiple emulsion system, Drug Dev. Ind. Pharm. 19 (1993) 1965-1980. https://doi.org/10.3109/03639049309073902.

[26] X. Wang, S. Jiang, X. Wang, J. Liao, Z. Yin, Preparation and evaluation of nattokinase-loaded self-double-emulsifying drug delivery system, Asian J. Pharm. Sci. 10 (2015) 386-395. https://doi.org/10.1016/j.ajps.2015.04.005.

[27] A. Vaziri, B. Warburton, Slow release of chloroquine phosphate from multiple taste-masked W/O/W multiple emulsions, J. Microencapsul. 11 (1994) 641-648. https://doi.org/10.3109/02652049409051114.

[28] S. Talegaonkar, S. Vyas, Inverse targeting of diclofenac sodium to reticuloendothelial system-rich organs by sphere-in-oil-in-water (s/o/w) multiple emulsion containing poloxamer 403, J. Drug Target. 13 (2005) 173-178. https://doi.org/10.1080/10611860500065104.

[29] A. Bozkir, G. Hayta, Preparation and evaluation of multiple emulsions water-in-oil-in-water (w/o/w) as delivery system for influenza virus antigens, J. Drug Target. 12 (2004) 157-164. https://doi.org/10.1080/10611860410001688018.

[30] A. Bozkir, G. Hayta, O. Saka, Comparison of biodegradable nanoparticles and multiple emulsions (water-in-oil-in-water) containing influenza virus antigen on the in vivo immune response in rats, Pharmazie, 59 (2004) 723-725. PMID: 15497758.

[31] H. Yanagie, H. Kumada, T. Nakamura, S. Higashi, I. Ikushima, Y. Morishita, A. Shinohara, F. Mitsuteru10, M. Suzuki11, H. Sugiyama, Dosimetric evaluation for neutron capture therapy to hapatocellular carcinoma using intra-arterial administration of boron-entrapped water-in-oil-in-water emulsion, Proc. 7th IASTED Int. Conf. Biomed. Eng. 2 (2010) 126-130. https://doi.org/10.2316/J.2010.216.680-0179.

[32] T. Takahashi, Increased concentration of anticancer agents in regional lymph nodes by fat emulsions, with special reference to chemotherapy of metastasis, Gann, 64 (1973) 345-350. PMID: 4752370.

[33] S. Higashi, M. Shimizu, T. Nakashima, K. Iwata, F. Uchiyama, S. Tateno, S. Tamura, T. Setoguchi, Arterial-injection chemotherapy for hepatocellular carcinoma using monodispersed poppy-seed oil microdroplets containing fine aqueous vesicles of epirubicin. Initial medical application of a membrane-emulsification technique, Cancer, 75 (1995) 1245-1254. https://doi.org/10.1002/1097-0142(19950315)75:6<1245::AID-CNCR2820750606>3.0.CO;2-U.

[34] S. Higashi, T. Setoguchi, Hepatic arterial injection chemotherapy for hepatocellular carcinoma with epirubicin aqueous solution as numerous vesicles in iodinated poppy-seed oil microdroplets: clinical application of water-in-oil-in-water emulsion prepared using a membrane emulsification technique, Adv. Drug Deliv. Rev. 45 (2000) 57-64. https://doi.org/10.1016/S0169-409X(00)00100-9.

[35] S. Zheng, R. Beissinger, D. Wasan, The stabilization of hemoglobin multiple emulsion for use as a red blood cell substitute, J. Colloid Interface Sci. 144 (1991) 72-85. https://doi.org/10.1016/0021-9797(91)90239-5.

[36] A.S. Cunha, J. Grossior, F. Puisieux, M. Seiller, Insulin in w/o/w multiple emulsions: preparation, characterization and determination of stability towards proteases in vitro, J. Microencapsul. 14 (1997) 311-319. https://doi.org/10.3109/02652049709051135.

[37] Y. Onuki, M. Morishita, K. Takayama, Formulation optimization of water-in-oil-water multiple emulsion for intestinal insulin delivery, J. Control Release 97 (2004) 91-99. https://doi.org/10.1016/j.jconrel.2004.03.010.

[38] E. Toorisaka, H. Ono, K. Arimori, N. Kamiya, M. Goto, Hypoglycemic effect of surfactant-coated insulin solubilized in a novel solid-in-oil-in-water (S/O/W) emulsion, Int. J. Pharm. 252 (2003) 271-274. https://doi.org/10.1016/S0378-5173(02)00674-9.

[39] T. Uno, T. Yamaguchi, X.K. Li, Y. Suzuki, H. Hashimoto, Y. Harada, T. Kimura, T. Kazui, The pharmacokinetics of water-in-oil-in-water-type multiple emulsion of a new tacrolimus formulation, Lipids, 32 (1997) 543-548. https://doi.org/10.1007/s11745-997-0069-1.

[40] S.Y. Tang, S. Manickam, A.M.-H. Ng, P. Shridharan, Anti-inflammatory and analgesic activity of novel oral aspirin-loaded nanoemulsion and nano multiple emulsion formulations generated using ultrasound cavitation, Int. J Pharm. 430 (2012) 299-306. https://doi.org/10.1016/j.ijpharm.2012.03.055.

[41] S.-Y. Lin, W. Wu, W. Lui, In vitro release, pharmacokinetic and tissue distribution studies of doxorubicin hydrochloride (Adriamycin HCl) encapsulated in lipiodolized w/o emulsions and w/o/w multiple emulsions, Pharmazie, 47 (1992) 439-443. PMID: 1409841.

[42] J.-L. Ma, Q.-M. Xiong, T. Tao, Physico-chemical properties and its release in vitro of multiple emulsion containing etoposide, Chin. J. Pharm. 24 (1993) 357-357. http://en.cnki.com.cn/Article_en/CJFDTotal-ZHOU199308050.htm.

[43] A. Khopade, N. Jain, Fine multiple emulsions bearing 6-mercaptopurine: In vitro and in vivo antitumor Studies, Drug Deliv. 6 (1999) 181-185. https://doi.org/10.1080/107175499266931.

[44] C.J. Benoy, R. Schneider, L. Elson, M. Jones, Enhancement of the cancer chemotherapeutic effect of the cell cycle phase specific agents methotrexate and cytosine arabinoside when given as

a water-oil-water emulsion, Eur. J. Cancer (1965), 10 (1974) 27-33. https://doi.org/10.1016/0014-2964(74)90034-6.

[45] B. Mishra, J. Pandit, Multiple water-oil-water emulsions as prolonged release formulations of pentazocine, J. Control Release, 14 (1990) 53-60. https://doi.org/10.1016/0168-3659(90)90060-7.

[46] H. Okochi, M. Nakano, Preparation and evaluation of w/o/w type emulsions containing vancomycin, Adv. Drug Deliv. Rev. 45 (2000) 5-26. https://doi.org/10.1016/S0169-409X(00)00097-1.

[47] M. Kaimainen, S. Marze, E. Järvenpää, M. Anton, R. Huopalahti, Encapsulation of betalain into w/o/w double emulsion and release during in vitro intestinal lipid digestion, LWT, 60 (2015) 899-904. https://doi.org/10.1016/j.lwt.2014.10.016.

[48] K. Frank, E. Walz, V. Gräf, R. Greiner, K. Köhler, H.P. Schuchmann, Stability of anthocyanin-rich w/o/w-emulsions designed for intestinal release in gastrointestinal environment, J. Food Sci. 77 (2012) N50-N57. https://doi.org/10.1111/j.1750-3841.2012.02982.x.

[49] K. Yoshida, T. Sekine, F. Matsuzaki, T. Yanaki, M. Yamaguchi, Stability of vitamin A in oil-in-water-in-oil-type multiple emulsions, J. Am. Oil Chem. Soc. 76 (1999) 1-6. https://doi.org/10.1007/s11746-999-0212-2.

[50] H.J. Giroux, S. Constantineau, P. Fustier, C.P. Champagne, D. St-Gelais, M. Lacroix, M. Britten, Cheese fortification using water-in-oil-in-water double emulsions as carrier for water soluble nutrients, Int. Dairy J. 29 (2013) 107-114. https://doi.org/10.1016/j.idairyj.2012.10.009.

[51] B.-K. Kim, A.-R. Cho, D.-J. Park, Enhancing oral bioavailability using preparations of apigenin-loaded W/O/W emulsions: In vitro and in vivo evaluations, Food Chem. 206 (2016) 85-91. https://doi.org/10.1016/j.foodchem.2016.03.052.

[52] S. Nakhare, S. Vyas, Multiple emulsion based systems for prolonged delivery of rifampicin: In vitro and in vivo characterization, Pharmazie, 52 (1997) 224-226. PMID: 9109169.

[53] World Health Organization, Cancer. https://www.who.int/health-topics/cancer#tab=tab_1/, 2018 (accessed on 01 August 2019).

[54] World Cancer Research Fund International, Worldwide cancer data: Global cancer statistics for the most common cancers. https://www.wcrf.org/dietandcancer/cancer-trends/worldwide-cancer-data/, 2018 (accessed on 15 November 2018).

[55] American Cancer Society, Key Statistics for lung cancer. https://www.cancer.org/cancer/lung-cancer/about/key-statistics.html/, 2019 (accessed on 01 August 2019).

[56] American Cancer Society, What is lung cancer. https://www.cancer.org/cancer/lung-cancer/about/what-is.html/, 2019 (accessed on 01 August 2019).

[57] National Cancer Institute, Non-small cell lung cancer. https://www.cancer.gov/publications/dictionaries/cancer-terms/def/non-small-cell-lung-cancer/, 2020 (accessed on 01 November 2020).

[58] T. Tamura, K. Kurishima, K. Nakazawa, K. Kagohashi, H. Ishikawa, H. Satoh, N. Hizawa, Specific organ metastases and survival in metastatic non-small-cell lung cancer, Mol. Clin. Oncol. 3 (2015) 217-221. https://doi.org/10.3892/mco.2014.410.

[59] A. Matsuda, T. Matsuda, A. Shibata, K. Katanoda, T. Sobue, H. Nishimoto, J.C.S.R. Group, Cancer incidence and incidence rates in Japan in 2007: A study of 21 population-based cancer registries for the monitoring of cancer incidence in Japan (MCIJ) project, Jpn. J. Clin. Oncol. 43 (2013) 328-336. https://doi.org/10.1093/jjco/hys233.

[60] A.G. Little, E.G. Gay, L.E. Gaspar, A.K. Stewart, National survey of non-small cell lung cancer in the United States: Epidemiology, pathology and patterns of care, Lung Cancer 57 (2007) 253-260. https://doi.org/10.1016/j.lungcan.2007.03.012.

[61] Y. Ren, C. Dai, H. Zheng, F. Zhou, Y. She, G. Jiang, K. Fei, P. Yang, D. Xie, C. Chen, Prognostic effect of liver metastasis in lung cancer patients with distant metastasis, Oncotarget. 7 (2016) 53245-53253. https://doi.org/10.18632/oncotarget.10644.

[62] S. Dasari, P.B. Tchounwou, Cisplatin in cancer therapy: Molecular mechanisms of action, Eur. J. Pharmacol. 740 (2014) 364-378. https://doi.org/10.1016/j.ejphar.2014.07.025.

[63] L. Kelland, The resurgence of platinum-based cancer chemotherapy, Nat. Rev. Cancer. 7 (2007) 573-584. https://doi.org/10.1038/nrc2167.

[64] Y. Takii, K. Mitsugi, K. Kimura, Y. Mihara, The effectiveness of hepatic arterial infusion chemotherapy with 5-fluorouracil/cisplatin and systemic chemotherapy with ramucirumab in alpha-fetoprotein-producing gastric cancer with multiple liver metastases, Case Rep. Oncol. Med. 2018 (2018) 5402313. https://doi.org/10.1155/2018/5402313.

[65] A.-M. Florea, D. Büsselberg, Cisplatin as an anti-tumor drug: cellular mechanisms of activity, drug resistance and induced side effects, Cancers, 3 (2011) 1351-1371. https://doi.org/10.3390/cancers3011351.

[66] U.B. Chaudhary, J.R. Haldas, Long-term complications of chemotherapy for germ cell tumours, Drugs, 63 (2003) 1565-1577. https://doi.org/10.2165/00003495-200363150-00004.

[67] C. Kosmas, N.B. Tsavaris, N.A. Malamos, M. Vadiaka, C. Koufos, Phase II study of paclitaxel, ifosfamide, and cisplatin as second-line treatment in relapsed small-cell lung cancer, J. Clin. Oncol. 19 (2001) 119-126. https://doi.org/10.1200/JCO.2001.19.1.119.

[68] R. Kotecha, A. Takami, J.L. Espinoza, Dietary phytochemicals and cancer chemoprevention: A review of the clinical evidence, Oncotarget. 7 (2016) 52517-52529. https://doi.org/10.18632/oncotarget.9593.

[69] M.H. Ng, A. Kushairi, The effect of pressure and solvent on the supercritical fluid chromatography separation of tocol analogs in palm oil, Molecules, 22 (2017) 1424. https://doi.org/10.3390/molecules22091424.

[70] P. Goh, M. Ng, Y. Choo, N. Amru, C. Chuah, Production of nanoemulsions from palm-based tocotrienol rich fraction by microfluidization, Molecules. 20 (2015) 19936-19946. https://doi.org/10.3390/molecules201119666.

[71] B.B. Aggarwal, C. Sundaram, S. Prasad, R. Kannappan, Tocotrienols, the vitamin E of the 21st century: Its potential against cancer and other chronic diseases, Biochem. Pharmacol. 80 (2010) 1613-1631. https://doi.org/10.1016/j.bcp.2010.07.043.

[72] K. Nesaretnam, W.W. Yew, M.B. Wahid, Tocotrienols and cancer: beyond antioxidant activity, Eur. J. Lipid Sci. Tech. 109 (2007) 445-452. https://doi.org/10.1007/s12263-011-0224-z.

[73] Y. Ding, Y. Peng, L. Deng, J. Fan, B. Huang, Gamma-tocotrienol reverses multidrug resistance of breast cancer cells with a mechanism distinct from that of atorvastatin, The J. Steroid Biochem. Mol. Biol. 167 (2017) 67-77. https://doi.org/10.1016/j.jsbmb.2016.11.009.

[74] M. Kaileh, R. Sen, Role of NF-κB in the anti-inflammatory effects of tocotrienols, J. Am. Coll. Nutr. 29 (2010) 334S-339S. https://doi.org/10.1080/07315724.2010.10719848.

[75] S.J. Wu, P.L. Liu, L.T. Ng, Tocotrienol-rich fraction of palm oil exhibits anti-inflammatory property by suppressing the expression of inflammatory mediators in human monocytic cells, Mol. Nutr. Food Res. 52 (2008) 921-929. https://doi.org/10.1002/mnfr.200700418.

[76] S. Wada, Y. Naito, Y. Matsushita, M. Nouchi, M. Kawai, E. Minami, W. Aoi, S. Ikeda, A. Higashi, T. Yoshikawa, δ-Tocotrienol suppresses tumorigenesis by inducing apoptosis and blocking the COX-2/PGE 2 pathway that stimulates tumor–stromal interactions in colon cancer, J. Funct. Foods. 35 (2017) 428-435. https://doi.org/10.1016/j.jff.2017.06.002.

[77] S.K. Park, B.G. Sanders, K. Kline, Tocotrienols induce apoptosis in breast cancer cell lines via an endoplasmic reticulum stress-dependent increase in extrinsic death receptor signaling, Breast Cancer Res. Tr. 124 (2010) 361-375. https://doi.org/10.1007/s10549-010-0786-2.

[78] J.K. Srivastava, S. Gupta, Tocotrienol-rich fraction of palm oil induces cell cycle arrest and apoptosis selectively in human prostate cancer cells, Biochem. Biophys. Res. Comm. 346 (2006) 447-453. https://doi.org/10.1016/j.bbrc.2006.05.147.

[79] Y. Jang, N.-Y. Park, A.L. Rostgaard-Hansen, J. Huang, Q. Jiang, Vitamin E metabolite 13′-carboxychromanols inhibit pro-inflammatory enzymes, induce apoptosis and autophagy in human cancer cells by modulating sphingolipids and suppress colon tumor development in mice, Free Radical Bio. Med. 95 (2016) 190-199. https://doi.org/10.1016/j.freeradbiomed.2016.03.018.

[80] J. Teixeira, F. Cagide, S. Benfeito, P. Soares, J. Garrido, I. Baldeiras, J.A. Ribeiro, C.M. Pereira, A.F. Silva, P.B. Andrade, Development of a mitochondriotropic antioxidant based on caffeic acid: proof of concept on cellular and mitochondrial oxidative stress models, J. Med. Chem. 60 (2017) 7084-7098. https://doi.org/10.1021/acs.jmedchem.7b00741.

[81] O.M. Agunloye, G. Oboh, A.O. Ademiluyi, A.O. Ademosun, A.A. Akindahunsi, A.A. Oyagbemi, T.O. Omobowale, T.O. Ajibade, A.A. Adedapo, Cardio-protective and antioxidant properties of caffeic acid and chlorogenic acid: Mechanistic role of angiotensin converting enzyme, cholinesterase and arginase activities in cyclosporine induced hypertensive rats, Biomed. Pharmacother. 109 (2019) 450-458. https://doi.org/10.1016/j.biopha.2018.10.044.

[82] M. Tyszka-Czochara, K. Bukowska-Strakova, M. Majka, Metformin and caffeic acid regulate metabolic reprogramming in human cervical carcinoma SiHa/HTB-35 cells and augment anticancer activity of Cisplatin via cell cycle regulation, Food Chem. Toxicol. 106 (2017) 260-272. https://doi.org/10.1016/j.fct.2017.05.065.

[83] M. Tyszka-Czochara, P. Konieczny, M. Majka, Caffeic acid expands anti-tumor effect of metformin in human metastatic cervical carcinoma HTB-34 cells: Implications of AMPK activation and impairment of fatty acids de novo biosynthesis, Int. J. Mol. Sci. 18 (2017) 462. https://doi.org/10.3390/ijms18020462.

[84] N.R. Prasad, A. Karthikeyan, S. Karthikeyan, B.V. Reddy, Inhibitory effect of caffeic acid on cancer cell proliferation by oxidative mechanism in human HT-1080 fibrosarcoma cell line, Mol. Cell. Biochem. 349 (2011) 11-19. https://doi.org/10.1007/s11010-010-0655-7.

[85] O. Catchpole, K. Mitchell, S. Bloor, P. Davis, A. Suddes, Antiproliferative activity of New Zealand propolis and phenolic compounds vs human colorectal adenocarcinoma cells, Fitoterapia 106 (2015) 167-174. https://doi.org/10.1016/j.fitote.2015.09.004.

[86] R.H. Liu, Health benefits of fruit and vegetables are from additive and synergistic combinations of phytochemicals, J. Am. Coll. Nutr. 78 (2003) 517S-520S. https://doi.org/10.1093/ajcn/78.3.517S.

[87] T. Tadros, P. Izquierdo, J. Esquena, C. Solans, Formation and stability of nano-emulsions, Adv. Colloid Interface Sci. 108 (2004) 303-318. https://doi.org/10.1016/j.cis.2003.10.023.

[88] J. Gutiérrez, C. González, A. Maestro, I. Sole, C. Pey, J. Nolla, Nano-emulsions: New applications and optimization of their preparation, Curr. Opin. in Colloid Interface Sci. 13 (2008) 245-251. https://doi.org/10.1016/j.cocis.2008.01.005.

[89] T.J. Wooster, M. Golding, P. Sanguansri, Impact of oil type on nanoemulsion formation and Ostwald ripening stability, Langmuir 24 (2008) 12758-12765. https://doi.org/10.1021/la801685v.

[90] C. Solans, J. Esquena, A.M. Forgiarini, N. Uson, D. Morales, P. Izquierdo, N. Azemar, M.J. Garcia-Celma, Nano-emulsions: formation, properties, and applications, in: K. L. Mittal, D. O. Shah (Eds.), Adsorption and Aggregatiion of Surfactants in Solution, Marcel Dekker Inc., New York, 2003, pp. 525-554.

[91] R. Mezzenga, B.M. Folmer, E. Hughes, Design of double emulsions by osmotic pressure tailoring, Langmuir, 20 (2004) 3574-3582. https://doi.org/10.1021/la036396k.

[92] J. Surh, G.T. Vladisavljević, S. Mun, D.J. McClements, Preparation and characterization of water/oil and water/oil/water emulsions containing biopolymer-gelled water droplets, J. Agric. Food Chem. 55 (2007) 175-184. https://doi.org/10.1021/jf061637q.

[93] N. Perez-Moral, S. Watt, P. Wilde, Comparative study of the stability of multiple emulsions containing a gelled or aqueous internal phase, Food Hydrocoll. 42 (2014) 215-222. https://doi.org/10.1016/j.foodhyd.2014.05.023.

[94] S. Neumann, I. Scherbej, U. Van Der Schaaf, H. Karbstein, Investigations on the influence of osmotic active substances on the structure of water in oil emulsions for the application as inner phase in double emulsions, Colloids Surf. A 538 (2018) 56-62. https://doi.org/10.1016/j.colsurfa.2017.10.073.

[95] G.R. Velderrain-Rodríguez, A. Acevedo-Fani, G.A. González-Aguilar, O. Martín-Belloso, Encapsulation and stability of a phenolic-rich extract from mango peel within water-in-oil-in-water emulsions, J. Funct. Foods, 56 (2019) 65-73. https://doi.org/10.1016/j.jff.2019.02.045.

[96] Y. Hemar, L.J. Cheng, C.M. Oliver, L. Sanguansri, M. Augustin, Encapsulation of resveratrol using water-in-oil-in-water double emulsions, Food Biophys. 5 (2010) 120-127. https://doi.org/10.1007/s11483-010-9152-5.

[97] J. Su, J. Flanagan, Y. Hemar, H. Singh, Synergistic effects of polyglycerol ester of polyricinoleic acid and sodium caseinate on the stabilisation of water–oil–water emulsions, Food Hydrocoll. 20 (2006) 261-268. https://doi.org/10.1016/j.foodhyd.2004.03.010.

[98] S. Iqbal, M.K. Baloch, G. Hameed, D.J. McClements, Controlling W/O/W multiple emulsion microstructure by osmotic swelling and internal protein gelation, Food Res. Int. 54 (2013) 1613-1620. https://doi.org/10.1016/j.foodres.2013.09.035.

[99] A. Oppermann, M. Renssen, A. Schuch, M. Stieger, E. Scholten, Effect of gelation of inner dispersed phase on stability of (w1/o/w2) multiple emulsions, Food Hydrocoll. 48 (2015) 17-26. https://doi.org/10.1016/j.foodhyd.2015.01.027.

[100] A. Oppermann, B. Piqueras-Fiszman, C. De Graaf, E. Scholten, M. Stieger, Descriptive sensory profiling of double emulsions with gelled and non-gelled inner water phase, Food Res. Int. 85 (2016) 215-223. https://doi.org/10.1016/j.foodres.2016.04.030.

[101] M.-N. Iancu, Y. Chevalie, M. Popa, T. Hamaide, Internally gelled w/o and w/o/w double emulsions, e-Polymers 9 (2009) 99. https://doi.org/10.1515/epoly.2009.9.1.1184.

[102] S. Mun, Y. Choi, S. Park, J. Surh, Y.-R. Kim, Release properties of gel-type W/O/W encapsulation system prepared using enzymatically-modified starch, Food Chem. 157 (2014) 77-83. https://doi.org/10.1016/j.foodchem.2014.02.017.

[103] M.L. Cole, T.L. Whateley, Release rate profiles of theophylline and insulin from stable multiple w/o/w emulsions, J. Control Release 49 (1997) 51-58. https://doi.org/10.1016/S0168-3659(97)00056-4.

[104] A. Benichou, A. Aserin, N. Garti, Double emulsions stabilized by new molecular recognition hybrids of natural polymers, Polym. Advan. Technol. 13 (2002) 1019-1031. https://doi.org/10.1002/pat.270.

[105] U. Schmidt, R. Bernewitz, G. Guthausen, H. Schuchmann, Investigation and application of measurement techniques for the determination of the encapsulation efficiency of O/W/O multiple emulsions stabilized by hydrocolloid gelation, Colloids Surf. A 475 (2015) 55-61. https://doi.org/10.1016/j.colsurfa.2014.12.040.

[106] M. Balcaen, L. Vermeir, P. Van der Meeren, Influence of protein type on Polyglycerol Polyricinoleate replacement in W/O/W (water-in-oil-in-water) double emulsions for food applications, Colloids Surf. A 535 (2017) 105-113. https://doi.org/10.1016/j.colsurfa.2017.09.034.

[107] Q. Zhu, L. Zhao, H. Zhang, M. Saito, L. Yin, Impact of the release rate of magnesium ions in multiple emulsions (water-in-oil-in-water) containing BSA on the resulting physical properties and microstructure of soy protein gel, Food Chem. 220 (2017) 452-459. https://doi.org/10.1016/j.foodchem.2016.10.016.

[108] Y. Kawashima, T. Hino, H. Takeuchi, T. Niwa, Stabilization of water/oil/water multiple emulsion with hypertonic inner aqueous phase, Chem. Pharm. Bull. 40 (1992) 1240-1246. https://doi.org/10.1248/cpb.40.1240.

[109] R. Sambanthamurthi, K. Sundram, Y.-A. Tan, Chemistry and biochemistry of palm oil, Prog. Lipid Res. 39 (2000) 507-558. https://doi.org/http://dx.doi.org/10.1016/S0163-7827(00)00015-1.

[110] O. Olafisoye, O. Oguntibeju, O. Osibote, Trace elements and radionuclides in palm oil, soil, water, and leaves from oil palm plantations: A review, Crit. Rev. Food Sci. Nutr. 57 (2017) 1295-1315. https://doi.org/10.1080/10408398.2014.886032.

[111] A. Kovács, I. Csóka, M. Kónya, E. Csányi, A. Fehér, I. Erős, Structural analysis of w/o/w multiple emulsions by means of DSC, J. Therm. Anal. Calorim. 82 (2005) 491-497. https://doi.org/10.1007/s10973-005-0922-0.

[112] A. Gupta, H.B. Eral, T.A. Hatton, P.S. Doyle, Nanoemulsions: Formation, properties and applications, Soft Matter. 12 (2016) 2826-2841. https://doi.org/10.1039/c5sm02958a.

[113] D.J. McClements, Theoretical analysis of factors affecting the formation and stability of multilayered colloidal dispersions, Langmuir, 21 (2005) 9777-9785. https://doi.org/10.1021/la0512603.

[114] F. Mohos, Confectionery and Chocolate Engineering: Principles and Applications, second ed., John Wiley & Sons Ltd., West Sussex, 2017. https://doi.org/10.1002/9781118939741.

[115] D.J. McClements, Food emulsions: Principles, Practice and Techniques, second ed., CRC Press, Boca Raton, 2005.

[116] R. Lochhead, Basic physical sciences for the formulation of cosmetic products, in: K. Sakamoto, R. Lochhead, H. Maibach, Y. Yamashita (Eds.), Cosmetic Science and Technology: Theoretical Principles and Applications. Elsevier Inc., 2017, pp. 39-76. https://doi.org/10.1016/B978-0-12-802005-0.00003-3.

[117] J. Jiao, D.J. Burgess, Rheology and stability of water-in-oil-in-water multiple emulsions containing Span 83 and Tween 80, AAPS Pharmsci. 5 (2003) 62-73. https://doi.org/10.1208/ps050107.

[118] N. Garti, Double emulsions—scope, limitations and new achievements, Colloids Surf. A 123 (1997) 233-246. https://doi.org/10.1016/S0927-7757(96)03809-5.

[119] B.S.B. Bamba, J. Shi, C.C. Tranchant, S.J. Xue, C.F. Forney, L.-T. Lim, W. Xu, G. Xu, Coencapsulation of polyphenols and anthocyanins from blueberry pomace by double emulsion stabilized by whey proteins: Effect of homogenization parameters, Molecules, 23 (2018) 2525. https://doi.org/10.3390/molecules23102525.

[120] S.Y. Tang, S. Manickam, Design and evaluation of aspirin-loaded water-in-oil-in-water submicron multiple emulsions generated using two-stage ultrasonic cavitational emulsification technique, Asia-Pac. J. Chem. Eng. 7 (2012) 145-156. https://doi.org/10.1002/apj.664.

[121] M. Bonnet, M. Cansell, A. Berkaoui, M. Ropers, M. Anton, F. Leal-Calderon, Release rate profiles of magnesium from multiple W/O/W emulsions, Food Hydrocoll. 23 (2009) 92-101. https://doi.org/10.1016/j.foodhyd.2007.11.016.

[122] J. Zhang, G.A. Reineccius, Preparation and stability of W/O/W emulsions containing sucrose as weighting agent, Flavour Fragr. J. 31 (2016) 51-56. https://doi.org/10.1002/ffj.3269.

[123] M. Yildirim, G. Sumnu, S. Sahin, The effects of emulsifier type, phase ratio, and homogenization methods on stability of the double emulsion, J. Disper. Sci. Technol. 38 (2017) 807-814. https://doi.org/10.1080/01932691.2016.1201768.

[124] D.J. McClements, J. Rao, Food-grade nanoemulsions: formulation, fabrication, properties, performance, biological fate, and potential toxicity, Crit. Rev. Food Sci. Nutr. 51 (2011) 285-330. https://doi.org/10.1080/10408398.2011.559558.

[125] E.J. Cook, A.P. Lagace, Apparatus for forming emulsions, US Patent No. 4533254A, Washington, 1985. https://patents.google.com/patent/US4533254A/en.

[126] C. Washington, Emulsion production by microfluidizer, Lab. Equip. Dig. 85 (1987) 69-71.

[127] T. Wang, X. Sun, Z. Zhou, G. Chen, Effects of microfluidization process on physicochemical properties of wheat bran, Food Res. Int. 48 (2012) 742-747. https://doi.org/10.1016/j.foodres.2012.06.015.

[128] D. Olson, C. White, R. Richter, Effect of pressure and fat content on particle sizes in microfluidized milk, J. Dairy Sci. 87 (2004) 3217-3223. https://doi.org/10.3168/jds.S0022-0302(04)73457-8.

[129] Y.-F. Maa, C.C. Hsu, Performance of sonication and microfluidization for liquid–liquid emulsification, Pharm. Dev. Technol. 4 (1999) 233-240. https://doi.org/10.1081/PDT-100101357.

[130] D. Dalgleish, S. Tosh, S. West, Beyond homogenization: the formation of very small emulsion droplets during the processing of milk by a microfluidizer, Ned. Melk Zui. 50 (1996) 135-148. http://pascal-francis.inist.fr/vibad/index.php?action=getRecordDetail&idt=3104995.

[131] T. Panagiotou, J.M. Bernard, S.V. Mesite, Deagglomeration and dispersion of carbon nanotubes using microfluidizer high shear fluid processors, Nano Sci. Technol. Inst. Conf. Expo Proc. 1 (2008) 39-42. https://briefs.techconnect.org/wp-content/volumes/Nanotech2008v1/pdf/916.pdf.

[132] M.R. Kasaai, Input power-mechanism relationship for ultrasonic irradiation: Food and polymer applications, Nat. Sci. 5 (2013) 35918. https://doi.org/10.4236/ns.2013.58A2003.

[133] D.M. Higgins, D.M. Skauen, Influence of power on quality of emulsions prepared by ultrasound, J. Pharm. Sci. 61 (1972) 1567-1570. https://doi.org/10.1002/jps.2600611004.

[134] K.S. Suslick, The chemical effects of ultrasound, Sci. Am. 260 (1989) 80-87. http://suslick.scs.illinois.edu/documents/sciamer8980.pdf

[135] S.M. Jafari, E. Assadpoor, Y. He, B. Bhandari, Re-coalescence of emulsion droplets during high-energy emulsification, Food Hydrocoll. 22 (2008) 1191-1202. https://doi.org/10.1016/j.foodhyd.2007.09.006.

[136] S.M. Jafari, Y. He, B. Bhandari, Optimization of nano-emulsions production by microfluidization, Eur. Food Res. Technol. 225 (2007) 733-741. https://doi.org/10.1007/s00217-006-0476-9.

[137] R. Santana, F. Perrechil, R. Cunha, High-and low-energy emulsifications for food applications: a focus on process parameters, Food Eng. Rev. 5 (2013) 107-122. https://doi.org/10.1007/s12393-013-9065-4.

[138] M.B. Schulz, R. Daniels, Hydroxypropylmethylcellulose (HPMC) as emulsifier for submicron emulsions: influence of molecular weight and substitution type on the droplet size after high-pressure homogenization, Eur. J. Pharm. Biopharm. 49 (2000) 231-236. https://doi.org/10.1016/s0939-6411(00)00069-2.

[139] A. Hartwig, M. Commission, White mineral oil, pharmaceutical, MAK Collection for Occupational Health and Safety 2 (2017) 1177-1191. https://doi.org/10.1002/3527600418.mb804247kske5917.

[140] A. Bach, V. Babayan, Medium-chain triglycerides: An update, Am. J. Clin. Nutr. 36 (1982) 950-962. https://doi.org/10.1093/ajcn/36.5.950.

[141] N.D. Shah, B.N. Limketkai, The use of medium-chain triglycerides in gastrointestinal disorders, Pract. Gastroenterol. 41 (2017) 20-28. https://med.virginia.edu/ginutrition/wp-content/uploads/sites/199/2014/06/Parrish-February-17.pdf.

[142] A. Chakravarti, S. Chowdhury, D. Mukherjee, Liquid membrane multiple emulsion process of separation of copper (II) from waste waters, Colloids Surf. A 166 (2000) 7-25. https://doi.org/10.1016/S0927-7757(99)00452-5.

[143] J.A. Omotosho, T.L. Whateley, T.K. Law, A.T. Florence, The nature of the oil phase and the release of solutes from multiple (w/o/w) emulsions, J. Pharm. Pharmacol. 38 (1986) 865-870. https://doi.org/10.1111/j.2042-7158.1986.tb03373.x.

[144] F. Ushikubo, R. Cunha, Stability mechanisms of liquid water-in-oil emulsions, Food Hydrocoll. 34 (2014) 145-153. https://doi.org/10.1016/j.foodhyd.2012.11.016.

[145] S. Chandel, P. Jain, S. Asati, V. Soni, Nanoemulsions: A New Application in Nutraceutical and Food Industry, in: B. Singh (Ed.), NanoNutraceuticals, CRC Press, Roca Baton, 2018, pp. 121-146. https://doi.org/10.1201/9781351138949-8.

[146] C. Lovelyn, A.A. Attama, Current state of nanoemulsions in drug delivery, J. Biomater. Nanobiotechnol. 2 (2011) 626-639. https://doi.org/10.4236/jbnb.2011.225075.

[147] N.R. Cameron, High internal phase emulsion templating as a route to well-defined porous polymers, Polymer, 46 (2005) 1439-1449. https://doi.org/10.1016/j.polymer.2004.11.097.

[148] I.W. Hamley, Introduction to soft matter: Synthetic and biological self-assembling materials, revised ed., John Wiley & Sons, 2013. https://books.google.com.my/books?id=Qd794-DI49wC.

[149] P. Walstra, Emulsion stability, in: P. Becher (Ed.), Encyclopedia of emulsion technology, Marcel Dekker Inc., New York, 1996, pp. 1-62. https://doi.org/10.1080/01932699708943748.

[150] J. Sjöblom, P.V. Hemmingsen, H. Kallevik, The role of asphaltenes in stabilizing water-in-crude oil emulsions, in: O.C. Mullins, E.Y. Sheu, A. Hammami, A.G. Marshall (Eds.), Asphaltenes, Heavy Oils, and Petroleomics, Springer, New York, 2007, pp. 549-587.

[151] J. Jiao, D.J. Burgess, Multiple emulsion stability: pressure balance and interfacial film strength, in: A. Aserin (Ed.), Multiple emulsions: Technology and Applications, John Wiley & Sons Inc., New Jersey, 2008, pp. 1-28. https://doi.org/10.1002/9780470209264.ch1.

[152] T.F. Tadros, Emulsion formation, stability, and rheology, in: T. F. Tadros (Eds.), Emulsion formation and stability, Wiley-VCH, 2013, pp. 1-75. https://doi.org/10.1002/9783527647941.ch1.

[153] A.S. Narang, D. Delmarre, D. Gao, Stable drug encapsulation in micelles and microemulsions, Int. J. Pharm. 345 (2007) 9-25. https://doi.org/10.1016/j.ijpharm.2007.08.057.

[154] S. Matsumoto, Y. Kita, D. Yonezawa, An attempt at preparing water-in-oil-in-water multiple-phase emulsions, J. Colloid Interface Sci. 57 (1976) 353-361. https://doi.org/10.1016/0021-9797(76)90210-1.

[155] J.J. Williams, Formulation of carpet cleaners, in: I. Johansson, P. Somasundaran (Eds.), Handbook for Cleaning/decontamination of Surfaces, Elsevier Science, 2007, pp. 103-123. https://doi.org/10.1016/B978-044451664-0/50004-8.

[156] T. Schmidts, D. Dobler, A.-C. Guldan, N. Paulus, F. Runkel, Multiple W/O/W emulsions—Using the required HLB for emulsifier evaluation, Colloids Surf. A. 372 (2010) 48-54. https://doi.org/10.1016/j.colsurfa.2010.09.025.

[157] C.-K. Kim, S.-C. Kim, H.-J. Shin, K.M. Kim, K.-H. Oh, Y.-B. Lee, I.-J. Oh, Preparation and characterization of cytarabine-loaded w/o/w multiple emulsions, Int. J. Pharm. 124 (1995) 61-67. https://doi.org/10.1016/0378-5173(95)00074-S.

[158] J. Wang, A. Shi, D. Agyei, Q. Wang, Formulation of water-in-oil-in-water (W/O/W) emulsions containing trans-resveratrol, RSC Adv. 7 (2017) 35917-35927. https://doi.org/10.1039/C7RA05945K.

[159] Q. Ye, T. Li, J. Li, L. Liu, X. Dou, X. Zhang, Development and evaluation of tea polyphenols loaded water in oil emulsion with zein as stabilizer, J. Drug Deliv. Sci. Technol. (2020) 101528. https://doi.org/10.1016/j.jddst.2020.101528.

[160] B. Mishra, J. Pandit, Prolonged tissue levels of pentazocine from multiple W/O/W emulsions in mice, Drug Dev. Ind. Pharm. 16 (1990) 1073-1078. https://doi.org/10.3109/03639049009114928.

[161] S. Nakhare, S. Vyas, Prolonged release of rifampicin from multiple W/O/W emulsion systems, J. Microencapsul. 12 (1995) 409-415. https://doi.org/10.3109/02652049509087253.

[162] R.K. Owusu, Q. Zhu, E. Dickinson, Controlled release of L-tryptophan and vitamin B2 from model water/oil/water multiple emulsions, Food Hydrocoll. 6 (1992) 443-453. https://doi.org/10.1016/S0268-005X(09)80030-1.

[163] Y. Kita, Permeation of water through the oil layer in W/O/W-type multiple phase emulsions, Nippon Kagaku Kaishi, 1 (1978) 11-14. https://doi.org/10.1246/nikkashi.1978.11.

[164] N. Garti, S. Magdassi, D. Whitehill, Transfer phenomena across the oil phase in water-oil-water multiple emulsions evaluated by Coulter counter: 1. Effect of emulsifier 1 on water permeability, J. Colloid Interface Sci. 104 (1985) 587-591. https://doi.org/10.1016/0021-9797(85)90067-0.

[165] M. Kanouni, H. Rosano, N. Naouli, Preparation of a stable double emulsion (W1/O/W2): Role of the interfacial films on the stability of the system, Adv. Colloid Interface Sci. 99 (2002) 229-254. https://doi.org/10.1016/s0001-8686(02)00079-9.

[166] R. Lutz, A. Aserin, L. Wicker, N. Garti, Double emulsions stabilized by a charged complex of modified pectin and whey protein isolate, Colloids Surf. B Biointerfaces, 72 (2009) 121-127. https://doi.org/10.1016/j.colsurfb.2009.03.024.

[167] A. Benichou, A. Aserin, N. Garti, Protein-polysaccharide interactions for stabilization of food emulsions, J. Disper. Sci. Technol. 23 (2002) 93-123. https://doi.org/10.1080/01932690208984192.

[168] B. Harzallah, V. Aguié-Béghin, R. Douillard, L. Bosio, A structural study of β-casein adsorbed layers at the air–water interface using X-ray and neutron reflectivity, Int. J. Biol. Macromol. 23 (1998) 73-84. https://doi.org/10.1016/s0141-8130(98)00035-x.

[169] A. Schuch, C. Helfenritter, M. Funck, H. Schuchmann, Observations on the influence of different biopolymers on coalescence of inner water droplets in W/O/W (water-in-oil-in-water)

double emulsions, Colloids Surf. A 475 (2015) 2-8. https://doi.org/10.1016/j.colsurfa.2014.06.012.

[170] M. Bonnet, M. Cansell, F. Placin, M. Anton, F. Leal-Calderon, Impact of sodium caseinate concentration and location on magnesium release from multiple W/O/W emulsions, Langmuir, 26 (2010) 9250-9260. https://doi.org/10.1021/la100078b.

[171] F. Leal-Calderon, S. Homer, A. Goh, L. Lundin, W/O/W emulsions with high internal droplet volume fraction, Food Hydrocoll. 27 (2012) 30-41. https://doi.org/10.1016/j.foodhyd.2011.09.004.

[172] Weiss, I. Scherze, G. Muschiolik, Polysaccharide gel with multiple emulsion, Food Hydrocoll. 19 (2005) 605-615. https://doi.org/10.1016/j.foohyd.2004.10.023.

[173] E. Dickinson, Hydrocolloids as emulsifiers and emulsion stabilizers, Food Hydrocoll. 23 (2009) 1473-1482. https://doi.org/10.1016/j.foodhyd.2008.08.005.

[174] M. Benna-Zayani, N. Kbir-Ariguib, M. Trabelsi-Ayadi, J.-L. Grossiord, Stabilisation of W/O/W double emulsion by polysaccharides as weak gels, Colloids Surf. A 316 (2008) 46-54. https://doi.org/10.1016/j.colsurfa.2007.08.019.

[175] B. Li, Y. Jiang, F. Liu, Z. Chai, Y. Li, X. Leng, Study of the encapsulation efficiency and controlled release property of whey protein isolate--polysaccharide complexes in W1/O/W2 double emulsions, Int. J. Food Eng. 7 (2011) 14. https://doi.org/10.2202/1556-3758.2321.

[176] A. Oppermann, L. Verkaaik, M. Stieger, E. Scholten, Influence of double ($w_1/o/w_2$) emulsion composition on lubrication properties, Food Funct. 8 (2017) 522-532. https://doi.org/10.1039/C6FO01523A.

[177] M. Balcaen, L. Vermeir, A. Declerck, P. Van der Meeren, Influence of internal water phase gelation on the shear-and osmotic sensitivity of W/O/W-type double emulsions, Food Hydrocoll. 58 (2016) 356-363. https://doi.org/10.1016/j.foodhyd.2016.03.011.

[178] A. Benichou, A. Aserin, N. Garti, Double emulsions stabilized with hybrids of natural polymers for entrapment and slow release of active matters, Adv. Colloid Interface Sci. 108 (2004) 29-41. https://doi.org/10.1016/j.cis.2003.10.013.

[179] S.L. Khokra, B. Parashar, H.K. Dhamija, K. Kumar, S. Arora, Formulation and evaluation of novel sustained release multiple emulsion containing chemotherapeutic agents, Int. J. PharmTech Res. 4 (2012) 866-872. ISSN: 09744304.

[180] M.P. Aronson, M.F. Petko, Highly concentrated water-in-oil emulsions: Influence of electrolyte on their properties and stability, J. Colloid Interface Sci. 159 (1993) 134-149. https://doi.org/10.1006/jcis.1993.1305.

[181] A.L. Márquez, A. Medrano, L.A. Panizzolo, J.R. Wagner, Effect of calcium salts and surfactant concentration on the stability of water-in-oil (w/o) emulsions prepared with polyglycerol polyricinoleate, J. Colloid Interface Sci. 341 (2010) 101-108. https://doi.org/10.1016/j.jcis.2009.09.020.

[182] I. Scherze, A. Knoth, G. Muschiolik, Effect of emulsification method on the properties of lecithin-and PGPR-stabilized water-in-oil-emulsions, J. Disper. Sci. Technol. 27 (2006) 427–434. https://doi.org/10.1080/01932690500357081.

[183] T. Hino, S. Shimabayashi, M. Tanaka, M. Nakano, H. Okochi, Improvement of encapsulation efficiency of water-in-oil-in water emulsion with hypertonic inner aqueous phase, J. Microencapsul. 18 (2001) 19-28. https://doi.org/10.1080/026520401750038575.

[184] A. Pawlik, P.W. Cox, I.T. Norton, Food grade duplex emulsions designed and stabilised with different osmotic pressures, J. Colloid Interface Sci. 352 (2010) 59-67. https://doi.org/10.1016/j.jcis.2010.08.049.

[185] S. Matsumoto, Y. Ueda, Y. Kita, D. Yonezawa, Preparation of water-in-olive oil-in-water multiple-phase emulsions in an eatable form, Agric. Biol. Chem. 42 (1978) 739-743. https://doi.org/10.1080/00021369.1978.10863054.

[186] J. Bibette, F.L. Calderon, P. Poulin, Emulsions: Basic principles, Rep. Prog. in Phys. 62 (1999) 969. https://doi.org/10.1088/0034-4885/62/6/203.

[187] E. Momeny, H. Mirhosseini, M.Z.I. Sarker, Effect of medium-high energy emulsification condition on physicochemical properties of β-Sitosterol multiple emulsion, Food and Bioprocess Technol. 10 (2017) 1642-1654. https://doi.org/10.1007/s11947-017-1932-1.

[188] M.S. Aston, T.M. Herrington, T.F. Tadros, Interfacial properties of mixtures of sorbitan sesquioleate with a block copolymer surfactant at the water/air and water/oil interfaces, Colloids Surf. 62 (1992) 31-39. https://doi.org/10.1016/0166-6622(92)80034-Y.

[189] S. Pimentel-Moral, J.M. Ochando-Pulido, A. Segura-Carretero, A. Martinez-Ferez, Stabilization of W/O/W multiple emulsion loaded with Hibiscus sabdariffa extract through protein-polysaccharide complexes, LWT, 90 (2018) 389-395. https://doi.org/10.1016/j.lwt.2017.12.054.

[190] J.L. Fraj, L.B. Petrović, J.R. Milinković-Budinčić, J.M. Katona, S.Đ. Bučko, L.M. Spasojević, Properties of double W/O/W emulsions containing vitamin C and E stabilized with gelatin/sodium caseinate complex, J. Serb. Chem. Soc. (2019) 75-75. https://doi.org/10.2298/JSC190515075F.

[191] O.Y. Altuntas, G. Sumnu, S. Sahin, Preparation and characterization of W/O/W type double emulsion containing PGPR–lecithin mixture as lipophilic surfactant, J. Disper. Sci. Technol. 38 (2017) 486-493. https://doi.org/10.1080/01932691.2016.1179121.

[192] P. Gharehbeglou, S.M. Jafari, A. Homayouni, H. Hamishekar, H. Mirzaei, Fabrication of double $W_1/O/W_2$ nano-emulsions loaded with oleuropein in the internal phase (W_1) and evaluation of their release rate, Food Hydrocoll. 89 (2019) 44-55. https://doi.org/10.1016/j.foodhyd.2018.10.020.

[193] J. Teixe-Roig, G. Oms-Oliu, G. Velderrain-Rodriguez, I. Odriozola-Serrano, O. Martin-Belloso, The effect of sodium carboxymethylcellulose on the stability and bioaccessibility of anthocyanin water-in-oil-in-water emulsions, Food Bioproc. Technol. 11 (2018) 2229-2241. https://doi.org/10.1007/s11947-018-2181-7.

[194] N. Aditya, S. Aditya, H.-J. Yang, H.W. Kim, S.O. Park, J. Lee, S. Ko, Curcumin and catechin co-loaded water-in-oil-in-water emulsion and its beverage application, J. Funct. Foods 15 (2015) 35-43. https://doi.org/10.1016/j.jff.2015.03.013.

[195] L.D. Rajasinghe, S.V. Gupta, Tocotrienol-rich mixture inhibits cell proliferation and induces apoptosis via down-regulation of the Notch-1/NF-κB pathways in NSCLC cells, Nutr. Diet. Suppl. 9 (2017) 103-114. https://doi.org/10.2147/NDS.S129891.

[196] K. Husain, S.M. Sebti, M.P. Malafa, Vitamin E delta-tocotrienol inhibits metastasis and targets cancer stem cell signaling in human pancreatic cancer, Cancer Res. 75 (2015) 4383. https://doi.org/10.1158/1538-7445.AM2015-4383.

[197] X. Ji, Z. Wang, F.H. Sarkar, S.V. Gupta, Delta-tocotrienol augments cisplatin-induced suppression of non-small cell lung cancer cells via inhibition of the Notch-1 pathway, Anticancer Res. 32 (2012) 2647-2655. PMID: 22753722.

[198] E. Pierpaoli, V. Viola, A. Barucca, F. Orlando, F. Galli, M. Provinciali, Effect of annatto-tocotrienols supplementation on the development of mammary tumors in HER-2/neu transgenic mice, Carcinogenesis. 34 (2013) 1352-1360. https://doi.org/10.1093/carcin/bgt064.

[199] J. Min, H. Shen, W. Xi, Q. Wang, L. Yin, Y. Zhang, Y. Yu, Q. Yang, Z.-n. Wang, Synergistic anticancer activity of combined use of caffeic acid with paclitaxel enhances apoptosis of non-small-cell lung cancer H1299 cells in vivo and in vitro, Cell. Physiol. Biochem. 48 (2018) 1433-1442. https://doi.org/10.1159/000492253.

[200] C.-L. Lin, R.-F. Chen, J.Y.-F. Chen, Y.-C. Chu, H.-M. Wang, H.-L. Chou, W.-C. Chang, Y. Fong, W.-T. Chang, C.-Y. Wu, Protective effect of caffeic acid on paclitaxel induced anti-

proliferation and apoptosis of lung cancer cells involves NF-κB pathway, Int. J. Mol. Sci. 13 (2012) 6236-6245. https://doi.org/10.3390/ijms13056236.

[201] R. Sirota, D. Gibson, R. Kohen, The timing of caffeic acid treatment with cisplatin determines sensitization or resistance of ovarian carcinoma cell lines, Redox Biol. 11 (2017) 170-175. https://doi.org/10.1016/j.redox.2016.12.006.

[202] A. Koraneekit, T. Limpaiboon, A. Sangka, P. Boonsiri, S. Daduang, J. Daduang, Synergistic effects of cisplatin-caffeic acid induces apoptosis in human cervical cancer cells via the mitochondrial pathways, Oncol. Lett. 15 (2018) 7397-7402. https://doi.org/10.3892/ol.2018.8256.

[203] N.N. Bouzaiene, S.K. Jaziri, H. Kovacic, L. Chekir-Ghedira, K. Ghedira, J. Luis, The effects of caffeic, coumaric and ferulic acids on proliferation, superoxide production, adhesion and migration of human tumor cells in vitro, Eur. J. Pharmacol. 766 (2015) 99-105. https://doi.org/10.1016/j.ejphar.2015.09.044.

[204] A.Y. Alayoubi, J.F. Anderson, S.D. Satyanarayanajois, P.W. Sylvester, S. Nazzal, Concurrent delivery of tocotrienols and simvastatin by lipid nanoemulsions potentiates their antitumor activity against human mammary adenocarcenoma cells, Eur. J. Pharm. Sci. 48 (2013) 385-392. https://doi.org/10.1016/j.ejps.2012.12.011.

[205] N. Steuber, K. Vo, R. Wadhwa, J. Birch, P. Iacoban, P. Chavez, T.A. Elbayoumi, Tocotrienol nanoemulsion platform of curcumin elicit elevated apoptosis and augmentation of anticancer efficacy against breast and ovarian carcinomas, Int. J. Mol. Sci. 17 (2016) 1792. https://doi.org/10.3390/ijms17111792.

[206] Ö.S. Aslantürk, In vitro cytotoxicity and cell viability assays: principles, advantages, and disadvantages, in: M. Larramendy, S. Soloneski (Eds.), Genotoxicity - A Predictable Risk to Our Actual World, Intech Open, 2018, pp. 1-18. https://10.5772/intechopen.71923.

[207] L. Śliwka, K. Wiktorska, P. Suchocki, M. Milczarek, S. Mielczarek, K. Lubelska, T. Cierpiał, P. Łyżwa, P. Kiełbasiński, A. Jaromin, The comparison of MTT and CVS assays for the assessment of anticancer agent interactions, PloS One, 11 (2016) e0155772. https://doi.org/10.1371/journal.pone.0155772.

[208] E. Chacon, D. Acosta, J.J. Lemasters, Primary cultures of cardiac myocytes as in vitro models for pharmacological and toxicological assessments, in J.V. Castell, M.J. Gmez-Lechn (Eds.), In Vitro Methods in Pharmaceutical Research, Academic Press, California, 1996, pp. 209–223. https://doi.org/10.1016/b978-012163390-5.50010-7.

[209] S. Elmore, Apoptosis: A review of programmed cell death, Toxicol. Pathol. 35 (2007) 495-516. https://doi.org/10.1080/01926230701320337.

[210] Z. Jin, W.S. El-Deiry, Overview of cell death signaling pathways, Cancer Biol. Ther. 4 (2005) 147-171. https://doi.org/10.4161/cbt.4.2.1508.

[211] B. Fadeel, D. Xue, The ins and outs of phospholipid asymmetry in the plasma membrane: Roles in health and disease, Crit. Rev. Biochem. Mol. Biol. 44 (2009) 264-277. https://doi.org/10.1080/10409230903193307.

[212] W. Lieberthal, J.S. Levine, Mechanisms of apoptosis and its potential role in renal tubular epithelial cell injury, Am. J. of Physiol. 271 (1996) F 477-F488. https://doi.org/10.1152/ajprenal.1996.271.3.F477.

[213] A.P. Demchenko, Beyond annexin V: Fluorescence response of cellular membranes to apoptosis, Cytotechnology, 65 (2013) 157-172. https://doi.org/10.1007/s10616-012-9481-y.

[214] D. Wlodkowic, W. Telford, J. Skommer, Z. Darzynkiewicz, Apoptosis and beyond: cytometry in studies of programmed cell death, in: Methods Cell Biol. 103 (2011) 55-98. https://doi.org/10.1016/B978-0-12-385493-3.00004-8.

[215] A.M. Rieger, K.L. Nelson, J.D. Konowalchuk, D.R. Barreda, Modified annexin V/propidium iodide apoptosis assay for accurate assessment of cell death, J. Vis. Exp. 50 (2011) e2597. https://doi.org/10.3791/2597.

[216] D.G. Pestov, M. Polonskaia, L.F. Lau, Flow cytometric analysis of the cell cycle in transfected cells without cell fixation, BioTechniques, 26 (1999) 102-106. https://doi.org/10.2144/99261st04.

[217] Z. Darzynkiewicz, Critical aspects in analysis of cellular DNA content, Curr. Protoc. Cytom. 56 (2011) 7.2. 1-7.2.8. https://doi.org/10.1002/0471142956.cy0702s56.

[218] S.Y. Shin, H. Yoon, S. Ahn, D.-W. Kim, D.-H. Bae, D. Koh, Y.H. Lee, Y. Lim, Structural properties of polyphenols causing cell cycle arrest at G1 phase in HCT116 human colorectal cancer cell lines, Int. J. Mol. Sci. 14 (2013) 16970-16985. https://doi.org/10.3390/ijms140816970.

[219] K.H. Kim, J.M. Sederstrom, Assaying cell cycle status using flow cytometry, Curr. Protoc. Mol. Biol. 111 (2015) 28.6.1-28.6.11. https://doi.org/10.1002/0471142727.mb2806s111.

[220] C.R. Reczek, N.S. Chandel, The two faces of reactive oxygen species in cancer, Annu. Rev. Cancer Biol. 1 (2017) 79-98. https://doi.org/10.1146/annurev-cancerbio-041916-065808.

[221] M. Katerji, M. Filippova, P. Duerksen-Hughes, Approaches and methods to measure oxidative stress in clinical samples: Research applications in the cancer field, Oxid. Med. Cell. Longev. 2019 (2019) 1279250. https://doi.org/10.1155/2019/1279250.

[222] S. Kollipara, R.K. Gandhi, Pharmacokinetic aspects and in vitro–in vivo correlation potential for lipid-based formulations, Acta Pharm. Sin B 4 (2014) 333-349. https://doi.org/10.1016/j.apsb.2014.09.001.

[223] V. Klang, C. Valenta, Lecithin-based nanoemulsions, J. Drug Deliv. Sci. Technol. 21 (2011) 55-76. https://doi.org/10.1016/S1773-2247(11)50006-1.

[224] D.J. McClements, L. Bai, C. Chung, Recent advances in the utilization of natural emulsifiers to form and stabilize emulsions, Annu. Rev. Food Sci. Technol. 8 (2017) 205-236. https://doi.org/10.1146/annurev-food-030216-030154.

[225] Lubrizol Standard Test Procedure, Peroxide value - AOCS Method, AATM 516-01, https://www.lubrizol.com/Personal-Care/Literature#/, 2006 (accessed 01 January 2018).

[226] Table 1: Principal IR absorptions for certain functional groups. http://academics.wellesley.edu/Chemistry/chem211lab/Orgo_Lab_Manual/Appendix/Instruments/InfraredSpec/Chem211%20IR%20Lit%20Value%20Table.pdf/ (accessed 01 February 2018).

[227] U. Nobbmann, Polydispersity – what does it mean for DLS and chromatography? http://www.materials-talks.com/blog/2014/10/23/polydispersity-what-does-it-mean-for-dls-and-chromatography/, 2014 (accessed 30 June 2017).

[228] W. Im-Emsap, J. Siepmann, O. Paeratakul, Disperse systems, in: G.S. Banker, C.T. Rhodes (Eds.), Modern Pharmaceutics, Marcel Dekker, Inc. New York, 2002, pp. 242–290. https://doi.org/10.1002/ardp.19803130919.

[229] American Society of the International Association for Testing and Materials, Standard test method for interfacial tension of oil against water by the ring method, ASTM D971. https://www.astm.org/Standards/D971.htm/, 2012 (accessed 01 January 2018).

[230] M.-A. Mehrnia, S.-M. Jafari, B.S. Makhmal-Zadeh, Y. Maghsoudlou, Crocin loaded nano-emulsions: factors affecting emulsion properties in spontaneous emulsification, Int. J. Biol. Macromol. 84 (2016) 261-267. https://doi.org/10.1016/j.ijbiomac.2015.12.029.

[231] A. Benichou, A. Aserin, N. Garti, Polyols, high pressure, and refractive indices equalization for improved stability of W/O emulsions for food applications, J. Disper. Sci. Technol. 22 (2001) 269-280. https://doi.org/10.1081/DIS-100105214.

[232] İ. Gülseren, M. Corredig, Interactions at the interface between hydrophobic and hydrophilic emulsifiers: Polyglycerol polyricinoleate (PGPR) and milk proteins, studied by drop shape tensiometry, Food Hydrocoll. 29 (2012) 193-198. https://doi.org/10.1016/j.foodhyd.2012.03.010.

[233] P.S. Goh, M. H. Ng, Y. M. Choo, N.B. Amru, C.H. Chuah, Production of tocols nanoemulsion by ultrasonication, J. Oil Palm Res. 28 (2016) 121-130. https://doi.org/10.21894/jopr.2016.2801.14.

[234] L.L. Lee, N. Niknafs, R.D. Hancocks, I.T. Norton, Emulsification: mechanistic understanding, Trends Food Sci. Technol. 31 (2013) 72-78. https://doi.org/10.1016/j.tifs.2012.08.006.

[235] M. Kaci, A. Belhaffef, S. Meziane, G. Dostert, P. Menu, E. Velot, S. Desobry, E. Arab-Tehrany, Nanoemulsions and topical creams for the safe and effective delivery of lipophilic antioxidant coenzyme Q10, Colloids Surf. B Biointerfaces, 167 (2018) 165-175. https://doi.org/10.1016/j.colsurfb.2018.04.010.

[236] F. Chemat, I. Grondin, P. Costes, L. Moutoussamy, A.S.C. Sing, J. Smadja, High power ultrasound effects on lipid oxidation of refined sunflower oil, Ultrason. Sonochem. 11 (2004) 281-285. https://doi.org/10.1016/j.ultsonch.2003.07.004.

[237] S.Y. Tang, S. Manickam, T.K. Wei, B. Nashiru, Formulation development and optimization of a novel Cremophore EL-based nanoemulsion using ultrasound cavitation, Ultrason. Sonochem. 19 (2012) 330-345. https://doi.org/10.1016/j.ultsonch.2011.07.001.

[238] N. Mollakhalili Meybodi, M. Mohammadifar, K. Abdolmaleki, Effect of dispersed phase volume fraction on physical stability of oil-in-water emulsion in the presence of gum tragacanth, J. Food Qual. Hazards Control 1 (2014) 102-107. http://jfqhc.ssu.ac.ir/article-1-95-en.pdf.

[239] Y.T. Shah, A.B. Pandit, V.S. Moholkar, Factors affecting cavitation behavior, Cavitation Reaction Engineering, Springer, Boston, 1999, pp. 55-83. https://doi.org/10.1007/978-1-4615-4787-7_3.

[240] R. Sadighi-Bonabi, F.A.F. Lahiji, F. Razeghi, The effect of viscosity, applied frequency and driven pressure on the laser induced bubble luminescence in water–sulfuric acid mixtures, Phys. Lett. A. 380 (2016) 2219-2226. https://doi.org/10.1016/j.physleta.2016.02.050.

[241] W.D. Pandolfe, Effect of dispersed and continuous phase viscosity on droplet size of emulsions generated by homogenization, J. Disper. Sci. Technol. 2 (1981) 459-474. https://doi.org/10.1080/01932698108943924.

[242] F. Wolf, K. Koehler, H.P. Schuchmann, Stabilization of water droplets in oil with PGPR for use in oral and dermal applications, J. Food Process Eng. 36 (2013) 276-283. https://doi.org/10.1111/j.1745-4530.2012.00688.x.

[243] A. Thompson, H. Singh, Preparation of liposomes from milk fat globule membrane phospholipids using a microfluidizer, J. Dairy Sci. 89 (2006) 410-419. https://doi.org/10.3168/jds.S0022-0302(06)72105-1.

[244] International Organization for Standardistion, Petroleum products - Determination of water - Coulometric Karl Fischer titration method, ISO 12937, https://www.iso.org/standard/2730.html/, 2000 (accessed 01 January 2019).

[245] K. Sawant, V. Mundada, V. Patel, Development and optimization of w/o/w multiple emulsion of lisinopril dihydrate using plackett burman and box-behnken designs, J. Nanomed. Nanotechnol. 8 (2017) 422. https://doi.org/10.4172/2157-7439.1000422.

[246] F. Tirnaksiz, O. Kalsin, A topical w/o/w multiple emulsions prepared with Tetronic 908 as a hydrophilic surfactant: formulation, characterization and release study, J. Pharm. Pharm. Sci. 8 (2005) 299-315. PMID: 16124940.

[247] Y. Hemar, M. Tamehana, P. Munro, H. Singh, Influence of xanthan gum on the formation and stability of sodium caseinate oil-in-water emulsions, Food Hydrocoll. 15 (2001) 513-519. https://doi.org/10.1016/S0268-005X(01)00075-3.

[248] E. Dickinson, Double emulsions stabilized by food biopolymers, Food Biophys. 6 (2011) 1-11. https://doi.org/10.1007/s11483-010-9188-6.

[249] Y. Zhang, J. Gou, F. Sun, S. Geng, X. Hu, K. Zhang, X. Lin, W. Xiao, X. Tang, Impact of electrolytes on double emulsion systems (W/O/W) stabilized by an amphiphilic block copolymer, Colloids Surf. B Biointerfaces, 122 (2014) 368-374. https://doi.org/10.1016/j.colsurfb.2014.07.008.

[250] N. Aditya, S. Aditya, H. Yang, H.W. Kim, S.O. Park, S. Ko, Co-delivery of hydrophobic curcumin and hydrophilic catechin by a water-in-oil-in-water double emulsion, Food Chem. 173 (2015) 7-13. https://doi.org/10.1016/j.foodchem.2014.09.131.

[251] T. C. Shekhar, G. Anju, Antioxidant activity by DPPH radical scavenging method of ageratum conyzoides linn. Leaves, Am. J. Ethnomedicine 1 (2014) 244-249. http://citeseerx.ist.psu.edu/viewdoc/download?doi=10.1.1.678.4869&rep=rep1&type=pdf.

[252] R. Sroynak, P. Srikalong, P. Raviyan, Radical scavenging capacity and antioxidant activity of the vitamin E extracted from palm fatty acid distillate by sequential cooling hexane, J. Agric. Sci. 5 (2013) 224. https://doi.org/10.5539/jas.v5n4p224.

[253] M.M. Rahman, M.B. Islam, M. Biswas, A.K. Alam, In vitro antioxidant and free radical scavenging activity of different parts of Tabebuia pallida growing in Bangladesh, BMC Res. Notes 8 (2015) 621. https://doi.org/10.1186/s13104-015-1618-6.

[254] S. Bhattacharya, R. Gachhui, P.C. Sil, Hepatoprotective properties of kombucha tea against TBHP-induced oxidative stress via suppression of mitochondria dependent apoptosis, Pathophysiology 18 (2011) 221-234. https://doi.org/10.1016/j.pathophys.2011.02.001.

[255] P. Schofield, D. Mbugua, A. Pell, Analysis of condensed tannins: A review, Anim. Feed Sci. Technol. 91 (2001) 21-40. https://doi.org/10.1016/S0377-8401(01)00228-0.

[256] Y.S. Tan, K.K. Ooi, K.P. Ang, A.M. Akim, Y.-K. Cheah, S.N.A. Halim, H.-L. Seng, E.R. Tiekink, Molecular mechanisms of apoptosis and cell selectivity of zinc dithiocarbamates functionalized with hydroxyethyl substituents, J. Inorg. Biochem. 150 (2015) 48-62. https://doi.org/10.1016/j.jinorgbio.2015.06.009.

[257] D.H.A. Ishak, K.K. Ooi, K.-P. Ang, A.M. Akim, Y.-K. Cheah, N. Nordin, S.N.B.A. Halim, H.-L. Seng, E.R. Tiekink, A bismuth diethyldithiocarbamate compound promotes apoptosis in HepG2 carcinoma, cell cycle arrest and inhibits cell invasion through modulation of the NF-κB activation pathway, J. Inorg. Biochem. 130 (2014) 38-51. https://doi.org/10.1016/j.jinorgbio.2013.09.018.

[258] K.K. Ooi, C.I. Yeo, T. Mahandaran, K.P. Ang, A.M. Akim, Y.-K. Cheah, H.-L. Seng, E.R. Tiekink, G2/M cell cycle arrest on HT-29 cancer cells and toxicity assessment of triphenylphosphanegold (I) carbonimidothioates, Ph3PAu [SC (OR)= NPh], R= Me, Et, and iPr, during zebrafish development, J. Inorg. Biochem. 166 (2017) 173-181. https://doi.org/10.1016/j.jinorgbio.2016.11.008.

[259] L. Salvia-Trujillo, M.A. Rojas-Graü, R. Soliva-Fortuny, O. Martín-Belloso, Impact of microfluidization or ultrasound processing on the antimicrobial activity against Escherichia coli of lemongrass oil-loaded nanoemulsions, Food Control 37 (2014) 292-297. https://doi.org/10.1016/j.foodcont.2013.09.015.

[260] P.K. Gupta, N. Bhandari, H.N. Shah, V. Khanchandani, R. Keerthana, V. Nagarajan, L. Hiremath, An update on nanoemulsions using nanosized liquid in liquid colloidal systems, in: K. S. Koh, V. L. Wong (Eds.), Nanoemulsions-properties, fabrications and applications, IntechOpen, 2019. https://doi.org/10.5772/intechopen.84442.

[261] R. Aboofazeli, Nanometric-scaled emulsions (nanoemulsions), Iran. J. Pharm. Res. 9 (2010) 325-326. PMID: 24381596.

[262] N. Garti, C. Bisperink, Double emulsions: progress and applications, Curr. Opin. Colloid Interface Sci. 3 (1998) 657-667. https://doi.org/10.1016/S1359-0294(98)80096-4.

[263] Horiba Scientific, Formulation stability. https://www.horiba.com/4-formula-stability/?fbclid=IwAR2Mmq0T-hNu2TZuu5qLg1sJ0blMrQwZAFPi8gAIep0Ia-YWkeVyHuM6_i4/, 2018 (accessed 15 October 2018).

[264] X. Chen, D.J. McClements, J. Wang, L. Zou, S. Deng, W. Liu, C. Yan, Y. Zhu, C. Cheng, C. Liu, Coencapsulation of (−)-epigallocatechin-3-gallate and quercetin in particle-stabilized W/O/W emulsion gels: Controlled release and bioaccessibility, J. Agr. Food Chem. 66 (2018) 3691-3699. https://doi.org/10.1021/acs.jafc.7b05161.

[265] B.V. Bonifacio, P.B. da Silva, M.A. dos Santos Ramos, K.M.S. Negri, T.M. Bauab, M. Chorilli, Nanotechnology-based drug delivery systems and herbal medicines: A review, Int. J. Nanomedicine. 9 (2014) 1-15. https://doi.org/10.2147/IJN.S52634.

[266] J.K. Patra, G. Das, L.F. Fraceto, E.V.R. Campos, M. del Pilar Rodriguez-Torres, L.S. Acosta-Torres, L.A. Diaz-Torres, R. Grillo, M.K. Swamy, S. Sharma, Nano based drug delivery

systems: Recent developments and future prospects, J. Nanobiotechnol. 16 (2018) 71. https://doi.org/10.1186/s12951-018-0392-8.

[267] A.A. Rahman, A.R.A. Jamal, R. Harun, N.M. Mokhtar, W.Z.W. Ngah, Gamma-tocotrienol and hydroxy-chavicol synergistically inhibits growth and induces apoptosis of human glioma cells, BMC Complement. Altern. Med. 14 (2014) 213. https://doi.org/10.1186/1472-6882-14-213.

[268] M. Yusof, S. Makpol, R. Jamal, R. Harun, N. Mokhtar, W. Wan Ngah, γ-Tocotrienol and 6-Gingerol in combination synergistically induce cytotoxicity and apoptosis in HT-29 and SW837 human colorectal cancer cells, Molecules 20 (2015) 10280-10297. https://doi.org/10.3390/molecules200610280.

[269] C. Wilankar, N. M Khan, R. Checker, D. Sharma, R. Patwardhan, V. Gota, S.K. Sandur, T. Devasagayam, γ-Tocotrienol induces apoptosis in human T cell lymphoma through activation of both intrinsic and extrinsic pathways, Curr. Pharm. Des. 17 (2011) 2176-2189. https://doi.org/10.2174/138161211796957463.

[270] K. Nishio, M. Horie, Y. Akazawa, M. Shichiri, H. Iwahashi, Y. Hagihara, Y. Yoshida, E. Niki, Attenuation of lipopolysaccharide (LPS)-induced cytotoxicity by tocopherols and tocotrienols, Redox Biol. 1 (2013) 97-103. https://doi.org/10.1016/j.redox.2012.10.002.

[271] S.K. Jaganathan, Growth inhibition by caffeic acid, one of the phenolic constituents of honey, in HCT 15 colon cancer cells, Sci. W. J. (2012) 372345. https://doi.org/10.1100/2012/372345.

[272] S. Thiagarajan, D.J. Arapoc, N. Husna Shafie, Y.Y. Keong, H. Bahari, Z. Adam, T. Ei, Momordica charantia (Indian and Chinese bitter melon) extracts inducing apoptosis in human lung

cancer cell line A549 via rOS-mediated mitochodria injury, Evid. Based Complement. Alternat. Med. 2019 (2019) 2821597. https://doi.org/10.1155/2019/2821597.

[273] Y.-M. Choi, H.-K. Kim, W. Shim, M.A. Anwar, J.-W. Kwon, H.-K. Kwon, H.J. Kim, H. Jeong, H.M. Kim, D. Hwang, Mechanism of cisplatin-induced cytotoxicity is correlated to impaired metabolism due to mitochondrial ROS generation, PloS One. 10 (2015) e0135083. https://doi.org/10.1371/journal.pone.0135083.

[274] R. Marullo, E. Werner, N. Degtyareva, B. Moore, G. Altavilla, S.S. Ramalingam, P.W. Doetsch, Cisplatin induces a mitochondrial-ROS response that contributes to cytotoxicity depending on mitochondrial redox status and bioenergetic functions, PloS One. 8 (2013) e81162. https://doi.org/10.1371/journal.pone.0081162.

[275] F. Chen, V. Vallyathan, V. Castranova, X. Shi, Cell apoptosis induced by carcinogenic metals, Mol. Cell. Biochem. 222 (2001) 183-188. https://doi.org/10.1023/A:1017970330982.

[276] K.K. Ooi, C.I. Yeo, K.-P. Ang, A.M. Akim, Y.-K. Cheah, S.N.A. Halim, H.-L. Seng, E.R. Tiekink, Phosphanegold (I) thiolates, Ph 3 PAu [SC (OR)= NC 6 H 4 Me-4] for R= Me, Et and iPr, induce apoptosis, cell cycle arrest and inhibit cell invasion of HT-29 colon cancer cells through modulation of the nuclear factor-κB activation pathway and ubiquitination, J. Biol. Inorg. Chem. 20 (2015) 855-873. https://doi.org/10.1007/s00775-015-1271-5.

[277] A. Boveris, E. Cadenas, Mitochondrial production of hydrogen peroxide regulation by nitric oxide and the role of ubisemiquinone, IUBMB Life 50 (2000) 245-250. https://doi.org/10.1080/713803732.

[278] F. Antunes, E. Cadenas, Cellular titration of apoptosis with steady state concentrations of H2O2: submicromolar levels of H2O2 induce apoptosis through Fenton chemistry independent of the cellular thiol state, Free Radic. Biol. Med. 30 (2001) 1008-1018. https://doi.org/10.1016/S0891-5849(01)00493-2.

[279] Y.M. Chung, Y.S. Bae, S.Y. Lee, Molecular ordering of ROS production, mitochondrial changes, and caspase activation during sodium salicylate-induced apoptosis, Free Radic. Biol. Med. 34 (2003) 434-442. https://doi.org/10.1016/s0891-5849(02)01301-1.

[280] J. Noh, B. Kwon, E. Han, M. Park, W. Yang, W. Cho, W. Yoo, G. Khang, D. Lee, Amplification of oxidative stress by a dual stimuli-responsive hybrid drug enhances cancer cell death, Nat. Commun. 6 (2015) 6907. https://doi.org/10.1038/ncomms7907.

[281] J. Yi, J. Yang, R. He, F. Gao, H. Sang, X. Tang, D.Y. Richard, Emodin enhances arsenic trioxide-induced apoptosis via generation of reactive oxygen species and inhibition of survival signaling, Cancer Res. 64 (2004) 108-116. https://doi.org/10.1158/0008-5472.can-2820-2.

[282] Y. Yang, W. Zhou, J. Wu, L. Yao, L. Xue, Q. Zhang, Z. Wang, X. Wang, S. Dong, J. Zhao, Antitumor activity of nimotuzumab in combination with cisplatin in lung cancer cell line A549 in vitro, Oncol. Lett. 15 (2018) 5280-5284. https://doi.org/10.3892/ol.2018.7923.

[283] M.C. Wang, X. Liang, Z.Y. Liu, J. Cui, Y. Liu, L. Jing, L.L. Jiang, J.Q. Ma, L.L. Han, Q.Q. GuO, In vitro synergistic antitumor efficacy of sequentially combined chemotherapy/icotinib in non-small cell lung cancer cell lines, Oncol. Rep. 33 (2015) 239-249. https://doi.org/10.3892/or.2014.3583.

[284] X. Ji, Z. Wang, A. Geamanu, A. Goja, F.H. Sarkar, S.V. Gupta, Delta-tocotrienol suppresses Notch-1 pathway by upregulating miR-34a in nonsmall cell lung cancer cells, Int. J. Cancer. 131 (2012) 2668-2677. https://doi.org/10.1002/ijc.27549.

[285] B. Aru, E. Güzelmeric, A. Akgül, G.Y. Demirel, H. Kırmızıbekmez, Antiproliferative activity of chemically characterized propolis from Turkey and its mechanisms of action, Chem. Biodivers. 16 (2019) e1900189. https://doi.org/10.1002/cbdv.201900189.

[286] N. Pabla, Z. Dong, Cisplatin nephrotoxicity: Mechanisms and renoprotective strategies, Kidney Int. 73 (2008) 994-1007. https://doi.org/10.1038/sj.ki.5002786.

[287] I. Arany, R.L. Safirstein, Cisplatin nephrotoxicity, Semin. Nephrol. 23 (2003) 460-464. https://doi.org/10.1016/S0270-9295(03)00089-5.

[288] X. Yao, K. Panichpisal, N. Kurtzman, K. Nugent, Cisplatin nephrotoxicity: A review, Am. J. Med. Sci. 334 (2007) 115-124. https: //doi.org/10.1097/MAJ.0b013e31812dfe1e.

[289] R.P. Miller, R.K. Tadagavadi, G. Ramesh, W.B. Reeves, Mechanisms of cisplatin nephrotoxicity, Toxins. 2 (2010) 2490-2518. https: //doi.org/10.3390/toxins2112490.

[290] D.-m. Zou, M. Brewer, F. Garcia, J.M. Feugang, J. Wang, R. Zang, H. Liu, C. Zou, Cactus pear: A natural product in cancer chemoprevention, Nutr. J. 4 (2005) 25. https: //doi.org/10.1186/1475-2891-4-25.

[291] J. Melzer, F. Iten, K. Hostanska, R. Saller, Efficacy and safety of mistletoe preparations (Viscum album) for patients with cancer diseases, Complement. Med. Res. 16 (2009) 217-226. https: //doi.org/10.1159/000226249.